

**Some parts of this thesis may have been removed for copyright restrictions.**

If you have discovered material in AURA which is unlawful e.g. breaches copyright, (either yours or that of a third party) or any other law, including but not limited to those relating to patent, trademark, confidentiality, data protection, obscenity, defamation, libel, then please read our [Takedown Policy](#) and [contact the service](#) immediately

INFLUENCE OF PRETREATMENT ON  
CORROSION BEHAVIOUR OF DUPLEX  
ZINC / POLYMER COATINGS  
ON STEEL SUBSTRATES

SAMSON OSARETIN AGBONLAHOR

A Thesis submitted for the degree of  
Doctor of Philosophy

THE UNIVERSITY OF ASTON IN BIRMINGHAM

JANUARY 1988

This copy of the thesis has been supplied on condition that anyone who consults it is understood to recognise that its copyright rests with its author and that no quotation from the thesis and no information derived from it, may be published without the author's prior, written consent.

**BEST COPY**

**AVAILABLE**

Variable print quality

**TEXT CUT  
OFF IN  
ORIGINAL**

'INFLUENCE OF PRETREATMENT ON CORROSION BEHAVIOUR OF  
DUPLEX ZINC/POLYMER COATINGS ON STEEL SUBSTRATES'

SAMSON OSARETIN AGBONLAHOR

DOCTOR OF PHILOSOPHY

1987

S U M M A R Y

An investigation has been undertaken to determine the major factors influencing the corrosion resistance of duplex polyester-zinc coatings on steel substrates.

Premature failure of these systems has been attributed to the presence of defects such as craters and pinholes in the polymer film and debonding of the polymer film from the zinc substrate.

Defects found on commercially produced samples have been carefully characterised using metallographic and scanning electron microscopy techniques. The influence of zinc substrate surface roughness, polymer film thickness and degassing of conversion coating films on the incidence of defects has been determined.

Pretreatments of the chromate, chromate-phosphate, non-chromate, and alkali-oxide types were applied and the conversion coatings produced characterised with respect to their nature and composition. The effect of degassing on the properties of the films was also investigated. Electrochemical investigations were carried out to determine the effect of the presence of the eta or zeta phase as the outermost layer of the galvanized coating.

Flow characteristics of polyester on zinc electroplated, hot-dip continuous and batch galvanized and zinc sprayed samples were investigated using hot-stage microscopy. The effect of different pretreatments and degassing after conversion coating formation, on flow characteristics were determined.

Duplex coatings were subjected to the acetic acid salt spray test. The effect on adhesion was determined using an indentation debonding test and the results compared with those obtained using cross-cut/peel and pull-off tests. The locus of failure was determined using scanning electron microscopy and X-ray photoelectron spectroscopy techniques.

KEYWORDS : Powder coating, Galvanized steel,  
Pretreatments, Polyester, Corrosion

## A C K N O W L E D G E M E N T S

The author wishes to thank the Science and Engineering Research Council for providing overall project funding. He also wishes to thank the academic and technical staff of the Department of Civil Engineering and Mechanical and Production Engineering at the University of Aston in Birmingham for their continuous support throughout the research.

In particular the author wishes to thank his supervisor Dr. N.R. Short and adviser Dr. J.K. Dennis for their considerable guidance throughout the work.

# L I S T   O F   C O N T E N T S

	<u>Page</u>
TITLE PAGE	1
SUMMARY	2
ACKNOWLEDGEMENTS	3
LIST OF CONTENTS	4
LIST OF FIGURES	12
LIST OF TABLES	20
1. INTRODUCTION AND OBJECTIVES	23
1.1. INTRODUCTION	23
1.2. OBJECTIVES	26
2. LITERATURE SURVEY	29
2.1. STEEL PROTECTION	29
2.1.1. INTRODUCTION	29
2.1.2. METHODS OF COATING STEEL WITH ZINC	31
2.2. ZINC COATING PRETREATMENTS	44
2.2.1. INTRODUCTION	44
2.2.2. PRE-CONVERSION COATING TREATMENT	46
2.2.3. CHROMATE CONVERSION COATING PROCESS	48
2.2.3.1. INTRODUCTION	48
2.2.3.2. DEVELOPMENT OF THE CHROMATING PROCESS	49
2.2.3.3. THE MECHANISM OF FOR- MATION OF CHROMATE CONVERSION COATINGS	50
2.2.3.4. FILM CHARACTERISTICS	54
2.2.3.5. ORGANIC COATING BONDIDNG PROPERTIES OF CHROMATE FILMS	58

	2.3.3.6. CHROMATE BATHS	61
2.2.4.	NO-RINSE PROCESSES	62
2.2.5.	PHOSPHATE CONVERSION COATINGS	63
2.2.6.	ALKALINE OXIDE	67
2.2.7.	CHROMETAN CONVERSION COATING PROCESSES	69
2.3.	POWDER ORGANIC COATINGS	71
2.3.1.	INTRODUCTION	71
2.3.2.	ADVANTAGES AND DISADVANTAGES OF POWDER ORGANIC COATING	72
2.3.3.	POWDER ORGANIC COATING FORMULATIONS	74
2.3.4.	PRODUCTION OF ORGANIC COATING POWDERS	78
2.3.5.	POWDER DEPOSITION	83
	2.3.5.2. ELECTROSTATIC ORGANIC POWDER COATING SYSTEMS	85
	2.3.5.3. POWDER PARTICLE CHARGING AND BEHAVIOUR	90
2.3.6.	CURING OF POWDER COATINGS	97
	2.3.6.1 CURING STUDIES	105
2.3.7.	ORGANIC COATING ADHESION MEASUREMENT	107
2.4.	PROBLEMS ASSOCIATED WITH POWDER COATED GALVANIZED STEEL	109
2.4.1.	DEGRADATION OF POLYMER FILM	109
2.4.2.	PINHOLING	112
2.4.3.	CRATERING	112
2.4.4.	LOSS OF ADHESION DUE TO CRACKING OF ZINC SPANGLES.	113

2.4.5.	CORROSION	117
3.	EXPERIMENTAL TECHNIQUES AND PROCEDURES	119
3.1.	MATERIALS AND SAMPLE PREPARATION	119
3.1.1.	MATERIALS	119
3.1.2.	SAMPLE PREPARATION	119
3.1.3.	POWDER	119
3.2.	CLEANING	120
3.2.1.	PROPRIETARY AC51 SOLUTION PREPARATION	120
3.2.2.	CLEANING PROCEDURE	121
3.3.	PREPARATION OF CONVERSION COATING SOLUTIONS	121
3.3.1.	PROPRIETARY CHROMATE-PHOSPHATE (ALOCROM 100) SOLUTION	121
3.3.2.	PROPRIETARY NON-CHROMATE (Chrometan) SOLUTION	121
3.3.3.	CHROMATE CONVERSION COATING SOLUTIONS	122
3.3.3.1.	CHROMIC ACID (NaCl as activator) SOLUTION	122
3.3.3.2.	CHROMIC ACID (activated with NaF) SOLUTION	122
3.3.3.3.	OTHER SOLUTIONS	122
3.4.	CONVERSION COATING PROCESS	123
3.5.	COUPON WEIGHT CHANGE STUDIES	124
3.6.	DETERMINATION OF ZINC DISSOLUTION RATE USING ATOMIC ABSORPTION SPECTROPHOTOMETRY	124
3.7.	ELECTROCHEMICAL STUDIES	128

3.7.1.	POTENTIODYNAMIC ANODIC POLARISATION	129
3.7.2.	POTENTIONSTATIC SCAN	130
3.7.3.	LINEAR POLARISATION	130
3.7.4.	REST POTENTIAL MEASUREMENT	131
3.8.	EXAMINATION AND ANALYSIS OF SAMPLE SURFACES	131
3.8.1.	SURFACE ROUGHNESS	131
3.8.2.	SCANNING ELECTRON MICROSCOPY (SEM)/ENERGY DISPERSIVE X-RAY ANALYSIS (EXDA) TECHNIQUES	132
3.8.3.	X-RAY PHOTOELECTRON SPECTROS- COPY (XPS) / AUGER ELECTRON SPECTROSCOPY (AES) TECHNIQUES	133
3.9.	POWDER COATING PROCESS	135
3.10.	POWDER FLOW STUDIES	137
3.11.	CORROSION TESTS	139
	3.11.1. ACETIC ACID SALT SPRAY TEST (ASTM B 287-74) (Reapproved 1980)	139
4.	THE NATURE OF DEFECTS FOUND IN POLYESTER POWDER FILMS ON ZINC COATED STEEL	147
4.1.	INTRODUCTION	147
4.2.	ANALYSIS OF DEFECTS ON POLYESTER POWDER COATED ZINC ELECTROPLATED STEEL SHEET (Sample i)	148
4.3.	ANALYSIS OF DEFECTS ON A POLYESTER POWDER COATED HOT-DIPPED GALVANIZED STEEL SECTION (Sample iia)	150
4.4.	ANALYSIS OF DEFECTS ON A POLYESTER POWDER COATED HOT-DIPPED GALVANIZED STEEL SECTION (Sample iib)	153
4.5.	LABORATORY PREPARED SAMPLES	155
4.6	CONCLUSIONS	158
5.	CHARACTERISTICS OF ZINC COATED STEEL SUBSTRATES	171

5.1.	INTRODUCTION	171
5.2.	RESULTS	171
5.2.1.	SURFACE ANALYSIS OF THE AS RECEIVED SPECIMENS	171
5.2.1.1.	SURFACE ROUGHNESS	171
5.2.1.2.	SURFACE CHEMISTRY AND COMPOSITION	172
5.2.2.	EFFECT OF AC51 CLEANING SOLU- TION ON THE SAMPLE SURFACE	173
5.2.3.	SPECIMEN CROSS-SECTION EXAMINATION AND ANALYSIS	174
5.2.3.1.	METALLOGRAPHY	174
5.2.3.2.	SAMPLE COATING THICKNESS AND HARDNESS	174
5.3.	DISCUSSION	174
5.4.	CONCLUSIONS	177
6.	CONVERSION COATING OF ZINC COATED SUBSTRATES	187
6.1.	INTRODUCTION	187
6.2.	CHROMIC ACID ACTIVATED WITH SODIUM CHLORIDE (L1) ( 0.12M/l $\text{CrO}_3$ + 0.3M/l NaCl)	187
6.2.1.	CONVERSION COATING FORMATION AND GROWTH	187
6.2.2.	ZINC DISSOLUTION RATE STUDIES	189
6.2.3.	EXAMINATION AND ANALYSIS OF THE CONVERSION COATING FILM FORMED	190
6.2.4.	EFFECT OF DEGASSING AFTER FOR- MATION OF THE CONVERSION COATING	191
6.2.5.	EFFECT OF VARIATION OF SOLUTION pH ON THE FORMATION OF CONVERSION COATING IN L1 (0.12M/l $\text{CrO}_3$ + 0.3M/l NaCl) SOLUTION	191

6.2.6.	EFFECT OF THE PRESENCE OF LEAD ON THE FORMATION OF CONVERSION COATING FILMS	192
6.2.7.	EFFECT OF USING NaF AS ACTIVATOR ( $\text{CrO}_3$ +NaF (L2)	194
6.3.	CHROMATE - PHOSPHATE (ALOCROM 100) SOLUTION	195
6.3.1.	FILM FORMATION AND Zn DISSOLUTION RATE STUDIES	195
6.3.2.	EXAMINATION AND ANALYSIS OF SAMPLE SURFACES AFTER PRETREATMENT	197
6.4.	NON-CHROMATE (CHROMETAN) CONVERSION COATING SOLUTION	197
6.4.1.	FILM FORMATION AND ZINC DISSOLUTION STUDIES	197
6.4.2.	EXAMINATION AND ANALYSIS OF CONVERSION COATING FILMS	198
6.5.	SODIUM HYDROXIDE SOLUTION	198
6.5.1.	FILM FORMATION AND ZINC DISSOLUTION RATE STUDIES	198
6.5.2.	EXAMINATION AND ANALYSIS OF SAMPLE SURFACE AFTER TREATMENT	199
6.6.	DISCUSSION	199
6.7.	CONCLUSIONS	205
7.	ELECTROCHEMICAL BEHAVIOUR OF ZINC COATED STEEL IN CONVERSION COATING SOLUTIONS	236
7.1.	INTRODUCTION	236
7.2.	SAMPLE AND SOLUTION PREPARATION	236
7.3.	ELECTROCHEMICAL STUDIES	237
7.4.	RESULTS AND DISCUSSION	239
7.4.1.	POTENTIODYNAMIC ANODIC POLARI- SATION	139
7.4.2.	POTENTIOSTATIC POLARISATION	250
7.5.	CONCLUSIONS	252
8.	POLYESTER POWDER FLOW STUDIES	268

8.1.	INTRODUCTION	268
8.2.	RESULTS	268
8.3.	DISCUSSION	269
8.4.	CONCLUSIONS	276
9.	ADHESION CHARACTERISTICS OF DUPLEX POLYESTER POWDER-ZINC COATED STEEL SUBSTRATES	288
9.1.	INTRODUCTION	288
9.2	CROSS-CUT/PEEL TEST	289
9.3.	PULL-OFF TEST	289
9.4.	INDENTATION DEBONDING	291
9.5.	RESULTS	293
9.6.	DISCUSSION	294
	9.6.1. CROSS-CUT/PEEL TEST	294
	9.6.2. PULL-OFF TEST	295
	9.6.3. INDENTATION DEBONDING TEST	298
9.7.	CONCLUSIONS	301
10.	CORROSION TESTING OF THE CONVERSION COATED ZINC AND THE DUPLEX POLYMER -ZINC COATINGS ON STEEL	315
10.1.	INTRODUCTION	315
10.2.	CORROSION RATE STUDIES OF CONVERSION COATED SAMPLES	316
10.3.	CORROSION TEST OF DUPLEX SAMPLES	317
10.4.	OBSERVATIONS DURING THE ACETIC ACID 5% SALT SPRAY TEST OF THE DUPLEX SAMPLES	317
10.5	DISCUSSION	319
	10.5.1 CONVERSION COATED SAMPLES	319
	10.5.2 CONVERSION AND POWDER COATED (DUPLEX) SAMPLES	321
10.6	CONCLUSIONS	323

11.	LOCUS OF FAILURE OF DUPLEX POLYMER - ZINC COATINGS ON STEEL SUBSTRATES	334
11.1.	INTRODUCTION	334
11.2.	RESULTS AND DISCUSSION	335
11.2.1.	CORROSION INDUCED FAILURE	335
11.2.2.	MECHANICAL INDUCED FAILURE	336
12	GENERAL DISCUSSION	346
13	RECOMMENDATION FOR FURTHER WORK	351
	REFERENCES	354

# LIST OF FIGURES

	<u>PAGE</u>
Figure 2.1 Typical hot-dip galvanized coatings <sup>(15)</sup>	42
Figure 2.2 The zinc rich end of the zinc-iron equilibrium diagram	43
Figure 2.3 Diagrammatic representation of the diffusion of iron and zinc through the alloy layer	43
Figure 2.4 Effect of sulphuric acid concentration on chromate passivation of zinc <sup>(40)</sup>	60
Figure 2.5 Bell curve <sup>(51)</sup> illustrating conversion coating film formation in relation to solution pH	60
Figure 2.6 Electrostatic fluidised bed coating system	89
Figure 2.7 Electrostatic powder spray coating system showing powder layer growth using corona-charge gun	89
Figure 2.8 Schematic illustration of the coalescence of molten powder particles	111
Figure 3.1 Schematic arrangement of the electrochemical test cell	142
Figure 3.2 Typical polarisation resistance plot	143
Figure 3.3 Potential - time equipment set-up	144
Figure 3.4 Schematic layout of Talysurf <sup>(132)</sup>	145
Figure 3.5 Schematic illustration of (a) X-ray photoelectron spectroscopy (XPS) (b) Auger electron spectroscopy (AES) techniques	146
Figure 3.6 Schematic illustration of major components of the XPS (ESCA model 550) system	146
Figure 4.1 Scanning electron micrographs of crater type defects in the coating on electroplated zinc	159

Figure 4.2	Optical micrograph of cross-section of crater defect showing incorporation of grit in powder coating on electrop- lated zinc (a) at the defect (x500) (b) just prior to defect (x220)	160
Figure 4.3	Optical micrograph of powder coated hot-dip galvanized specimen showing defects	161
Figure 4.4	Optical micrograph of cross-section through the powder coated hot-dip galvanized section	161
Figure 4.5	Scanning electron micrographs of crater type defect	162
Figure 4.6	Scanning electron micrograph of cross-section of crater defect showing rough zeta regions	163
Figure 4.7	Scanning electron micrograph of cross-section showing very large gas bubble which could lead to pinholing	163
Figure 4.8	Surface of defective powder coating showing craters	164
Figure 4.9	Surface view of one crater (x100)	164
Figure 4.10	Optical micrographs of cross-sections showing defect free areas on the polymer film	165
Figure 4.11	Optical micrographs of cross-sections showing defects in the galvanized layer (zinc coat)	166
Figure 4.12	Optical micrograph of cross-section through one crater	167
Figure 4.13	An illustration of Faraday cage effect	167
Figure 4.14	Scanning electron micrographs of a crater -viewed from the surface	168
Figure 4.15	Scanning electron micrographs of cross-section: (a&b) of defective galvanized areas covered by polymer coating (c) through one crater	169
Figure 4.16	Optical micrograph of sound powder coating on hot-dip galvanized sample	170

Figure 5.1	Traces of surface roughness (Ra) of samples (A) electroplated (B) hot-dip continuous (C) hot-dip batch (D) sprayed	181
Figure 5.2	X-ray photoelectron/Auger electron spectroscopy traces of HDC sample surfaces (A) before cleaning (B) After cleaning	182
Figure 5.3	Scanning electron micrographs of samples before and after cleaning in AC51 solution A electroplated degreased only by acetone swab A(i) Electroplated after cleaning B HDC degreased only by acetone swab B(i) HDC after cleaning	183
Figure 5.3 continued;	C HDB degreased only by acetone swab C(i) " after cleaning D sprayed degreased only by acetone swab D(i) " after cleaning	184
Figure 5.4	Optical micrographs of sample cross-sections (A) electroplated (B) HDC	185
Figure 5.4 continued -	(C) HDB (Ci) HDB showing the outburst of zeta (D) sprayed	186
Figure 6.1	Rest potential vs immersion time in 0.12M/l $\text{CrO}_3$ + 0.3M/l NaCl solution (L1)	210
Figure 6.2	Coupon weight change vs immersion time in 0.12M/l $\text{CrO}_3$ + 0.3M/l NaCl Solution (L1)	210
Figure 6.3	Dissolved zinc weight vs immersion time in 0.12M/l $\text{CrO}_3$ + 0.3M/l NaCl (L1)	210
Figure 6.4	Scanning electron micrographs showing the appearance of coatings formed on (a) electroplated, (b) HDC, (c) HDB and (d) sprayed samples in 0.12M/l $\text{CrO}_3$ + 0.3M/l NaCl solution (L1) at 25°C	211

Figure 6.5	Scanning electron micrographs showing the appearance of coatings formed on (a) electroplated, (b) HDC, (c) HDB and (d) sprayed samples in 0.12M/l $\text{CrO}_3$ + 0.3M/l NaCl solution (L1) at 25°C and degassed at 220°C for 20 minutes	215
Figure 6.6 (a)	Effect of variation of 0.12M/l $\text{CrO}_3$ + 0.3M/l NaCl solution (L1) pH on coupon weight change of HDC samples treated for 120s	219
Figure 6.6 (b)	Effect of variation of 0.12M/l $\text{CrO}_3$ + 0.3M/l NaCl solution (L1) pH on at.% Cr content of conversion coating formed on HDC samples treated for 120s	219
Figure 6.7	Scanning electron micrographs showing the appearance of conversion coatings formed on HDC samples treated for 120s in 0.12M/l $\text{CrO}_3$ + 0.3M/l NaCl (L1) solution at different pH values	220
Figure 6.8	Coupon weight change of HDB vs time of immersion in L1 and L3	221
Figure 6.9	Scanning electron micrographs showing the appearance of conversion coatings formed on HDB in 0.03M/l $\text{CrO}_3$ + 0.07M/l NaCl (L3) solution	222
Figure 6.10	Rest potential vs immersion time in 0.12M/l $\text{CrO}_3$ + 0.1M/l NaF (L2) solution	224
Figure 6.11	Scanning electron micrographs showing the appearance of conversion coatings formed on HDC in 0.12M/l $\text{CrO}_3$ + 0.1M/l NaF (L2) solution	225
Figure 6.12 (a)	Coupon weight change vs immersion time in 0.12M/l $\text{CrO}_3$ + 0.1M/l NaF (L2) solution	226
Figure 6.12 (b)	At. % Cr vs immersion time of HDB in 0.12M/l $\text{CrO}_3$ + 0.1M/l NaF (L2) solution	226
Figure 6.13	Potential vs immersion time in Alocrom 100 solution	227
Figure 6.14	Coupon weight change vs immersion time in Alocrom 100 solution	227

Figure 6.14	Weight of Zn dissolved vs immersion time in Alocrom 100 solution	228
Figure 6.16 (a)	Scanning electron micrographs showing the appearance of conversion coatings formed on pure Zn samples in Alocrom 100 solution	229
Figure 6.16 (b)	Scanning electron micrographs showing the appearance of conversion coatings formed on HDC samples in Alocrom 100 solution	230
Figure 6.17 (a)	Coupon weight change of electroplated sample vs immersion time in Chrometan solution	231
Figure 6.17 (b)	Weight of zinc dissolved of electroplated sample vs immersion time in Chrometan solution	231
Figure 6.18	Scanning electron micrographs showing the appearance of conversion coatings formed on electroplated samples in Chrometan solution	232
Figure 6.19	Rest potential vs time of immersion in NaOH solution	233
Figure 6.20	Scanning electron micrographs showing the appearance of conversion coatings formed on electroplated samples in NaOH solution	234
Figure 6.21	XPS survey spectra of chromated electroplated zinc	235
Figure 7.1	Simplified potential - pH diagrams (a) Zn-H <sub>2</sub> O (b) Cr-H <sub>2</sub> O (c) Fe-H <sub>2</sub> O (d) a, b & c combined	256
Figure 7.2	(a -h) Groups of potentiodynamic polarisation curves of zeta and zinc in various solutions shown in TABLE 7.1	258
Figure 7.3	Effect of pH on the rate of corrosion of zinc <sup>(139)</sup>	262
Figure 7.4	Theoretical and actual potentiodynamic polarisation plots of active - passive metals	262

Figure 7.5 (a - h) Groups of potentiostatic polarisation curves of zeta and zinc in the various solutions shown in TABLE 7.1	263
Figure 7.6 (a) Instantaneous current vs solution pH of zeta and zinc in NaOH (b) Final current of zeta and zinc in NaOH solution vs pH of the solution	267
Figure 8.1 The effect of type of zinc coating as cleaned on powder flow	278
Figure 8.2 The effect of short chromating time (30s) on powder flow	279
Figure 8.3 The effect of chromate pretreatment (120s) on powder flow	280
Figure 8.4 The effect of degassing after pretreatment (120s) on powder flow	281
Figure 8.5 The effect of alkali pretreatment on powder flow	282
Figure 8.6 The effect of different pretreatments on the powder flow on electroplated samples	283
Figure 8.7 The effect of different pretreatments on the powder flow on continuous hot-dip samples	284
Figure 8.8 The effect of different pretreatments on the powder flow on batch hot-dip samples	285
Figure 8.9 The effect of different pretreatments on the powder flow on sprayed zinc samples	286
Figure 8.10 Comparison of final coverage on different pretreatment surfaces	287
Figure 9.1 (a) Schematic diagram for the case of indentation debonding film on metal substrate <sup>(151)</sup> (b) Illustration of indenter radius 'a' and debonded radius 'b'	308
Figure 9.2 Micrograph of an indent produced in polyester film on zinc	308

Figure 9.3	Peeling strain vs time for samples not degassed	309
Figure 9.4	Comparison of peeling strain vs time for degassed samples	310
Figure 9.5	Comparison of peeling strain vs time for samples no degassed (Peeled after 700 hours in acetic 5% salt spray corrosion test)	311
Figure 9.6	Comparison of peeling strain vs time for samples degassed (peeled after 700 hours in acetic 5% salt spray corrosion test)	312
Figure 9.7	Effect of polymer coating thickness on peeling strain (pretreated in 0.12M/l $\text{CrO}_3$ + 0.3 M/l NaCl solution for 120s and degassed)	313
Figure 9.8	Powder organic coating on zinc sprayed samples (a) Thin film (55 - 65 u) (b) Thick film (80-100 u)	314
Figure 10.1	(a) Comparison of corrosion current of samples immersed in acetic acid salt spray solution after treatment in different pretreatment solutions	327
Figure 10.1	(b) Comparison of corrosion rate in mm/yr. of samples immersed in acetic acid salt spray solution after treatment in different pretreatment solutions	328
Figure 10.2	Comparison of polarisation resistance ( $R_p$ ) of samples immersed in acetic acid salt spray solution after treatment in different pretreatment solutions	329
Figure 10.3	Optical macrographs showing the appearance of the significant face of the acetic 5% salt spray corrosion tested (for 700 hours) pannels (a - e)	330
Figure 10.4	Optical micrographs showing the appearance of powder coated zinc sprayed sample cross-section before (a) and after (b) corrosion test	332
Figure 10.5	Relative disbonded areas of samples cleaned only and samples conversion coated in 0.12M/l $\text{CrO}_3$ + 0.3M/l NaCl (L1) for 30s and 120s	333

Figure 11.1	Scanning electron micrographs showing the appearance of disbonded interfaces of corrosion induced failure	
(a)	electroplated sample; metal face	
(b)	" " polymer face	
(c)	HDB sample; metal face	
(d)	" " polymer face	343
Figure 11.2	Scanning electron micrographs showing the appearance of disbonded interfaces of mechanical induced failure	
(a)	electroplated sample; metal face	
(b)	" " polymer face	
(c)	HDB sample; metal face	
(d)	" " polymer face	344
Figure 11.3(a)	Schematic illustration of the duplex polymer - zinc coating on steel	345
Figure 11.3 (b)	Good's model illustrating the five possible regions for the locus of failure of interfaces A and B	345
Figure 11.3 (c)	Possible regions for the locus of failure of the duplex polymer - zinc coating on steel applying Good's model	345

# LIST OF TABLES

		<u>PAGE</u>
TABLE 2.1	Comparison of zinc coatings (from data sheet of Zinc Development Association)	40
TABLE 2.2	Suitable pretreatment processes for cold rolled steel zinc and zinc alloy coatings	45
TABLE 2.3	Classification of chromate conversion coatings	50
TABLE 2.4	Composition (%) of a number of chromate conversion coatings on zinc	51
TABLE 3.1	Laboratory prepared conversion coating solutions	141
TABLE 4.1	Thickness of zinc and polymer coatings at and around a crater (figure 4.12)	154
TABLE 4.2	Incidence of defects on different powder coated substrates	156
TABLE5.1	The surface roughness of as-received and cleaned samples	179
TABLE5.2	Elements detected on surface of samples	179
TABLE5.3	Effect of AC51 on weight change of samples	179
TABLE5.4	SEM/EDXA analysis of cross-section of samples	180
TABLE 5.5	Micro-hardness and thickness of steel substrate and zinc coatings	180
TABLE6.1	Elements detected by EDXA of conversion coating films formed in L1 solution	207
TABLE 6.2	Elements detected by XPS of conversion coating formed in L1 solution	208
TABLE 6.3	Elements detected by EDXA of samples treated in Alocrom 100	208
TABLE6.4	Elements detected by EDXA of conversion coating film formed in Chrometan solution on electroplated samples	209

TABLE 6.5	Weight change and weight of zinc dissolved of HDC treated in NaOH (L17)	209
TABLE 7.1	Laboratory prepared conversion coating solutions (repeat of of TABLE 3.1)	253
TABLE7.2	Dissolution rate ( $i_{corr}$ ) of zeta and zinc in solutions L1, L2 and L3 at a constant potential of 0.0 V during potentiodynamic anodic polarisation from -1.5 V to +1.5 V	254
TABLE 7.3	Range of passive potential ( $E_p$ ) and passive log current density <sup>p</sup> ( $i_p$ ) of zeta and zinc in different conversion coating solutions	254
TABLE7.4	The initial and final log current density ( $\text{mA}/\text{cm}^2$ ) of zeta and zinc in various solutions during potentiostatic anodic polarisation at a constant potential of +1.5 V	255
TABLE 8.1	Final powder coverage	277
TABLE 8.2	Flow temperature ranges	
TABLE9.1	Classification of cross-cut/peel test results	303
TABLE 9.2	Cross-cut tests	304
TABLE9.3	Classification of the nature of failure of pull-off adhesion test	304
TABLE 9.4	Pull-off adhesion test results	305
TABLE9.5	Indentation debonding test results before corrosion test	306
TABLE 9.6	Indentation debonding test after corrosion test	307
TABLE 9.7	Effect of organic powder coating film thickness on peeling strain	307
TABLE10.1	Results of electrochemical corrosion rate tests on conversion conversion coated samples	325
TABLE10.2	Results of acetic 5% salt spray test on conversion coated samples	325

TABLE10.3	Rest potential of powder coated samples immersed in 5% NaCl (acetic) solution	326
TABLE11.1	Surface analysis of the interfaces of samples from corrosion induced disbondment experiments	342
TABLE 11.2	Surface analysis of the interfaces of samples from mechanical induced disbondment experiments	342

## 1. INTRODUCTION AND OBJECTIVES

### 1.1 INTRODUCTION

Demand from a wide range of industries for high performance coatings on metals has led to an intensified scientific and practical interest in the behaviour of organic films on metallic substrates. This is particularly so from the point of view of corrosion control<sup>(1,2,3)</sup>. In the case of steel an alternative system of protection is the application of zinc coatings. However, further protection by application of organic films (solution paints and powder coatings) on the zinc coated steel is essential when (a) it is used in an aggressive environment, (b) an extra long life is required, and (c) the surface appearance needs to be modified. This 'duplex' system is considered to have a corrosion resistance higher than the sum of the individual systems.

The main methods of applying a zinc coating to the steel surface are: batch hot-dip galvanizing after fabrication, continuously coating strip (e.g. Galvatites), electroplating (e.g. Zintec), Sherardizing, spraying with zinc powder, and painting with zinc containing paints. The surface composition and properties of the zinc coating depends on the method of coating treatment used. The size, orientation and possible cracking of the spanple in galvanized coatings will determine surface roughness and adsorption of impurities<sup>(4)</sup>. Any additions to the zinc, such as Sn, Al or Pb may not be evenly distri-

buted at the surface<sup>(5)</sup>. The composition and morphology of the oxide at the surface will depend on whether the surface is 'fresh' or 'weathered'.

Prior to the application of an organic film the zinc surfaces are subjected to cleaning, inorganic chemical reactions, drying and degassing operations. The inorganic chemical reactions produce a conversion coating which replaces the 'normal' oxide and presents to the organic film, a substrate with different properties. These changes in properties include a roughening of the substrate surface and the formation of a less conductive interfacial region, which may also act as a poorer catalyst to the oxygen reduction reactions, and give improved organic film/zinc substrate adherence and maximum resistance to deterioration under service conditions. The more common conversion coatings include chromates, phosphates, and alkaline oxide. Despite widespread use of these, relatively little is known about the formation and composition of conversion coatings. With recent developments in X-ray photoelectron spectroscopy (XPS) and Auger Electron Spectroscopy (AES) some advances have been made<sup>(5)</sup> but many questions remain unanswered. Furthermore new environmental regulations particularly those controlling the concentration of chromates in effluents have resulted in the introduction of new formulations<sup>(6)</sup>.

Powder organic coatings are one of the more important recent developments which have taken place in the surface coating field. Methods of application include fluid-

dised bed, electrostatic fluidised bed and electrostatic spraying. Commercially, electrostatic thermosetting powder coatings technology is expanding rapidly. It represents an important potential for keeping a clean environment by efficient use of the coating material, very low or nil volatilization during curing cycles, and a healthy work climate for the coater. Organic films of the polyester type applied by powder coating, are often used since they offer particularly good weathering properties.

The application and curing conditions of the organic film may well depend on the chemical nature of the substrate surface and therefore will require careful control. Zinc oxide was once used as a white pigment in various paints and it is known that it can react with many organic surface coating formulations<sup>(7)</sup>. For instance, cross-linking of low MW polyesters by zinc oxide may cause changes in the rheology of the formulations. Also, saponification of oil-based paints and the formation of soluble zinc salts can result in moisture-induced blistering of the polymer film. It is quite possible that the various conversion coatings may also affect the polymer properties but their exact behaviour is not known.

To avoid defects such as cratering, pinholing, delamination, and to promote long term adhesion of the organic film to substrate, each of the above operations require critical control. Due to the variability of substrate surface composition and morphology, and pre-coating ope-

ration variables, this is not always achieved and defects do occur. This problem is highlighted by the difficulty which has been experienced in formulating a BSI specification BS6497<sup>(8)</sup> and which has largely been based on customer experience and practice. In the view of many manufacturers and users this standard is unsatisfactory.

Apart from the degradation of the organic film itself, of which much work has been published, performance of the duplex system will depend on the continuity of the organic film and the ability of the interfacial bond between polymer and zinc to resist failure induced, during the coating process, by corrosion or by mechanical loading.

## 1.2 OBJECTIVES

This project was initiated to conduct a systematic investigation in order to:

- (a) Establish the nature of defects such as pinholing and cratering and other defects if any, by carrying out a systematic analysis of these defects using metallographic and scanning electron microscopy (SEM)/energy dispersive x-ray analysis (EDXA) techniques.
- (b) Ascertain the chemical nature and properties of the interfacial bond between polyester films and zinc coated substrates to determine the critical process variables which affect long term adhesion.
- (c) Make clear the type of defect likely to be associated with different types of zinc coating substrates.

The investigation proceeded in the following way:

(i) A thorough investigation was made of the nature and causes of defects in polyester powder coatings on zinc coated steels, produced both commercially and in the laboratory.

(ii) Samples representing the wide variety of zinc coated steel available, with respect to surface structure and composition, were characterised using metallographic, SEM/EDXA and XPS/AES techniques.

(iii) Pretreatments of the chromate, chromate-phosphate, non-chromate and alkali-oxide type were applied to the various zinc substrates. The mechanisms of film formation and nature, composition and surface chemistry of the conversion coatings produced was investigated using SEM-/EDXA and XPS/AES techniques. The effect of degassing on the films formed was also studied.

(iv) A study of the mechanisms of film formation and passivity of the various zinc coated steel surfaces, in both laboratory and commercial pre-treatment solutions, using micro-processor controlled electro-chemical techniques was carried out.

(v) The flow characteristics of the polyester powder on the different zinc coating surfaces, both before and after the application of the above mentioned pre-treatments, were investigated using hot-stage microscopy and image analysis techniques.

(vi) The adhesion of the polyester powder film on the the various zinc coatings, before and after corrosion tests, was measured using cross-cut/peel test, pull-off

test and indentation debonding techniques.

(vii) The locus and mechanisms of failure after accelerated corrosion tests and mechanical debonding was studied using SEM/EDXA and XPS/AES techniques.

## 2. LITERATURE SURVEY

### 2.1 STEEL PROTECTION

#### 2.1.1 INTRODUCTION

Mild Steel, because of its excellent properties, is one of the main materials used in civil engineering structures and in the manufacture of many industrial and domestic goods. Unfortunately, it has a major disadvantage, in that in moist atmospheres it rusts readily. The Zinc Development Association reported in 1983<sup>(9)</sup> that corrosion destroys one-fifth of the world production of steel, worth £50000m annually. It is therefore not surprising that great efforts are made to protect steel from corrosion.

Most methods of protection involve putting a layer of some corrosion-resistant material between steel and the environment. Zinc is commonly applied and more than 2m tonnes are used annually for this purpose<sup>(9)</sup>.

There are two main reasons why zinc coatings are used to protect steel against corrosion. The first arises from the fact that zinc is more electronegative than iron<sup>(10,11,12)</sup>, and when the two metals are in contact in an electrolyte, zinc tends to dissolve, leaving the steel unattacked. This sacrificial protection of steel by zinc coatings can extend, to some extent, over adjacent areas, if the zinc coating has been removed locally to expose the underlying steel. Thus, around cracks or other dis-

continuities in the coating, the zinc corrodes preferentially and the steel is protected. However, this advantageous electro-chemical relationship between zinc and steel is reversed at about 60°C and localised pitting corrosion can be a serious problem with hot waters of certain composition or characteristics.

The second reason for using zinc to protect steel is that, in most atmospheric conditions, the rate of attack on zinc is only 3 - 10 per cent that of steel, and this is due mainly to the grey impermeable films which form over the surface of Zn exposed to air and resist further attack. In industrial atmospheres containing sulphur dioxide the film is less stable because it consists largely of basic zinc carbonate which reacts with the sulphurous acid present. Hence, a coating of metallic zinc on steelwork forms a durable barrier affording considerable protection under normal conditions. Another complementary reason for using zinc to protect steel is the economy of application of zinc coatings such as hot-dip galvanizing as compared to other forms of protection.

Zinc is a bluish-white metal with a silver lustre on freshly exposed surfaces. This lustrous appearance is seen in the spangle on some newly galvanized surfaces, and where they are present they consist of actual crystals of metallic zinc. Zinc is hard, crystalline, brittle, has a density of 7.14 (g/cm<sup>3</sup>), melting point of about 420°C, boiling point of 907°C and coefficient of thermal expansion of  $31 \times 10^{-6} / \text{K}$  (13).

## 2.1.2 METHODS OF COATING STEEL WITH ZINC

There are five main methods of applying a zinc coating to steel:

- (i) Hot-dip galvanizing
- (ii) Zinc spraying
- (iii) Zinc plating (electrogalvanizing)
- (iv) Sherardizing
- (v) Zinc dust paints

A comparison of the above methods as given by the "Zinc Development Association" is shown in table 2.1.

### (i) HOT-DIP GALVANIZING

Hot-dip galvanizing was first reported in 1741, by the French chemist Melouin. It is the oldest and most important zinc coating process and over 2,000,000 tonnes of zinc are used in this method, to coat about 30,000,000 tonnes of steel, each year<sup>(14)</sup>. Nearly one-half of the steel in the form of sheet, a quarter is fabricated work and the remainder is tube and wire. Hot-dip galvanizing has widespread use throughout every continent. The reasons for its popularity are as follows:

- (a) The process is not complicated and therefore can be controlled accurately.
- (b) Due to immersion in molten zinc the entire surface of the object is covered uniformly, including parts of difficult access, which is not always so with many other methods of protection

(c) Due to reason of alloy formation a compact layer system is obtained which is firmly bonded to the steel and which consists of almost a pure zinc layer on top of several iron-zinc alloy layers.

(d) After removal of the zinc patina (consisting chiefly of zinc carbonate which forms on top of pure zinc) and the pure zinc layer in the course of time, the alloy layers provide further protection. In industrial atmospheres these layers are even more corrosion resistant than a pure zinc layer.

Some major applications of hot-dip galvanized coatings include:

(a) Structural steel for power generating plants, petrochemical facilities, heat exchangers, cooling coils and electrical transmission towers and poles.

(b) Bridge structural members, culverts, steel pipe, and arches.

(c) Reinforcing steel for cooling towers and concrete.

There are two types of hot-dipping process:

(a) batch hot-dip, (b) continuous hot-dip

(a) Batch hot-dip

Batch hot-dip galvanizing can be divided in to two categories- (a) wet galvanizing and (b) dry galvanizing. In wet galvanizing, a blanket of flux is built up on the surface of the zinc bath to act as a wetting and cleaning agent to the work as it passes through to the molten zinc. In dry galvanizing, the work is dipped in a flux

bath, usually zinc ammonium chloride, and dried in an oven. This forms a thin film over the work, protecting it from surface oxidation and acts as a wetting agent as the work enters the molten zinc. A wide variety of fabricated parts or articles and cut lengths of sheets are dipped in batches mounted on suitable jigs, if small, or singly if large. A considerable degree of mechanization is employed and manual handling is reduced to a minimum. Intermediate times (minutes) are used in the case of batch processes for fabricated articles.

#### (b) Continuous hot-dip

In the continuous hot-dip process, wire, strip or sheet is coated continuously, often at high speeds. In general, an article to be galvanized is cleaned, and heat treated in a reducing atmosphere to remove surface oxide. It is then immersed in a bath of molten zinc for a time sufficient for it to wet and alloy with the zinc. Short immersion times (seconds) are used in continuous processes.

The coating formed is chemically bonded to the article and it consists of Fe - Zn alloy layers followed by a layer of almost pure zinc. Typical galvanized coatings are shown in figure 2.1<sup>(15)</sup>.

The composition of the galvanizing bath depends on the purity of the zinc and other deliberate additions. For example, tin is added to the galvanizing bath to make it

possible to operate the bath at lower temperatures, to achieve better spangle appearance on the product, and to obtain thinner and more adherent coatings. The addition of aluminium suppresses the formation of the brittle zinc-iron alloy and improves the coating surface brightness. However, the Fe-Zn interaction in the presence of Al can be inconsistent and unpredictable owing to the breaking away of layers which can lead to irregular and unsightly coatings.

In practice about 0.1-0.3 wt% Al is added to the bath and a galvanizing temperature of about 450°C is used, although an interest has been shown, in a number of investigations, in an increased Al content and higher bath temperatures<sup>(16,17)</sup>.

Lead is often added to the bath to reduce drossing and researchers have now established that the lead is present as scattered globules predominantly at the surface of the solidified zinc<sup>(18,19)</sup>.

The usual temperature of galvanizing is 450-460°C. The zinc rich end of the zinc-iron equilibrium phase diagram, figure 2.2, shows the phases which can form at various temperatures and concentrations under equilibrium conditions. When steel is immersed in the galvanizing bath, zinc atoms begin to diffuse immediately into the iron lattice, and iron atoms move outwards. Some authors<sup>(11)</sup> claimed that the mobility of zinc atoms is greater than that of iron due to the lower melting point of zinc.

Others support the idea that the progress of the reaction is governed by the diffusion of iron<sup>(20,21)</sup>. It has also been proposed that both metals migrate at a rate which is more or less equal<sup>(22,23)</sup>. However, the interaction of iron and zinc atoms leads to the formation of a series of alloy layers as indicated diagrammatically in figure 2.3. There are three main phases of interest: (a) gamma (69 - 89 at.% zinc), (b) delta (87 - 93 at.% zinc) and (c) zeta (94 at.% zinc).

The composition of the steel to be galvanized affects considerably both the weight of coating applied and its structure. Steel containing 0.05 to 0.15 per cent silicon or a combination of high phosphorous and high carbon will increase the zinc-iron alloy growth producing a heavy, almost complete alloy coating with a dull grey finish often known as "grey galvanizing". Reactions at higher temperatures are now of major interest to galvanizers. For example, developments in the galvanizing of Si-containing steels involve the use of temperatures of about 530°C.

It can be seen that by relating observations made during galvanizing to the equilibrium phase diagram, a direct correlation is not always found. For example, the gamma phase is often missing or not detected. The stability of zeta phase seems to vary depending on the exact conditions of treatment. The delta<sub>(1)</sub> consists of delta<sub>(1k)</sub>, delta<sub>(1p)</sub>, and various forms of disintegrated delta<sub>(1)</sub> - phase. It is claimed that the delta-phase is never found

as a layer even with fast quenching and, if it does form, it transforms to  $\delta_{(1)}$  on cooling.

## (ii) ZINC SPRAYING

A sprayed coating is obtained by melting zinc powder or zinc wire in a flame or electric arc and projecting the molten droplets, by air or gas, on to the grit blasted surface to be coated. Although first described in 1909, its use for the protection of large structures has expanded very rapidly only in recent years.

Each year about one million tonnes of steel are protected by about 30,000 tonnes<sup>(24)</sup> of sprayed non-ferrous metals, mostly zinc. For example, in the United Kingdom around 3,000 tonnes of zinc<sup>(24)</sup> are used each year for this purpose. Zinc spraying usually comprises of two stages: (a) surface preparation, which consists essentially of grit-blasting, preceded when the steel is very greasy, by a cleaning process; (b) spraying. In this process there is no alloying between zinc and steel and so the mechanical bond must be strong enough to maintain good adhesion and electrical contact.

Coatings produced by zinc spraying are rough and porous, but when compared with other methods of applying zinc to steel, are equally effective for most purposes (see table 2.1 for comparison with other methods).

### (iii) ZINC PLATING

Zinc is electroplated on to steel to give a fine, smooth finish. It is used to protect objects where rough or uneven finishes cannot be tolerated (e.g. instrument parts) and for articles that cannot withstand the pretreatment or temperature in the other coating processes. The Zinc coating is also sufficiently ductile to enable the process to be adapted for the continuous plating of strip and wire where severe subsequent deformation may be required.

As with other plating processes, there are two common limitations:

- (a) The size of the article to be coated is limited by the size of the plating bath available.
- (b) Its shape is limited by the ability (throwing power) of the particular bath composition to reach recesses and other parts distant from the anode.

Various solutions are available for the electrodeposition of zinc, these differ considerably both in composition and in characteristics, but may be classified generally as being either of the acid or the alkaline type<sup>(25)</sup>.

The choice of solution is influenced by many factors: the nature of the base metal, whether cast iron or steel, its form, whether flat strip or complex pressing; its initial condition, whether it needs extensive or simple cleaning; the type of deposit, the tolerance of the solution to impurities and above all, the problems of

effluent treatment. For steel pressings, it is usual to employ a cyanide zinc solution to give a matt or bright deposit.

#### (iv) SHERARDIZING

This method is the least known of the major zinc coating processes. The articles to be coated are tumbled in a barrel containing zinc dust at a temperature just below its melting point - typically around 380°C but lower in the case of spring steels. The zinc bonds to the steel by a diffusion process which forms a hard layer of zinc/iron compounds.

The article to be sherardized is first cleaned by acid-pickling or grit-blasting and then thoroughly dried. The clean dry work is then placed in the sherardizing barrel with the appropriate amount of zinc dust. Fine sand may be added to aid even distribution of the dust, the barrel is rotated and the temperature raised until the desired coating is produced.

The uniformity of coating over complicated shapes together with its abrasion resistance make this process very useful for nuts and bolts. Even temperature distribution imposes a size limitation on the process. It is generally used for small and fairly intricate components where a dull finish is acceptable.

#### (v) ZINC DUST PAINTS

Zinc dust paints consist of very fine dust suspended in an organic or inorganic medium. In order to get the effect of a true zinc coating from such paints, it is essential that the dry paint film should be in contact with the base metal. To ensure good contact, the steel should be shot or grit blasted before application of zinc dust paints.

Zinc dust paints may be used alone for protection or as a primer followed by a conventional top coat. The bonding of zinc rich paints to steel is essentially a physical and not a chemical process

**TABLE 2.1** Comparison of zinc coatings (from data sheet of Zinc Development Association)



Page removed for copyright restrictions.



Figure 2.1 Typical hot-dip galvanized coatings<sup>(15)</sup>

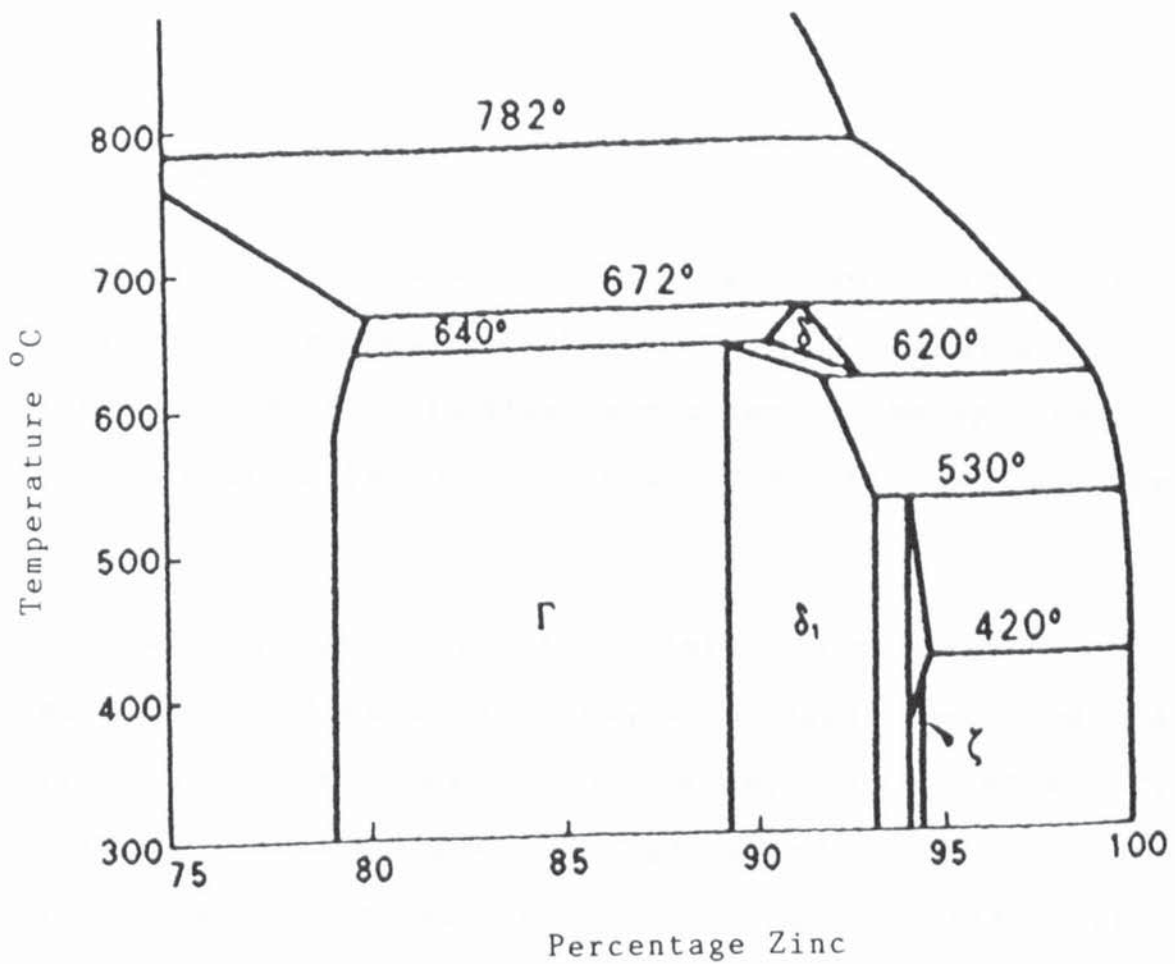


Figure 2.2 The zinc rich end of the zinc-iron equilibrium diagram

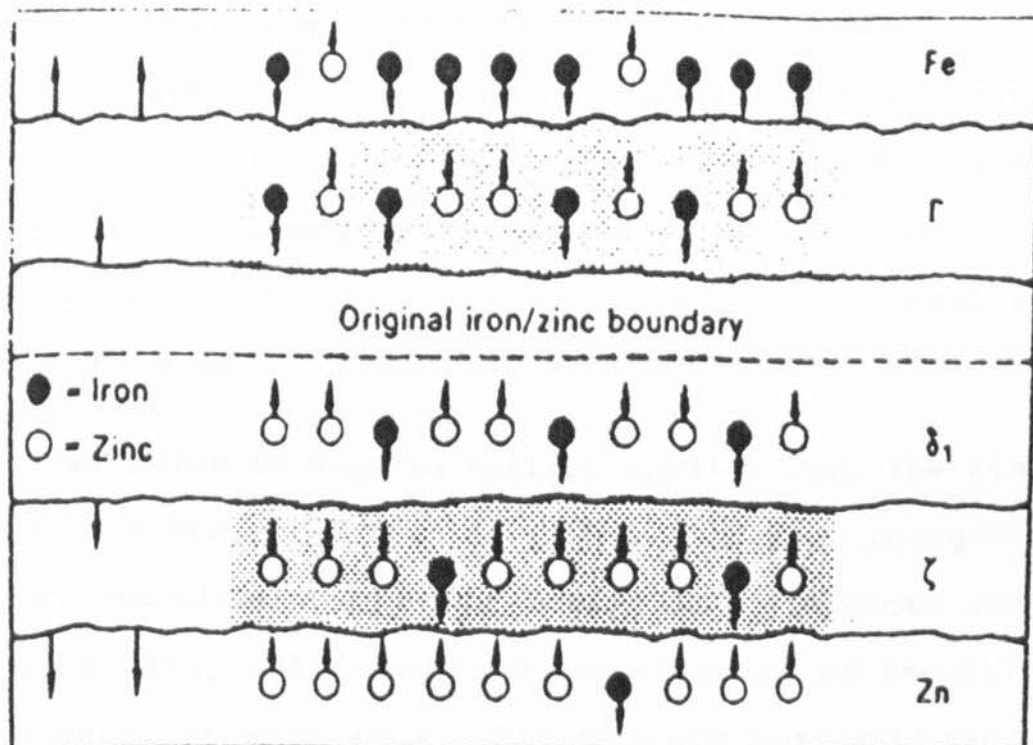


Figure 2.3 Diagrammatic representation of the diffusion of iron and zinc through the alloy layer

## 2.2 ZINC COATING PRETREATMENTS

### 2.2.1 INTRODUCTION

When zinc coated steel is to be exposed in aggressive environments or when extra long life and a pleasing appearance is required, further protection by the application of organic films on the zinc coated steel may be desirable.

Even scrupulously clean and relatively oxide-free zinc surfaces tend to bond poorly to organic coatings. A fresh zinc coated steel surface may consist of a very thin and unstable layer of ZnO providing a poor substrate for organic coatings. Also during the galvanizing process, it is possible that Al, Pb and other impurities present in the zinc coating may be segregated at the surface. This contrasts sharply with some other substrates like aluminium and cold rolled steel sheets which normally contain no segregated Pb or impurities on the surface. Consequently, organic coating systems suitable for the latter two metals rarely adhere well to zinc coated steel.

Therefore, prior to organic coating application, the zinc surfaces are subjected to a series of cleaning, inorganic chemical reactions and drying processes to promote long term durability and to improve the adhesion of the film to the metallic substrate. Pre-organic coating treatments known as conversion coatings are used. These can be either phosphate, chromate or alkaline oxide type. The

term "conversion coating" refers to the fact that surface metal is converted into a non-metallic form in the film-providing reaction. Generally, there are two groups of conversion coatings, those that thicken the naturally occurring oxide film and those that produce phosphate or chromate coatings. Of the latter there are again many types, the one chosen will depend upon the alloy. Coatings vary greatly in both appearance and protective value.

Conversion coating processes for use on zinc coated steel surfaces prior to powder coating, are mainly of the chromate and phosphate types<sup>(26)</sup>. However, other processes such as chromium-phosphate coating (an aluminium pretreatment process which is also used for zinc pretreatment industrially), the non-chromate passivation treatments developed recently by B.N.F. Metals Technology Centre, alkaline oxide and no-rinse are also available. Suitable processes for different zinc coating surfaces are shown in table 2.2 below <sup>(27)</sup>:

Table 2.2 Suitable Pretreatment Processes for Cold Rolled Steel, Zinc and Zinc Alloy Coatings



### 2.2.2 PRE-CONVERSION COATING TREATMENT

It is of prime importance to maintain an absolutely clean surface prior to phosphating or chromating. Typical contaminants that must be removed include white rust, soils that are picked up as the metal travels through the factory and also, grease or oil used as a temporary protective or during metal forming operations.

Cleaning methods suitable for zinc coating surfaces may be conveniently classified under the following headings:

Mechanical - This group includes wet or dry abrasive blasting, rotary wire brushing, etc and is most suited to the removal of corrosion products and to "roughen-up" bright spangled surfaces. As mechanical cleaning removes some zinc, it should only be applied to hot-dip galvanized sheets or parts having coating thickness of over 20 microns.

Solvent Wiping - This is only applicable to components too large for handling in existing plant or for low volume production. If the material is bright spangled, surface roughening will be necessary (mechanical or suitable hand applied acid etch).

Vapour Degreasing - This is Ideal for degreasing complex shapes. If material is bright spangled a further cleaning operation will be required to roughen the surface.

Emulsion Cleaning - This is used in a multi-stage spray

pretreatment plant. There is no zinc dissolved in this process and hence it is more suitable for zinc surfaces that require no further roughening.

**Alkali Cleaning** -This can be either non-etch cleaners suitable for matt zinc material, or controlled etch cleaners for bright spangled zinc. Activated cleaners are recommended prior to zinc phosphating. Alkali cleaning can be carried out by spray or immersion application.

**Acid Cleaning** - Weak acid dips can be used on any material where the surface requires "opening up" prior to conversion coating. Stronger acid baths may be used on thick galvanized surfaces to remove corrosion products or for etching under carefully controlled operating conditions. Due to the corrosive nature of these solutions they are normally used for immersion only.

It has been reported<sup>(26,27)</sup> that the coating topology of the crystalline phosphating processes is strongly influenced by the method of cleaning used. The use of acid cleaners or strong alkali cleaners will cause the formation of coarser, thicker crystalline coatings, which will be less able to withstand deformation and hence paint adhesion will be significantly impaired. Chromate, amorphous phosphate and chromate-phosphate processes are tolerant of precleaning and only require that the surface be receptive to processing.

## 2.2.3 CHROMATE CONVERSION COATING PROCESS

### 2.2.3.1 INTRODUCTION

Chromates are widely used in solution as corrosion inhibitors. Under atmospheric exposure an alternative method is used which consists of depositing, on the metal, a chromate film which acts as a reservoir for soluble chromate. Chromate coatings, which rose to prominence during World War II, can be considered as films generally not more than about 25 $\mu$ m in thickness. They are used on zinc primarily for improving the adhesion of powder organic coatings/paints but their own inhibiting action makes a useful contribution to the total protection. Some chromate films function as a decorative film on such materials as aluminium, copper, brass, magnesium, tin, zinc, cadmium, silver, and the ferrous metals.

Chromate conversion coatings result from simple immersion of metals for a short period, in a chemical solution containing either chromic acid or one of its soluble salts along with a source of hexavalent chromium, accelerators, and surface etchants or activators. Other methods of application include spraying, brushing and, in a few cases, electrodeposition and the resultant coating becomes an integral part of the metal surface. Depending upon the bath composition, immersion time, temperature, and pH, the protective coating will vary in quality and appearance.

#### 2.2.3.2 DEVELOPMENT OF THE CHROMATING PROCESS

After their discovery by Wilhelm<sup>(28)</sup>, Anderson<sup>(29)</sup> made a comprehensive study of the formation of chromate conversion coatings on zinc. He developed the Wilhelm Cronak solution which consisted of 200g  $\text{Na}_2\text{Cr}_2\text{O}_7 \cdot 2\text{H}_2\text{O}$  + 6.9 ml  $\text{H}_2\text{SO}_4$  (s.g. 1.84) in a litre of  $\text{H}_2\text{O}$  and operated at room temperature with immersion times of 5-15s. These chromate conversion coatings were an iridescent yellow colour. Other chromating solutions were developed later but these continued to rely on an acidic dichromate solution with added anions<sup>(30)</sup> such as sulphate, chloride, formate, phosphate and fluoride. These anions have been claimed to have effect on the rate of formation of films on zinc<sup>(31)</sup>. The Cronak process was equivalent in corrosion prevention to other proprietary solutions tested<sup>(32,33)</sup>.

Some standards, such as the Australian Standard 1971-1976, have separated chromate conversion coatings on zinc into four categories, as shown in Table 2.3. Type A, C and D coatings are formed by one immersion process, whilst type B involves a second immersion in an alkaline solution. Although this alkaline solution usually contains a bleaching agent, it is not essential and the term "bleached" can be a misnomer when used to describe category B coatings.

Table 2.3 Classification of chromate conversion coatings.

Coating type	Typical appearance	Typical coating weight (g/m <sup>2</sup> )	Typical Cr(VI) content (mg/m <sup>2</sup> )
A-Clear	Transparent, clear sometimes with a bluish tinge	0 - 0.5	5
B-Bleached	Transparent with slight iridescence	0 - 1.0	5 - 10
C-Iridescent	Yellow iridescent	1.0 - 1.5	50 - 100
D-Opaque	Olive green shading or bronze	>1.5	100-200

#### 2.2.3.3 THE MECHANISM OF FORMATION OF CHROMATE CONVERSION COATINGS

Since the early work of Anderson<sup>(29)</sup> and Clarke and Andrew<sup>(34)</sup> there have been few publications on the rate of formation of films<sup>(35)</sup> or on the effect of added anions on the chromating reaction<sup>(31,36)</sup>. Chemical analyses of the films formed on zinc (Table 2.4)<sup>(37)</sup> are consistent with the following reactions:



The reduced  $\text{Cr}^{3+}$  is precipitated on the surface of the zinc probably as a hydrated oxide<sup>(33)</sup>. Zinc is only found in the film in trace quantities and normally accumulates in the chromating solution. It is claimed that these reactions, are dependent on anions which do not appear in the above equations. For example, in pure  $\text{CrO}_3$

solutions, it is reported<sup>(37)</sup> that zinc does not dissolve to any appreciable extent. On the addition of sulphate, zinc dissolves and a visible coating is formed on the zinc surface.

Table 2.4 Composition (%) of a number of chromate conversion coatings on zinc.

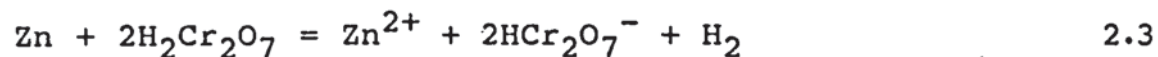
Composition	Process	
	Cronak	CrO <sub>3</sub> , NaCl
Chromium (VI)	8.7	5
Chromium (III)	28	24
Sulphate	3.3	
Chloride		>1
Zinc	2.1	
Water	19	
Reference	23	31

The loss of zinc and the weight of film deposited as a function of immersion period and of variation of sulphuric acid content above and below the normal 6ml/l, is shown in figure 2.4<sup>(38)</sup>. The solution is made up of 182g/l of NaCr<sub>2</sub>O<sub>7</sub> .2H<sub>2</sub>O + H<sub>2</sub>SO<sub>4</sub> as indicated; temp 18°C.

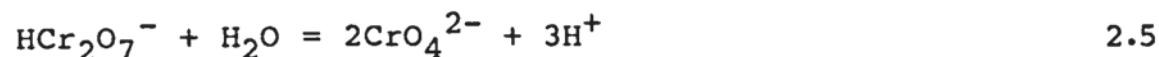
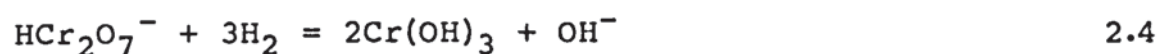
The curves show that in a normal bath the weight of film deposited is equal to the weight of metal dissolved and that as the H<sup>+</sup> ions are consumed, so more metal is converted to film in the solution. The curves also show that the dissolution of zinc during film formation is small, which is an important consideration when parts with thin Zn coatings are being treated.

Film formation is considered by some authorities<sup>(28,32,39)</sup> to be via a dissolution - precipitation mechanism as follows:

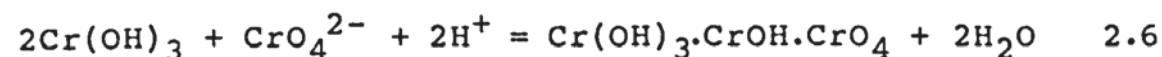
(1) Zinc is dissolved by dichromic acid, thus raising the pH in the neighbourhood of the surface:



(2) The rise in pH allows some precipitation of hydroxide and the chromate ion becomes more stable:



(3) A basic chromium film forms on the metal surface



As can be seen from the above equations, the end result of the reactions is the formation of basic chromium chromate, as suggested by Anderson<sup>(29)</sup> and supported by many others<sup>(27,30,39,40,41,42,)</sup>. Some authors<sup>(31)</sup> support the proposal by McLaren et al<sup>(41)</sup>, that chromate conversion coatings are hydrated chromium(III) oxide films with absorbed anions such as chromate and sulphate.

On the other hand, electron diffraction studies<sup>(26,43,44)</sup> have shown that the chromate conversion coating contained zinc chromate and zinc oxide as the main constituents, suggesting the formation of a basic zinc chromate.

The chromium (III) hydroxide should precipitate if the pH in the vicinity of the zinc surface is approximately 2. Although the pH of most chromating solutions is lower than this value, the hydrogen ion is consumed by the

first reaction above and the pH change at the surface permits the precipitation of  $\text{Cr}(\text{OH})_3$ .

The surface pH value is reported to have been measured for a 0.07 mol/l  $\text{Cr}(\text{VI})$  solution containing added sulphuric acid<sup>(45)</sup>. At low  $\text{H}_2\text{SO}_4$  concentrations, a pH of 1.75 was measured immediately on immersion and this was maintained for some minutes. At higher  $\text{H}_2\text{SO}_4$  concentrations the pH decreased linearly with time before reaching a constant value. For example, with 0.02 mol/l  $\text{H}_2\text{SO}_4$  it took 1 minute for the pH to stabilize at the zinc surface. This work also showed that the pH was independent whether cast or plated zinc was used. It is unfortunate that  $\text{H}_2\text{SO}_4$  additions were used during these experiments because, the sulphate ion as well as the hydrogen ion directly affects the chromating reaction.

The role of added anions during chromating is intriguing. They are unlikely to affect directly either of the redox reactions and probably act by either complexing with chromium (III) in the film or altering the properties of the precipitated chromium (III) hydroxide by adsorption. It is reported that a maximum was observed in the film weight versus sulphate added curve, and that this does not occur with the chloride ion<sup>(31)</sup>. As the stability constants for chromium (III) complexes of  $\text{Cl}^-$  and  $\text{SO}_4^{2-}$  are similar, a maximum would also be expected for  $\text{Cl}^-$  additions if the complexing reaction was the main reason for the shape of the curves. This suggests that the

sulphate or chloride is incorporated in the film by adsorption similar to the mode of incorporation of chromium (VI). The well-known difference in adsorption properties between  $\text{SO}_4^{2-}$  and  $\text{Cl}^-$  can account for the difference in film weight versus concentration of added anion curves<sup>(31)</sup>. This explanation is further reinforced by the chemical analyses in Table 2.4 which show that a higher proportion of  $\text{SO}_4^{2-}$  than  $\text{Cl}^-$  is retained in the films.

An interesting recent study has been carried out in the USA on the characterisation of chromate coatings on Zn/Al alloy (Gavalume)<sup>(27)</sup>. This study showed that alkaline cleaning of Gavalume produced a zinc-covered hydrous aluminium oxide layer. Reaction of this layer with acid chromate results in preferential deposition of a protective chromium coating in the zinc-rich area, apparently leaving the aluminium surface sites unprotected. But treatment with a hexavalent/trivalent chromium preparation preferentially deposits chromium on aluminium rich areas.

#### 2.2.3.4 FILM CHARACTERISTICS

Chromate conversion coating is amorphous. Directly after formation of the film, care must be taken since the coating is quite soft; however, after rinsing and drying, the film becomes relatively tough and flexible. In the event that the film loses its water of hydration through a drying treatment at a temperature of 66° C or higher,

the hardness of the film increases. It is reported that although both resistance to abrasion and corrosion resistance to weak acids and alkalies improve after dehydration the protective value of the film to water immersion or salt spray is reduced<sup>(46)</sup>. This reduction in protective value is frequently attributed to the conversion of soluble chromates to insoluble compounds. Some authors<sup>(26)</sup> claimed that the dehydration of the amorphous coating structure and the formation of cracks also contributed to the reduction in protective value. The above effect varies with the material coated, the time and temperature of drying, the amount of water vapour in the air (if saturated no deterioration occurs)<sup>(26)</sup>, the formulation and operating parameters of the particular chromate process.

It is claimed that a particular yellow chromating process operated<sup>(26)</sup> under specific conditions is capable of withstanding drying temperature of 20 minutes at up to 250°C prior to powder coating without total loss of performance. This pretreating operation is essential to "degas" hot-dip galvanized steel sections prior to powder coating. Failure to degas results in an unacceptable incidence of pinholing in the cured powder coating<sup>(47)</sup>. Film coating weights of chromate pre-treatments vary widely depending on the particular proprietary composition being employed. Coating weights of 54mg/m<sup>2</sup> to 162mg/m<sup>2</sup> are recommended. The chromate film weight is not a critical determinant of quality because of its

virtual insolubility even at the lowest film weight. The concentration of hexavalent chromium in the film is the criterion used to establish the presence of the treatment at prescribed levels.

It was stated earlier that during the conversion coating process, oxidation-reduction occurs, resulting in the formation of a film containing both trivalent and hexavalent chromium complexes plus water of hydration. The hexavalent chromium complex, which is frequently termed the "soluble" portion of the film, is believed to provide resistance to water corrosion. In addition, by virtue of a leaching action of hexavalent chromium, the well known self-healing mechanism is realized<sup>(46)</sup>. Scratches and abraded areas on the surface will heal and thus, retain corrosion resistance. The trivalent chromium complex, which is recognized as the "insoluble" portion of the film, is believed to increase coating hardness. It is believed too that the trivalent chromium complex contributes subsequently to corrosion resistance. Thus Pocock<sup>(48)</sup> has cited the high corrosion resistance of clear bright films on both cadmium and zinc which contain very little hexavalent chromium. It was noted that during the salt spraying of films that contain considerable amounts of hexavalent chromium, the complete leaching of this compound is evident by loss of colour<sup>(48)</sup> and occurs long before corrosion breakdown occurs.

The colours that are obtained with a chromate conversion cycle have also been linked to the coating composition.

A typical yellow film formed on zinc by the dichromate-sulphuric acid treatment was found<sup>(29)</sup> to contain largely trivalent and hexavalent chromium compounds. The chromium in this particular coating is thought to be<sup>(49)</sup> in the form of either a basic chromium chromate or chromic hydroxide and soluble chromates. Brown and black coatings may contain basic chromium chromates of varying composition<sup>(50)</sup>, whereas, olive drab coatings on zinc very likely owe their colour to trivalent chromium compounds. The colourless films resulting from a leaching process are relatively insoluble and are thought to contain chromium hydroxide or oxide along with water of hydration<sup>(50)</sup>.

The corrosion resistance of the chromate film is mainly dependent upon the environment to which the coating is exposed. Under a specific set of conditions, other factors that would influence corrosion resistance would include the basis metal that is coated, the bath type chosen and variables of bath operation, such as immersion time, temperature, pH and, in the case of electrodeposited coatings, the thickness of the plated metal. In general, corrosion resistance will increase with film thickness, but this factor has been disclaimed as the sole determinant since those factors given above as well as both pre and post-treatments have a definite influence. Galvanic corrosion is effectively retarded by a chromate film, and maximum protection is obtained where a chromate film can be applied to both metals that would

have provided the galvanic couple.

On the debit side, chromate conversion coatings have a low resistance to abrasion. A properly dried coating will withstand the abrasion related to press room drawing and stamping operations, but they are readily removed by severe rubbing or brush abrasion. As mentioned previously, a freshly formed film is quite soft and easily damaged.

#### 2.2.3.5 ORGANIC COATING BONDING PROPERTIES OF CHROMATE FILMS

In considering chromate conversion coatings as basis for organic finishing, the two factors of importance are:

- (a) improvement of initial adhesion of the organic coating to the metal, and
- (b) increased life of the organic coating.

Chromate coatings are believed to provide bonding through molecular adhesion. The chromate film is bonded to the surface by molecular attraction and, in turn, holds the organic film by the same mechanism.

The chromate films have advantages over paint bonding coatings which do not in themselves have a corrosion inhibiting effect. The chromate film forms an effective barrier against either corrosive attack through pores or scratches in the organic coating or a reaction between the metal and the organic coating itself. It is also reported that the films are thin and non-porous, which

results in little or no absorption of paint or other applied organic material. This will provide a more economical use of the organic coating as compared with certain crystalline type paint base coatings.



Aston University

Illustration removed for copyright restrictions

**Figure 2.4** Effect of sulphuric acid concentration on chromate passivation of zinc<sup>(40)</sup>



Aston University

Illustration removed for copyright restrictions

**Figure 2.5** Bell curve<sup>(51)</sup> illustrating conversion coating film formation in relation to solution pH

#### 2.2.3.6 CHROMATE BATHS

Although the mechanism affecting the formation of chromate coatings of good thickness and colour is not well understood, the basis for developing treatment formulations may be illustrated in principle by a "bell curve" given in Fig 2.5<sup>(46)</sup>. Certain concentrations of chemical dip constituents attack a metal and corrode it, whereas, others completely prevent the corrosion of the same metal.

Over a range between the attacking and inhibiting concentrations, a chromate conversion coating is formed, varying in thickness and quality from poor to optimum to poor. The position of the optimum "peak" changes from one type formulation to another, and from one metal to another. Occasionally, dissimilar metals can be treated successfully in the same bath under similar conditions of temperature, pH, etc, but, in most cases, composition and process modifications are necessary.

The type of coating that will be obtained or whether a coating will be obtained at all, at a given temperature and immersion time depend on the hexavalent chromium concentration, type and concentration of activator, pH and the chemical balance of the solution. As the solution is depleted through use, it is replenished by maintenance additions as indicated by control tests. Usually the most critical factor is control of pH. A very

effective control method uses pH and hexavalent chromium determination.

Normally chromate baths cannot be maintained indefinitely but must be dumped periodically and made up fresh. The inoperative point is reached when coatings are no longer obtained even though control tests show the solution to be in correct chemical balance, or when excessive additions are required to keep the bath in operation. This inoperative condition is apparently due to the build up of contaminants such as trivalent chromium from the film forming reaction, dissolved metal from the work being treated, and miscellaneous contaminants dragged into the solution. Expected life of the bath varies with the treatment and depends also on the thoroughness of the cleaning, rinsing, and dragout.

#### 2.2.4 NO-RINSE PROCESSES

These do not fall into one chemical type although those in widespread commercial use are mainly chromate based. Apart from the plant advantages mentioned earlier, the process is claimed to have the additional advantage of being applicable to all substrates, although it may not necessarily match the best conventional treatments on specific substrates. Some no-rinse treatments include organic resinous materials which can improve performance but can give rise to chemical stability problems and compatibility problems with subsequent finishes.

No-rinse processes free from chromate have also been introduced recently but production experience is limited.

#### 2.2.5 PHOSPHATE CONVERSION COATINGS

The term "phosphate conversion coating" refers to an adherent surface layer that consists in general, of insoluble metallic phosphates produced on metal surfaces by the action of suitably balanced and controlled baths<sup>(51)</sup>. Phosphating processes have been given a great number of names in the patent and proprietary literature; Coslettizing, Parkerizing, Bonderizing - all refer to phosphate treatments.

The contribution of the phosphate coating in promoting organic coating adhesion is ascribed by Lorin<sup>(52)</sup> to the following factors:

- (a) an increase in the surface area of the substrate leading to an increased possibility of bond formation,
- (b) absorption of paint (or organic powder melts) at microfissures in the coating before polymerisation, giving better inter-penetration of the two coatings,
- (c) chemical reactions between unsaturated resins and phosphate crystals.

The quality and type of phosphate coating is interdependent on a number of factors including the metal concentration, the accelerator type, and the pH of the solution. The present-day formulations, the details of which are very seldom found in the literature, seem to be

on the basis of the accelerator type employed; the more common accelerators being nitrates, nitrites, peroxides, and chlorates. They are used alone, in combination with each other, or with metallic as well as other organic and inorganic accelerators. A survey of the chlorate accelerated bath has been given by Heinzelmann<sup>(53)</sup>, who indicated that this bath type permits the growth of fine crystalline deposits with consequent low porosity of coating. The nitrate bath generally produces deposits that have a coarse crystalline structure, whereas, the nitrite bath has the ability to produce a fine crystalline deposit, however, there are complications in balancing the solution. In general, all accelerators do not produce the same result nor are the optimum operating conditions the same for every bath. The pH would depend upon the type of heavy metal phosphate used and the soluble phosphate content of the solution with the specific oxidizing agent employed. Since pH control is quite important in preventing undesirable reactions to occur, acids other than phosphoric acid and/or certain buffers may be employed to control this variable. Details are seldom found in the literature although methods of control to obtain optimum performance are incorporated in various proprietary compounds

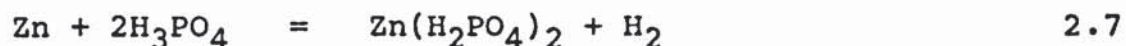
The phosphating process is claimed<sup>(54)</sup> to be dependent upon the fact that divalent zinc forms primary, secondary and tertiary phosphates, the first of which is soluble, the second sparingly soluble and the last insoluble.

The mechanism of film formation is not understood completely due to its complexity but attempts have been made to rationalize the reaction, based on electrochemical theory. Thus, the first step upon the immersion of a material in a phosphate solution is the chemical attack on its surface at anodic areas. At the cathodic areas of this same surface, there is a reaction with the solution which reduces the acidity of the solution immediately surrounding these areas. Since metal phosphate solubility decreases as acidity decreases, the normal reaction is the precipitation of the secondary and tertiary phosphates and, depending upon the conditions of the bath, an adherent film will form over the entire surface to be coated. Due to the solution of zinc from the immersed material, the deposited coating will invariably contain a substantial proportion of the insoluble phosphate of the treated metal. In those baths that contain either ammonium or sodium phosphates, the resultant phosphate coating will be composed entirely of zinc phosphate.

As mentioned previously, acceleration of the bath reaction is necessary to reduce the time period for the phosphate film formation. Thus, there is normally considerable hydrogen gassing, which it is claimed<sup>(51)</sup> serves as a barrier at the cathodic areas and thus prevents rapid deposition of the phosphate coating. The addition of an oxidizer will reduce this objectionable gassing action, eliminate its effect, and permit a more rapid deposition of the phosphate film.

The precipitation of tertiary phosphate on the metal surface can be represented by the following sequence of reactions.

Metal dissolution -



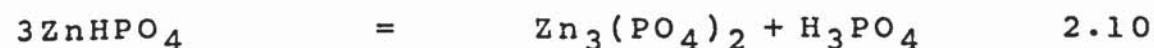
The oxidizing accelerators depolarize this reaction and the formation of soluble primary phosphate may be regarded as partially rate-controlling. At this stage, the pH rises due to loss of  $\text{H}^+$  ions and the secondary phosphate begins to precipitate:



If the rise in pH is sufficient, tertiary phosphate is formed rapidly by hydrolysis:



or



The acid ratio - the relation between free phosphoric acid content and total phosphate content in a processing bath - is claimed<sup>(38)</sup> to be an important factor affecting the process. An excess of free acid will retard the dissociation of the primary and secondary phosphates and hinder the deposition of the tertiary phosphate coatings. Sometimes excessive loss of metal takes place and the coating is loose and powdery. If the free acid is too low it is claimed that it causes dissociation of phosphates in the solution as well as at the metal/solution interface which leads to precipitation of insoluble phosphates as sludge.

Another factor in the initiation of the phosphate coating reaction is the presence in the processing solution of tertiary phosphate, either as a colloidal suspension or as fine particles<sup>(55)</sup>. These tertiary phosphate particles act as nuclei for the growth of many small crystals on the metal surface, thereby promoting the formation of a smoother coating.

There are two main phosphating processes which are used for zinc pretreatment:

(a) Zinc (crystalline) phosphate

Crystalline zinc phosphate processes are widely used on hot-dip galvanized and electrogalvanized but their popularity varies in different parts of the world. They are mostly used in Japan but are less frequently used in the USA and Europe. Pre-activation is necessary to obtain a uniform fine crystal size.

(b) Iron (non crystalline) phosphate

This process produces an iridescent to grey amorphous coating consisting of a mixture of iron phosphates and Zinc oxide. Optimum performance with this type of process is only obtained in conjunction with a suitable chromate after treatment.

#### 2.2.6 ALKALINE OXIDE

In this type of pre-treatment process an alkaline solution, containing cobalt or nickel ions, is employed. The



coating formed consists essentially of zinc oxide containing heavy metal ions such as iron, cobalt or nickel. The mechanism which makes this type of coating effective is not fully understood but it is of interest that Leidheiser and Suzuki<sup>(56)</sup> showed that cobalt and nickel ions are effective corrosion inhibitors for zinc. After post-treatment (rinsing in dilute chromic acid solution) the coatings also contain chromium, which is an important factor in performance

The alkaline nature of this type of process opens up the possibility of combining cleaning with coating by the incorporation of a suitable surfactant system. This permits a contracted processing sequence to be employed:

- (a) Clean/Coat
- (b) Rinse
- (c) Chromium coating rinse

The alkaline oxide type of process is extensively employed for the treatment of hot-dip galvanized and electrogalvanized steels and will also give satisfactory results on zinc/iron and zinc/aluminium alloys. At the present time, it is the treatment most widely used by coil coaters.

Another major advantage of this process is the outstanding adhesion it gives to organic films - especially to the types of epoxy coatings employed in coil-coating production.

The complete complex oxide treatment film when properly

applied will contain (5.4 to 18 mg/m<sup>2</sup>) of cobalt or nickel and (6.5 to 16 mg/m<sup>2</sup>) of chromium. The appearance varies from a very light gold colour to a lustrous brownish gold colour. Although the degree of colour is not used as a measure of treatment quality it serves to verify the presence of the treatment.

The alkaline oxide treatment is comparatively simple to control chemically, has good bath stability and little tendency for sludge formation, and requires relatively little attention from the line operator to provide consistent quality in paint adherence over long periods.

The coatings formed are predominantly amorphous chromium phosphate and vary from a light iridescence to an attractive malt green sometimes referred to as architectural green. It is difficult to achieve constant colour due to a build up of trivalent chromium and other dissolved metals. Longer processing times and increasing additions of flouride are needed to maintain the coating colour and weight until a point is reached where the bath has to be discarded.

#### 2.2.7 CHROMETAN CONVERSION COATING PROCESSES

Chromates are extremely toxic hence their handling in factories and discharge to the atmosphere and water are controlled by stringent legislation. These toxic effects of chromates are being noticed more and more frequently, making even more stringent regulations in future inevitable. These future regulations can be complied with only

by making substitutes for chromates wherever possible.

Non-chromate conversion coating processes have been developed recently at the BNF Laboratories. In these processes, trivalent chromium cations and aluminium cations are induced to precipitate on to the zinc surface as the pH rises<sup>(6)</sup>. Factors affecting the formation of coating film, coating colour and its protective value are solution composition, pH, temperature and time of immersion.

It is reported that several metal cations can be induced to precipitate<sup>(6)</sup> on to zinc surfaces as pH rises but only two appear to offer an alternative to chromates, these being trivalent chromium and aluminium cations.

The authors<sup>(6)</sup> also developed a different solution for use to deposit passivation coatings on hot dip galvanized products. In this case, they claimed that it is advantageous to operate the passivation treatment in the quench tank used to cool the work after galvanizing.

## 2.3 POWDER ORGANIC COATINGS

### 2.3.1 INTRODUCTION

BS 6497 (1984) defines powder organic coatings as products containing pigments, resins and other additives which are applied in the form of powder to a metallic substrate and are then fused to form a coherent continuous film. Powder organic coating is one of the more important recent developments which has taken place in the surface coating field and its characteristics are now well known.

Since its conception in the USA in 1951<sup>(57)</sup> powder coating technology has developed progressively. There have been many conferences, since 1969, dealing with powder coatings and innumerable statistics have been presented to illustrate the growth rate of this new market. Harris<sup>(58)</sup>, when considering the market for powder coatings in the early 70's, claimed that an annual growth rate of 25-30% was reported in many countries and stated that by 1976, the growth rate had gone up to between 50 and 100%. However, in 1980, Gormley<sup>(59)</sup> reported that the use of powder coating only increased from about 3% of the relevant surface coating markets in 1970 to about 4% in 1980 in the USA (a growth of 33% in ten years (annual growth rate of 3.3%)). Also, contrary to the Harris report, only 2.3% annual growth rate was reported in the EEC countries<sup>(60,61)</sup>.

### 2.3.2 ADVANTAGES AND DISADVANTAGES OF POWDER ORGANIC COATINGS

Powder organic coatings have many advantages and some disadvantages<sup>(62,63,64,65,66)</sup> over the conventional wet paint system. The main advantage of powder coatings over wet paints is that they contain no solvent. The first benefit resulting from this is that they reduce the problems of storage in terms of space and the fact that wet paints require safe storage due to the fire risk. If powders are stored in a cool, dry place they have long shelf life. As there are no solvents in powder coatings and the minimum ignition energy of powders used is normally high, the risk of fire is very small. Stringent pollution control legislation is being introduced, for example, in the United States and Japan, while in all countries there is a growing awareness of the need to protect the environment. Powder coating offers the best means to comply with these requirements as no odour or toxic fumes are generated in the powder coating process.

There are no runs, sags, or blisters in the final coating and due to the fact that the powder and air mixture behaves as a liquid<sup>(67)</sup>, powder coating is suited ideally to automation. Labour costs can be reduced as powder coating operations require less skill than wet painting operations.

New developments with polyester, polyurethane and acrylic resins are increasing the scope of powder coatings.

Today, powder coatings can be "tailor made" for a variety of applications. It is no longer necessary to compromise properties or economics to accommodate powder coatings, but rather to expect higher performance at lower overall costs. A powder coating of higher quality can be applied at the same cost as a lower quality solution coating.

There is no overspray sludge or contaminated water to be disposed of with powder as there is with liquid coatings, and a high utilization of powder can be realized by a properly designed recovery system<sup>(68)</sup>.

Air used to exhaust the powder spray booth is recirculated directly to the plant, eliminating heating or cooling costs of the make-up air that occur when air is exhausted from the plant. The cost of heating the curing oven is less, since large volumes of the air are not exhausted from the oven to remove solvent fumes.

Since powder coatings develop full cure during the bake and usually resist abuse better than solution coatings, there is less damage during handling and assembly operations. Also, they do not have to be packed as carefully for shipment. Badly sprayed parts can be blown clean with an air gun prior to baking instead of stripping in solvent.

Powder application equipment requires only about two-thirds as much floor space as solution system for the same volume of work. Powder can be sprayed from both sides at once eliminating one spray booth. Among the

areas eliminated are paint mixing rooms and powder coatings are supplied ready for use and do not require thinning or mixing before application. Cure ovens may be hotter and shorter. Polyester and epoxy powders require no primer, which means a one-coat finish. Modern powder coatings may be applied at thickness equivalent to modern liquid coatings.

A disadvantage of organic powder coatings which has not been overcome properly is the change from one colour to another in production without contamination. Powder paints cannot be tinted like liquid paints so colour must be carefully controlled during manufacture. It is claimed that if any particles of one colour find their way into another powder, they will be seen as speckles in the finished coating. Thus if the colour being coated on a coating line is to be changed, the line must be thoroughly cleaned to avoid contamination of the next coating. This is a very time consuming, and often a difficult task.

### 2.3.3 POWDER ORGANIC COATING FORMULATIONS

There are two main classes of powder coating; the thermoplastic and the thermosetting types. The thermoplastic resins are generally characterised as materials of comparatively high molecular weight which exhibit excellent chemical resistance qualities, toughness and flexibility. Those suitable for use in powder coatings include polyvinyl chloride, polyvinyl butyral, nylons, polyester, acry-

lics and certain high molecular weight epoxies<sup>(58)</sup>.

The thermosetting powder coatings were introduced in the United States during the late 1950's. Thermosetting resins are initially of low molecular weight and a high molecular weight, complex structure, is built up during the curing cycle. As a low molecular weight material they show better flow properties, good surface wetting characteristics and excellent adhesion to substrates. Over 90% of all thermosetting powder coatings are based upon the epoxy, acrylic and polyester resins. Other suitable resins which can be used in thermosetting powders include heat convertible forms of many in the thermoplastic class.

Epoxies were the first thermosetting powder coating resins produced, and still retain a good proportion of the market share. Epoxies exhibit good friability in pigment formulations thus contributing to their ease of manufacture. They store well with good physical and chemical package stability. They have a low melt viscosity which aids good flow-out and levelling prior to curing. The thermosetting reaction is not gradual: once a threshold temperature is reached, curing is rapid and complete. There are no volatiles from crosslinking reactions, thus blistering, pinholing and bubbling are not problems with epoxy resins. They possess good electrostatic charging properties and excellent deposition characteristics.

Epoxies also exhibit excellent protective properties

against chemicals. In addition they have good wetting properties at the melt temperature with excellent adhesion and mechanical properties plus good appearance.

The major drawback of this class of resin is their poor outdoor performance. Yellowing occurs quite rapidly, especially if cured at temperatures slightly above that recommended and erosion of the surface occurs when subjected to exterior weathering with the formation of "chalk". Also, pretreatment and a minimum thickness of about 80 microns are essential for protection against climatic conditions or a corrosive environment.

The polyester resins are polycondensation products of the reaction of polybasic acids with polyhydric alcohols. The polyester backbone can be formulated having free hydroxyl groups, free carboxyl groups, or both. Low molecular weight polyesters (500-2500 MW) with high aromatic content can be formulated readily to give friable solids with a glass transition temperature over 50°C. Polyesters, being polar molecules, are noted for their excellent electrostatic spray properties. One of the carboxyl groups is Triglycidyl Isocyanurate (TGIC) polyester. It is based on a carboxy functional polyester cross-linked by Triglycidyl Isocyanurate.

The main advantages of this formulation include:

Excellent appearance with outstanding gloss and good flow, good mechanical and technological properties, good

resistance to discolouration at elevated temperatures and excellent durability.

Powder organic coatings contain five major components: resin, hardener, pigments, fillers and additives. In order to obtain a satisfactory powder formulation, it is necessary to consider the following :

- (i) The method by which the product will be compounded.
- (ii) Correct choice of pigment to maintain good rheological properties during the important premixing operation.
- (iii) Correct choice of resin/hardener to give the required blend of film properties.
- (iv) The need to ensure the correct colour match and the required level of gloss.
- (v) Good storage stability and freedom from caking etc.

#### 2.3.4 PRODUCTION OF ORGANIC COATING POWDERS

The appearance and performance of finished coatings depend on the success of spraying and curing of the powder coatings. It has been suggested that best results are achieved from powders of uniform particle size with each particle having the same composition<sup>(58)</sup>. Uniform powder particles of the same composition can only be obtained by homogeneous compounding of all the powder ingredients resins, pigments, hardners and additives. Good homogeneity is ensured by first blending the components before the compounding operation.

In practice uniformity is not realisable in view of the wide disparity in the particle sizes of resins and pigments as supplied. Harris<sup>(58)</sup> reported that the problem of particle disparity of powder components can be avoided by predispersing these ingredients in the base resin by master-batch techniques; the ingredients are melt mixed at known concentrations into a portion of the base resin, cooled to solidify, granulated and then added in the calculated amounts to the premix stage of the powder manufacturing process.

There are three main methods of producing powders

(i) dry processing, (ii) wet processing and (iii) melt processing. Melt processing is mostly favoured by industry as it is both economic and reliable.

#### (i) Dry processing

This is the simplest and cheapest method for producing powders. It was the first one to be employed by the industry. The ingredients are dry blended in a Ball mill for 12-18 hours. This results in a mechanical mix only, and all the constituents of the powder-pigment, resin and additives, are chemically separate. The coating produced from dry mixed powder has a low gloss, and due to problems with controlling particle size, recovery and recycling is difficult. However, the initial cost is low, making this a suitable powder for low performance applications.

#### (ii) Wet processing

This involves dispersing the ingredients in a solvent to form a homogenous mixture. The solvent is then extracted by evaporation or freeze drying. Finally, a finished powder product is obtained by micro pulverisation and screening. Another method often used in wet processing is spray drying. This method eliminates the pulverisation and sizing stages. The spray drier is a large chamber in which the solution is atomised. A volume of gas, which is sufficient to completely evaporate the solvent and allows the resulting spherically shaped powder to be removed, is then fed into the chamber.

The main advantage of this method is that the powder is uniform in size and shape as well as being homogeneously mixed. The disadvantage is that the presence of solvents

removes some of the advantages gained by powder over wet paints (e.g. production cost, fire and health hazard). Secondly, some solvent gets trapped in the powder causing problems such as agglomeration during use.

### (iii) Melt processing

This was used initially to improve dry blend powders but now, it is the process used by almost all commercial manufacturers of powders. In this process, the compounding trough or chamber is heated to a temperature, in the range of 75-105°C in which the resin is a highly viscous liquid. The pigments, hardeners and additives are then mixed thoroughly to produce a homogeneous powder. During the mixing period, the components are subjected to high shear forces which result in the breakdown and dispersion of pigment agglomerates, the melting of the resin particles, and the compatible distribution of flow additives and hardeners evenly throughout the resin media. This technique requires skill to control the process temperature; it must be above the glass transition temperature of the resin and well below the curing temperature. The efficiency of the shearing action, the working temperature and the time taken during compounding are the major factors affecting the optimum development of film characteristics. However, it is thought that the reactivity of the hardner system will largely dictate the temperature and time factors. A temperature of about 80°C is recommended for epoxy or polyester resins<sup>(69)</sup>.

In this melt method of powder production, the compounding processes fall into three classes:

- (a) the batch process, typified by Z-blade mixers
- (b) the semi-continuous process using heated rolls or Banbury mixers
- (c) the fully continuous manufacture by extrusion.

The Z-blade mixer has been in use since the beginning of this century but unfortunately does not produce a homogeneous mixture. It is simple to operate and sufficiently robust to require little servicing.

The semi-continuous method is not widely used for powder compounding but it is suggested that the use of heated two-roll mills or Banbury-mixers may make it a feasible method for compounding thermoplastic powders.

Today, powders are melted and mixed in an extruder which has the advantage of being a continuous operation and, if a cooling table is attached, several functions can be carried out in one operation<sup>(70)</sup>. The melt is mixed either in a Z- blade mixer or an extruder and the molten mixture is cooled on a table and pulverised to give the desired particle size. Particle size is controlled by screening the pulverised powder and returning any coarse particles to the mill.

Additions can be made to powders to improve their performance, cellulose acetate butyrate reduce the caking tendency of heat sensitive powders and can enhance interior

durability, 0.1% silica improves fluidity and reduces caking. Ultra-violet screening agents can be added to improve resistance to breakdown by sunlight.

Powder coatings can be designed to give particular coating finishes such as textured, low gloss satin and metallic finishes by additions. Textured finishes can be achieved simply by either having a high pigment loading or adding flow control agents such as barium sulphate which restrict the flow of the powder in a controlled way during curing to give a textured appearance. However, this technique loses much of the flexibility and impact resistance of untextured coatings. An alternative is to use a mix of two hardeners 'A' and 'B' (as detailed later in this review), this gives a fine textured surface by allowing a particle containing hardener 'B' to continue to flow when a particle containing hardener 'A' has gelled.

Gloss can be reduced by adding incompatible film formers such as ethyl cellulose, the reduction in gloss being proportional to the amount added. However chemical resistance is reduced as the proportion of ethyl cellulose is increased. Techniques used to reduce gloss in liquid paints cannot be applied to powder paints because these additions i.e. stearates, cannot float to the surface of powder paints during curing (as they do with liquids) because of the vastly increased viscosity.

### 2.3.5 POWDER DEPOSITION

There are many ways in which powder deposition can be carried out. The technique to be used is dictated by the shape and size of the object to be coated and the type of powder used<sup>(71,72,73,74,75,76,77,78)</sup>.

The main techniques used include: fluidised bed, electrostatic fluidised bed, flock coating, flame spraying and electrostatic spraying.

#### Fluidised bed

A fluidised bed is a chamber in which powder is placed and gas is passed through, giving the appearance that the powder is boiling. This system is described as somewhat analogous to dipping in wet paint systems<sup>(78)</sup> and consists basically of a powder hopper with a porous tile base. The object to be coated is pre-heated to a temperature above the sintering range of the powder and immersed in the fluidised bed. The powder is fluidised by means of air supplied through the tile.

#### Electrostatic fluidised bed

This technique is illustrated in figure 2.6<sup>(79)</sup>. Charging electrodes are normally placed on top of the tile which are connected to high voltage power supply. Ions generated from corona discharge at the electrodes charge the powder particles. There is danger of electrostatic sparking if the workpiece falls into the bed. A system developed to eliminate this danger is called "the intrinsic-

lly safe fluidised bed system"<sup>(79)</sup>. In this system, the charging electrodes are placed on the underside of the porous tile.

The main problem with this technique is a limitation of size; large objects can not be coated in this way as fluidised beds become unstable and "streaming" occurs once a critical size is reached. A second disadvantage is that coating thickness is difficult to control. However there is no waste powder or recycled powder to deal with.

The electrostatic fluidised bed was introduced to overcome coating thickness problems. A fluidised bed is used as above but the powder is electrically charged. The work piece is earthed and hence the powder is attracted to the work piece, but a limiting thickness is reached due to the mutual repulsion between the particles. This improves coating thickness control while size limitations still remain.

To overcome constraints on work piece size, various techniques of powder spraying, from hand held or mounted gun have been reported; flock spraying being the simplest. This consists of spraying powder onto a pre-heated work piece and curing subsequently.

An alternative method of flock spraying, often used where preheating is a problem, is flame spraying. In this method, a gas - oxygen supply is arranged in such a way

that the powder is heated as it is sprayed on the substrate. The temperature of the flame is above the degradation point of the powder but due to the high velocity of the powder particles passing through the flame degradation does not occur.

Both methods have major disadvantages, finish is dependent upon the skill of the operator and recycling is difficult especially in the latter case. Thicker coatings tend to build up on the lower half of the object hence it is unsuitable for large workpieces and can not coat round corners. The methods can all be automatically controlled to give consistent products with repeatable results.

#### 2.3.5.2 ELECTROSTATIC ORGANIC POWDER COATING SYSTEMS

The electrostatic powder spraying process was first introduced in to the metal finishing industry in the early 1960's. It was seen as the best way to overcome problems related to finish, recycling and size<sup>(80,81,82)</sup>. In the initial stages the process was developed semi-empirically but recently extensive studies have been carried out on electrostatic powder coating processes<sup>(83,84,85,86)</sup>. The coating thickness is dependent upon the charge applied to the particles and/or back-ionisation. The process's "throwing power" is very good, thus mechanisation is relatively easy. Recycling overshot powder is also easy. Initially, it was accepted, as with the electrostatic fluidised bed, that the mutual repulsion of the charged particles would act as a

self-limiting mechanism controlling film thickness but now self-limiting is recognised as being a direct result of back-ionization<sup>(87)</sup>. The good throwing-power enables complicated shapes to be coated. The powder requires regrading as certain sized particles are more likely to overshoot but this is a simple operation using a balanced air-flow to size the powder. The main problem is that thermoplastic powders tend to become sticky and form clusters causing blockage in the gun, thus only thermosetting powders are used. A second problem is only apparent if a colour change is required. The equipment must be cleaned very carefully as any powder left in the equipment will show up as specks in the coating. Notwithstanding, the process has a lot to offer in terms of application, good control, and efficient powder deposition. The adhesion of the particles is strong enough for the work piece to be transferred to an oven for curing to give a thin continuous film.

An electrostatic powder coating system consists of a source at which powder particles are charged, a space or transport region between source and target, and an earthed target which is the object to be coated. Particle charging is achieved by spray gun either electrostatically, or by an induction method.

The first powder electrostatic spray gun was developed by the French company SAMES in 1962<sup>(58)</sup>. This incorporated a single short pointed electrode at the gun nozzle. The

electrode is normally fixed in position, the only degree of adjustment offered being the potential applied to it. The majority of corona-charged guns in use today are similar to the earlier basic arrangement. Recently designed powder spray guns have the needle electrode inside the gun<sup>(82,88,89)</sup>. These are run at relatively low voltage (10KV) and use some form of Electro-Gas-Dynamic charging system. Some of the advantages claimed for this technique include the withdrawing of the corona discharge into the barrel so improving corona charge efficiency and the free ion density is reduced thus reducing the chances of back-ionization occurring. An excessive number of free ions are produced in the case of the earlier designed guns.

Another effort aimed at improving the corona charging efficiency, made recently by electrostatic powder spray equipment manufacturers, is the introduction of non-conductive spraying booths. For a conductive booth, it is claimed<sup>(82)</sup> that if a small workpiece is placed in a large booth, the largest and the most dominant earthed object is the booth itself. Many of the electric field lines originating at the gun head will terminate on the booth walls, with the booth therefore presenting itself as a major competitor for powder deposition. The result is that the coating efficiency on the workpiece will be unacceptably low, and the deposition on the booth walls will extend considerably the time required for powder colour change. Also with a large workpiece relative to

overall booth size wrap-around properties will be affected, resulting again in poor coating efficiency and possibly necessitating the doubling of the number of guns necessary to ensure even coating on all sides. All these drawbacks are eliminated by using a non-conductive booth.

A major problem with powder handling systems is the risk of fire or explosion. This is increased when combined with high voltages as in the case of powder coating where voltages as high as 60 KV are often used to charge the power. The risk is combated by using well earthed metallic booths which prevent the build-up of charge and subsequent possibility of sparking. However, it has been shown that some non-conductive materials such as Perspex cannot release sparks with sufficient energy to ignite a powder cloud<sup>(69)</sup>. The reason given for this is that the energy is released from only a small area as the resistance of the material is high, whereas an unearthed metallic booth releases all of its stored up energy at once causing a high energy spark.

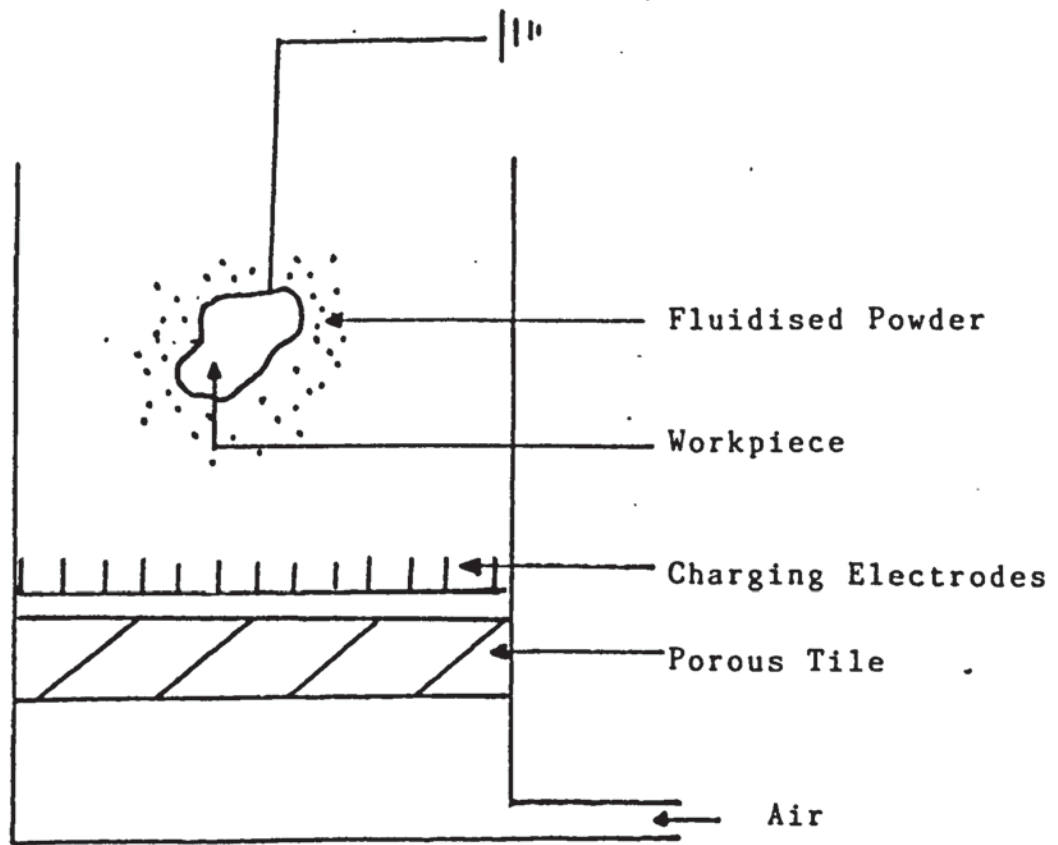


Figure 2.6 Electrostatic fluidised bed coating system

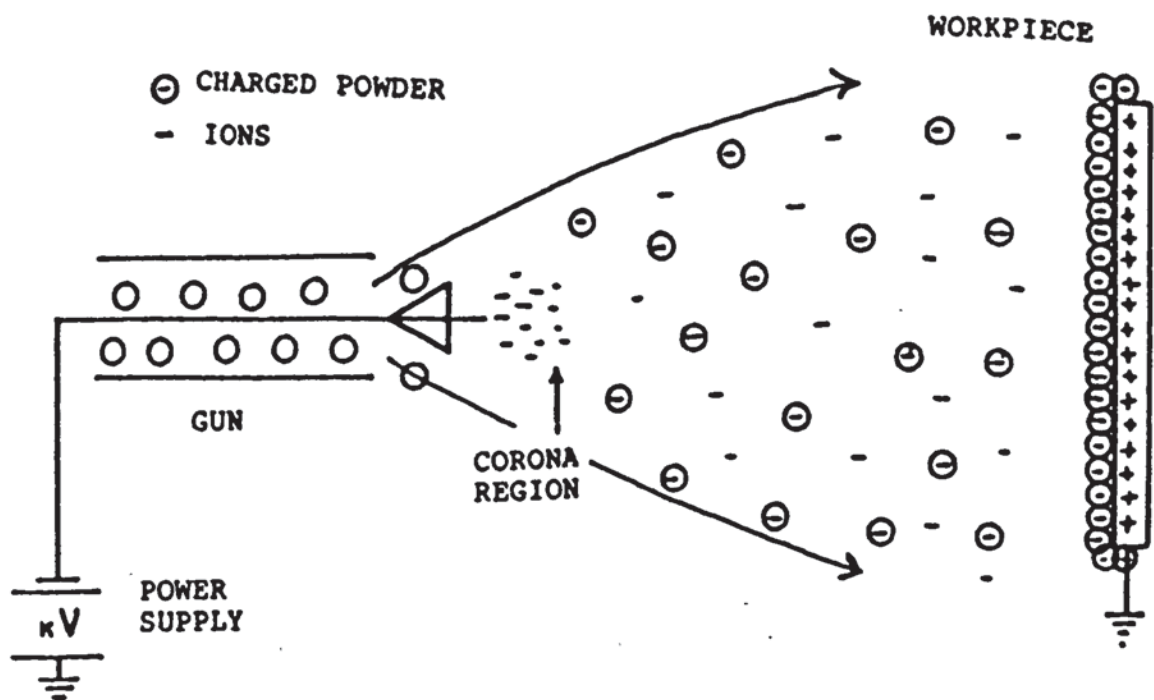


Figure 2.7 Electrostatic powder spray coating system showing powder layer growth using corona-charge gun

### 2.3.5.3 POWDER PARTICLE CHARGING AND BEHAVIOUR

The prime requirement of powder coating systems is that of imparting electrical charge, usually unipolar, to individual particles. The charged particles are then manipulated such that they alight and adhere on a grounded metal substrate. The movement of the particles between the charging station and substrate is usually governed by either electrical or mechanical forces or a combination of both. Electrical forces are created by the interaction between the charged particles and the electric field between substrate and gun, while mechanical forces are those resulting from air being driven through the gun. The success of all these operations is reported<sup>(58)</sup> to be greatly dictated by the particle size distribution, although particle shape is a contributory factor. In most reported studies of imparting charge to a particle, it has always been assumed that the particle is spherical even though the inherently brittle nature of thermosetting powders ensures that they are of irregular (or angular) shape. Acceptance of charge by these irregular shaped particles results in the concentration of charge at the peaks and corners and hence the behaviour of such particles in an electrostatic field is far from uniform as would be expected of spherical particles. Little has so far been published about the relationship between particle size distribution and the charging properties of an electrostatic spray powder. Freshwater<sup>(90)</sup>, Bright<sup>(91)</sup>, Huneke<sup>(92)</sup> and Kut<sup>(93)</sup> assumed that the par-

particle size influences a whole series of important technical properties, e.g. the fluidity, the charging and discharging mechanism during the electrostatic spray process, the degree of electrostatic efficiency, the risk of dust explosion and the degree of levelling of the stoved lacquer film. Oesterle and Szasz,<sup>(94)</sup> Bright, Makin and Corbett<sup>(95)</sup> and Lever<sup>(96)</sup> have considered the theory of the charging mechanism, in which the importance of the particle size distribution is mentioned, but with no experimental evidence in support.

De Lange and Selier<sup>(97)</sup> have carried out detailed studies of particle size distribution and properties of the electrostatic spraying powders. They reported that particle size distribution plays an important part both in the powder application and in powder reclamation. Some of their findings reported include:

- (a) A narrow size powder spectrum is favourable for powder reclamation.
- (b) The maximum layer thickness that can be attained is clearly dependent on the mean particle size.
- (c) The voltage that is optimal for powder coating is independent of particle size. Further, they reported that the electrostatic coating efficiency is raised by increasing the particle size. Indirect coating of flat plates is also dependent on the particle size and is claimed to be improved by coarser powders. This appears somewhat surprising bearing in mind the effect of gravity on coarser powders compared with finer powders. They

attributed this to the fact that the coarser particles are less attracted to the object because of their higher kinetic energy, spread wider and form a broader, more enveloping powder cloud.

(d) The electrostatic coating efficiency is raised by increasing the particle size.

(e) Gloss and levelling fall off ambiguously with increasing particle size; attributed to roughness of the film surface with coarser powders.

(f) There is melting delay for the coarser particles and commencement of the hardening reaction during the course of melting, so that the coarser particles cannot flow together sufficiently.

#### Corona charging of particles

This is perhaps the most widely used method of particle charging in both pistol and fluidised bed coaters. In its simplest embodiment, the charging electrode may be a sharp pointed needle-like electrode, or a fine gauge wire. The electrode is connected, via a high resistive load, to a high voltage generator. Corona charging in pistol applicators and the principle of electrostatic powder coating operation are illustrated in figure 2.7. Powder particles size between 1 and 80 microns diameter are blown past a sharp point held at high voltage between 50 and 100KV from which there is a corona discharge. The powder is charged by ion bombardment close to the point and carried by the field to an earthed object to which it

adheres. The corona discharge is obtained by subjecting the point electrode to a high voltage of negative polarity, this leads to local discharge or ionization of the air, resulting in charge separation and the creation of unipolarly charged molecules, or ions.

The charge acquired  $q$  (negative charging) in time  $t$  by a spherical particle is given by Pauthenier's equation<sup>(98)</sup>.

$$q(t) = 12 e_0 E a^2 (e_s / e_s + 2) (1 + 4e_0 E / J t)^{-1} \quad 2.11$$

where  $a$  = Particle radius

$E$  = Electric field

$J$  = Ion current density

$e_s$  = The relative permittivity of the particles

$e_0$  = Permittivity of free space.

This relationship shows that the charge acquired by the particles is a function of the applied field and the powder flow rate. The magnitude of the charge determines the velocity with which the particles travel and adhere to the object.

For a spherical particle its mass ' $m$ ' will be:

$$m = \frac{4\pi a^3}{3} p \quad 2.12$$

where  $p$  = density of the particle

If positive charging is used, although the Pauthenier relationship is still valid, the actual mechanism of the corona discharge at the electrode point will be different. With high positive potential applied to the electrode, electrons will have to be stripped from neutral

air molecules thus creating positive ions, which in turn migrate towards the earthed workpiece and interact with powder particles in a manner identical to that of negative ions.

Although negative polarity has been chosen as the standard commercial configuration and, perhaps is of greatest importance, it is claimed that the present availability of electronic voltage multiplier units ensures that polarity offers no limitation to design and performance. It has also been reported that the electrical discharging associated with the release of substantial energy leads to serious disruption of the deposited layer causing the familiar surface defect known as 'orange-peel'. This surface disruption varies according to the polarity used on the charging gun<sup>(99)</sup>.

With negative gun charging polarity, the spark associated with back-ionization is a bulk phenomenon. That is, the spark channel actually penetrates the depth of the deposited layer and can create the familiar 'pin-holing', together with some degree of cratering which is associated with 'orange-peel'. The nature of back-ionization changes considerably when positive corona charging is used. The discharge does not penetrate the deposited layer, but is more of a surface phenomenon. There is no pin-holing, but the surface disruption usually tends to be more severe.

When insulating powder particles are blown through a gun,

a net electrical charge which can either be positive or negative, is retained by the particles. Some commercial guns utilise this phenomenon, relying entirely on tribo or frictional charging to effect particle charging. In relation to the coating process, there is a subtle difference between corona charged and purely tribo-charged particles. In tribo-charged guns, no free ions are created, resulting in a system producing two species only - charged particles and uncharged particles compared with three species identified with corona charged guns (figure 2.7). It is claimed that a tribo-charged gun deposits a far superior quality coating than a corona charged gun. Since no free ions are created by a tribo-gun, the charge build-up on the deposited layer is entirely due to the charged particles. Thus the charge density in the layer is low and the layer breakdown potential will not be reached until a considerable thickness is achieved. Tribo-charged coating tests have indicated that layer breakdown or back-ionization may be initiated after about 10 seconds of coating time. The corresponding value for corona charging is about one second, or in most cases when the first monolayer of powder is deposited. Thus, with a tribo-charged gun, there is no back-ionization within the first 10 seconds; and consequently there is no disruption of the deposited layer which would lead to pin-holing and cratering. At the same time, there is no self-limiting and thick layers are created. This situation is not acceptable in most

industrial coating applications. However, some authorities<sup>(82)</sup> suggested that this may be compensated by careful control of conveyor speed and powder throughput.

### 2.3.6 CURING OF POWDER COATINGS

Curing of a powder coating is a chemical reaction which is aided by heat. In the case of thermosetting powder, the cross-linking network is three dimensional.

After electrostatic deposition, the powder is held on the surface solely by electrostatic forces. Unbaked powder coatings consist of agglomerations of particles whose major dimensions are much greater (approximately x5) than the final coating thickness. To produce a continuous film, the powder coated article is baked in an oven capable of providing a rate of temperature increase of about 30°C/min. As the powder heats up it softens, melts and flows over the surface. Initially, from its irregular shape, each particle tends to form a spherical shape before melting and coalescing into adjacent particles to form a continuous film. Then the continuous film flows from an irregular surface to a smoother surface (figure 2.8 After flow, the cross-linking reactions occur at the onset of curing. At the end of the stoving cycle, the cross-linking reactions should be complete and mechanical properties fully developed<sup>(100)</sup>.

It is assumed and adequately supported in the literature<sup>(101,102)</sup> that surface tension is the major driving force to cause flow. The major resistance to flow is the .PA viscosity of the molten coating at baking conditions. If surface tension is the cause of the flow,

the radius of curvature of the particles should be important, since the pressure causing two spherical powder particles to flow together is proportional to the surface tension of the coating, divided by the particle radius.

Surface tension arises from molecular forces which act on the surface of molten powder to provide a minimum surface area. For example, consider a liquid in contact with its vapor, the molecule in the middle of the liquid is in equilibrium in a uniform field, but a molecule at the surface of the liquid undergoes an attraction from the liquid phase. The attraction from the more dispersed vapour phase is not able to compensate the former and the molecules at the surface have a higher free energy.

To reach equilibrium, the system will tend to minimize its free energy per unit area and consequently to contract its surface to a minimum. It results in a surface tension parallel to the surface, preventing any attempt to increase the interface.

According to Fowkes<sup>(103)</sup> the surface tension  $Y$  is the sum of two forces, namely the non-polar intermolecular attractions (or dispersion tension  $Y_d$ ) and the polar intermolecular attractions (or association tension  $Y_p$ ), or:

$$Y = Y_d + Y_p \quad 2.13$$

By increasing temperature,  $Y$  decreases as the intermolecular attraction forces diminish.

Interfacial tension is defined as the result of the surface tensions of two materials in contact with each other, resulting from the intermolecular attractions of these two materials at their common interface. The equilibrium between these tensions is governed by Young's equation:

$$Y_{sv} = Y_{sp} + Y_{pv} \cdot \cos \Theta \quad 2.14$$

where

$Y_{sv}$  = surface tension of substrate in contact with vapour from the molten powder drop.  $Y_{sv}$  tends to decrease the substrate/vapour interface by spreading the liquid over the surface.

$Y_{pv}$  = surface tension of molten powder drop (powder coating film) in contact with its vapour. This force tends to minimize the liquid/vapour interface.

$Y_{sp}$  = interfacial tension between the molten powder coating drop (film) and its substrate.  $Y_{sp}$  reduces the substrate/liquid interface.

$\Theta$  = angle between  $Y_{pv}$  and the substrate, the so-called contact angle.

From Young's equation it is clear that the maximum of wetting of the substrate is achieved when  $\Theta \longrightarrow 0$  ( $\cos \Theta \longrightarrow 1$ ) or when

$$Y_{sv} > Y_{pv} \cdot \cos \Theta + Y_{sp}.$$

Consequently, there are two possibilities for improving the wetting characteristics:

(a) reduce the surface tension of the molten powder  $Y_{pv}$  ;  
and (b) reduce the interfacial tension between the liquid and the substrate  $Y_{sp}$  .

Gabriel<sup>(104)</sup> claimed that wetting can be improved by reducing contact angles, and that contact angle can be reduced with additives such as ethylacrylate copolymer of mean molecular weight of nearly 8000. Additives like epoxidized soyabean fatty acid and hydroabietyl alcohol were reported<sup>104</sup> to have improved molten powder flow by raising the surface tension. Relating these to Young's equation, the influence of the above mentioned additives can be interpreted as follows:

The copolymers (or Type A-additives) reduce  $Y_{pv}$  therefore raising the spreading pressure  $Y_{sv} - (Y_{pv} \cdot \cos\theta + Y_{sp})$  and promoting wetting between molten resin and substrate. But, as the effect on surface tension of the epoxy resin caused by the addition of the acrylic additive decreases with increasing temperature, it was considered that the improvement of wetting should also be attributed to the reduction of the interfacial tension  $Y_{sp}$ . Epoxidized soyabean fatty acid and hydroabietyl alcohol (or type B-additives) raise contact angle  $\theta$ , which means that  $\cos\theta$  is reduced, and with nearly constant values of  $Y_{sv}$  and  $Y_{sp}$ ,  $Y_{pv}$  will be increased.

In powder coating technology, the influence of both types of additives have been interpreted by de Langer<sup>(101)</sup> as follows:

Epoxy resin without additives leads to "cratering" and "orange peel".

Epoxy resin + Type B-additives leads to "cratering", but no "orange peel".

Epoxy resin + Type A-additives leads to "orange peel" but no "cratering".

Epoxy resin + both types of additives leads to good flow (no craters, no "orange peel").

These theoretical aspects of surface tension consideration have shown that the requirements of maximum surface tension for good flow and minimum surface tension for good substrate and pigment wetting can be combined to a suitable compromise by combination of both types of additives.

It has been reported by some authors<sup>(101)</sup> that expoxidized soyabean fatty acid reduces the surface tension of acrylic and certain polyester powder coatings. The rather poor flow of these powder types will become even worse (more "orange peel") and normal practice in such cases is to use only the acrylic additive to prevent cratering. It is also a normal practice with most types of epoxy, epoxy/polyester, and pure polyester powder coatings, to use only a type A (acrylic)-additive and not two conflicting additives.

One of the requirements for a good powder melt flow and hence good film formation is a sufficiently long time at which the viscosity is low. For thermoplastic powders this depends only on the molecular weight of the polymer and on its curing temperature. For thermosetting powders (containing a curing agent) the reactivity of the system also plays an important role, as well as the heating rate<sup>(105)</sup>. Ghijsels and Klaren<sup>(106)</sup> showed with epoxy powders, that they attained lower minimum viscosities, and as a consequence better flow, by the use of higher heating rates. This agrees well with observations made in practice, that better flow is found with powders applied on thin or preheated substrates. Interaction between pigment and binder (e.g., adsorption, chemisorption) may play a role. Ghiljadov, et al<sup>(107)</sup> showed that, with increasing interaction between pigment and resin particles, improved wetting of the pigment by the binder takes place on the one side, whereas, on the other side, the mentioned rise in viscosity by pigment addition will be smaller.

The effect of pigment on melt viscosity or flow is dependent on the extent to which a pigment is dispersed within the resin matrix. Nix and Dodge<sup>(102)</sup> found that, with equal pigment levels, a powder with finely dispersed pigments showed lower melt viscosity than the same powder with badly dispersed pigments. By improving the degree of dispersion, the melt viscosity may be reduced in some cases by a factor of approximately 10.

Particle size has a dramatic effect on film flow (and gloss), as small particles need less time to melt and to coalesce than coarse particles. When the maximum particle size is reduced, the minimum film thickness required to give good flow and gloss is also reduced.

Another important factor affecting flow is the initial profile of the dry, deposited (unbaked) powder layer on the substrate. Photographic evidence<sup>(101)</sup> has indicated that if "clusters" or large agglomerates of powder particles are present they can become the "hills" of the orange peel effect. This view agrees with that of Nix and Dodge<sup>102</sup> who have shown that poor levelling or orange peel is not always a result of high melt viscosity as claimed by Klaren and Ghijsels<sup>(106)</sup>. They say clusters may be caused by low molecular weight materials at the surface, which may cause sticking of particles to one another. Other suggested causes of clusters include:

(a) Electrostatic attraction or repulsion, which may cause clusters to form either before spraying, during transport to the substrate, or upon deposition.

(b) Too many powder particles of less than 5 microns in diameter, which cling to larger particles of 50 to 60 microns in diameter.

Entrapped air and vapour bubbles in stoved powder coatings interfere considerably with powder melt flow. Flow must occur simultaneously with at least partial displace-

ment of air (and possibly vapour, produced during stoving) from between individual powder particles. Release of this air will be retarded or partly prevented, as the powder melts first at the air interface to form a continuous layer. Furthermore, air trapped within powder particles will raise the melt viscosity and interfere with flow. Sometimes the air bubbles just reach the air interface during stoving, resulting in "micro-pinholing". For a complete removal of air bubbles, Zorll<sup>(108)</sup> calculated that the release time may amount to 26 seconds in some cases. Hoeflaak and Selier<sup>(109)</sup> found a critical film thickness above which air-bubbling occurs. They also showed that there exists a relation between that critical film thickness, stoving temperature, and flow time. Trapped air and vapour bubbles and micro-pinholes can be prevented or reduced by low melt viscosity, long flow time, and reduced film thickness. It is suggested that the critical film thickness can be increased by:

- (i) Increasing stoving temperature; and
- (ii) Pretreatment (chromating or phosphating) of the metal substrate.

#### 2.3.6.1 CURING STUDIES

The extent of cure or degree of cross-linking of a polymer/binder is very important since it can affect certain film properties such as chemical resistance, durability and mechanical behaviour (e.g. tensile strength, ultimate strain, hardness and impact resistance). The curing of powder coatings has been studied by many researchers using different techniques. These techniques include the measurement of melt viscosities using the Weissenburg Rheogoniometer<sup>(102)</sup>, the measurement of kinetics and thermodynamics of cure using Differential Thermal Analysis (DTA)<sup>(110)</sup> or Differential Scanning Calorimetry (DSC), determining the onset of cross-linking, the gel point and the time available for flow using a Dielectric Spectrometer<sup>(105)</sup>.

Commercial differential thermal analysers were introduced in the 1950's and since then there have been numerous publications describing their use. Pope and Judd<sup>(111)</sup> have reviewed the history, techniques and applications of differential thermal analysis. DTA is a technique which involves heating the test sample and an inert reference sample under identical conditions and measuring any temperature difference between them, either against time or against a fixed temperature. The fields of application of DTA and DSC, are practically identical, but the two techniques are distinctly different. DSC measures the heat flux required to maintain an equal temperature in the sample and a reference either against time or tempe-

rature. In DTA, a single heater is used and thermocouples are used to measure the temperature difference between the sample and the reference. In DSC the sample and reference have two separate heaters. The kinetics of cure (reactivity), and heat of cure can be studied using these techniques. Information can also be found about the glass transition and the onset of fusion using these techniques.

DSC can also be used to study the effect of state of cure on bond performance of epoxy resin coatings<sup>(112)</sup>. For example, it was used to find that bond strength increased with degree of cure, bond failure being cohesive in the range 70-90% cure and adhesive in the range 90-100% cure. Also Klaren has shown, by using DSC that increasing the heating rate from 20°C/minute to 80°C/minute moves the cure peak maxima, i.e the curing temperature, up by 30°C for epoxy resins.

Powder melt temperature and flow have been studied<sup>(64,69,110)</sup> by using a hot stage microscope technique incorporating the Quantimet television microscope (QTM).

### 2.3.7 ORGANIC COATING ADHESION MEASUREMENT

Adhesion of polymer films to substrates is one of the most important coating properties as far as performance and durability are concerned. Its importance has increased with the trend toward more applications of powder polymer coatings to engineering products.

There are many methods of assessing coating adhesion to substrates. These methods vary from qualitative tests such as cross-cut (peel-off), bending etc to quantitative measurements such as indentation - debonding. However, adhesion tests of coatings that are likely to be satisfactory, necessarily involve some degree of failure within either the substrate or coating, so that exact prediction of strength of adhesion is impossible.

In almost all the methods of adhesion testing, a force of increasing magnitude is applied to the paint film/-substrate joint, until the joint is disrupted. Either the maximum force applied is measured, or some other criterion such as area of "detachment", is used to designate the "adhesion"

This force, in most cases, is applied to the interface by way of the paint film which is invariably a viscoelastic material whose mechanical properties are a function of temperature and rate of test. There is always the suspicion that the manner of performing the test will affect the result. Indeed, trials with a thumbnail or knife will readily demonstrate this to be the case.

Methods of detaching the film in the direction normal to the plane of the interface (e.g. pull-off test) have been devised to reduce interference from film properties as much as possible. This allows the whole area of the film to be detached simultaneously when the joint is broken.

The cross-cut or scratch test involves making a series of cuts through the polymer film with a knife or diamond cone and assessing for adhesive failure either before or after peeling off weakly bonded areas with pressure sensitive tape.

Another test is the water displacement test which depends on film permeability and swelling characteristics as well as on adhesion which, in this case, relates to the relative energies of wetting by water and the film.

The final group of methods are the non-destructive test methods such as the ultrasonic probe test.

## 2.4 PROBLEMS ASSOCIATED WITH POWDER COATED GALVANIZED STEEL

### 2.4.1 DEGRADATION OF POLYMER FILM

As applications of powder organic coatings become more diverse, the environments in which coatings are expected to perform become harsher. When exposed outdoors the coatings must withstand the combined effects of moisture, oxygen, heat, ultra-violet light and micro-organisms in order to meet the required standards.

It is normally recognised that progressive loss of gloss, chalking and mass loss that occur on exterior weathering is due to the effect of ultra-violet light in the presence of oxygen and moisture<sup>(113)</sup>. Two different mechanisms have been proposed to explain this:

- (i) degradation by hydroxyl radical formation, due to the photocatalytic activity of the pigment (e.g. titanium dioxide in white pigments),
- (ii) direct photodegradation of the binder.

Most of the ultraviolet radiation adsorbed by a paint film pigmented with titanium oxide is adsorbed by the pigment and this is also expected to be the same for other types of pigment<sup>(114)</sup>. Although adsorption is expected to reduce the amount of damage done by ultraviolet radiation, titanium oxide and other pigments are photoactive and as a result can catalyse breakdown in the binder. Thus the presence of pigment can accelerate or retard degradation depending on the photoactivity of the

pigment. When pigment crystals are irradiated with sufficient energy, electrons are excited from valence bands to the conduction bands thus allowing both the electrons and the holes created by missing electrons to move about within the crystal lattice. Some electrons and holes reach the surface where they are capable of initiating chemical reactions in the surrounding medium. The positive holes react with hydroxyl groups to form adsorbed hydroxyl radicals.



The electrons react with adsorbed oxygen to form the  $\text{O}_2$  radical ion which then reacts with water to form the perhydroxy radical.



Both radicals can initiate breakdown of organic compounds and hence the process of paint film degradation is started.

The photochemical degradation of the binder is mainly due to an oxidation process with oxygen adsorbed from the atmosphere. Energy must be adsorbed for this process to start and has been found to come from ultraviolet radiation. The molecular bonds in the binder are broken by UV quanta or protons which collide with electrons, the rate of breakdown being dependent upon the energy adsorbed. The shorter the wavelength of the incident ultraviolet light the greater the energy but the

intensity of the radiation and absorption characteristics of the binder also affect the total energy absorbed.

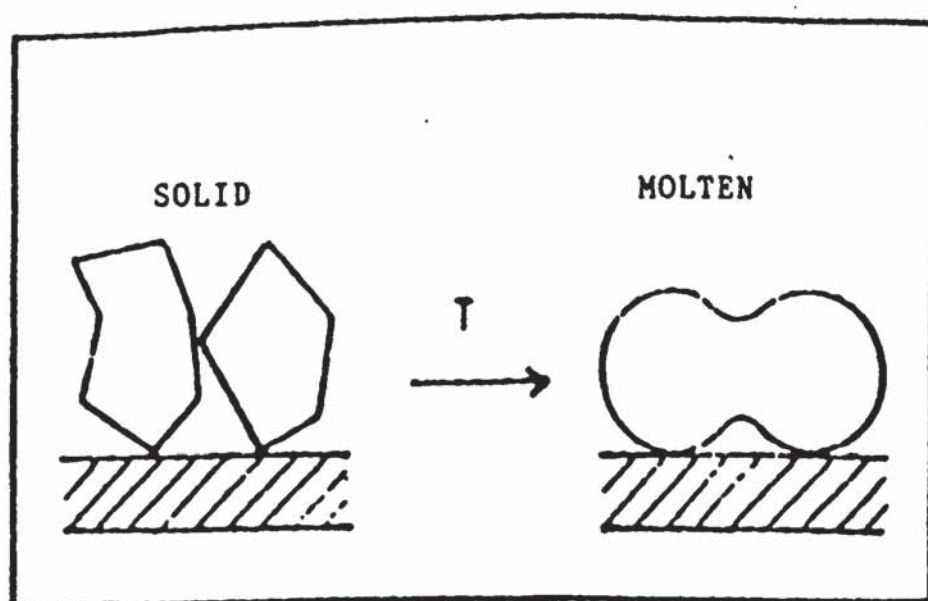


Figure 2.8 Schematic illustration of the coalescence of molten powder particles

#### 2.4.2 PINHOLING

Pinholing is a type of defect that occurs in organic powder coatings and it appears to the naked eye as depressions in polymer films. This defect has been attributed to<sup>(49)</sup>:

- (a) Back ionization, -ve corona charging
- (b) Entrapped air or
- (c) Volatile condensation products.

#### 2.4.3 CRATERING

This is another type of defect often found in organic powder coatings. Initially, it was attributed to a defect, some distance away, in the zinc layer. It was considered that a pore present in the zinc layer was joined to the defect in the film by a fissure. This cratering defect is often associated with coatings produced by the batch hot-dip galvanizing process rather than those produced on sheet in continuous galvanizing lines (Galvatites) or zinc electroplate (Zinctec). Recent research work has linked this type of defect with (details in section 2.3):

- (a) Back ionization, +ve corona charging
- (b) Surface contamination and
- (c) Absence or wrong type of flow control agents.

#### 2.4.4 LOSS OF ADHESION DUE TO CRACKING OF ZINC SPANGLES

The papers of Leidheiser and Kim<sup>(115-118)</sup> and Leidheiser and Suzuki <sup>(119)</sup> have outlined some of the factors affecting the adhesion of paint to galvanized steel and have given methods of predicting adhesion. Both were reported to be strongly related to the fracturing tendencies of the grains (spangles) of zinc.

In their papers, Harvey and others<sup>(120,121)</sup> and Sebisty and co-authors<sup>(122)</sup>, established that:

- (a) There are two clearly distinguishable modes of failure - Boundary cracking and intragrannular "straight-line" cracking.
- (b) The cracking tendency of the spangles does not depend on the coating weight (i.e, zinc layer thickness)
- (c) The intragrannular cracks are usually in long parallel groups or in groups of right-angled cracks which are typical zinc cleavage cracks, although Leidheiser and Kim<sup>(118)</sup> established that intragranular cracks formed on (0001) or (0020) planes.
- (d) The influence of zinc alloying additions, Sn and Pb, on propensity to cracking were small.
- (e) During bend tests, the boundary cracking occurs after only a small amount of bending and is very prevalent when the spangle size is small.
- (f) Many of the cracks are too fine to be visible to the naked eye. They widen and become more apparent as bending proceeds.

However, Jaffrey, Browne, and Howard, in their work<sup>(123)</sup> established that:

- (a) Both forms of cracks, boundary and intragranular cracks, occurred at low and high strains but at low strains the former were observed more frequently than were the intra-granular cracks.
- (b) At low strains, the crystallographic cracks were detected exclusively in one direction within a grain and in low reflectivity grains only intragranular cracks ran at angles which varied between 40 and 90 degrees to the tensile axis and they did not cross into contiguous grains.
- (c) As the strain increased, the cracking within basal grains become more extensive, the other grains began displaying parallel cleavage cracks and finally some of these grains developed a second set of cracks.
- (d) Grains with their (0001) plane in the plane of the sheet displayed cracking only during the final phase of specimen failure.
- (e) The smaller the spangle (grain) size, the lower the density of the cleavage type cracks after a given strain.
- (f) Variation in test temperatures between - 24°C and 47°C had no detectable effect on the initiation or growth of either type of crack.

The latter authors (Jaffrey and others) concluded that boundary cracking is the most common failure due to

strain. It appears to be little influenced by factors such as alloy purity, temperature, strain rate, and grain size. The relative dominance of the boundary mode of cracking was also found by Barlow and Harvey<sup>(124)</sup>.

Detailed study of the results of Leidheiser and Kim<sup>(115)</sup> and that of Jaffrey, et al<sup>(123)</sup> revealed some important differences. For example, the former authors said that the best paint adhesion was for sheets displaying the largest proportion of basally oriented grains which was initially considered to be due to the presence of numerous fine cracks in basally oriented grains. They also reported<sup>(118)</sup> that in tension cracking occurred only rarely within grains and that mechanical twinning was the major mechanism of plastic deformation. Subsequently, they put forward the view that basally oriented grains are fractured less extensively than other grains during bending. The results of Jaffrey and co-authors and those of Harvey and co-authors<sup>(120,121,124)</sup> are consistent with and reinforce the later view. They question the observation regarding mechanical twinning during tension. Given that the estimated shear stress to nucleate a twin in pure zinc<sup>(125)</sup> is  $980 \text{ N/mm}^2$  at  $0^\circ\text{C}$  compared with a flow stress<sup>(126)</sup> of  $70 \text{ N/mm}^2$ . It seems highly unlikely that twinning would dominate at a low level of tensile strain.

Spangle orientation and surface topography studies were also carried out by Jaffrey et al using both optical and electron microscopy and they indicated that there are

four spangle types (127).

(a) Mirror-like flat, featureless surface - high reflectivity.

(b) Feathery - high reflectivity but an underlying dendritic pattern.

(c) Dimpled - relatively low reflectivity - small scale regular hills but without preferred direction.

(d) Ridged - low reflectivity - small scale hills and valleys but arranged in one, or occasionally two, systems of ridges.

In all cases examined in this study, it was found that the grains with a ridged topography, fractured most readily at low levels of tensile strain. As the strain increased they cracked more extensively and eventually cracks began appearing in the other types of spangles. This demonstrates that it is those grains which have their basal plane running at an angle to the plane of stress which crack most readily. Such behaviour is entirely consistent with basal plane cleavage. This phenomenon is well known in zinc crystals and has been demonstrated to occur in spangles.

Jaffrey and co-authors<sup>(123)</sup> indicated that it is possible that the surface topography plays much greater role in determining paint adhesion, either directly or indirectly than has been previously acknowledged. Kim and Leidheiser<sup>(117)</sup> have already shown that paint adhesion is dependent upon the orientation of the spangle and that the

basal grains were smoother, cleaner and had better paint retention. The non-basal grains have a much more complex and rougher surface than do the other types.

#### 2.4.5 CORROSION

Corrosion resistance properties of powder coatings are to large extent influenced by the pretreatment given to the underlying metal and the powder type. It is reported<sup>(110)</sup> that Polyester and mixed polymer powder coatings provide more corrosion protection than any of the epoxy types on steel and aluminium substrates. Powder storage conditions before use have been reported to have significant effect on the corrosion resistant of the finished products<sup>(110)</sup>. Storage conditions that allowed powder access to a moist, or warm environment adversely affect the corrosion resistance of the powder coating.

Corrosion problems with organic coated metals range from improper application procedures to those which are not correctable because of an absence of understanding. The tendency of a coated metal to corrode is a function of three major factors:

- (i) The nature of the substrate metal
- (ii) The character of the interfacial region between the coating and the substrate, and
- (iii) The nature of the coating.

In many cases, the coatings are required to compensate for the inadequacies of surface preparation prior to coating. An organic coating protects a metal substrate

from corroding primarily by two mechanisms:

- (i) Serving as a barrier for water, oxygen, and ions, and
- (ii) Serving as a reservoir for corrosion inhibitors that assist the surface in resisting attack.

The barrier properties of the coating are improved by increasing thickness, by presence of pigments and fillers that increase the diffusion path for water and oxygen, and by the ability to resist degradation. The common degradation mechanisms of the coating include abrasion and impact, cracking or crazing at low or high temperature, bond breakage, oxidation and freeze-thaw cycling. The result of such degradation allows access of reactants to the coating/substrate interface without the necessity for diffusion through the polymer matrix.

Six types of corrosion beneath paint coatings have been identified. These include blistering, early rusting<sup>(128)</sup>, flash rusting<sup>(129,130)</sup>, anodic undermining, filiform corrosion, and cathodic delamination<sup>(131)</sup> .

There is little evidence in the literature to suggest which, if any, of these mechanisms is applicable in the case of powder coatings.

### 3 EXPERIMENTAL TECHNIQUES AND PROCEDURES

#### 3.1 MATERIALS AND SAMPLE PREPARATION

##### 3.1.1. MATERIALS

The materials used for this work included

- (i) Pure zinc sheet (99.95% pure)
- (ii) Electroplated zinc (Zintec)
- (iii) Galvanized steel sheets - (a) Hot-dip continuous (HDC) and (b) Hot-dip batch (HDB)
- (iv) Arc zinc sprayed

##### 3.1.2 SAMPLE PREPARATION

Samples for pretreatment studies were cut to measure 5cm long and 1.5 cm wide. The edges were carefully lacquered and left to dry at room temperature for three days and then stored in desiccators. Those samples to be powder coated after pretreatment were cut to measure 15cm long and 10cm wide.

##### 3.1.3 POWDER

The powder used for this project was a white polyester having the following formulation, as stated by the supplier

Polyester Resin	58%
T.G.I.C. (TRIGLYCIDYL ISOCYANURATE)	4.4%
Pigment	35%
Additives	1.7%

It was recommended to be stoved at 200°C for 15 minutes.

### 3.2 CLEANING

The performance of organic coatings may vary from failure in a matter of a few weeks to years depending on the efficiency of cleaning, rinsing and pretreatment stages. The majority of failures are undoubtedly due to insufficient or unsatisfactory preparation of the metal surface. Hence, it was deemed essential to ensure thorough cleaning to remove all traces of dirt, grease, oil, silicone compound, and corrosion products.

#### 3.2.1 PROPRIETARY AC51 SOLUTION PREPARATION

AC51 is a proprietary product of Robertsons Chemicals Limited. It is a phosphoric acid based aluminium cleaner which also works well when used to clean zinc. Undiluted, AC51 has a pH of about 0.6. It has a working temperature range of 0 to 60°C and chemical degradation occurs above 60°C.

Batches of one litre of working solution were prepared by making a 10% by volume solution of AC51, using cold distilled water. After thorough mixing the solution was heated up to 40±2°C and kept at this temperature when in use, in a thermostatically controlled water bath. Evaporation of the working solution was prevented by covering the solution with a watchglass. A freshly prepared solution has pH of about 1.8.

### 3.2.2 CLEANING PROCEDURE

In all cases, samples were degreased in acetone for two minutes before chemical cleaning in AC51 at 40°C for 60 seconds. This was followed by rinsing in distilled water for two minutes and then dried in a stream of warm air.

### 3.3 PREPARATION OF CONVERSION COATING SOLUTIONS

#### 3.3.1 PROPRIETARY CHROMATE-PHOSPHATE (ALOCROM 100) SOLUTION

The chemicals used were Alocrom 100 liquid, Alocrom 100 Make-up powder and Alocrom 100 Replenishing powder. The make-up for every batch of 1 litre was as follows:

Distilled water	900 ml
Alocrom 100 liquid	100 ml
Alocrom 100 make-up powder	22 g
Alocrom 100 Replenishing powder	5 g

The solution was made up in a 1 litre plastic beaker by pouring in the distilled water, adding Alocrom 100 liquid and stirring well. The Alocrom 100 make-up powder and Alocrom 100 replenishing powder were added and mixed thoroughly. The pH was found to be 2.3.

#### 3.3.2 PROPRIETARY NON-CHROMATE (Chrometan) SOLUTION

Batches of 1 litre of this solution were made by first pouring half a litre of distilled water into a 1 litre beaker, and then measuring the proportions of the different chemicals<sup>(6)</sup> before topping up to the 1 litre level

with distilled water. The solution was stirred thoroughly using a magnetic stirrer. Sodium hydroxide was added until a slight permanent precipitate of chromium hydroxide was present and sulphuric acid was then added until the precipitate just dissolved. The pH was measured and found to be 4.5. The solution make up was

Chrometan	48g/l
Sodium hypophosphite	24g/l
Sodium nitrate	8g/l
Boric acid	8g/l

### 3.3.3 CHROMATE CONVERSION COATING SOLUTIONS

#### 3.3.3.1 CHROMIC ACID (NaCl as activator) SOLUTION

One litre batches of this solution were made with distilled water in a plastic beaker. The make up of the solution was 0.12M/l (12g/l) of  $\text{CrO}_3$  + 0.3M/l (17.5g/l) of NaCl. The solution was thoroughly mixed by stirring with the magnetic stirrer and the pH was found to be 1.2. It was then stored at room temperature.

#### 3.3.3.2 CHROMIC ACID (activated with NaF) SOLUTION

Batches of this solution were made up as above using 0.12M/l (12g/l) of  $\text{CrO}_3$  and 0.1M/l (4.2g/l) of NaF. Its pH was found to be 3.4.

#### 3.3.3.3. OTHER SOLUTIONS

One litre batches of all other pretreatment solutions, detailed in table 2.1, used in this project were made by

mixing the correct proportions of chemicals required in a 1 litre plastic beaker with distilled water. In each case the solution was well mixed by stirring it with a magnetic stirrer. The pH of every solution was measured using a digital pH meter. The solutions were coded in order to facilitate easy reference (see table 3.1).

### 3.4 CONVERSION COATING PROCESS

All the conversion coating operations were carried out at  $22 \pm 2^{\circ}$ . The samples were conversion coated by simple immersion and without agitation. Coupons used for these studies were numbered with a sharp scribe before treatment. The samples were suspended in the solution, both during chemical cleaning and conversion coating operations, using a crocodile clip connected to a stiff wire. Care was taken to avoid galvanic coupling between the zinc-iron layer and the mild steel and between the coupon and the mild steel crocodile clip by covering the sample edges with protective lacquer and ensuring that the crocodile clip did not enter the solution. The general sequence of operations were -

Degrease (immersed in acetone for 2 minutes);

Chemically clean in AC51 solution for 1 minute;

Rinse in distilled water for 2 minutes;

Dry in stream of warm air;

Conversion coat (for the time required; a fresh 100 ml of solution in small plastic container was used for every coupon);

Rinse in distilled water for 1 minute;

Dry in warm air (temperature not greater than 50°C.)

### 3.5 COUPON WEIGHT CHANGE STUDIES

For the purpose of these studies, samples were dried in a warm stream of air for 5 minutes after the two rinses in the above sequence. In each case, the samples were weighed after drying, using a balance, accurate to  $\pm 0.00001\text{g}$ . Each coupon was weighed 5 times and the average taken. The weight difference before and after conversion coating was determined and divided by the calculated area of the sample immersed in the solution. This gives a weight change per unit area ( $\text{g}/\text{mm}^2$ ).

### 3.6 DETERMINATION OF ZINC DISSOLUTION RATE USING ATOMIC ABSORPTION SPECTROPHOTOMETRY

The principle of atomic absorption spectroscopy is based on the fact that if a solution containing a metallic species is aspirated into a suitable flame, an atomic vapour of the metal will generally be formed. Some of the metal atoms may be raised to an energy level sufficiently high to emit the characteristic radiation of that metal, a phenomenon that is exploited in emission flame photometry. The overwhelming majority of the metal atoms, however, remain in the non-emitting, ground state. If irradiated with light of their own characteristic resonance wavelength, these ground-state atoms will absorb some of the radiation, the absorbance being proportional to the population density of atoms in the flame.

The technique thus offers the outstanding intrinsic advantage of specificity, since the atoms of a particular element can only absorb radiation of their own characteristic wavelength conversely, light of a particular frequency can only be absorbed by the specific element to which it is characteristic. Spectral interferences, which are so troublesome in emission methods, therefore rarely occur.

A Perkin-Elmer Model 560 Atomic Absorption Spectrophotometer, calibrated to read directly the zinc concentration in the test solution, was used for these experiments. The readings were integrated over a period of 5 seconds. The source of radiation is a hollow cathode lamp. It consists of a hollow cylindrical cathode made from, or containing material of the element to be determined, together with a tungsten wire anode housed in a glass envelope containing a rare gas at low pressure. The atomic vapour of the sample solution is produced using atomizers and burners. The compressed air normally used for atomizing the liquid also feeds the supporting gas within the flame.

If a parallel beam of radiation is considered of intensity  $I_0$ , at frequency  $\nu$ , incident on atomic vapour of thickness  $x$  cm, then if  $I_\nu$  is the intensity of the transmitted radiation, the absorption coefficient,  $K_\nu$  of the vapour at frequency  $\nu$  is defined by the relation, similar to Beer-Lambert's law;

$$I_v = I_o \exp(-K_v x) \quad 3.1$$

For the purpose of making measurements, a useful parameter is the absorbance A, defined as-

$$A = \log_{10} I_o / I_v \quad 3.2$$

Substituting for  $I_o / I_v$  from equation 3.1,

$$A = k_v x \log_{10} e = 0.4343 k_v x \quad 3.3$$

It follows that the absorbance is directly proportional to the absorption coefficient.

### Solution preparation

In order to read directly the concentration of zinc in test solutions, the concentration of the samples and standard were made within the linear working range of the instrument. Calibration was then made with only a reagent blank and a standard at the bottom and upper ends of the linear concentration range.

### Blank solution

Fresh test solution containing no zinc was diluted the same amount as the sample solution with distilled water

### Standard solution

One ml of zinc nitrate (1000 ppm) was pipetted in a volumetric flask and made up to 100 ml with blank solution. Ten ml of this solution was then pipetted into another volumetric flask and made up to 100 ml with blank solution. This brought the zinc concentration in the solution to 1 ppm.

## Sample solutions

In all cases, the sample was diluted with distilled water by the number of times required to bring the zinc concentration in the sample solution to within the bottom and top set limits ie within the linear range of the zinc calibration curve.

## Analytical procedures

The blank solution was first aspirated to set the lower end of the linear concentration range. The standard was then aspirated to set the upper end of the concentration range. This was followed by aspiration of the sample solutions. The results obtained were converted to weight of zinc dissolved per unit area of sample immersed in the solution using the following equation:

$$Zw = VX/KAC \quad 3.4$$

where

$Zw$  = weight of zinc dissolved per unit area  $\text{mg/mm}^2$ )

$V$  = volume of solution used (ml)

$X$  = zinc concentration measured in ppm

$K$  = number of ppm of zinc in one litre of distilled water containing 1g of zinc

$A$  = estimated area of sample immersed in the solution ( $\text{mm}^2$ )

$C$  = number of ml in 1 litre

### 3.7 ELECTROCHEMICAL STUDIES

A Princeton Applied Research microprocessor controlled Corrosion Measurement System, Model 350, was used for these studies. The microprocessor controls the program to be applied to the specimen as well as the nature and frequency of the measurements. It additionally makes possible interactions between the operator, the controls, and the display panel. This interaction aids and directs the operator in setting up the equipment for an analysis or playback.

Figure 3.1 is a schematic illustration of the arrangement of the test cell. It consists of two beakers; one containing the test solution and the other containing salt bridge solution. The bridge solution was saturated KCl bridged to the test solution by an inverted 'U' shaped glass tube filled with conductive gel consisting of a mixture of 2.5% Agar, 1% potassium nitrate and 96.5% deionised water. The test electrode (sample) and the counter electrode, which in this case was platinum wire, were immersed in the test solution whilst the reference electrode was immersed in the bridge solution.

The solutions used in these studies were those described in section 3.3. The experiment was performed under aerated condition and at room temperature of 25°C. Appreciable care was taken in preparing the samples to ensure that there was no galvanic effect and that the same area was exposed in the solution in each case.

Samples were degreased in acetone for two minutes and chemically cleaned in AC51 for 1 minute. After cleaning all samples were rinsed thoroughly in deionised water for two minutes before making electrochemical measurements. A fresh portion of test electrolyte was used for each sample.

### 3.7.1 POTENTIODYNAMIC ANODIC POLARISATION

This is the characterization of a metal specimen by its current-potential relationship. The specimen is forced to act as an anode so that it corrodes or forms a passive coating. These measurements are used to determine corrosion characteristics of metal specimens in the environment of interest. A complete current-potential plot of a specimen can be determined in a few minutes. Hence, investigations of passivation tendencies and effects of inhibitors or oxidizers on specimens can be performed easily and quickly. This permits comparison of the corrosion and passivation characteristic of different metals and environments and enables compatible specimen-environment combinations to be chosen to provide long service life. Potentiodynamic anodic polarisation plots can yield important information such as:

- (a) The ability of the material to passivate spontaneously in the particular medium.
- (b) The potential region over which the specimen remains passive.
- (c) The corrosion rate in the passive region.

Polarisation experiments were performed over the range -1.5V to +1.5V and using an automatically controlled scanning rate of 25mV/s.

### 3.7.2 POTENTIOSTATIC SCAN

In this technique, the current is measured periodically with constant potential applied to obtain a plot of current versus time. This gives the rate of current increase or decrease and hence indicates the rate of passivating film formation or anodic dissolution rate. The potentiostatic scan was performed measuring current at intervals of 1 second for a time of 3 minutes, using the chromate and alkaline solutions. A constant polarisation potential of + 1.5V was used.

### 3.7.3 LINEAR POLARISATION

The electrochemical technique of Linear Polarization is another method of measuring corrosion rates. The technique is performed by applying a controlled-potential scan over a small voltage range, typically -25mV to +25mV with respect to  $E_{\text{corr}}$ . The resulting current is linearly plotted versus potential. The slope of this potential-current function at  $E_{\text{corr}}$  is the Polarization Resistance which is used, together with the Tafel Constants, to determine  $I_{\text{corr}}$ . Figure 3.2 shows a typical polarization resistance plot.

Linear polarisation is an extremely rapid procedure and thus makes linear polarisation useful for less rigorous

experiments, such as qualitative evaluation of inhibitors. Additionally, since the applied potential is never far removed from the corrosion potential, the surface of the specimen is not materially affected by the experiment, and thus can often be used for other studies. In the present work all samples were scanned over a range of 20 mV either side of the corrosion potential ( $E_{\text{corr}}$ ). A stable  $E_{\text{corr}}$  was established before starting the polarization scan which was done at a scan rate of 0.166 mV/second in all cases.

#### 3.7.4 REST POTENTIAL MEASUREMENT

Figure 3.3<sup>(69)</sup> shows the Schematic diagram of the potential-time apparatus. The potential was recorded on a single pen chart recorder and a saturated calomel electrode was used in conjunction with a salt bridge as a reference electrode. Different samples were treated in solutions detailed in section 3.3 for the time chosen.

### 3.8 EXAMINATION AND ANALYSIS OF SAMPLE SURFACES

#### 3.8.1 SURFACE ROUGHNESS

The Talysurf is a convenient method of measuring surface roughness. Schematic layout of the Taylor-Hobson Talysurf<sup>(132)</sup> which was used for this work is shown in figure 3.4. It has a measuring head which consists of a stylus and a shoe (T) which are drawn across the surface under test by an electric motor and gear box. The arm carrying the stylus forms an armature which pivots about

the centre piece of a stack of E shaped stampings and around each of the outer pole pieces is a coil carrying an a.c current. As the armature pivots about point M it causes the air gaps to vary and thus modulates the amplitude of the original a.c current flowing in the coil. These form part of bridge circuits, hence the output consists of modulation only. This modulation is fed to an amplifier which operates a pen recorder to produce a permanent record and a meter to give a direct numerical assessment. This instrument incorporates an integrating device which analyses the information to give a result in terms of centre line average (CLA)<sup>(132)</sup>. This is defined as the average height from a main line of all ordinates of the surface regardless of sign; i.e.-

$$CLA (R_a) = h/n \quad 3.5$$

where h = height of ordinates

n = number of ordinates

For each sample, readings were taken along both the 'x' and 'y' axes and an average of five readings on each axis were taken. A cut-off length of 2.5 mm was chosen and different scales were used to suit the anticipated roughness.

### 3.8.2 SCANNING ELECTRON MICROSCOPY (SEM)/ENERGY DISPERSIVE X-RAY ANALYSIS (EDXA) TECHNIQUES

In the Scanning Electron Microscope (SEM) a beam of electrons is focused to a very small spot, and scanned over the area to be examined. Secondary electron current

emitted by the sample is collected, amplified and used to modulate the brightness of a cathode - ray tube (Video screen) the spot of which is moving in synchronism with the primary electron beam. If any property of the sample causes the secondary electron current to change from point to point, the image recorded on the cathode - ray tube will constitute a map of the variation of this over the area of the sample being scanned. Thus scanning electron microscopy is very sensitive to the topography of a sample.

If an X-ray energy dispersive spectrometer is coupled with the SEM it is possible to perform microanalysis with a resolution equal to  $1\mu\text{m}^3$ .

Samples to be examined were cut to about 5mm square and mounted on conductive metal stubs. In order to make the samples conducting, they were either carbon or gold coated. Samples, were examined, analysed and their spectra plotted.

### 3.8.3 X-RAY PHOTOELECTRON SPECTROSCOPY (XPS)/AUGER ELECTRON SPECTROSCOPY (AES) TECHNIQUES

This is the study of electrons ejected from a sample's molecular or atomic orbitals due to ionization by a beam of monoenergetic photons. X-ray Photoelectron Spectroscopy (XPS), more commonly known as electron spectroscopy for Chemical analysis (ESCA) is used for surface analysis by irradiating a sample with monoenergetic soft x-rays

and energy analysing the electron emitted. Mg K $\alpha$  x-rays (1253.6 eV) or Al K' x-rays (1486.6 eV) are ordinarily used. These photons have limited penetrating power of the order of 1-10 micrometers in a solid. Although ionization occurred to a depth of a few micrometers only those electrons that originate within tens of Angstroms below the solid surface can leave the surface without energy loss. It is these electrons which produce the peaks in the spectra.

The emitted electrons have kinetic energies (KE) given<sup>(133)</sup> by

$$KE = hv - BE \quad 3.6$$

where  $hv$  = the energy of the photon,  $BE$  = binding energy or ionization energy of the atom for the particular shell involved. The quantity measured most directly in photoelectron spectroscopy is the ionization energy for the removal of electrons from different molecular or atomic orbitals. Since ionization energies are characteristic properties of atoms and molecules, the method therefore provides a direct means of chemical analysis. The spectra are direct representations of the molecular orbital energy diagrams.

Auger Electron Spectra are obtained from the electrons emitted due to the relaxation of the energetic ions left after photoemission. Figure 3.5 (a&b) shows both the Photoelectron process and the Auger process. In the later case an outer electron falls in to the inner orbital vacancy, and a second electron is emitted, carrying

off the excess energy. The Auger electron process kinetic energy is equal to the difference between the energy of the initial ion and final ion, and is independent of the mode of the initial ionization. Thus, Photoionization normally leads to two emitted electrons, a photoelectron and an Auger electron.

Figure 3.6 is a schematic illustration of the ESCA (model 550) system used for this work. It shows the relationship of the major components, including the electron energy analyser, the x-ray source, and the ion gun used for sputter-etching. The samples were cut to measure exactly 15 x 7 mm so as to cover completely the sample probe area in order to ensure accurate results. The samples were mounted carefully on the end of a sample introduction probe at an angle of  $50^{\circ}$  with respect to the analyser axis as shown in figure 2.6

During the analysis, low resolution with a scanning width of 1250 K E, starting from 150 to 1400 K E, was used to obtain the whole spectra while medium resolution with scanning of 25 K E was used for the specified peaks such as C, Zn and Cr. The carbon peak was taken as a standard and hence used for calibration of the spectra throughout the analysis.

### 3.9 POWDER COATING PROCESS

The powder spraying equipment was installed in a fume cupboard the walls of which were covered with polyethene

sheeting. The powder equipment manufactured by Controsion Ltd was made up of three main units:

- (i) The generator
- (ii) The powder spray gun
- (iii) The powder feed system

(i) The generator provides the high tension source required to charge the powder particles. It is a PET - SRF series 6000 generator which is designed around a Piezo - electric solid - state transformer and has a self regulating field built into its design. To allow maximum penetration of recessed areas and improved quality of finish, the SRF series is designed so that as the discharge electrode is moved closer to earth, the intensity of the electrostatic field reduces proportionately. It uses -ve corona charging system

A safety device is built into the generator so that it is switched off immediately should the operator touch the discharge electrode.

(ii) The powder spray gun is a hand held gun with a trigger mechanism to begin and cease operations. Powder is fed to the gun via a powder feed unit and is transported by medium pressure ( $27.6 \text{ N/m}^2$ ) compressed air to the rear of the gun. As the powder moves forward it comes into contact with the electrostatic field produced by the discharge electrode which runs up the inside of the powder tube half way up the gun. At the front of the gun is a discharge disc which is designed to prevent the

powder moving forward entirely by the kinetic energy obtained from the compressed air flow. This improves covering efficiency. The powder should move towards the work piece as a slow moving cloud.

(iii) The powder feed system consists of a vibrating hopper which is powered by pulsing compressed air ( $27.6 \text{ N/m}^2$ ) via a solenoid which is controlled by the trigger of the powder spray gun. The air supply is split into two as it enters the hopper; one tube goes to the spray gun while the other powers the vibrator.

Jigging was achieved by holding the sample with a crocodile clip. A complete circuit was obtained by connecting the clip to earth. To ensure that the same amount of powder was supplied in each case the same alternate vertical and horizontal movements of the spray gun were made across each face of the pannel while pausing for a few seconds between each movement to allow the pressure to rise up to the set value of  $550 \text{ kN/m}^2$ . For thin coatings, ten alternate movements were made on each side and twenty for thick coatings. Curing of the coated pannels was carried out in a thermostatically controlled oven at a temperature of  $200^\circ\text{C}$  for 15 minutes.

### 3.10 POWDER FLOW STUDIES

These studies were carried out using a Hot-stage Microscope which is made up of following units -

(a) Variac - this unit provides and controls the voltage applied to the hot-stage;

- (b) Hot-stage - this is the heat source that provides the heat to melt the powder on the sample;
- (c) Automatic exposure and lighting units;
- (d) Camera - used for photographing the melt flow of the powder;
- (e) Microscope - used for viewing the powder particles, the melt and the flow;
- (f) Chart recorder for monitoring temperature;
- (g) Thermocouple which is spot welded to the sample and connected to the chart recorder.

Samples used for these studies were cut to measure 50 mm long by 20 mm wide. They were pretreated as required before applying the powder with a fine brush and a constant heating rate of 5°C/min was applied at all times. The powder was applied to cover initially, approximately 20% of the exposed area (as viewed through the microscope aperture). The heating rate was achieved by pre-plotting a straight-line graph of temperature against time on the chart recorder and manipulating the Variac so that the trace of the chart recording pen followed this straight line. The Chart recorder was set to zero at room temperature and heating was applied up to 200°C mark on the chart. With the aid of the camera and the automatic exposure unit, photographs of the melting powder were taken every 5°C. The proportion of the area covered at 5°C intervals was measured with the aid of the Tektronix void measuring computer. The areas covered by powder in each photograph were circled round with the computer's

pencil head. The computer then calculated and printed out the proportion of the area covered. The results were later corrected for errors due to variation of area covered when the powder was applied initially, using a correcting factor as defined below

$$A = 20a/i \quad 3.7$$

Where

A = the actual proportion of the area covered,

a = the measured proportion of the area covered,

i = the actual initial proportion of area covered by the applied powder.

### 3.11 CORROSION TESTS

#### 3.11.1 ACETIC ACID SALT SPRAY TEST (ASTM B 287-74) (Reapproved 1980)

The aim of this test was to subject the duplex polyester-zinc coatings to a prolonged period of exposure in a standard corrosive atmosphere. This should help evaluate the coating's resistance to aggressive environments and to lateral corrosion when the polymer film is penetrated through to the zinc coating.

The temperature of the salt spray cabinet was maintained at  $35 \pm 3^\circ\text{C}$  whilst the spray pressure was kept between 7 and 17  $\text{N/cm}^2$  (10 and 25 psi).

The corrosive medium was made up by dissolving 1kg of sodium chloride in 19 l of distilled water; (5% sodium

chloride, 95% distilled water). The pH of the solution was reduced to between 3.0 and 3.1 by adding acetic acid.

#### Procedure

Two intersecting diagonal lines were scored on one side of the test panel through the polymer film, to the zinc. The panels were suspended in the the cabinet at 30 degrees from the vertical. The flow of the corrosive medium and of the compressed air to the nozzle were adjusted to give a fine spray. Two mist collectors were employed, one near to the nozzle and the other away from the nozzle.

Funnels of 10 cm diameter were fitted to the mist collectors and the condensate collection rate measured to ensure that it was within the specified limits of 1-2 ml/h. Daily examination of the samples under test in the spray cabinet was made during the period of the test. After the selected test time, the samples were removed and rinsed by single immersion in warm water. They were then dried in a warm air stream at a temperature of less than 38°C.

TABLE 3.1 Laboratory prepared conversion coating solutions

Code	Composition M/l	pH	Group
L1	CrO <sub>3</sub> 0.12, NaCl 0.30	1.2	
L2	CrO <sub>3</sub> 0.12, NaF 0.10	3.4	1
L3	CrO <sub>3</sub> 0.03, NaCl 0.07	1.2	_____
L4	CrO <sub>3</sub> 0.03, NaCl 0.07, NaOH 0.03	5.5	
L5	CrO <sub>3</sub> 0.03, NaOH 0.03	6.1	2
L6	CrO <sub>3</sub> 0.12, NaCl 0.30	5.5	_____
L7	CrO <sub>3</sub> 0.12, NaCl 0.30, NaOH 0.12	5.8	3
L8	CrO <sub>3</sub> 0.6, NaOH 1.25	13.0	_____
L9	CrO <sub>3</sub> 0.6, NaOH 1.25, NaCl 0.30	13.0	4
L10	CrO <sub>3</sub> 0.6, NaOH 1.25, NaF 0.1	13.0	
L11	CrO <sub>3</sub> 1.0, NaOH 1.0	5.5	_____
L12	CrO <sub>3</sub> 1.0, NaOH 1.25	7.0	5
L13	CrO <sub>3</sub> 1.0, NaOH 2.0	10.0	
L14	NaOH 0.000001	8.0	_____
L15	NaOH 0.00001	9.0	6
L16	NaOH 0.0001	10.0	
L17	NaOH 0.001	11.0	_____
L18	NaOH 0.01	12.0	7
L19	NaOH 0.1	13.0	_____
L20	NaOH 1.0	14.00	8

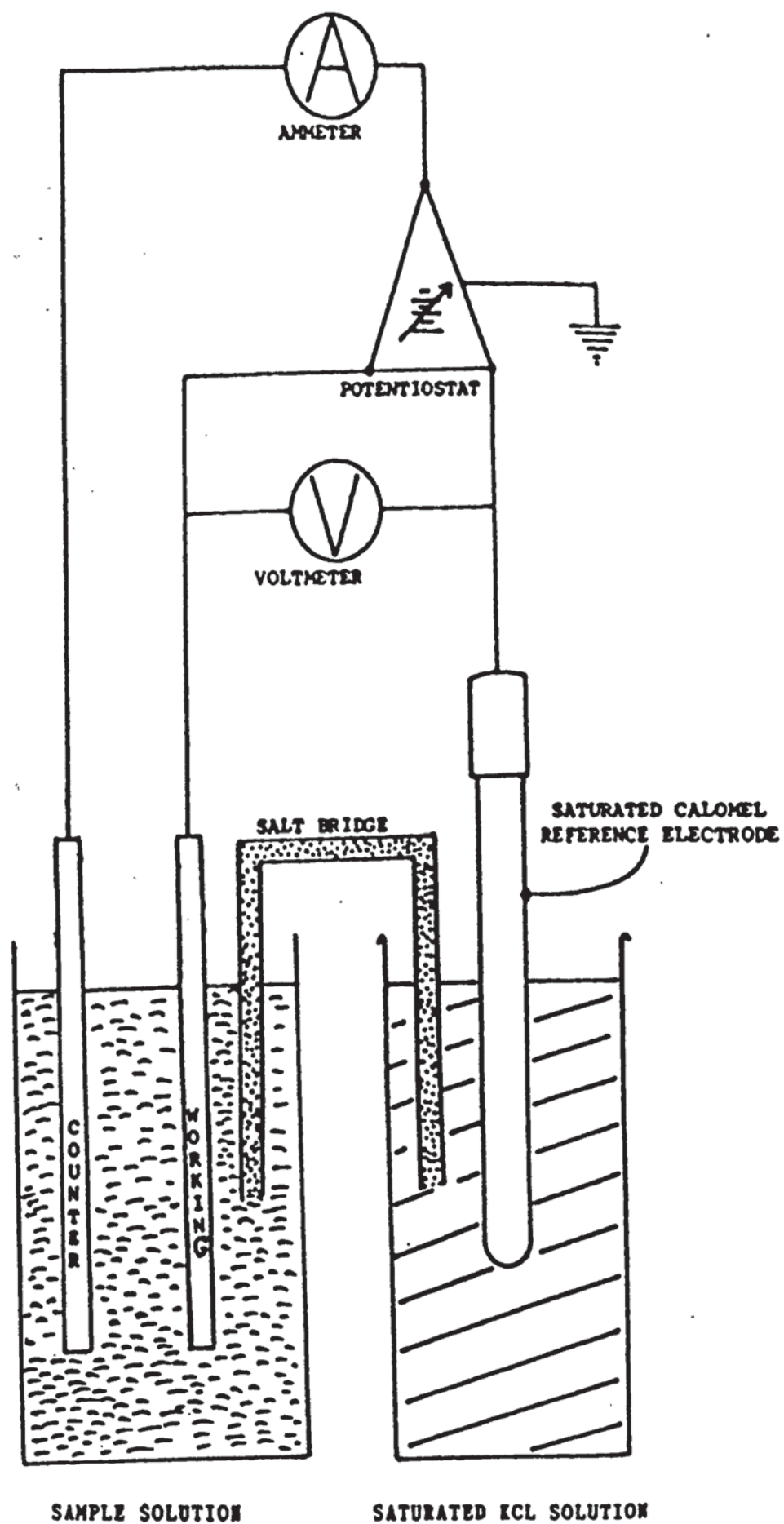


Figure 3.1 Schematic arrangement of the electrochemical test cell

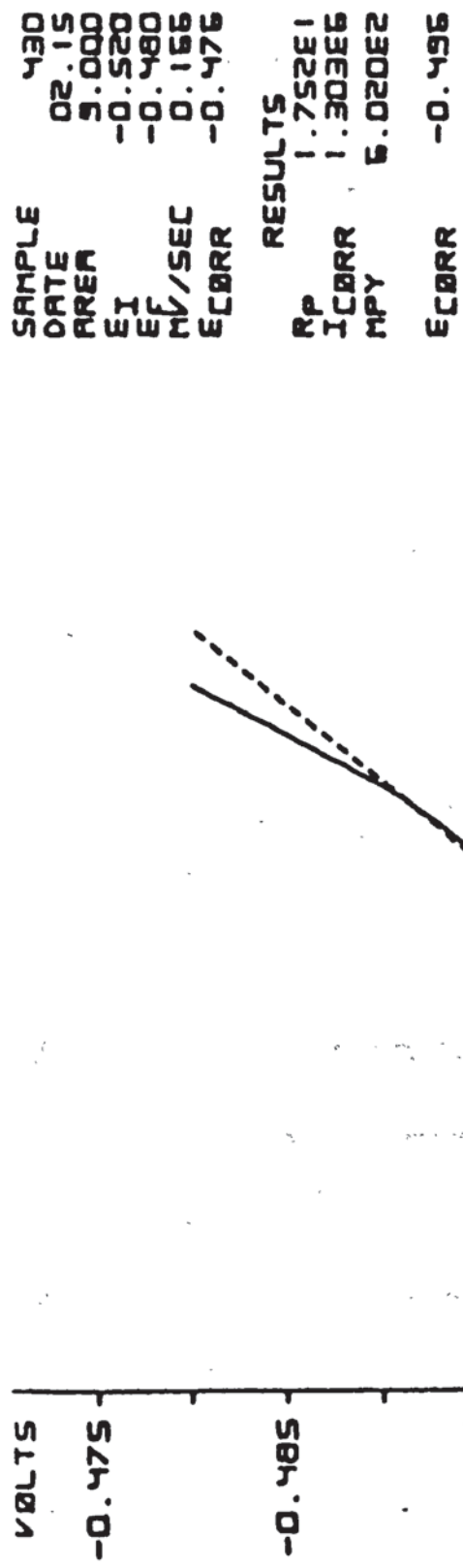


Figure 3.2 Typical polarisation resistance plot

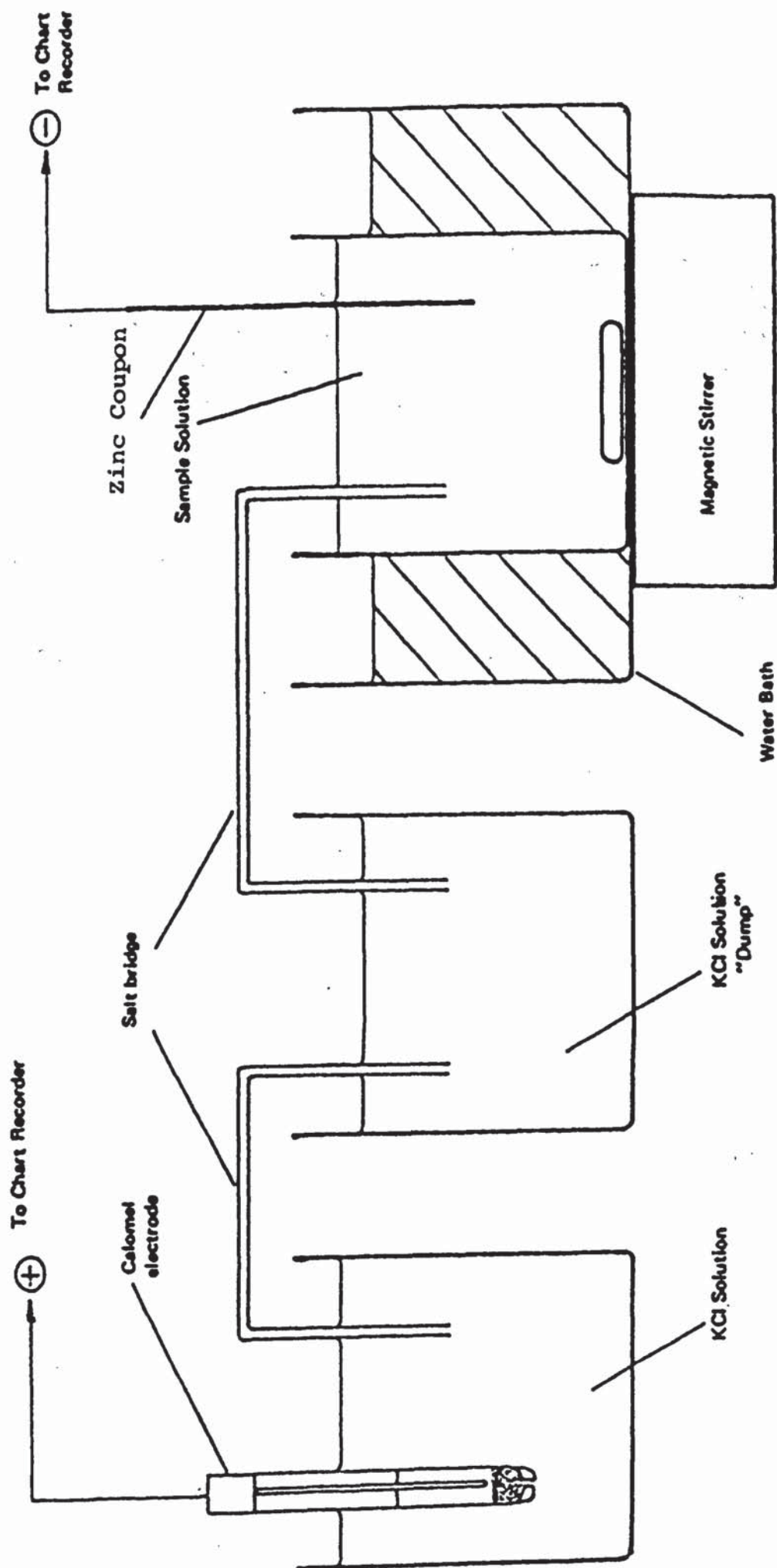


Figure 3.3 Potential - time equipment set-up



Illustration removed for copyright restrictions

**Figure 3.4 Schematic layout of Talysurf<sup>(132)</sup>**

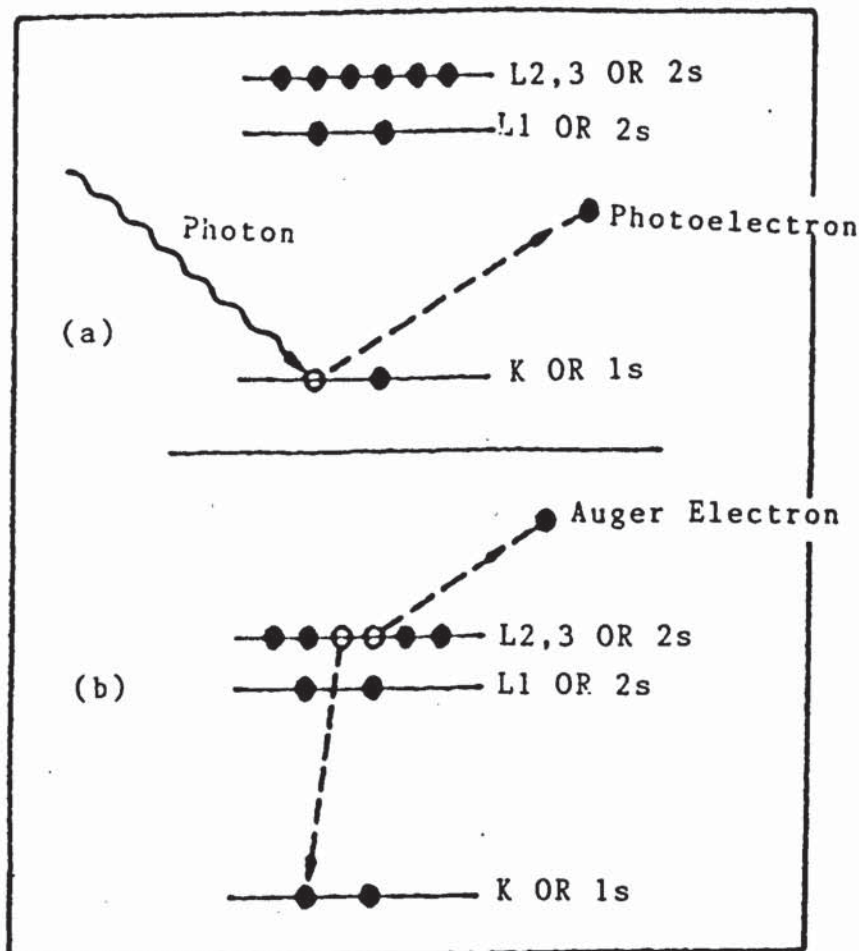


Figure 3.5 Schematic illustration of  
 (a) X-ray photoelectron spectroscopy (XPS)  
 (b) Auger electron spectroscopy (AES)  
 techniques

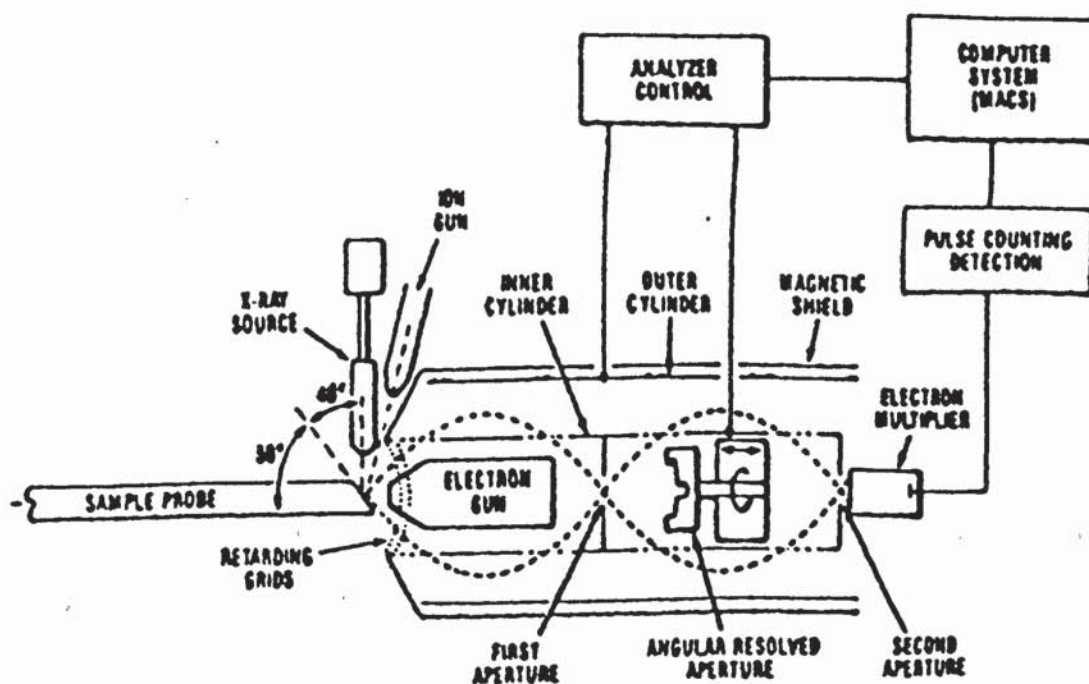


Figure 3.6 Schematic illustration of major components  
 of the XPS (ESCA model 550) system

## 4 THE NATURE OF DEFECTS FOUND IN POLYESTER POWDER FILMS ON ZINC COATED STEEL

### 4.1 INTRODUCTION

It has been reported that when powder coating steel substrates, cratering and pinholing defects often occurred and were usually evident immediately after the powder had been cured. Some authors<sup>(101,134,)</sup> have attributed the cratering defects to surface contamination, powder particle clustering or the absence of flow control agents in the powder, whilst others<sup>(87)</sup> link it with back ionisation when using +ve corona charging of the powder. Pinholing has been attributed to air or vapour entrapped within powder particles<sup>(134)</sup> and back ionisation when using -ve corona charging of the powder<sup>(87)</sup>.

On zinc substrates the situation is more complicated since the surface composition and properties of the zinc depend on the method of coating treatment used, viz batch hot-dip galvanizing after fabrication, continuous coated strip (e.g. Galvatites), electroplating (e.g. Zintec) and spraying with zinc powder. Pinholing has been associated with defects in the galvanized coating some way from the defect in the polymer film, particularly in the case of batch hot-dipped samples, and it is recommended that this type of material be degassed by preheating above the powder curing temperature after pre-treatment<sup>(26)</sup>.

Industrially, these defects continue to appear. This

presents difficulties to the firms associated with powder coating as claims and counter claims are constantly made by companies and their customers regarding the incidence of these defects. It was, therefore, decided to investigate, in detail the nature and causes of these defects. An ideal way of carrying out these investigations was to analyse defects found on commercially produced samples and then attempt to reproduce them in the laboratory. The samples used for the investigation include:

- (i) Commercially produced polyester powder coated zinc-electroplated steel sheet.
- (iia) Commercially produced polyester powder coated, hot-dipped galvanized steel sections.
- (iib) Commercially produced, polyester powder coated, hot-dipped galvanized steel sections, of different source to (iia).
- (iii) Laboratory prepared samples.

#### 4.2 ANALYSIS OF DEFECTS ON POLYESTER POWDER COATED ZINC ELECTROPLATED STEEL SHEET (SAMPLE i)

A commercially produced, polyester powder coated zinc electroplated steel component, containing defects in the powder coating, was made available. A similar component in a state prior to powder coating was also available. The samples were first examined visually. The defects appeared to be concentrated on one side of the sample.

Examination of the zinc electroplate in the SEM showed it to be sound and EDXA revealed a trace of Cr suggesting

that a chromate conversion treatment had been applied. Cross section examination revealed a coating thickness of approximately 7  $\mu\text{m}$ .

Figs. 4.1(a) & (b) are SEM micrographs of two typical defects found in the powder coating. EDXA of the surrounding polymer revealed Ti with traces of Al, Si and S presumably arising from the pigment used in the polyester powder. Analysis of the particles found in the defect shown in Fig 4.1(a) revealed large amounts of Cl, K and Zn. From this it was deduced that these particles were various corrosion products of zinc, e.g. zinc hydroxide and various chloride salts of potassium and zinc arising from chloride contamination of the electroplate prior to powder coating. Fig 4.1(b) shows that complete powder flow has been prevented by the presence of particulate matter. EDXA of these particles and similar debris found in other defects revealed high concentrations of Si, Ca, Al, and K, suggesting that the particles were sand or grit.

Fig 4.2(a) is a cross-section of one of these defects showing that film flow has been halted, thus preventing complete cover of the surface. The mechanism of film formation involves coalescence and spreading of molten powder on the substrate (section 2.3.6) and if this process is not complete, craters will be present in the final film.

Corrosion products, sand or grit will inevitably inter-

fere with wetting of the surface but probably of more importance is the fact that although polymer will enclose the debris (see for example Fig 4.2(b)) there is such an increase in viscosity that complete flow is not possible.

#### 4.3 ANALYSIS OF DEFECTS ON A POLYESTER POWDER COATED HOT-DIPPED GALVANIZED STEEL SECTION (sample iia)

A commercially produced polyester powder coated steel section containing numerous defects was made available for examination. An optical macrograph of the surface is shown in Fig 4.3. Two types of defect are clearly evident viz, cratering and pinholing, both of which were of variable size and randomly distributed. Since both types of defect were present in the same sample, it is difficult to explain how a particular type of defect can be related to the polarity of the charged powder as reported<sup>(87)</sup> A defect free sample was cut out, mounted in cold-setting bakelite for cross-section examination, polished and etched in Palmerton's reagent. Optical microscopy, Fig 4.4, revealed a galvanized coating typical of that found when galvanizing a silicon containing steel. The galvanized coating was of variable thickness from 25-100um. The thicker regions were composed of outbursts of the zeta phase (Fe-Zn alloy), which in some cases had consumed all the zinc so that the surface in these areas was Fe-Zn. The polymer coating was between 150-200um thick, having flowed during heating so that irregularities of the galvanized layer were not evident at the surface of the polymer layer.

#### (a) Cratering defect

Fig 4.5 is an SEM micrograph of a typical defect, and it is evident that powder has not flowed over part of the galvanized layer. There is no evidence of grit or corrosion products so the reasons for this lack of flow may not be the same as for the electroplated sample. EDXA analysis of this and other defects of similar type have shown:

- (i) that the polymer contains Ti, Ca and traces of Si and Al, presumably from the pigment;
- (ii) that islands of polymer may exist within the defect;
- (iii) that P and some Cr is present, presumably from the pretreatment;
- (iv) that Zn, Fe and Pb are detected because of the underlying galvanized coating.

Neither the SEM micrographs, Fig 4.5, nor cross-section examination of the defect, Fig 4.6, shows any evidence of debris hindering flow, and the reason for poor flow must be different from that for the electroplated sample. It was thought that the presence of Pb at the surface may be a problem and so an attempt was made to determine whether Pb is present only in the areas not covered by polymer. This was done by attempting to remove the polymer from around the defect using an organic solvent and then analysing these areas. The solvents utilised were nitrobenzene and dichloromethane. Total removal of the poly-

mer was not achieved but analysis was still possible and revealed the presence of Pb in areas where there were no defects. Use of techniques such as ESCA/AES may prove more valuable for further study.

It is possible that the lack of flow may be associated with the roughness of the surface, particularly at outbursts of zeta e.g. on the right in Fig 4.6. It has been found<sup>(135)</sup> that surface characteristics such as roughness and surface treatments may affect the flow of molten powders on metal surfaces.

#### (b) Pinholing

Fig 4.7 shows quite clearly the presence of voids in the polymer coating and the collapsed form of these gives rise to the pinholing defects shown in Fig 4.3. Observation of a large number of defects of this type suggests that they are located in regions where the galvanized coating is thinnest. Flow must occur simultaneously with at least partial displacement of air and vapour from between powder particles. Release of air is retarded if powder melts at the air interface to form a continuous layer. Also, entrapped air or vapour will raise viscosity and interfere with flow. Release times for removal of air bubbles may be quite excessive<sup>(108)</sup> and it has been suggested that there is a critical film thickness above which bubbles will not escape<sup>(109)</sup>. The origin of the gas may be entrapped air, condensation products from curing, dehydration of the conversion coating film or

moisture trapped in the troughs or irregularities on the very rough surface. This would be most likely at depressions between outbursts of zeta and hence the observation that they appear to be associated with the thinner parts of the zinc coating

#### 4.4 ANALYSIS OF DEFECTS ON A POLYESTER POWDER COATED HOT-DIPPED GALVANIZED STEEL SECTION (SAMPLE iib)

Another sample of powder coated galvanized steel section which contained defects was submitted for examination. Sections were cut from the sample and cross-sections examined using optical microscopy and scanning electron-microscopy together with x-ray analysis.

##### Results of optical microcopy examination

The surface appearance is shown in figure 4.8 at low magnification. To the naked eye it was apparent that some of these defects were orientated in straight lines. Figure 4.9 shows these defects to be of the crater type and to have a diameter of 1.16 mm.

Cross-sections through a 'good' area illustrate that the thickness of the galvanized layer is very uneven but that the powder coating has been able to flow and provide a reasonably smooth outer surface. However, the powder coating is inevitably thin at regions where peaks occur in the galvanized layer eg figures 4.10 (a-c). Figure 4.10 (c) illustrates a region which has also been covered by the powder coating and which would not appear as a

defective area immediately after coating. However, the cross-section shows that part of the galvanized layer is detached and so poor protection would be likely to result. Figures 4.11 (a&b) show other examples of defects which have resulted in thin powder coatings due to irregular growth of the galvanized layer.

### Crater region

A cross-section through a crater is shown in figure 4.12. and table 4.1 shows the thickness of both zinc and polymer coatings at and around this crater.

TABLE 4.1 Thickness of zinc and polymer coatings at and around a crater (figure 4.12)

Position where

thickness measured	Zinc (mm)	Polymer (mm)
Centre of crater	0.028	0.0
Just right of crater	0.174	0.026
Just left of crater	0.200	0.019

The micrograph (fig.4.12) illustrates that a pit up to 160 um deep was present in the galvanized layer and that the powder had been unable to flow into the cavity during baking. This is because, in addition to the problem of covering a rough zeta outcropping surface, it would be difficult for electrostatically sprayed powder to penetrate into holes as large as the ones shown in the galvanized layer - figure 4.12. This would be as a direct result of Gauss' Law<sup>(82)</sup>; no field lines can exist, nor penetrate, areas that approximate to being surrounded by

the earthed metal boundary of the workpiece. This effect is known in powder coating as the Faraday cage effect. As illustrated in figure 4.13, most lines of electric field will terminate on the peaks of the flared zeta layer. With low gun velocity, particles will tend to follow more predictably the field line pattern, resulting in minimal penetration of the inside surface of the pit in the galvanized coating.

Figure 4.14 (SEM) illustrates the appearance of a crater viewed from the surface. It is evident that it is deep, as would be expected from the cross-section results.

Cross-sections of other defects are shown in figure 4.15 (a), (b) & (c) These essentially provide the same information as that shown by optical microscopy ie. uneven galvanizing, particles breaking away and pits in the galvanizing. All these features lead to problems at the powder coating stage.

The powder coating did not contain any porosity such as was observed in some of the other samples reported in the previous section.

#### 4.5 LABORATORY PREPARED SAMPLES

Samples of electroplated, continuous hot-dipped galvanized, batch hot-dipped galvanized and zinc sprayed steel were obtained in the form of thin sheet. A Talysurf was used to compare surface profiles by measuring centre line average values, CLA. These values are given in Table 2

where it can be seen that the zinc sprayed sample is very rough compared to the electroplated or continuous hot-dipped galvanized samples.

Specimens were cleaned using a proprietary acid cleaner and chromated for 2 min at 25°C in a laboratory prepared solution consisting of 12.0g/l CrO<sub>3</sub> + 17.4g/l NaCl and then coated with a white polyester powder. Some samples were degassed after chromating by heating to 220°C for 20 min, two different powder coating thicknesses were applied and the polymer cured by heating to 200°C for 15 min.

Visual examinations of the samples showed clearly the effect of different process parameters and substrates, the incidence of defects being given in Table 4.2.

TABLE 4.2 Incidence of Defects on Different Powder Coated Substrates

Zinc Substrate	Surface Roughness CLA (μ)	Not Degassed Coating Thickness 55-65μ	Not Degassed Coating Thickness 90-110μ	Degassed Coating Thickness 90-110μ
ELECTRO-PLATE	1.0	No Defects	Isolated Pinholes	No Defects
CONTINUOUS HOT-DIP	0.9	No Defects	Isolated Pinholes	No Defects
BATCH HOT-DIP	1.7	No Defects	Very Bad Pinholing	A Few Pinholes
SPRAY	>5	No Defects	Severe Pinholing & Cratering	A Few Pinholes

It was clearly evident that defects were absent when thin polymer films were applied. However these films do not comply with BS 6497 which requires a minimum film thickness of  $60\mu\text{m}$  on significant surfaces. In the case of the hot-dip galvanized and zinc sprayed samples the coating thickness could be as low as  $10\mu\text{m}$ . at the thickest points in the zinc coating (figure 4.16). These regions will have the minimum corrosion resistance. Coherent polymer films can be formed, as demonstrated in figure 4.16 even in the presence of Pb at the zinc surface and outbursts of zeta will not in themselves hinder the formation of good polymer films.

When thicker polymer films are applied the situation is quite different. It was evident that the incidence of defects increased quite markedly on the rougher zinc surfaces which suggests that release of gases from the polymer is more difficult from depressions in the zinc coating. An interesting point was that in the case of the hot-dip galvanized samples, pinholes were distributed in a pattern similar to that of spangle boundaries of the zinc substrate, suggesting nucleation of gas bubbles at grain boundaries. It would appear from these results that pinholing is influenced more by the surface roughness of the sample than by its metallographic structure and that the major source of vapour is from the dehydration of the chromate conversion coating. Degassing the samples after chromating reduced considerably the incidence of pinholing.

#### 4.6 CONCLUSIONS

(1) Two distinct types of defect in polyester powder coatings have been confirmed, these being craters and pinholes.

(2) Craters appear to result from impeded flow of the polymer film due to:

(a) entrapped corrosion products, dirt or gases in the case of electroplated samples and

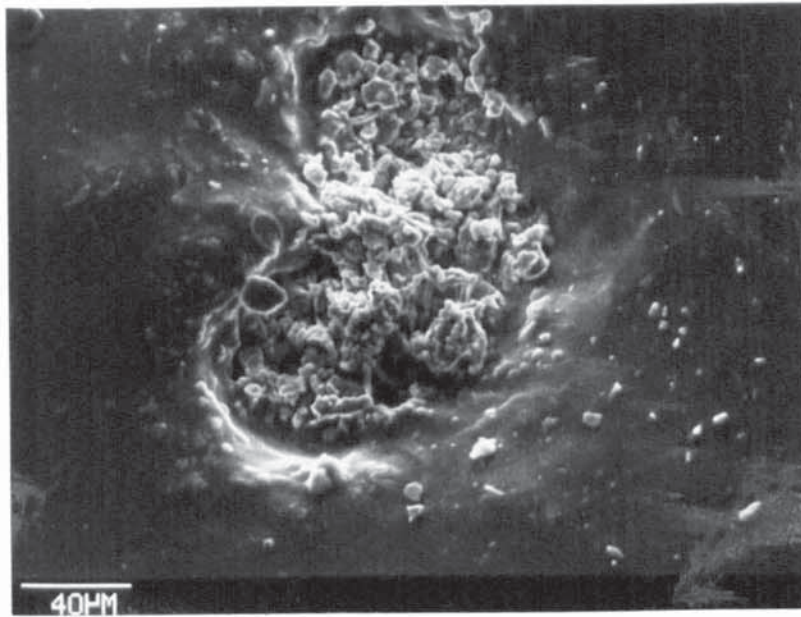
(b) defects (pits) in the galvanized layer in the case of hot-dip galvanized sections.

(3) Pinholes appear to result from the dehydration of the chromate conversion coating but their incidence is very dependent on the thickness of the polymer layer and the roughness of the zinc substrate. Thus zinc spray coatings and hot-dip galvanized coatings, with protruding outbursts of the zeta phase, are particularly susceptible. This problem is considerably reduced by degassing the chromate conversion coating prior to powder coating.

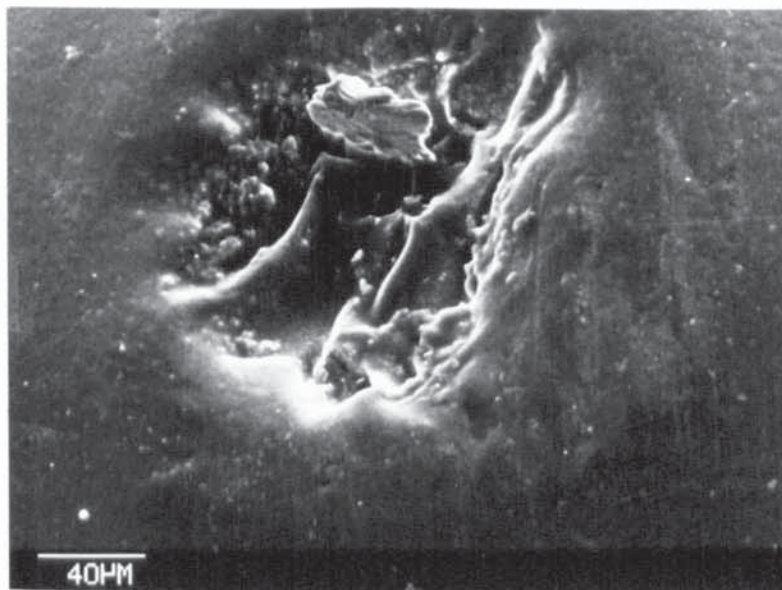
(4) In addition, batch hot-dipped galvanized sections revealed other unsatisfactory aspects such as

(a) uneven surface finish on the galvanizing resulted in uneven powder coatings, which may be very thin in places (not to BS 6497) and thus offer poor corrosion resistance and

(b) defects in the galvanized layer are covered but would be weak points in the powder coating.

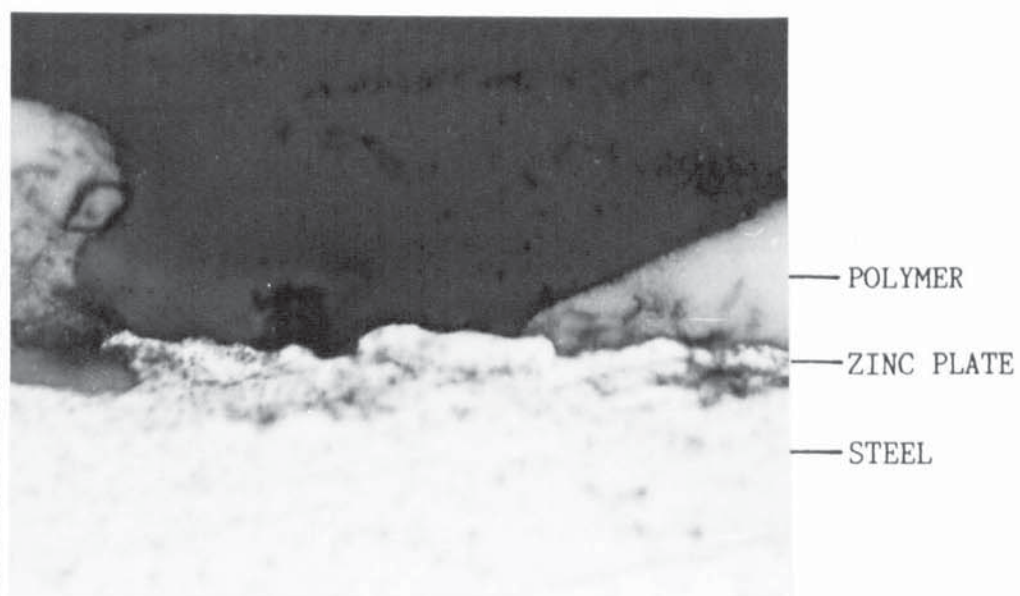


(a)

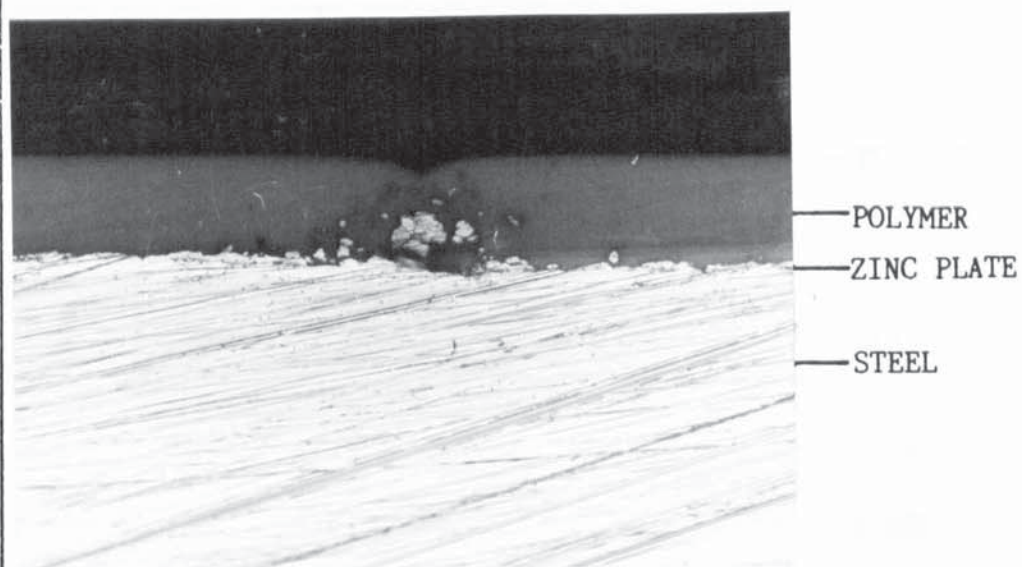


(b)

Figure 4.1 Scanning electron micrographs of crater type defects in the coating on electroplated zinc

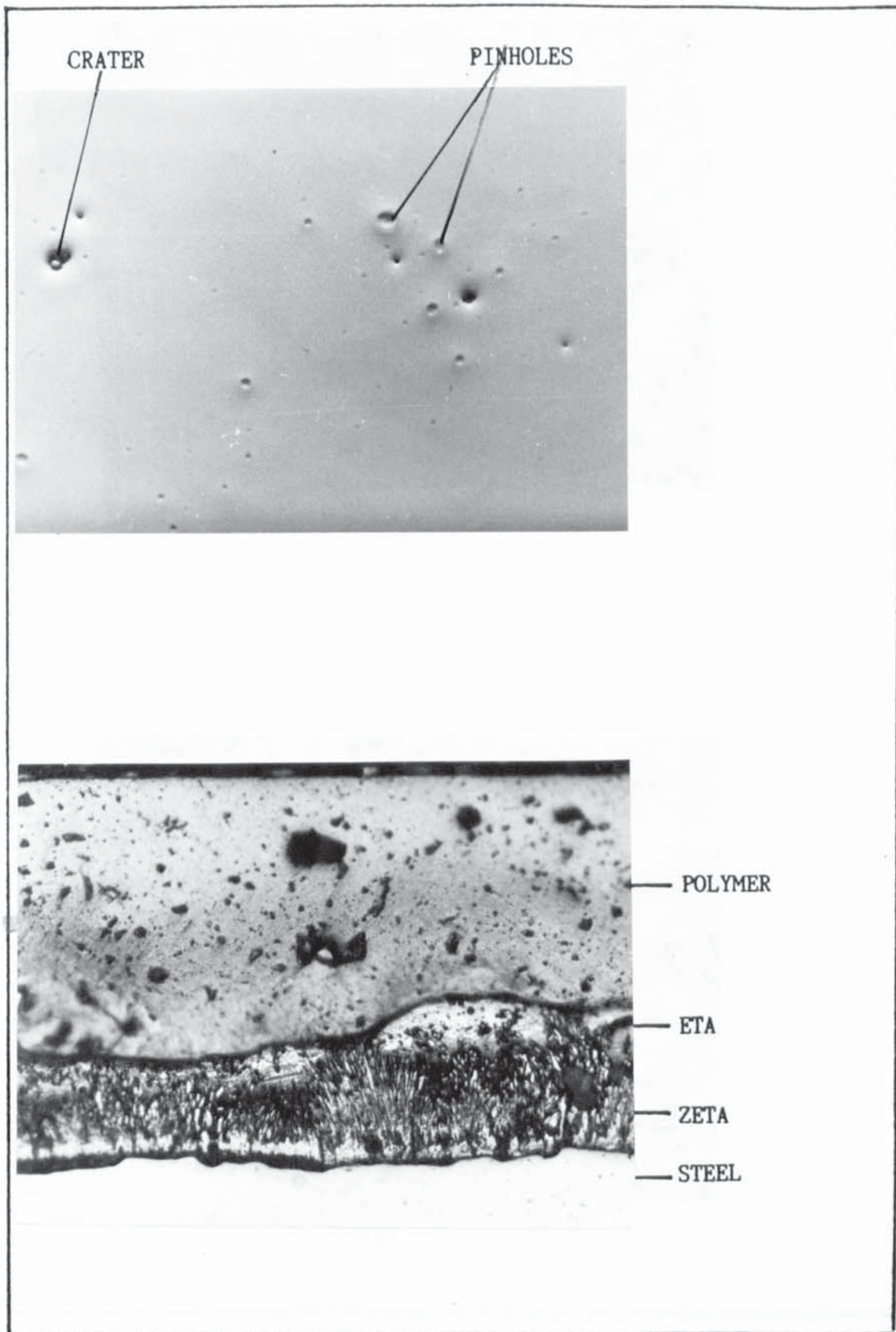


(a)



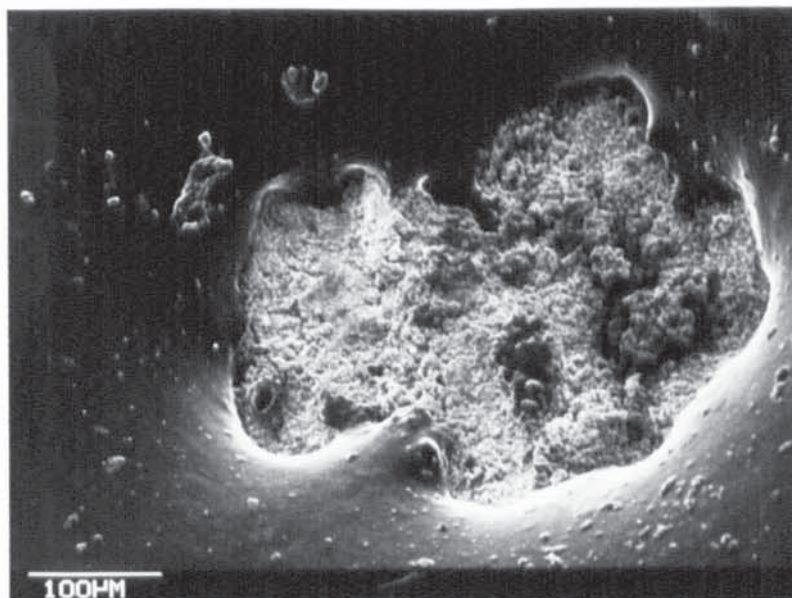
(b)

Figure 4.2 Optical micrograph of cross-section of crater defect showing incorporation of grit in powder coating on electroplated zinc  
 (a) at the defect (x500)  
 (b) just prior to defect (x220)

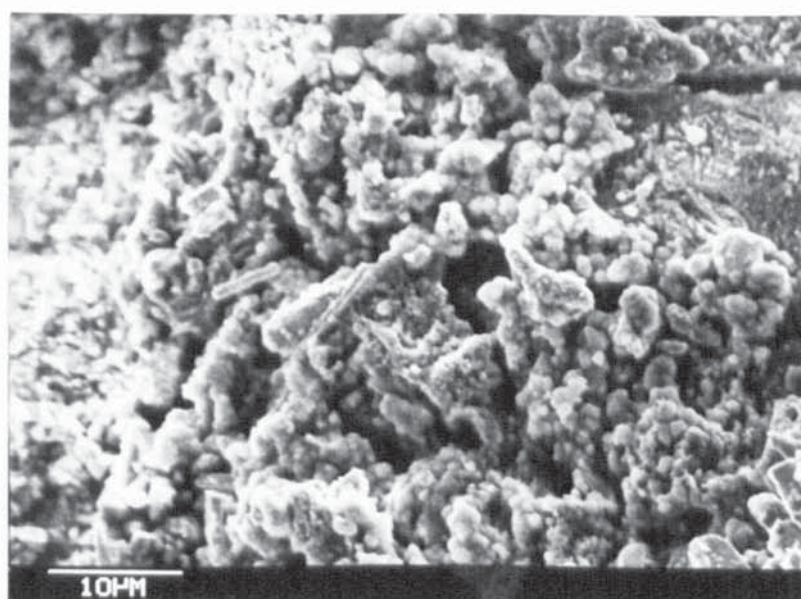


TOP: Figure 4.3 Optical micrograph of powder coated hot-dip galvanized specimen showing defects (x3.8)

BELOW: Figure 4.4 Optical micrograph of cross-section through the powder coated hot-dip galvanized section (x220)

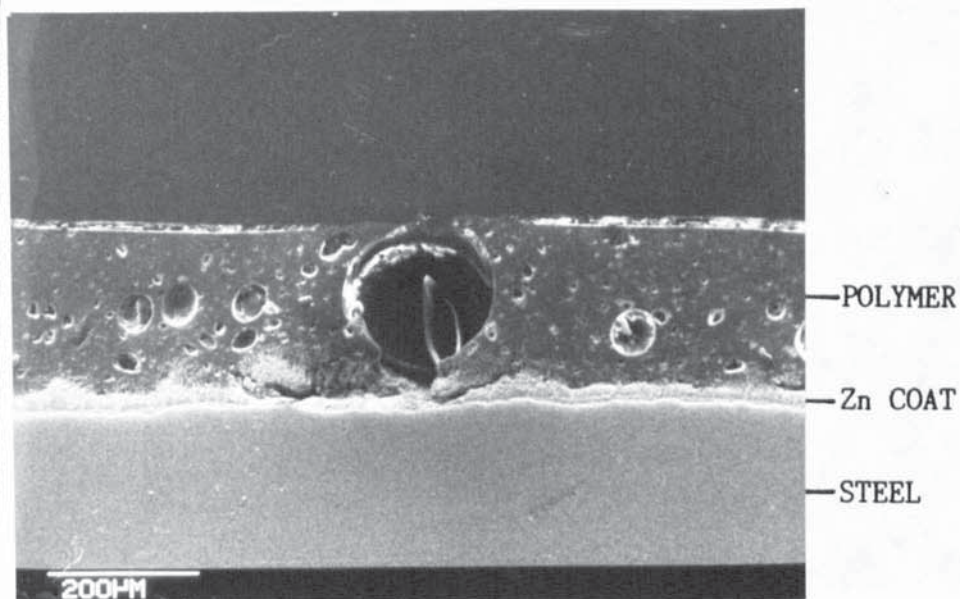
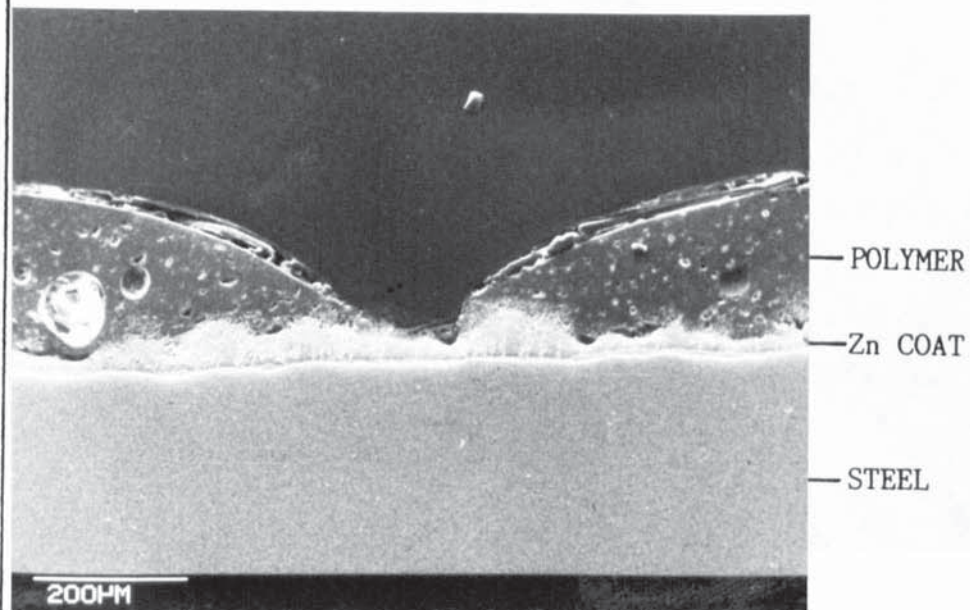


(a)



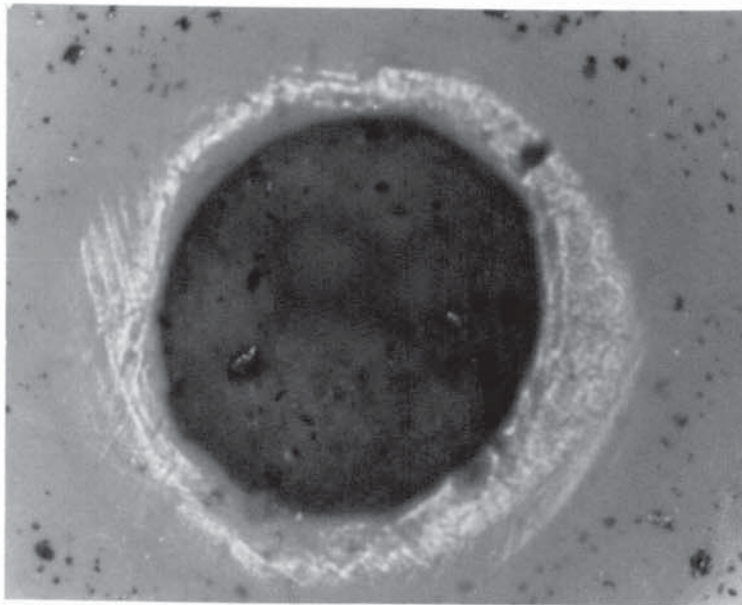
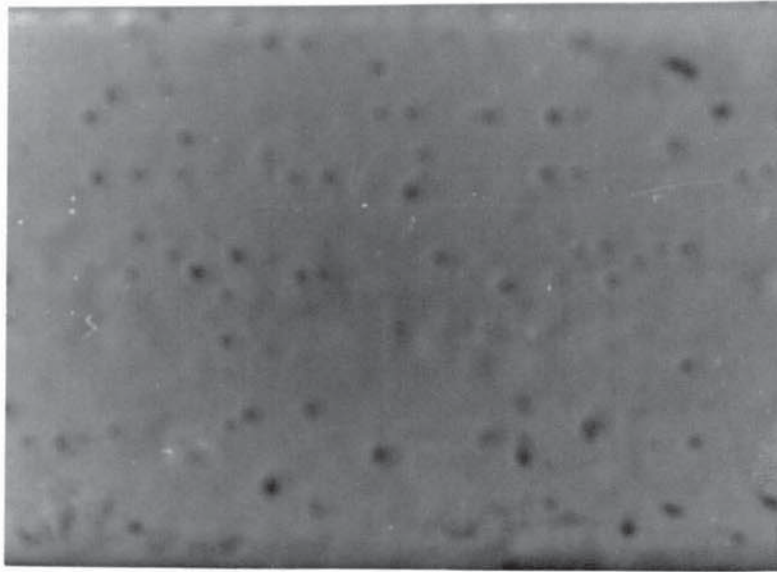
(b)

Figure 4.5 Scanning electron micrographs of crater type defect



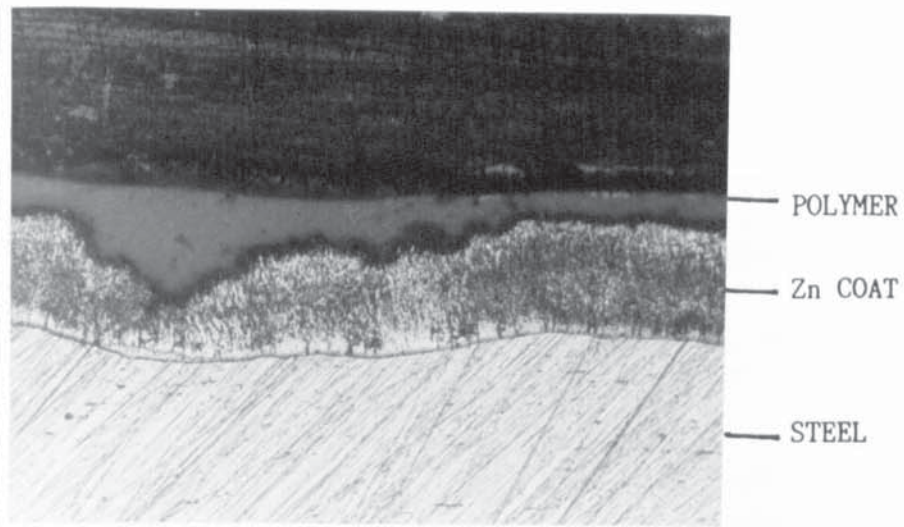
TOP: Figure 4.6 Scanning electron micrograph of cross-section of crater defect showing rough zeta regions

BELOW: Figure 4.7 Scanning electron micrograph of cross-section showing very large gas bubble which could lead to pinholing

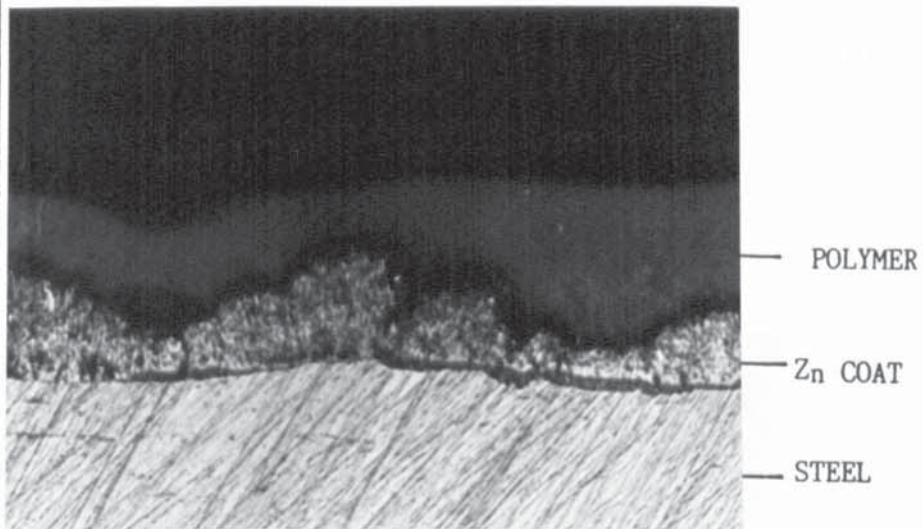


TOP: Figure 4.8 Surface of defective powder coating showing craters (x5)

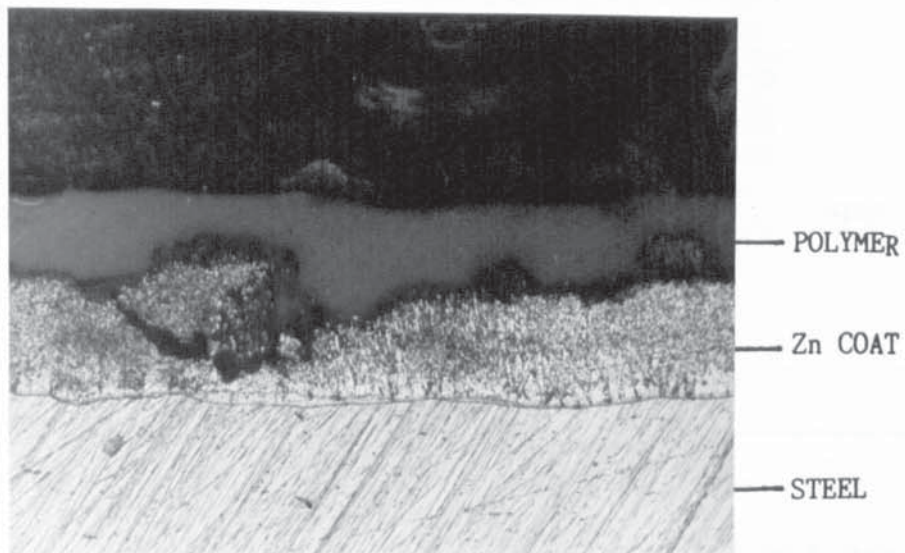
BELOW: Figure 4.9 Surface view of one crater (x100)



(a)

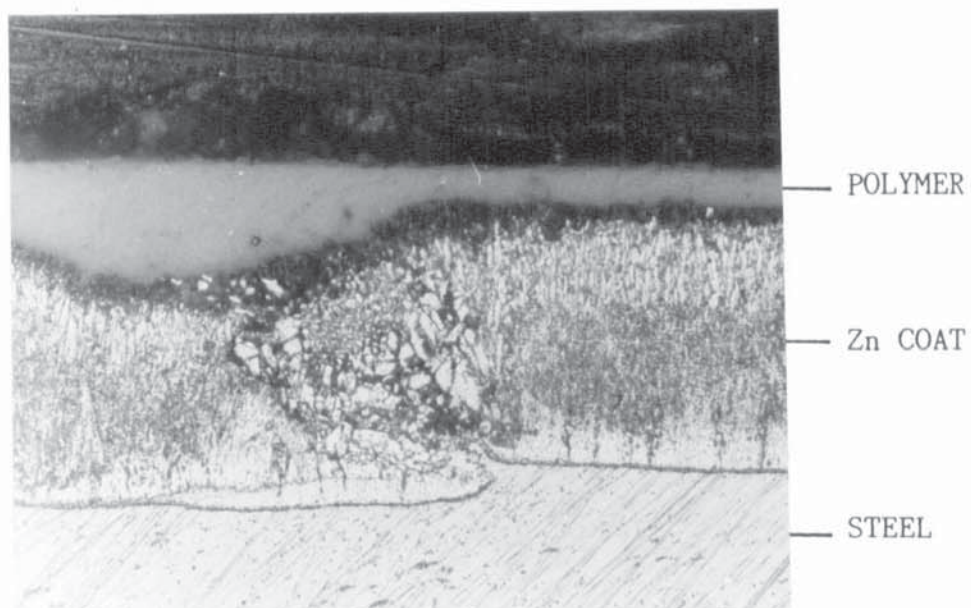


(b)

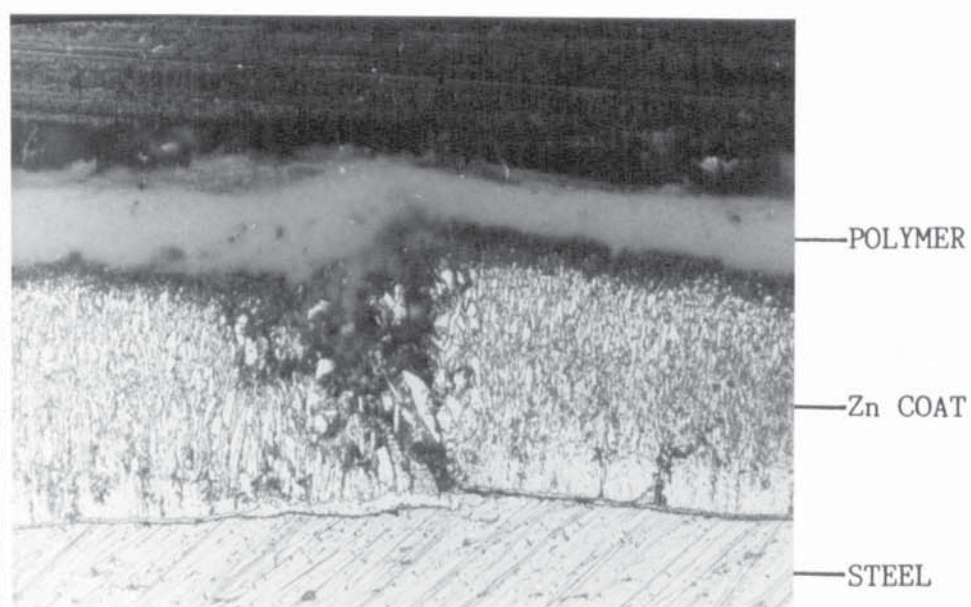


(c)

Figure 4.10 Optical micrographs of cross-sections showing defect free areas on the polymer film (x100)

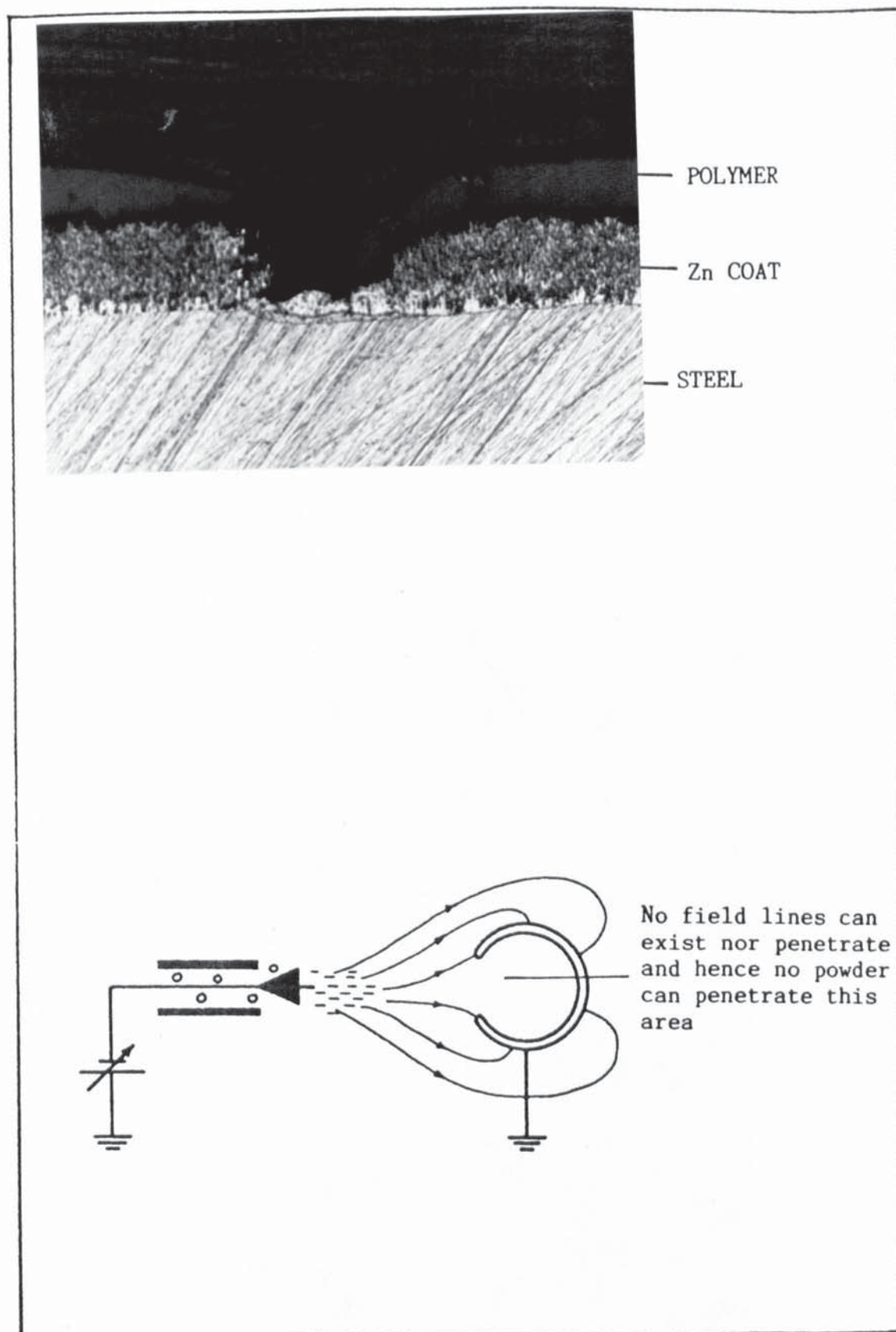


(a)



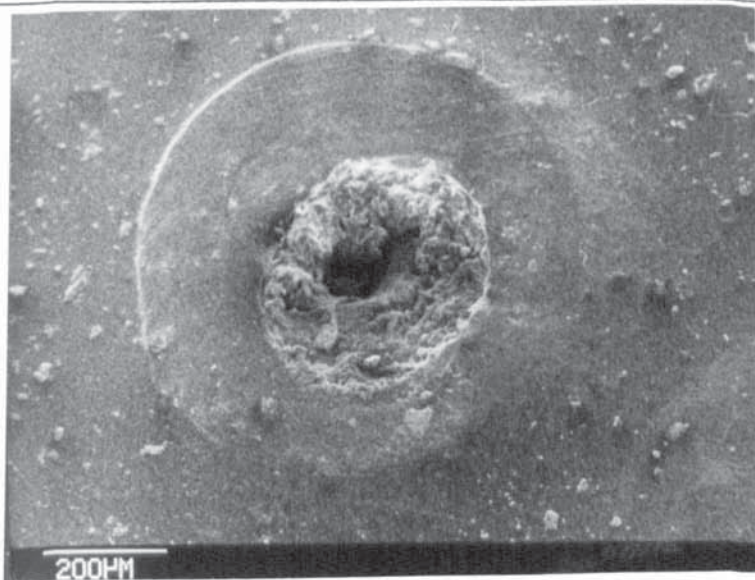
(b)

Figure 4.11 Optical micrographs of cross-sections showing defects in the galvanized layer (zinc coat) (x150)

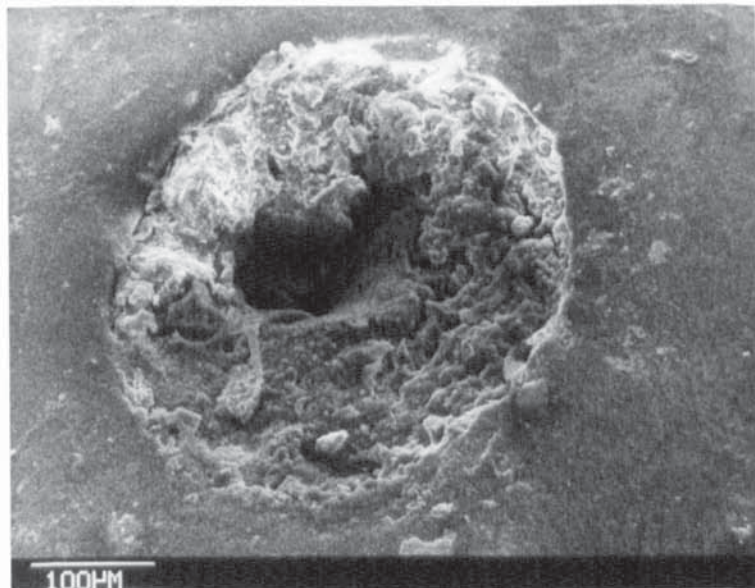


TOP: Figure 4.12 Optical micrograph of cross-section through one crater

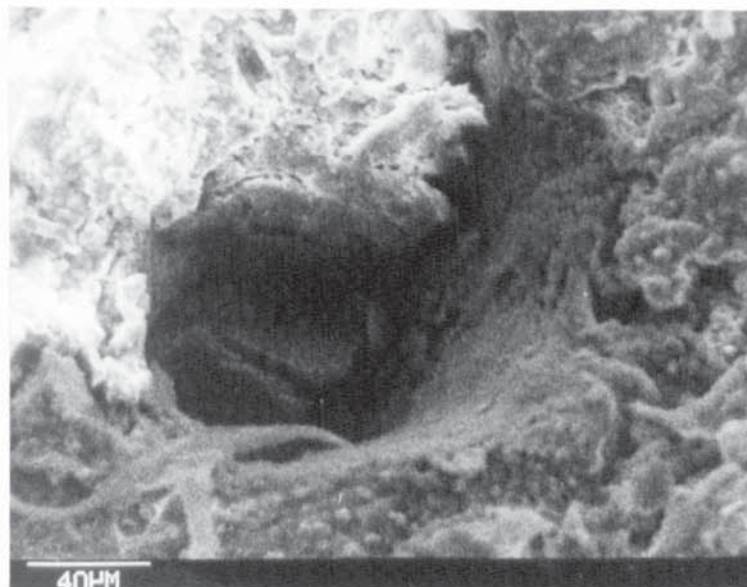
BELOW: Figure 4.13 An illustration of Faraday cage effect



(a)

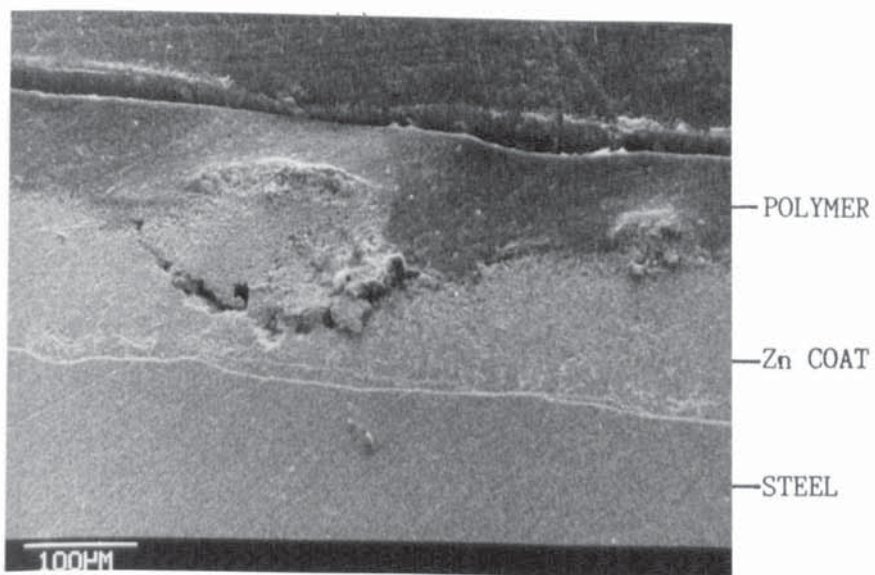
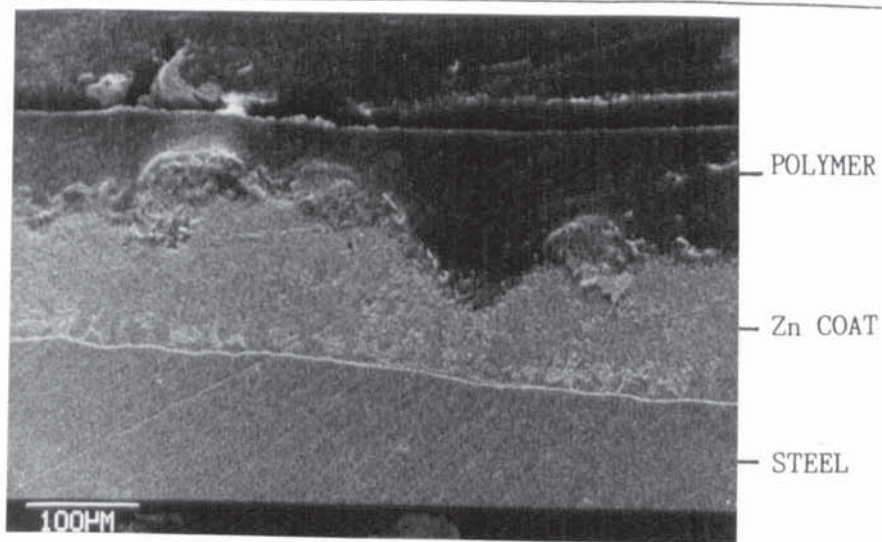


(b)

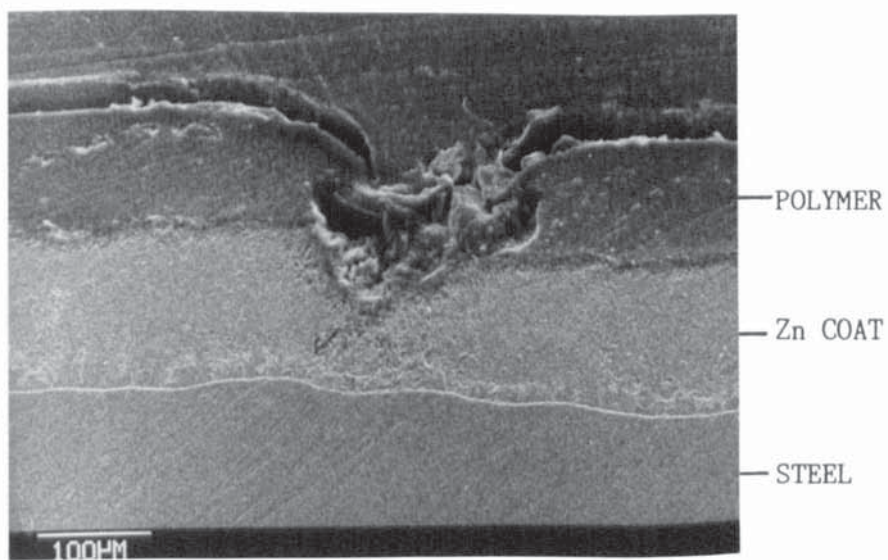


(c)

Figure 4.14 Scanning electron micrographs of a crater - viewed from the surface



(b)



(c)

Figure 4.15 Scanning electron micrographs of cross-section:  
 (a&b) of defective galvanized areas covered by polymer  
 coating  
 (c) through one crater

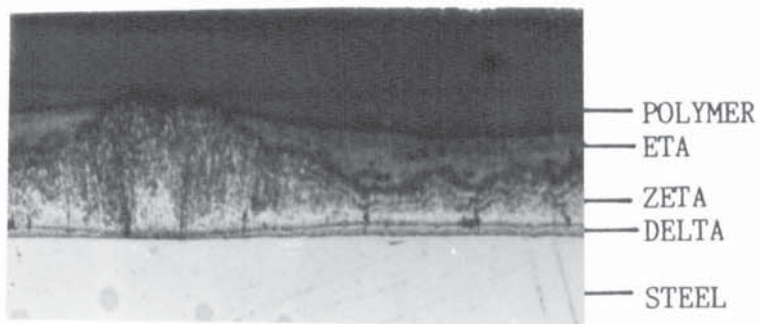


Figure 4.16 optical micrograph of sound powder coating on hot-dip galvanized sample (x220)

## 5 CHARACTERISATION OF ZINC COATED STEEL SUBSTRATES

### 5.1 INTRODUCTION

The four zinc coated steel sheet specimens used for this project were prepared under industrial conditions. These specimens were first characterised with regard to:

- (i) surface roughness
- (ii) surface chemistry and composition, and
- (iii) coating thickness, structure and composition.

Also the effect of proprietary AC51 cleaning solution on substrate surface chemistry and composition, was investigated.

### 5.2 RESULTS

#### 5.2.1 SURFACE ANALYSIS OF THE AS RECEIVED SPECIMENS

##### 5.2.1.1 SURFACE ROUGHNESS

The Ra values for surface roughness of the four specimens are given in table 5.1. Figure 5.1 shows the Talysurf traces of the four sample surfaces in the as received state. The roughest surface was that of the sprayed sample and it can be seen from Fig 5.1(D) that the top of the peaks are clipped and the equipment was unable to measure an exact Ra value. In the case of the electroplated and hot dipped continuous samples the Ra values were about the same, although the Talysurf traces are somewhat different in that the distance between peaks is shorter in the case of the electroplated sample. The

scanning electron micrographs of the surfaces in the as received state Fig 5.3 (A & B) reflect this effect. In addition the surface of the HDC sample is pitted. The Talysurf trace for the HDB sample, Fig 5.1 (C) is similar to that of the HDC. The Ra value was, however, somewhat greater.

#### 5.2.1.2 SURFACE CHEMISTRY AND COMPOSITION

Table 5.2 shows the elements detected on the surface of the samples. SEM/EDXA examination revealed that the as received surface of HDC and HDB samples contained Zn and Pb. The zinc sprayed sample showed only Zn whilst the electroplated surface contained Zn and Fe. XPS analysis showed that the surfaces of the four samples contained Zn, C, O and that the electroplated samples had a trace of Cr presumably from some chromate rinse treatment after electroplating.

Energy Dispersive X-ray analysis of the as received samples revealed that the continuous hot-dip sample surface had a negligible Pb content of about 0.05% whilst HDB had up-to 3% Pb which was unevenly distributed over the surface. A similar analysis on the electroplated sample showed that the iron content was up-to 15%. This was due to the penetration of the electron beam through the thin electroplate coating to the steel base.

### 5.2.2 EFFECT OF AC51 CLEANING SOLUTION ON THE SAMPLE SURFACES

The effect of AC51 cleaning solution on the surface of the samples can be seen from tables 5.1 and 5.2 and in figures 5.2 and 5.3. XPS traces of HDC surfaces, as received and cleaned are shown in figure 5.2. From these, it can be seen that the zinc peaks increased considerably after cleaning suggesting removal of some compound or oxide. It has been reported<sup>(136)</sup> that the relative sensitivity of detection of an element depends in some way upon chemical composition.

The surface roughnesses of the samples as given by Ra values were reduced after cleaning. Scanning electron micrographs for the electroplated sample showed little difference before and after cleaning, whilst the HDC sample appeared to be more pitted after cleaning.

In the case of the HDB sample, scanning electron micrograph after cleaning appeared to show some form of etching although this aspect has not been pursued.

The Pb content of the HDC surface was reduced to zero suggesting that it had all been removed during cleaning whilst that of HDB was reduced to 2.4%.

Table 5.3 shows the weight loss of different samples as a result of cleaning them in AC51 solution. These are all of the same order suggesting the same mechanism of zinc removal in each case.

### 5.2.3 SPECIMEN CROSS-SECTION EXAMINATION AND ANALYSIS

#### 5.2.3.1 METALLOGRAPHY

Figure 5.4 shows the metallography of the zinc coatings. SEM/EDXA semi-quantitative analysis of the different coating layers and the substrates (mild steel) are shown in table 5.4. It can be seen from figure 5.4, that the hot-dip continuous galvanized coating has 2 layers whilst that of hot-dip batch has 3 layers. The two hot-dip continuous galvanized coating layers are eta and Fe/Zn compound, probably delta, and the layers for hot-dip batch include the eta, zeta, and delta phases. The Zn spray coating is porous whilst the electroplated coating can hardly be detected even at high magnification.

#### 5.2.3.2 SAMPLE COATING THICKNESS AND HARDNESS

The thickness and hardness values of both the substrate and the zinc coating (one side) are shown in table 5.5.

### 5.3 DISCUSSION

The above results show that the surface roughness of a zinc coatings depends on the method of applying the zinc. It is also dependent on the cleaning operation applied before and after zinc coating. For example, prior to zinc spraying, the mild steel substrate is usually grit-blasted to remove soil and also to roughen the substrate surface so as to provide the mechanical keying required for good adhesion. This is reflected in the

surface of the zinc coating. Another reason for the high surface roughness of the sprayed sample was that the zinc is deposited at the steel substrate as solid particles which are mechanically bonded and surrounded by pores and oxide. This is why sprayed zinc coatings are sometimes sealed, usually with paint, to give a smooth surface texture. The difference in roughness of the hot-dip continuous and hot-dip batch samples is linked with the method of withdrawing and subsequent cooling of the workpiece and the amount of dross on the galvanizing bath which is picked up by the work piece.

The difference in roughness of these samples means that if uniform polymer coatings of sufficient thickness (e.g. BS 6497) at the peaks are to be obtained a great amount of powder has to be applied to the samples of rougher surfaces than the smoother ones. This is likely to be uneconomical and require modification of the powder coating system. The powder coating at the valleys will be relatively too thick and may lead to pinholing (sections 2.3.6, & 4.3 -4.5).

The results of the analysis obtained after cleaning the samples in AC51 show that the solution etched off the upper -most layers of samples to obtain clean active surfaces. A very clean bright surface was obtained for each sample after cleaning even though the samples were immersed in the solution for a relatively short time of 1 minute. The reduction in Ra value (average surface roughness) after cleaning tends to suggest that chemical

polishing rather than etch-cleaning had taken place. The Ra values for the electroplated and HDC samples are almost the same and tends to suggest that the surfaces are similar. This similarity of the surfaces is not confirmed by the scanning electron micrographs (Fig 5.3). It is interesting to note that dissimilar surface profiles can have the same Ra value. Therefore the Ra value of a surface as obtain from the Talysurf is only a qualitative assessment. The weight loss due to cleaning were generally the same for the whole samples, suggesting that the samples were equally affected by the cleaning solution (AC51).

The steel substrates contain no Pb and therefore the Pb found in the coating would have come from the galvanizing bath either as a contamination or deliberate addition. In the case of HDB, the lead was found below the uppermost layer of the galvanized coating. This was revealed by the fact that when the surface was analysed using SEM/EDXA, Pb was picked up, but XPS analysis of the same surface failed to detect Pb, only Zn, O, and C were detected. This is due to the greater depth of penetration of SEM/EDXA x-rays compared with the XPS which can only penetrate a few nm. In fact, it has been reported<sup>(18,19)</sup> that the Pb is present as scattered globules in the solidified zinc.

The difference in the sample coating thickness was as expected but the differences in hardness were surprising.

The HDC coating had a Vickers hardness value of 95 (eta) whilst the equivalent layer in the case of HDB had a hardness value of 118 Hv, a difference of 23 Hv (24%) (see table 5.5). The possible cause of this difference in hardness would be the method of cooling applied after dipping (coating). The relatively low hardness value of the sprayed coating was due to the porosity of the coating.

#### 5.4 CONCLUSIONS

- (1) The structure and composition of the zinc coatings produced by the four methods were very different.
- (2) The surface roughnesses of zinc coatings on mild steel depends on methods of applying the zinc coating, and cleaning operations applied before and after the coating operation.
- (3) The sprayed sample had the highest surface roughness (Ra value). This was followed by HDB, and then the electroplated and HDC which had about the same values.
- (4) The Ra values of the samples were reduced after cleaning, particularly that of electroplated and HDC samples.
- (5) The weight changes after cleaning were all the same.
- (6) The scanning electron micrographs of sample surfaces after cleaning revealed that :
  - (a) there was no effect on the electroplated sample
  - (b) The HDC surface became more pitted,
  - (c) The HDB surface was slightly etched.

(d) Evidence regarding the sprayed sample was inconclusive

(7) Elements segregated at the zinc surface or present from subsequent treatment e.g. chromating were removed during cleaning.

(8) The Pb in galvanized coatings lies below the surface layer.

**TABLE 5.1      The surface roughness of as-received and cleaned samples**

Sample	Roughness (CLA)		
	As Received	Cleaned	% Reduction in Roughness
ELECT	1.0	0.74	- 26%
HDC	0.9	0.66	- 27%
HDB	1.7	1.50	- 11%
SPRAY	>5	>5	

**TABLE 5.2      Elements detected on surface of samples**

Sample	SEM Analysis		XPS Analysis	
	As Received	Cleaned	As Received	Cleaned
ELECT	Zn, Fe	Zn, Fe	Zn, Cr, C, O	Zn, C, O
HDC	Zn, Pb	Zn	Zn, C, O	Zn, C, O
HDB	Zn, Pb	Zn, Pb	Zn, C, O	Zn, C, O
SPRAY	Zn	Zn	Zn, C, O	Zn, C, O

**TABLE 5.3      Effect of AC51 on weight change of samples**

Sample	Weight Loss g/m <sup>2</sup>
ELECT	-13
HDC	-14
HDB	-12
SPRAY	-13

TABLE 5.4 SEM/EDXA analysis of cross-section of samples

Sample	Area Of Sample Analysed	Composition at %			
		Fe	Zn	Pb	Si
ELECT	Top of Sample M/S (Substrate)	Too Thin to Analyse			
		99.93	0.00	0.00	0.00
HDC	Galva. Coating -				
	ETA	0.80	98.95	0.00	0.00
	Zn-Fe Alloy	10.07	89.03	0.00	0.00
	Mild Steel(Sub)	98.82	0.00	0.00	0.12
HDB	Galva. Coating -				
	ETA	0.84	99.14	0.00	0.02
	ZETA	6.41	90.94	0.65	0.00
	DELTA	9.35	90.22	0.44	0.00
	STEEL	99.90	0.00	0.00	0.05
SPRAY	Zn Coating -	0.00	100.00	-	-
	M/S (Substrate)	99.99	0.00	0.00	0.01

TABLE 5.5 Micro-hardness and thickness of steel substrate and Zn coatings

Samples	Thickness (µm)		Micro-Hardness (Hv)	
	Steel	Zn (one side)	Steel	Zn Coat
ELECT	723	7	140	
HDC	725	38	143	95
HDB	943	80	188	(ETA) 118 (ZETA) 172
SPRAY	946	108	185	41

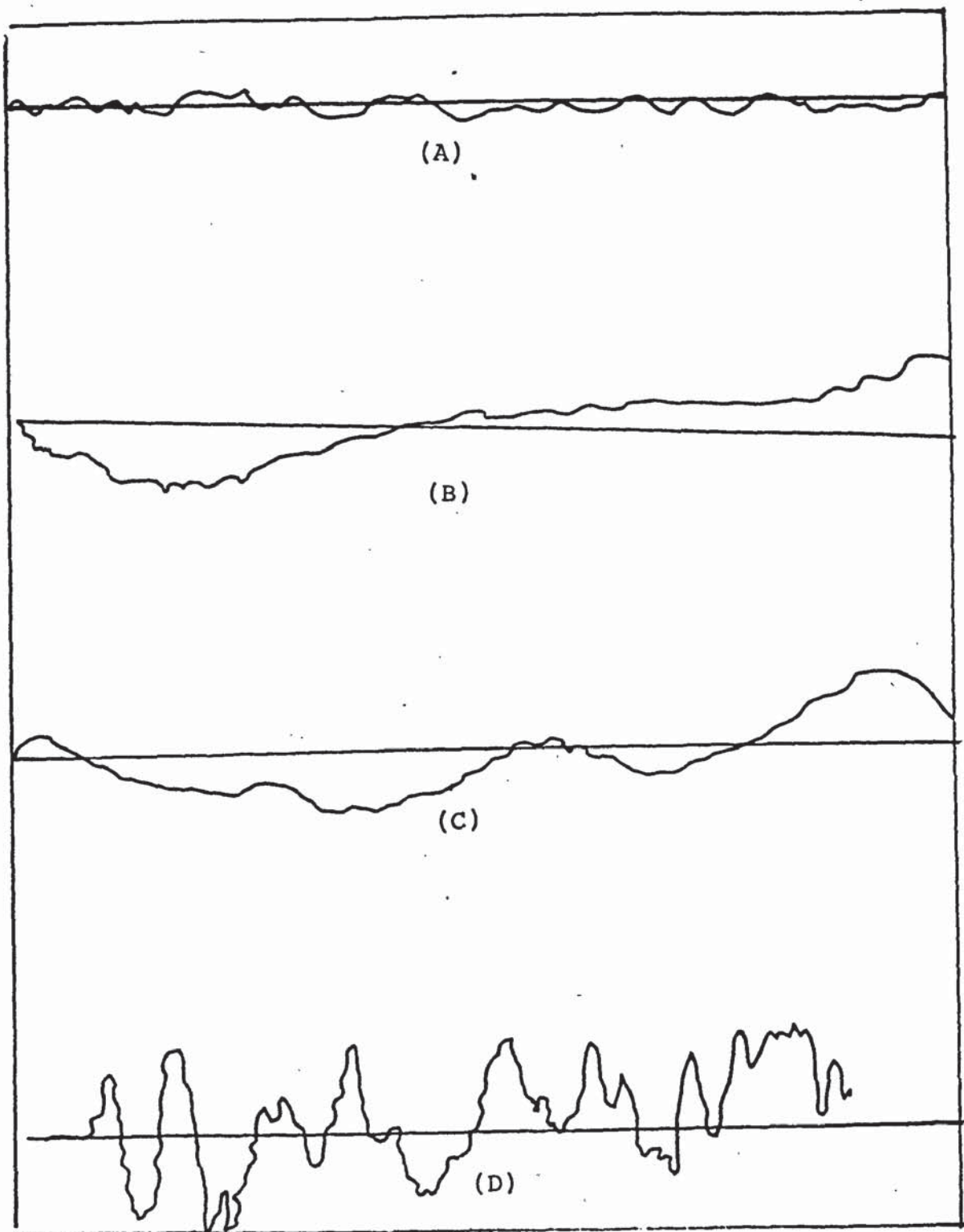


Figure 5.1 Traces of surface roughness ( $R_a$ ) of samples  
(A) electroplated  
(B) hot-dip continuous  
(C) hot-dip batch  
(D) sprayed

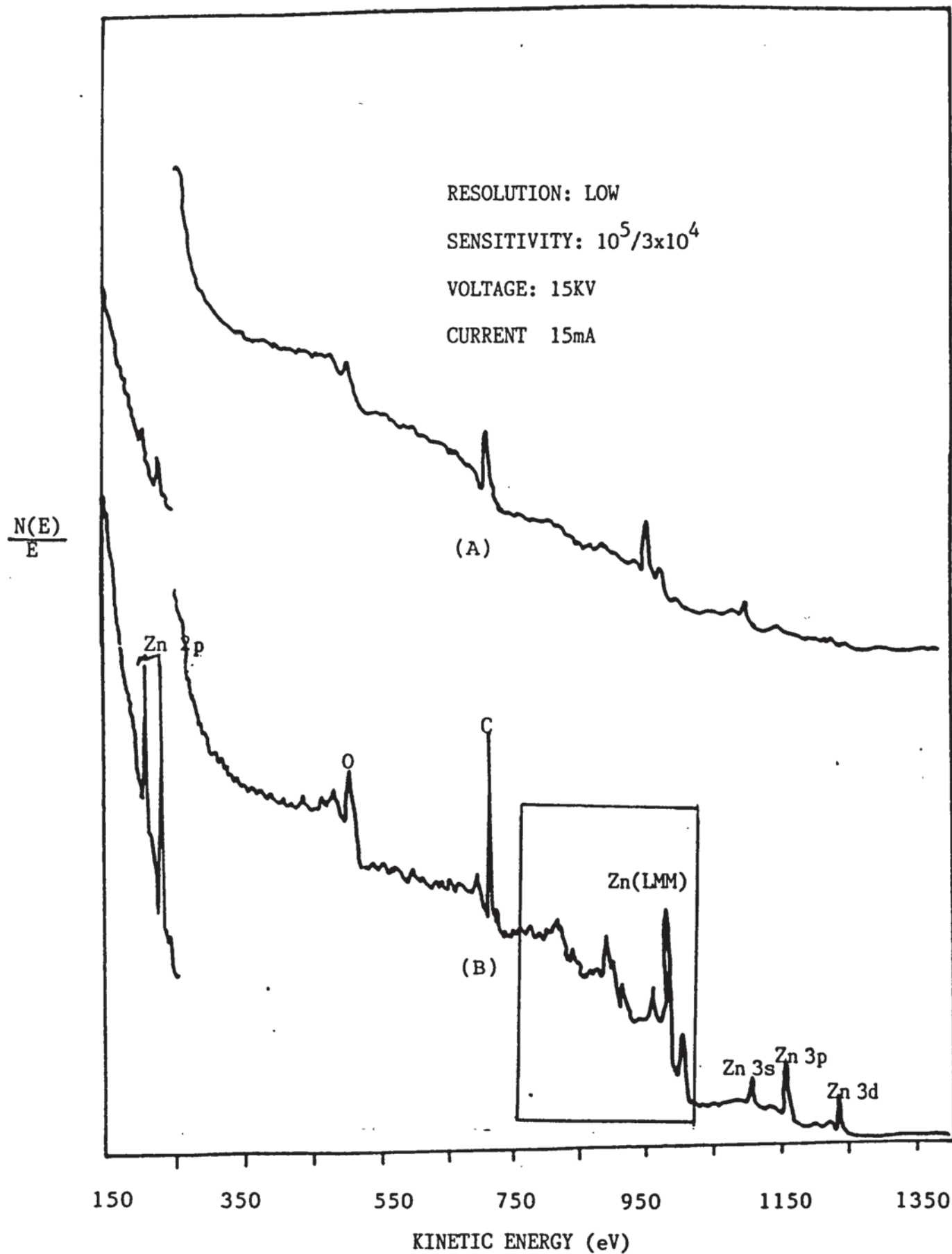
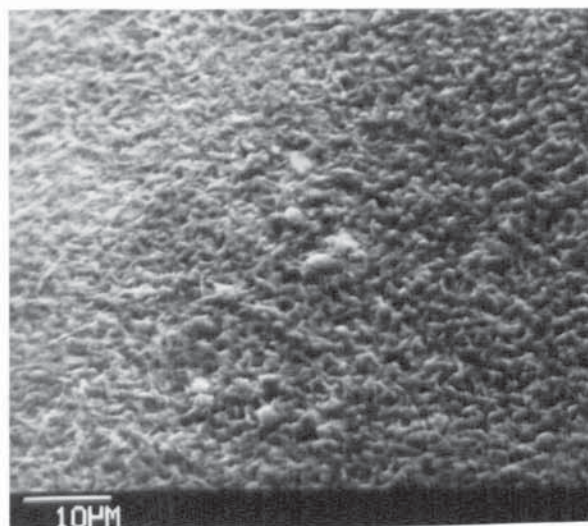
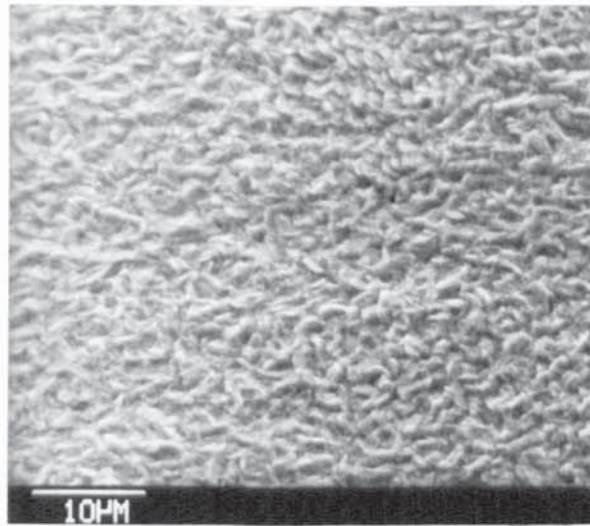


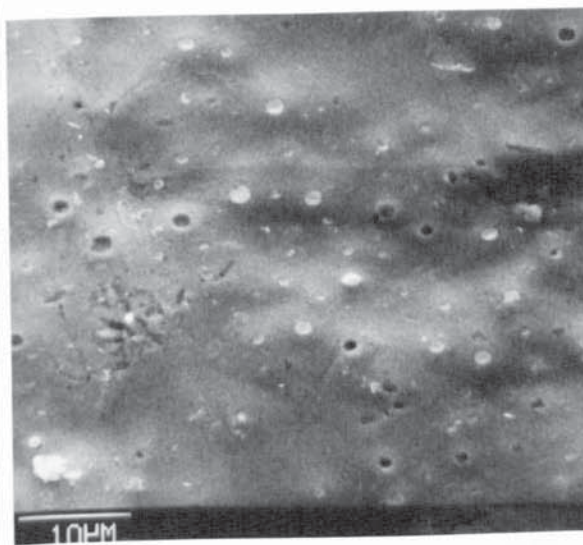
Figure 5.2 X-ray photoelectron/Auger electron spectroscopy traces of HDC sample surfaces  
(A) before cleaning  
(B) After cleaning



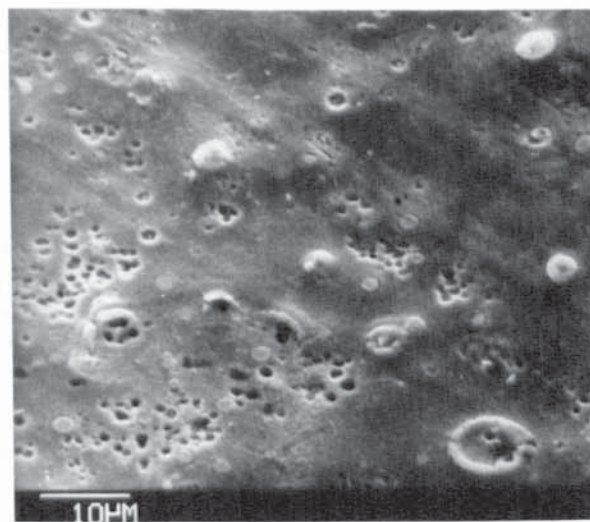
A



A(i)

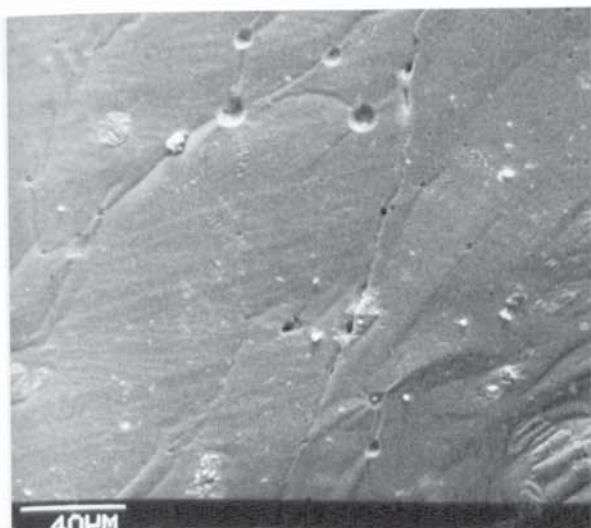


B

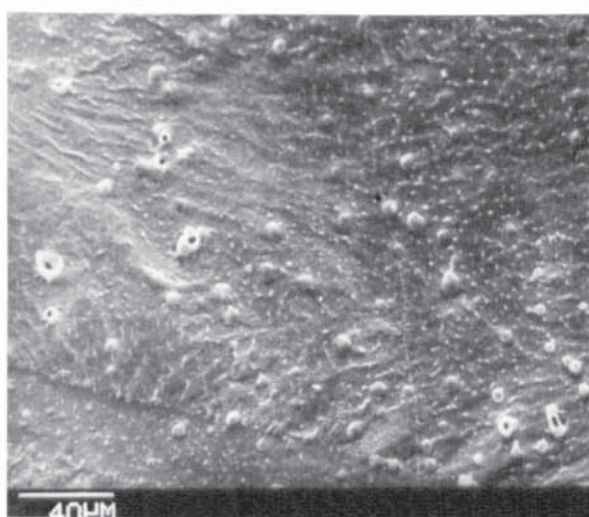


B(i)

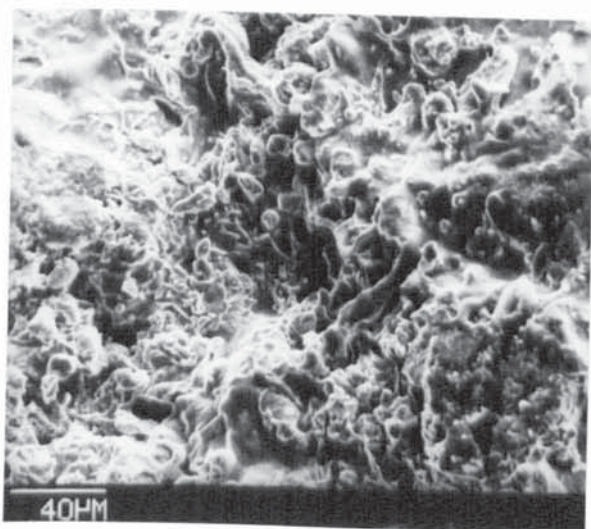
Figure 5.3 Scanning electron micrographs of samples before and after cleaning in AC51 solution  
 A electroplated degraded only by acetone swab  
 A(i) " after cleaning  
 B HDC degraded only by acetone swab  
 B(i) " after cleaning



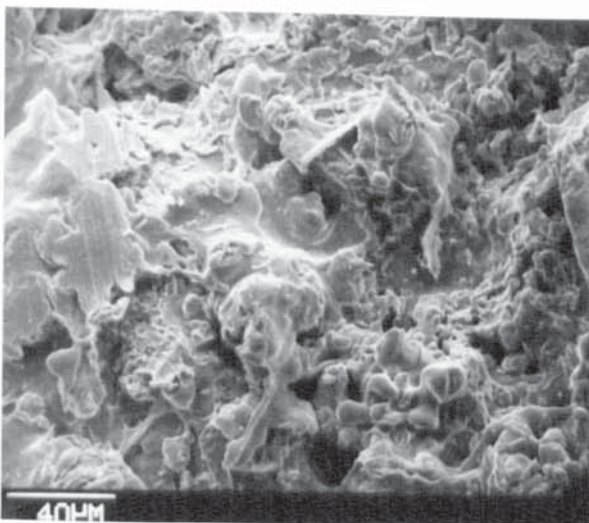
C



C(i)



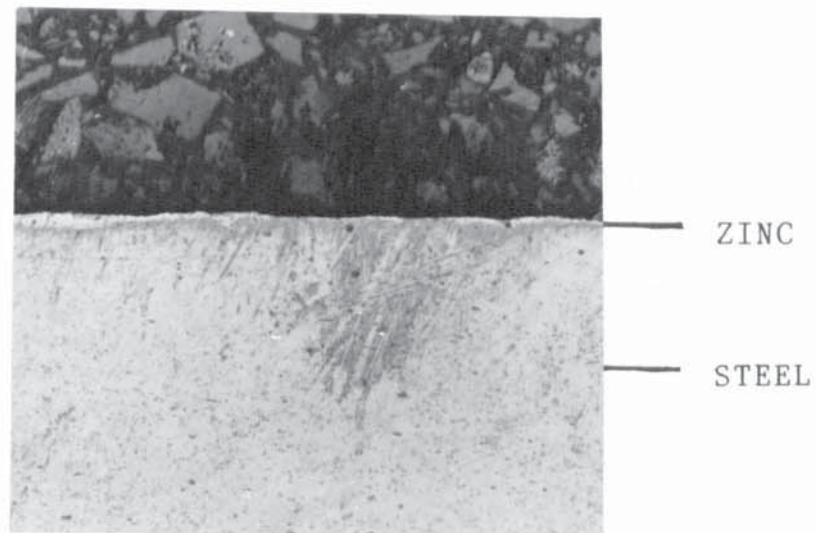
D



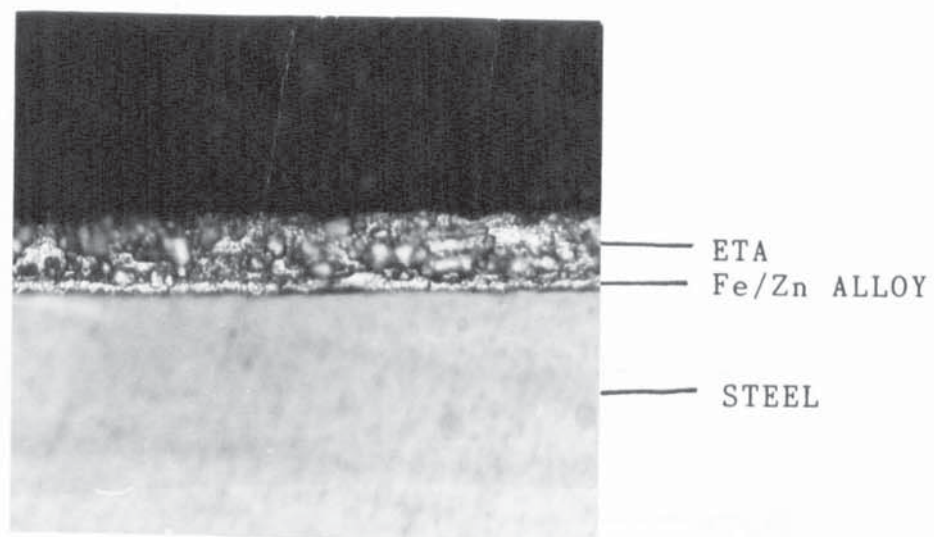
D(i)

Figure 5.3 continued

C	HDB degraded only by acetone swab
C(i)	" after cleaning
D	sprayed degraded only by acetone swab
D(i)	" after cleaning

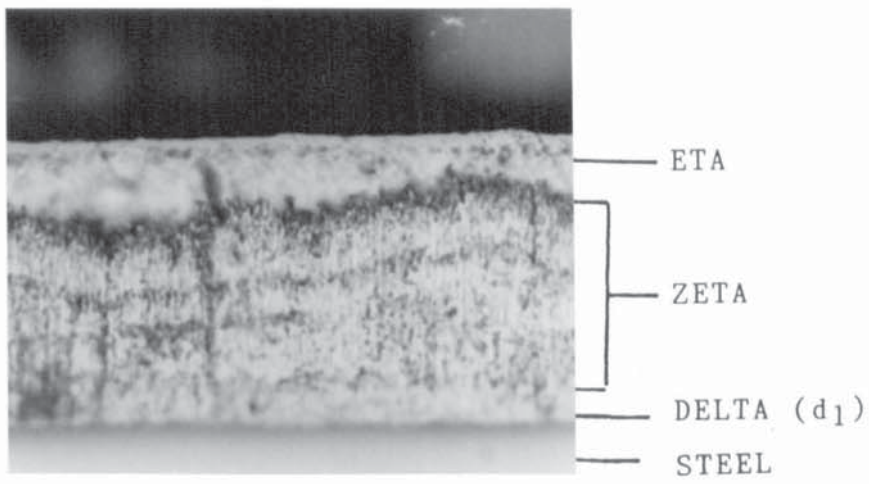


(A)

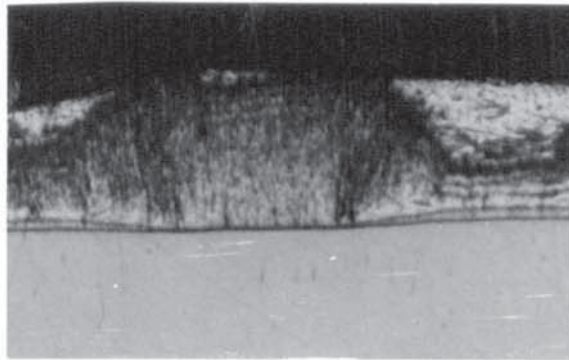


(B)

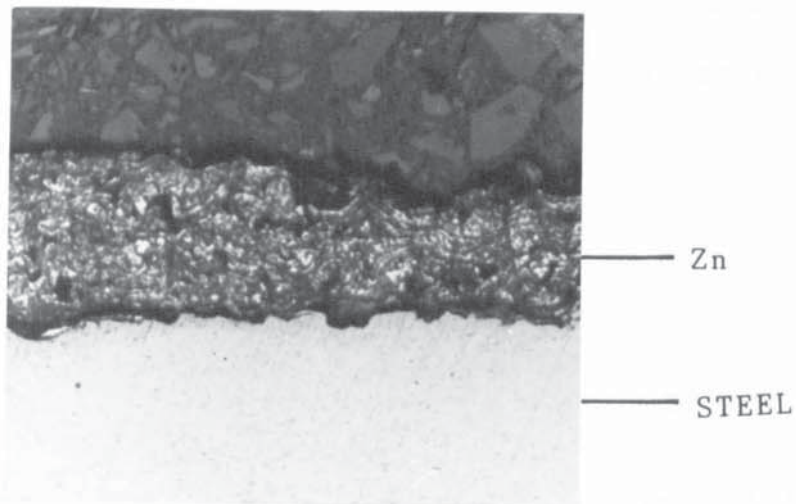
Figure 5.4 Optical micrographs of sample cross-sections  
 (A) electroplated  
 (B) HDC



(C)



(Ci)



(D)

Figure 5.4 continued- (C) HDB  
 (Ci) HDB showing the out burst of zeta  
 (D) sprayed

## 6 CONVERSION COATING OF ZINC COATED SUBSTRATES

### 6.1 INTRODUCTION

Chromate conversion coatings are the most widely used pretreatments employed prior to powder coating of zinc. Most chromate treatments in use at present are of the proprietary type. Users are supplied with powdered compounds or liquid concentrates, from which working solutions are made up and operated according to manufacturers recommendations. A variety of formulations, tailored to meet specific requirements, are available and generally simple to operate. Reports on the mechanisms of film formation have been published but much of the work was carried out using proprietary solutions and is not easy to reproduce. This chapter is concerned with studies of the mechanisms of film formation, their composition and surface chemistry, for both laboratory prepared solutions and commercial proprietary solutions. Laboratory solutions of known chemical composition were chosen and made to resemble proprietary solutions as close as possible.

### 6.2 CHROMIC ACID ACTIVATED WITH SODIUM CHLORIDE (L1) (0.12M/l $\text{CrO}_3$ + 0.3M/l $\text{NaCl}$ )

#### 6.2.1 CONVERSION COATING FORMATION AND GROWTH

The formation and growth of conversion coatings on zinc coated steel substrates was investigated using :

(a) Measurement of open potential relative to saturated

standard Calomel Electrode (S.C.E.) with time.

(b) Coupon weight change measurement with time.

Figure 6.1 shows the rest potential versus time curve for different samples. All the samples exhibited rapid fall in potential within seconds of immersion. A careful examination of the curves revealed that it took approximately 20 seconds for pure Zn, electroplated and sprayed samples to reach a steady potential in this solution, whilst the hot-dipped continuous and hot-dipped batch galvanized samples did not reach steady potential, even after the minute immersion.

Figure 6.2 is a plot of weight change against immersion time. The best fitting curve obtained for all the plots, using a commercial curve fitting package, was a polynomial of the 2nd order. The equations obtained, for times  $t =$  or  $> 5$  seconds, for the curves were:

$$\text{ELECT} \quad h = 19.2719 + 19.6940t - 0.1138t^2 \quad 6.1$$

$$\text{HDC} \quad h = 95.4812 + 25.7257t - 0.2656t^2 \quad 6.2$$

$$\text{HDB} \quad h = 9.9754 + 8.9741t - 0.0612t^2 \quad 6.3$$

$$\text{Sprayed} \quad h = 22.5963 + 30.6447t - 0.1106t^2 \quad 6.4$$

Where  $h$  = weight change ( $\text{mg}/\text{m}^2$ ) and  $t$  = immersion time (s). They have correlation coefficients ( $R$ ) of 1.0, 0.97, 1.0 and 0.98 respectively. From the plots, it can be seen that at all times, the sprayed sample had the greatest weight change, probably due to the sample's greatest effective surface area due to surface roughness which

made it impossible to measure the exact surface area. The HDB galvanized sample had the lowest weight change. Simple extrapolation of the curves suggest that this statement would not be true if the samples were immersed for longer times. The HDC galvanized samples attained a peak weight change. The importance of these equations is that the weight change for any time of immersion can be predicted before treatment. For example, using the above equations, the weight changes for 100 seconds immersion time were calculated to be:

$$\begin{aligned}\text{Elect} &= 850.7 \text{ mg/m}^2 \\ \text{HDC} &= 12.1 \text{ mg/m}^2 \\ \text{HDB} &= 295.4 \text{ mg/m}^2 \\ \text{Sprayed} &= 1981.1 \text{ mg/m}^2\end{aligned}$$

## 6.2.2 ZINC DISSOLUTION RATE STUDIES

Figure 6.3 shows the curves of weight of zinc dissolved against immersion time in L1 solution for all the samples. The HDC galvanized sample has the lowest zinc dissolution rate. Comparison of these curves with surface roughness values suggests that the rougher the surface, the higher the rate of zinc dissolution. The best fitted curve for the respective samples was the polynomial curve. Again, for  $t = \text{or} > 5$ , the curves have the following equations:

$$\begin{aligned}\text{Elec} \quad h &= -40.8862 + 44.0198t - 0.4215t^2 & 6.5 \\ \text{HDC} \quad h &= 7.7055 + 28.5724t - 0.2039t^2 & 6.6 \\ \text{HDB} \quad h &= 157.3466 + 63.4501t - 0.5507t^2 & 6.7 \\ \text{Sprayed} \quad h &= 844.8012 + 76.3959t - 0.0927t^2 & 6.8\end{aligned}$$

where  $h$  = weight of zinc dissolved ( $\text{mg}/\text{m}^2$ ) and  $t$  = time (s) The correlation coefficients for the curves were calculated to be 0.98, 0.99, 1.0 and 0.99 respectively.

### 6.2.3 EXAMINATION AND ANALYSIS OF THE CONVERSION COATING FILM FORMED

The scanning electron micrographs (SEM) of samples treated in solution (L1) are shown in figure 6.4. It can be seen from these micrographs figure 6.4(a) to 6.4(d), that a significant conversion coating had formed after just fifteen seconds immersion. The film had a gel-like structure and when dried, it cracked to form blocks or grains. It can be seen from the micrographs in figure 6.4(d) that the conversion coating is not as easily noticeable on sprayed samples due to their surface roughness.

Table 6.1 (a-d) shows the semi-quantitative analysis (atomic %), as determined by EDXA, of the elements detected on the surface of the conversion coating on the different samples at the various times of immersion. It is evident that the % of chromium detected increases with time of immersion in conversion coating solution. This is probably a result of increasing conversion coating thickness with time. In the case of the electroplated and HDB samples Fe and Pb were found respectively. These elements are probably in the substrate and are detected since the electron beam penetrates the thickness of the conversion coating film. It is not possible to determine

if Fe or Pb are present in the film using this technique.

Table 6.2 contains the results of XPS analysis of the conversion coating surface for the different samples. The results are the same in each case, the conversion coating surface being composed of Zn, Cr, O, C and Cl. Thus zinc is present in the coating itself.

#### 6.2.4 EFFECT OF DEGASSING AFTER FORMATION OF THE CONVERSION COATING

Figure 6.5 shows scanning electron micrographs of the degassed conversion coating surfaces. Degassing probably causes the film to dehydrate and shrink resulting in a thinner curled film with wider cracks which expose the substrate. The EDXA results of the conversion coating surface before and after degassing for the samples are also shown in table 6.2 (a-d). Degassing reduces the proportion of Cr and increases the proportion of other elements detected as would be expected for thinner film and more exposed substrate.

#### 6.2.5 EFFECT OF VARIATION OF SOLUTION pH ON THE FORMATION OF CONVERSION COATING IN L1 (0.12M/l $\text{CrO}_3$ + 0.3M/l NaCl) SOLUTION

The pH of the solution was varied by adding sodium hydroxide solution to obtain pH values of 1.2, 1.5, 2.0, 3.0, 4.0, 5.0 and 6.0 respectively. These solutions were used to pretreat HDC galvanized samples. The film formation was studied using the weight change

technique and the surfaces of the samples after treatment were analysed using SEM/EDXA.

Figure 6.6 (a) shows the change in weight with solution pH for a treatment time of 120 seconds. Figure 6.6 (b) shows the amount of Cr (atomic %) detected on the sample surfaces treated in the solution used in figure 6.6(a). These curves suggest that an increase in pH reduces the conversion film growth rate and hence lowers the proportion of Cr on the surface. The weight change is reduced rapidly as pH is increased and above a pH value of 3 there is little weight change at all. The rest potentials of these solutions were measured and it was found that an increase in pH of this solution had no effect. The scanning electron micrographs shown in Fig. 6.7 illustrates that the amount of conversion coating formed was reduced as the pH of the solution was increased. Film formation did not occur at high pH values but preferential attack resulted in pitting.

#### 6.2.6 EFFECT OF THE PRESENCE OF LEAD ON THE FORMATION OF CONVERSION COATING FILMS

When the specimens used for this project were characterised, it was found that the surface of the HDB galvanized samples contained lead as well as zinc (table 6.2). It is not known whether lead has any effect on the formation of conversion coatings. However it is known that Pb is not wetted by many solutions and the author thought

it wise to study the effect lead has on chromate film formation in the case of the HDB galvanized samples. Since film formation in the solution (L1) is very rapid, a lower concentration of this solution (L3), which has a lower film growth rate (see figure 6.8), was used to carry out these studies. This solution (L3) had the same pH as the parent solution (L1).

Figure 6.9 shows scanning electron micrographs of surfaces at various times of treatment. After 15 seconds, small precipitates had nucleated on specific sites over the surface. After 30 seconds, the precipitates became well defined and after 60 seconds, had grown and coalesced to form larger particles.

After 120 seconds, the precipitates had much reduced in number and become larger in size. A discontinuous, smoother coating can be seen surrounding the precipitates. These features are shown at a higher magnification figure 6.9 (e) At this magnification, the precipitates (A), the exposed zinc substrate (B) and the smoother coating (C) were analysed using EDXA, and typical results were as follows:

Position	% Zn	% Pb	% Cr
A	41.03	3.27	55.70
B	98.17	0.15	1.64
C	97.48	0.19	2.37

Several precipitates (white spots) were analysed and the same profile of results was obtained in each case. The

results of this analysis suggest that lead globules provide sites for easy precipitation of chromate.

#### 6.2.7 EFFECT OF USING NaF AS ACTIVATOR (L2)

(0.12 M/l  $\text{CrO}_3$  + 0.1 M/l NaF)

The potential-time profiles of all the samples immersed in solution L2 are shown in figure 6.10. On immersion, the rest potential of the HDB galvanized and the electroplated samples were about - 600 mV whilst that of HDC and sprayed were - 700 mV. HDC potential falls rapidly in first 5s followed by very gradual decrease. Spray stays at -700 mV for 10s and then falls rapidly and HDB increases gradually. Contrary to initial potential decay with time exhibited by the HDC up to 20 seconds, and electroplated and sprayed samples up to 45 seconds, the HDB galvanized samples potential increases with time throughout the one minute of immersion. When the rest potentials were measured for five minutes, the potential for electroplated, HDC and sprayed samples remained the same and steady whilst that of HDB galvanized continue to increase.

The scanning electron micrographs of the surfaces of HDC treated in this solution (L2) for a time of 60s, 120s and 300s are shown in figure 6.11. The micrograph for 60s shows the pattern of growth of conversion film. It appeared from this micrograph for 60s that coating layers start to form at some preferential areas, and then

spread to cover the whole surface and smoothed over. The smooth surface can be seen from the micrographs for 120 seconds and 300 seconds immersion times. The coating looks more adherent, compact and less cracked compared with those obtained when sodium chloride was used as the solution activator. However, it took a considerably longer time to obtain conversion films which covered the whole surface and coupon weight change studies revealed a continuing weight loss with increasing time of immersion as shown in figure 6.12 (a). The best fit curve for the plots of weight loss against time was polynomial of the second order, suggesting a reduction of the rate of weight loss with increasing immersion time. Figure 5.12 (b) is a plot of atomic % Cr content on the surface against time. It can be seen that the % Cr is directly proportional to the immersion time.

### 6.3 CHROMATE - PHOSPHATE (ALOCROM 100) SOLUTION

#### 6.3.1 FILM FORMATION AND ZINC DISSOLUTION RATE STUDIES

The potential versus time of immersion plots for zinc and HDC galvanized sheets are shown in figure 6.13. The curve for zinc lies below that of HDC galvanized sample at all

times of immersion. In the case of the later, the potential starts at  $-800\text{mV}$ , falls rapidly to  $-850\text{mV}$  within 1 minute and then rises to  $-830\text{mV}$  after 3 minutes of immersion. The potential then continues to rise slightly through longer times of immersion. In the case of pure zinc, the potential starts at  $-820\text{mV}$ . and falls rapidly to  $-870\text{mV}$  within 1 minute. It then rises slowly and becomes stable after 5 minutes at  $-860\text{mV}$ . The possibility of film formation at long immersion times was investigated by treating some samples for times up to 60 min. Both the zinc and galvanized steel samples decreased in weight after treatment in chromate solution and figure 6.14 shows a plot of weight loss with time. Figure 6.15 shows the weight of Zn dissolved with time. It can be seen from these figures 6.14 and 6.15 that the lower weight change obtained with HDC compared to pure zinc by coupon weight measurement method, is consistent with the lower weight of zinc dissolved obtained for the same sample using atomic absorption analysis method. The curves show a trend of increasing weight loss and zinc dissolution with increasing time of immersion but rate of increase decreases with increasing time. The rate of dissolution of Zn was relatively high during the first five minutes of immersion.

### 6.3.2 EXAMINATION AND ANALYSIS OF SAMPLE SURFACES AFTER PRETREATMENT

Scanning electron micrograph (SEM) of some of the samples treated in Alocrom 100 solution are shown in figure 6.16. The SEM/EDXA results are shown in table 6.3. It can be seen from table 6.3 that the pretreated surface contained Zn, Cr and P. For both samples and at all times of immersion, the atomic % of P was generally higher than that of Cr. The proportions of Cr and P increase with time up to 5 min immersion and thereafter decrease.

The micrographs shown in figure 6.16, illustrates that background pits and hills are covered by a thin conversion coating film. A relatively thicker film can be seen on the micrographs of samples immersed for 5 minutes but the background pits can still be seen easily.

### 6.4 NON CHROMATE (CHROMETAN) CONVERSION COATING SOLUTION

#### 6.4.1 FILM FORMATION AND ZINC DISSOLUTION STUDIES

Figure 6.17 shows the plot of coupon weight change and weight of zinc dissolved against time of immersion. The curves show the negligible value of zinc dissolved as compared with the coupon weight change. This suggest that film growth is responsible for most of the weight change. Maximum film weight was recorded from the sample immersed for 2 minutes and at the same time, the least zinc dissolved weight was obtained.

#### 6.4.2 EXAMINATION AND ANALYSIS OF CONVERSION COATING FILMS

Semi-quantitative analyses of elements detected on the surface after different treatment times were made using SEM/EDXA and the results are shown in table 6.4. It can be seen from the table that the elements detected are Zn, Fe, Cr, P and S. The atomic % of Cr, P and S generally follow the same trend, increasing with time of immersion up to 2 minutes when they reached a maximum and then started to decrease for longer immersion times. The micrographs of the sample surface after treatment are shown in figure 6.18. It can be seen that a thick cracked film had already formed even after 15s of immersion.

Examination of the micrographs revealed that the coatings were powdery and handling difficulties suggested that they possessed negligible adhesion. Areas where film has been removed can be seen easily on the micrographs of the sample immersed for 2 minutes and hence the reduction of film weight at this immersion time.

#### 6.5 SODIUM HYDROXIDE SOLUTION

##### 6.5.1 FILM FORMATION AND ZINC DISSOLUTION RATE STUDIES

Figure 6.19 shows graphs of open potential against immersion time for samples treated in NaOH (pH = 11) solution. Sprayed samples had the most active potential which remain steady throughout the whole time of immersion. Electroplated and HDC samples became more noble with increa-

sing immersion time. After 60 seconds immersion the HDB and HDC galvanized samples had the same potential, which was also the most noble potential.

Electroplated samples were used to study the weight change and Zn dissolution rate. The weight change and the weight of zinc dissolved are shown in table 6.5. The weight loss increased with time of immersion but the amount of zinc dissolved was not related to the time of immersion. This is because the zinc coating on this sample was very thin and so weight loss was not only due to zinc dissolution but also to base metal (Fe) attack.

#### 6.5.2 EXAMINATION AND ANALYSIS OF SAMPLE SURFACE AFTER TREATMENT

The surfaces of samples treated in sodium hydroxide solution were examined using SEM/EDXA but only zinc could be detected on the surface. XPS examination showed the surfaces to be composed of Zn, O and C. Figure 6.20 shows the scanning electron micrographs of the treated sample surfaces. All the surfaces showed pitting, being most severe in the case of the sample treated for 60 seconds.

#### 6.6 DISCUSSION

Potential-time curve relationships have been widely used<sup>(41)</sup> for studying film formation and film break-down, as indicated by an increase or decrease in the rest potential (corrosion potential) respectively. For example, May<sup>(137)</sup> studied the corrosion of 70/30 brass in

sea-water and showed that scratching the surface resulted in a sudden fall in potential to a more negative value followed by a rapid rise due to reforming of a passive film. This hypothesis can be used therefore to explain the curves in figure 6.1, 6.10, 6.13 and 6.16.

The curves in figure 6.1 show an initial drop of potential, indicating dissolution of the Zn substrate. This is consistent with dissolution of zinc as shown in figure 6.3. The potential then becomes relatively steady throughout the rest of the time of immersion. The steady potential range could be explained as follows: after the early dissolution, the liquid near the surface of the substrate became saturated with the dissolved  $\text{Zn}^{2+}$  ions. This results in steady  $\text{Zn}^{2+}/\text{Zn}$  exchange and the interfacial potential of  $\text{Zn}^{2+}/\text{Zn}$  was then indicated by the steady part of the potential time curve.

A film is formed as shown in the scanning electron micrographs and confirmed by increase in coupon weight change despite the dissolution of zinc. Since film formation is not followed by a rise in potential it is possible to conclude that the conversion film was not passive.

Lin and co-authors in their studies of film growth kinetics<sup>(138)</sup>, concluded that the migration of oxygen anions or oxide ion vacancies was the essential factor for passive film growth and on the other hand, the diffusion of metal cations or cation vacancies results in metal dissolution. That a passive film is not formed in the

present work is probably due to the presence of  $\text{Cl}^-$  or  $\text{F}^-$  which are known to prevent passivity in other systems.

Conversion film formation is considered to be via a dissolution - precipitation mechanism (sect. 2.2.4.2). The halide ions ( $\text{Cl}^-$ ) are strongly absorbed by zinc and have a strong complex forming tendency with zinc cations; thus, removal of a lattice cation already partly complexed with adsorbed chloride, may well be kinetically easier than oxide - film formation.

A closer examination of the potential-time curves in figures 6.1, and 6.10 revealed that the HDB had the noblest potential. It should be remembered that when the sample surfaces were analysed using EDXA, Pb was detected. It is therefore not surprising for this sample to be more noble as lead will tend to increase the potential since it is a more noble element. In fact figure 6.10 suggests that the HDB becomes passive; judging from the increasing noble potential for this sample, as soon as it was immersed in L2 solution. Figure 6.12(a) shows coupon weight loss. Therefore the film could be very thin and not truly passive.

This work had revealed that the theory of higher dissolution rate resulting in higher film weight growth rate does not satisfy all solutions. For example, in the case of Alclom 100, zinc dissolved at a relatively higher rate (figures 6.14 and 6.15) than that observed for solution L1 but only a thin film could be detected on the

treated sample surface. Also, for this solution, the rise of rest potential as an indication of formation of film appeared to apply quite well. The potential rises to about its peak value at about five minutes of immersion (see figure 6.13) and more film was noticed on the sample treated for this time (5 minutes). Pretreatment times greater than 5 minutes resulted in etching or pitting of the surface (figure 6.16) and probably covered by very thin film as revealed by the x-ray analysis (table 6.3). The continuous coupon weight loss in Alocrom 100 and the relatively higher weight of zinc dissolved could be due to either the redissolution of the film formed or the solution formulation is not suitable to form conversion film on zinc substrates. Alocrom 100 is actually for pretreating aluminium substrates. However this result shows that not all the conversion coating solutions give conversion film formation on all metals. Also, examination of the scanning electron micrographs shown in figures 6.4 and 6.11 indicated that these films were formed and grown by different mechanisms.

Three different chemical structures of chromate conversion coatings on zinc have so far been reported in the literature (sec. 2.2.4.2). These include:

- (a) Basic chromium chromate<sup>(33,35,36,)</sup> of composition  $\text{Cr}(\text{OH})_3 \cdot \text{Cr}(\text{OH})\text{CrO}_4 \cdot \text{H}_2\text{O}$ ,
- (b) Hydrated chromium (III) oxide films with absorbed anions such as chromate and sulphate<sup>(31,38)</sup> of composition  $\text{Cr}_2\text{O}_3 \cdot \text{CrO}_3 \cdot \text{H}_2\text{O}$ ,

(c) Basic Zinc chromate<sup>(26,43,44)</sup> of composition  $\text{ZnCrO}_4 \cdot 4\text{Zn}(\text{OH})_2 \cdot \text{H}_2\text{O}$ .

SEM x-ray link analysis (EDXA) of samples treated in different solutions revealed that the composition of the surfaces depend strongly on the composition of the treatment solution. Samples treated in Alocrom 100 and in non-chromate (chrometan) solutions had different surface compositions as compared with the same samples treated in 0.12M/l  $\text{CrO}_3$  + 0.3M/l NaCl (L1) solutions. Also when the effect of Pb on the conversion coating formation on HDB galvanized samples was studied (section 6.2.6), it was found that lead globules provided sites for nucleation of conversion films. It would be unlikely that the composition of this film would be the same as that formed on HDC galvanized sample immersed in the same solution. It would be more satisfactory therefore to state the composition of conversion coatings on zinc coatings in relation to the solution formulation and type of zinc coating.

Examination of the sample surfaces treated in solution L1 using XPS showed that all the samples surfaces had the same composition or chemistry. The elements found on the surfaces of all the samples were Cr, O, Zn, C with little traces of Cl. The presence of Zn on the surface again throws doubt on the validity of the suggestion that the composition of chromate conversion coating on zinc is basic chromium chromate.

The morphologies of the chromate layers, before and after degassing, on all the samples were studied (Figures 6.4 a-d and 6.5 a-d). The equivalent EDXA analyses are shown in table 6.2 (a-d). From this table, it can be generally concluded that degassing reduces the % (atomic) of Cr and increases that of zinc in the conversion coating film. A comparison of figures 6.4 and 6.5 revealed the effect of degassing on the conversion film layer. Dehydration of the film at the degassing temperature resulted in greater shrinkage of the film so that the cracks between the blocks were much greater (presumably exposing the zinc substrate) and the blocks themselves appeared to be curled up at the edges. Film weights of samples immersed for 2 minutes were found to have been reduced by 51% after degassing whereas drying in a warm air only reduce the weight by only 15%. Typical XPS Spectra are shown in figure 6.21. It can be seen that the spectra are essentially the same although the zinc peaks are now more pronounced when degassed. This could be due to diffusion of zinc into the chromate layer or, more likely, widening of the crack to expose the zinc substrate. High resolution XPS spectra of the Cr (2p) lines showed binding energies of 578.7 and 577.0 eV (relative to the C 1s line at 284.6 eV) before and after degassing respectively. The shift of 1.7 eV indicated a conversion of Cr(VI) to Cr(III)

- (1) Weight change and zinc dissolution rate of all samples treated in chromate solution ( $\text{CrO}_3 + \text{NaCl}$ ) have the same polynomial curve of the 2nd order relationship with immersion time.
- (2) Undried conversion coating films formed on zinc were not passive.
- (3) Degassing after chromate film formation led to:
  - (a) dehydration which in turn resulted in shrinking of the film and widening of cracks and subsequent exposure of the substrate.
  - (b) conversion of  $\text{Cr(VI)}$  to  $\text{Cr(III)}$
- (4) The theory that higher dissolution rate of substrate results in higher rate of conversion coating film formation was not applicable to all chromate solutions studied.
- (5) Alocrom 100 pretreatment solution is not a suitable pretreatment solution for zinc.
- (6) The possibility of a solution forming conversion coating depend on its formulation, concentration, pH and the type of metal treated.
- (7) There was no generalised mechanisms for conversion coating film formation; the mechanism of a conversion coating formation depended on the formulation, composition and concentration of the solutions.
- (8) The type of coating, nature and composition of conversion coating formed is affected by the formulation of that solution and the substrate's surface chemistry.

(9) There is evidence to suggest that the chemical structure of the conversion coating formed in 0.12M/l  $\text{CrO}_3$  + 0.3M/l NaCl (L1) solution was basic zinc chromate.

(10) Pb globules in hot-dipped batch galvanized steel stimulate the formation of conversion coating and the film formed may contain some Pb compounds which may improve the corrosion resistance of the coating.

**TABLE 6.1 Elements detected by EDXA of conversion coating films formed in L1 solution**

**(a) Electroplated**

Immersion time(s)	Elements (Atomic %)					
	Before degassing			After degassing		
	Zinc	Iron	Chromium	Zinc	Iron	Chromium
5	88.15	4.22	7.63	89.14	5.11	5.75
10	85.08	5.84	9.08	87.18	4.98	7.84
15	83.57	4.85	11.58	84.50	5.35	10.35
20	84.75	5.20	10.06	81.19	5.25	9.56
30	80.92	6.13	12.95	80.56	6.98	12.14
40	74.17	5.41	20.42	75.65	5.34	19.01
60	69.98	4.67	25.35	70.61	4.22	25.17

**(b) HDC**

Immersion time(s)	Elements (Atomic %)			
	Before degassing		After degassing	
	Zinc	Chromium	Zinc	Chromium
5	95.13	4.87	96.55	3.45
10	86.76	13.24	90.76	9.24
15	88.67	11.33	89.96	10.02
20	85.6	14.4	88.85	11.15
30	84.21	15.75	86.46	13.54
40	77.50	22.50	81.43	18.57
60	64.71	35.29	78.31	21.69

**(c) HDB**

Immersion time(s)	Elements (Atomic %)					
	Before degassing			After degassing		
	Zinc	Lead	Chromium	Zinc	Lead	Chromium
5	93.59	2.16	4.25	94.68	2.21	3.11
10	91.72	0.70	7.58	93.15	0.83	6.02
15	85.42	2.21	12.37	86.46	2.63	10.91
20	88.15	1.21	10.63	90.07	1.21	8.72
30	82.97	0.67	16.36	84.57	1.14	14.29
40	79.20	0.08	20.72	81.21	0.98	17.81b
60	75.37	0.01	24.61	76.44	0.75	22.81

(d) Sprayed

Immersion time(s)	Elements (Atomic %)			
	Before degassing		After degassing	
	Zinc	Chromium	Zinc	Chromium
5	94.69	5.31	95.84	4.16
10	92.45	7.55	94.05	5.95
15	90.23	9.77	92.14	7.86
20	90.45	9.55	91.03	8.97
30	88.33	11.67	89.16	10.84
40	87.45	12.55	86.68	13.32
60	78.10	21.90	85.24	14.76

TABLE 6.2 Elements detected by XPS of conversion coating formed in L1 solution

Samples	Elements
1 ELECT	Zn, Cr, O, C, Cl
2 HDC	Zn, Cr, O, C, Cl
3 HDB	Zn, Cr, O, C, Cl
4 SPRAYED	Zn, Cr, O, C, Cl

TABLE 6.3 Elements detected by EDXA of samples treated in Alocrom 100

Immersion time(s)	Elements (Atomic %)					
	Zinc			HDC		
	Zn	Cr	P	Zn	Cr	P
1	84.8	7.6	7.6	84.0	7.5	8.4
2	81.88	8.8	9.32	81.9	8.5	9.6
5	76.6	10.8	12.6	80	10.0	10.0
10	78.2	10.4	11.4	82.1	8.2	9.7
20	80.5	9.21	10.29	84.3	7.7	8
40	85	6.3	8.7	88.1	5.0	69
60	88.3	3.7	7.8	91.7	3.1	5.2

**TABLE 6.4** Elements detected by EDXA of conversion coating film formed in Chrometan solution on electrop-  
lated samples

Immersion Time (mins)	Elements (Atomic %)				
	Zn	Fe	Cr	P	S
0.5	79	5.06	7.36	6.37	1.29
1.0	74.42	4.03	10.59	8.23	2.73
1.5	71.48	3.48	11.08	10.68	2.95
2.0	63.44	4.41	15.60	14.17	2.39
3.0	69	4.59	13.52	10.54	1.64

**TABLE 6.5** Weight Change and Weight of Zn Dissolved of Elect-  
Treated in NaOH (L17)

Immersion Time Minutes	Weight Change		Weight of Zn Dissolved	
	g/m <sup>2</sup> x 10 <sup>-2</sup>		g/m <sup>2</sup> x 10 <sup>-2</sup>	
0.5	-	40		4
1	-	60		3
2	-	78		3
3	-	88		4
5	-	100		4

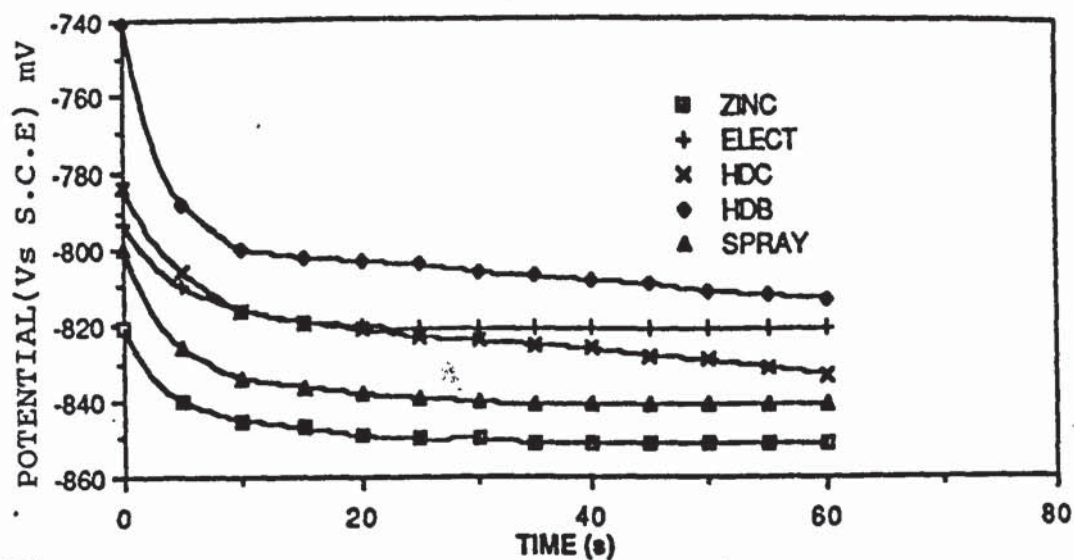


Figure 6.1 Rest potential vs immersion time in 0.12M/l  $\text{CrO}_3$  + 0.3M/l NaCl solution (L1)

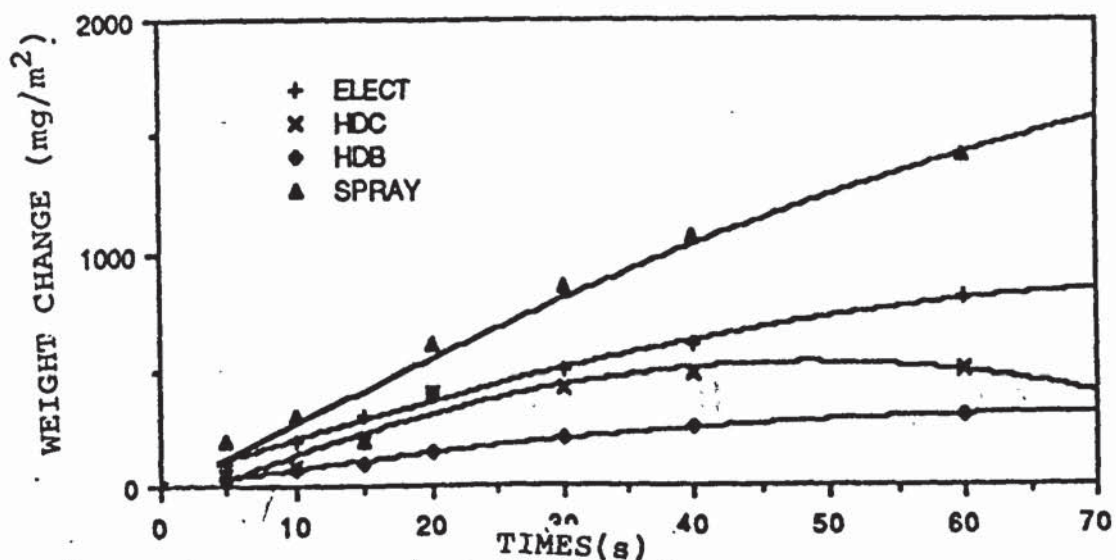


Figure 6.2 Coupon weight change vs immersion time in 0.12M/l  $\text{CrO}_3$  + 0.3M/l NaCl Solution (L1)

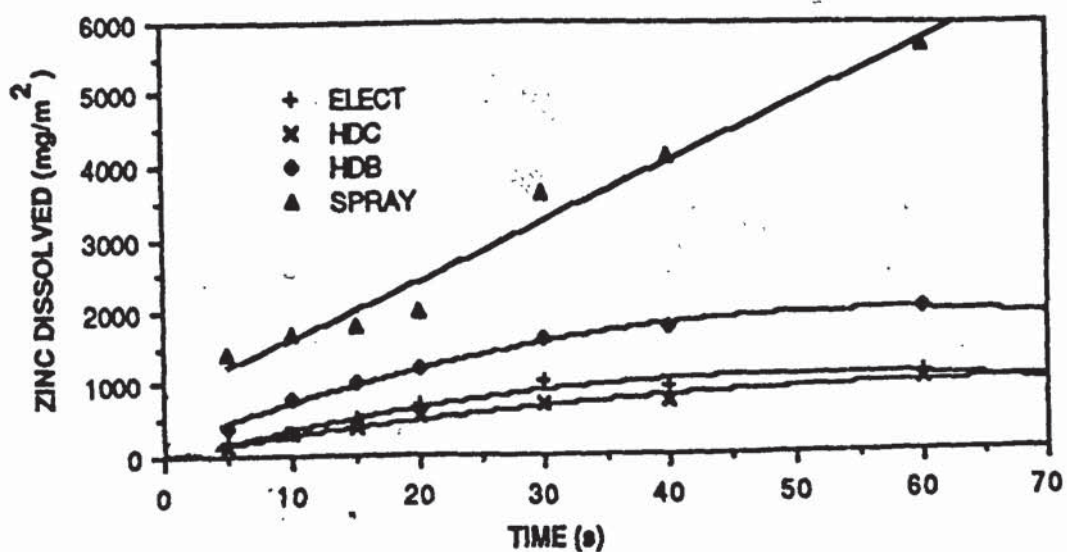
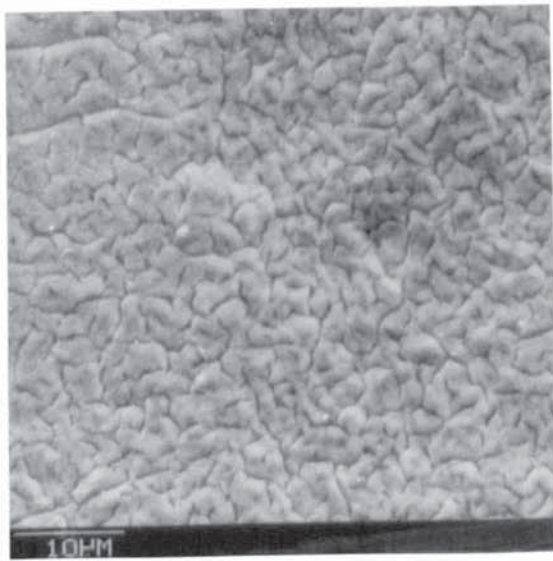
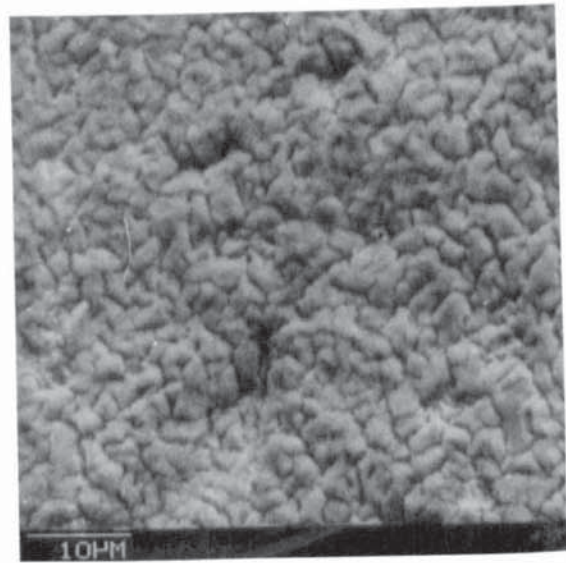


Figure 6.3 Dissolved zinc weight vs immersion time in 0.12M/l  $\text{CrO}_3$  + 0.3M/l NaCl (L1)

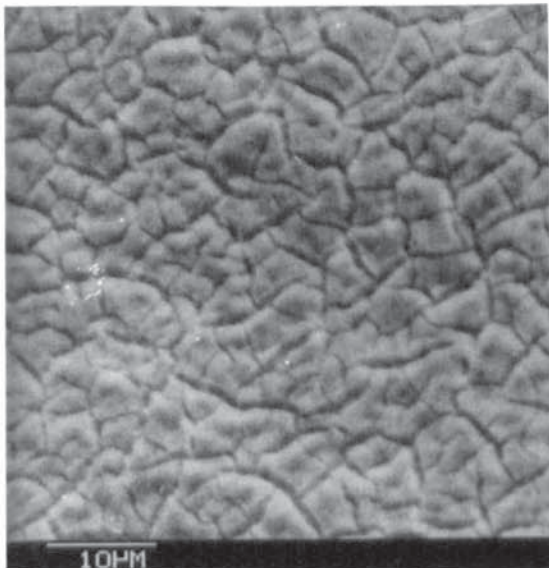
(a)



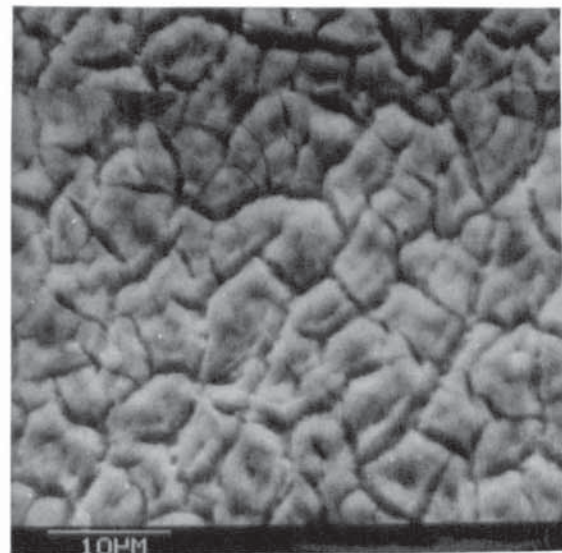
15 Seconds



30 Seconds



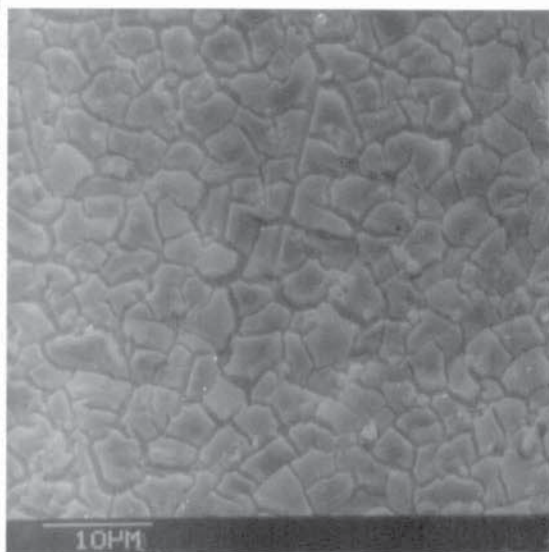
60 Seconds



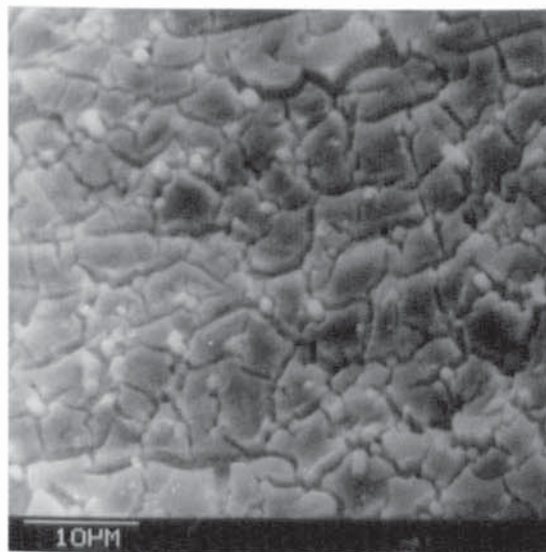
120 Seconds

Figure 6.4 Scanning electron micrographs showing the appearance of coatings formed on (a) electroplated, (b) HDC, (c) HDB and (d) sprayed samples in 0.12M/l  $\text{CrO}_3$  + 0.3M/l NaCl solution (L1) at 25°C

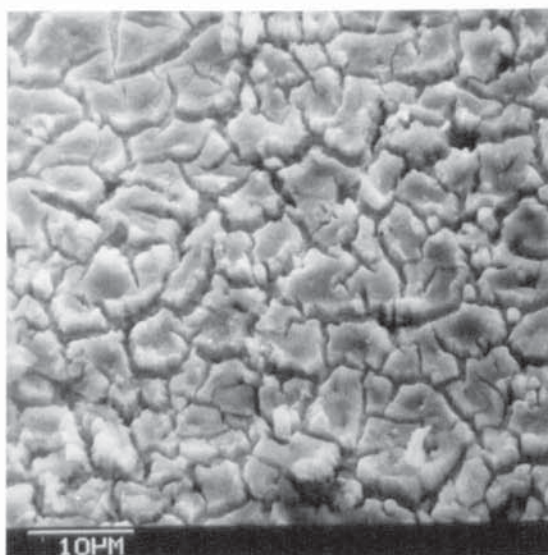
(b)



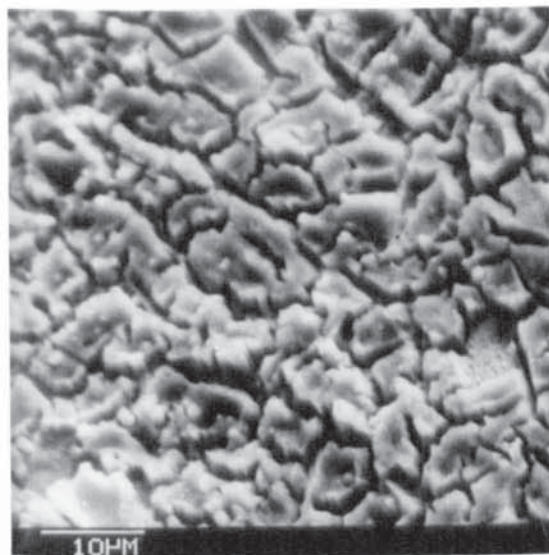
15 Seconds



30 Seconds



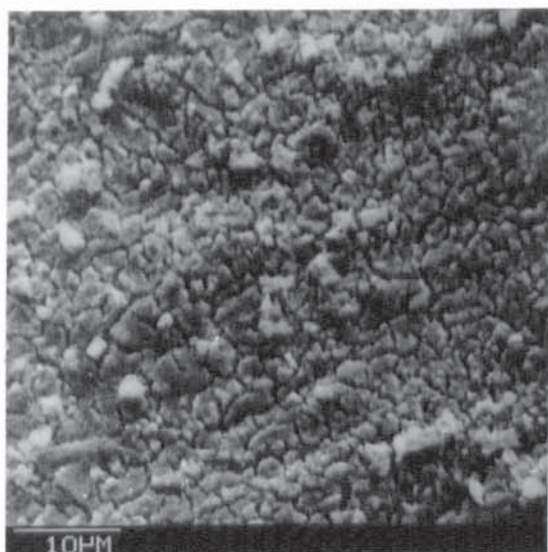
60 Seconds



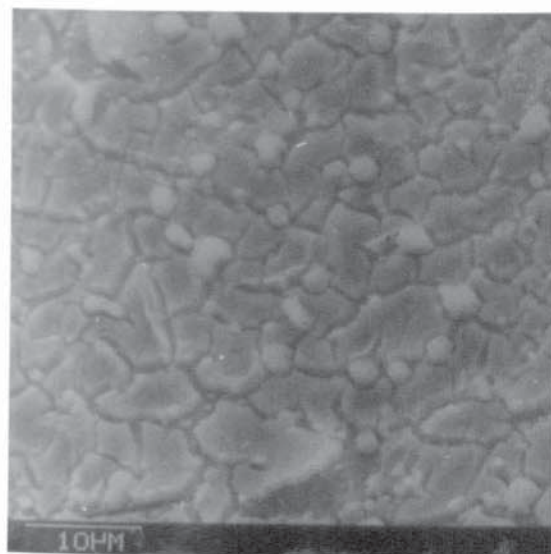
120 Seconds

Figure 6.4 continued

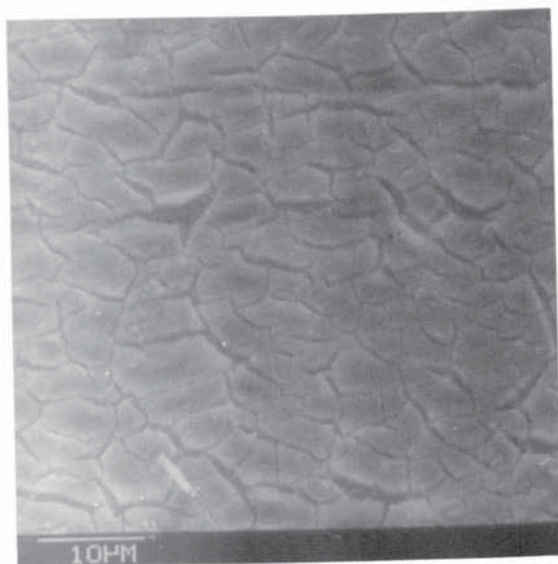
(c)



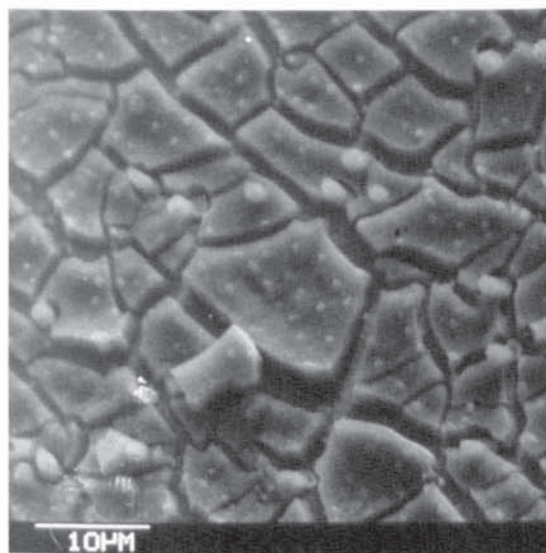
15 Seconds



30 Seconds



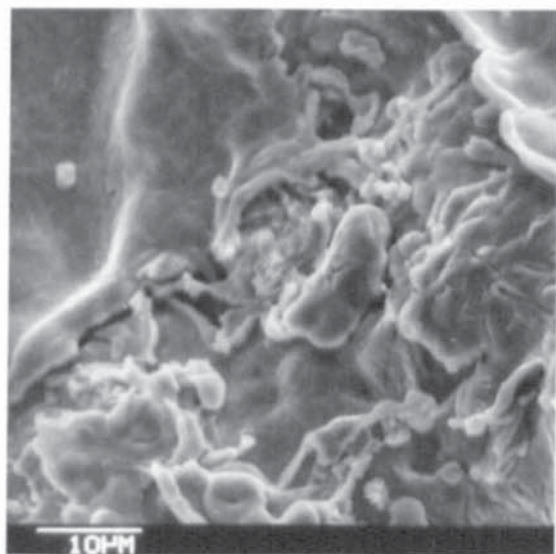
60 Seconds



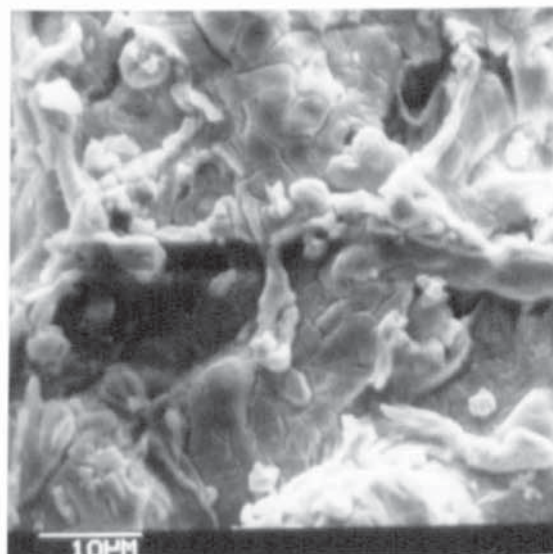
120 Seconds

Figure 6.4 continued

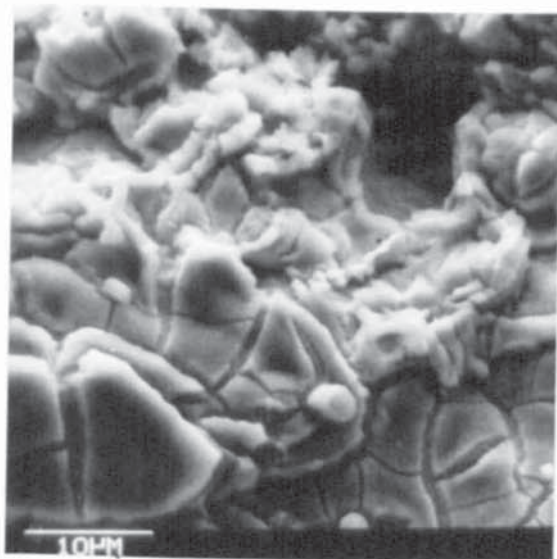
(d)



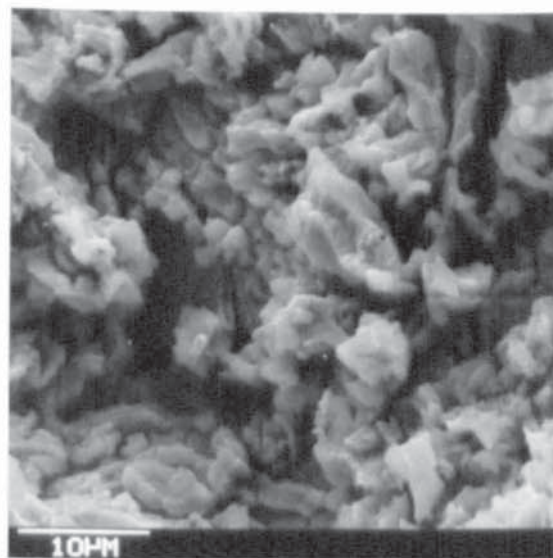
15 Seconds



30 Seconds



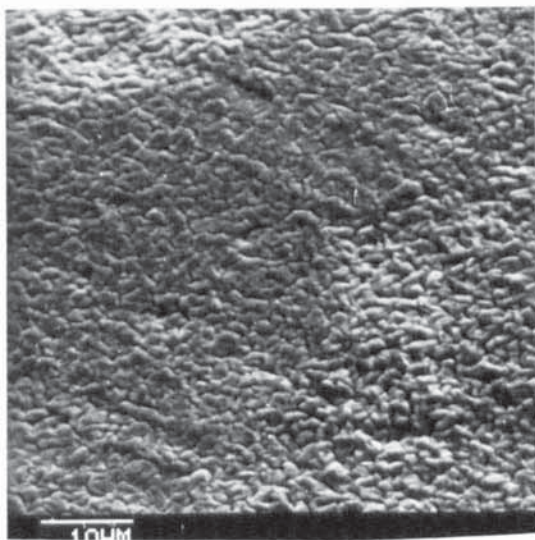
60 Seconds



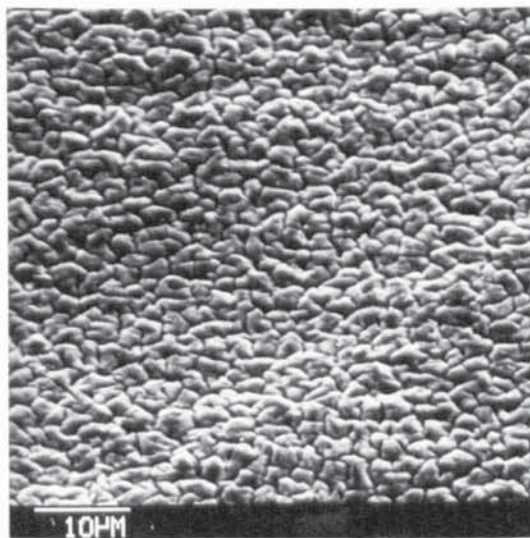
120 Seconds

Figure 6.4 continued

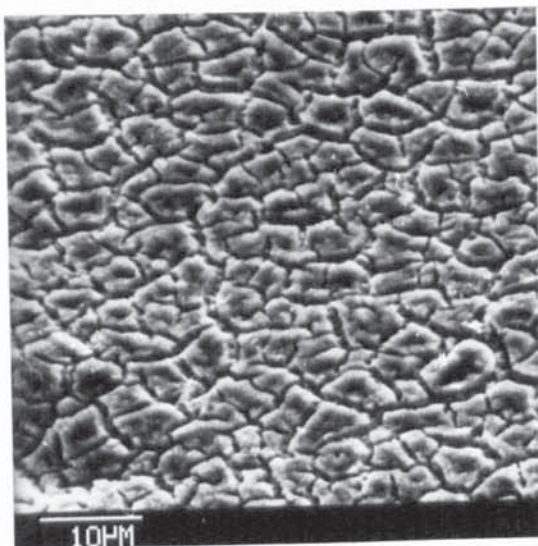
(a)



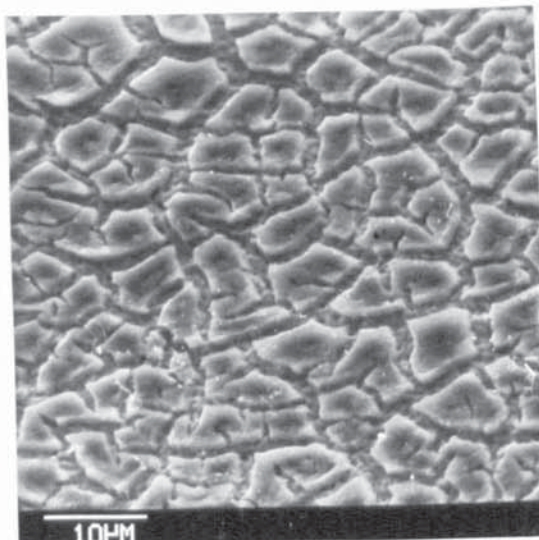
15 Seconds



30 Seconds



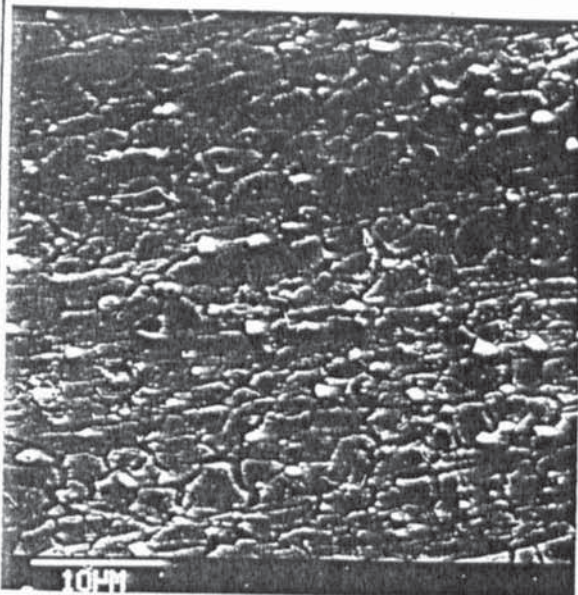
60 Seconds



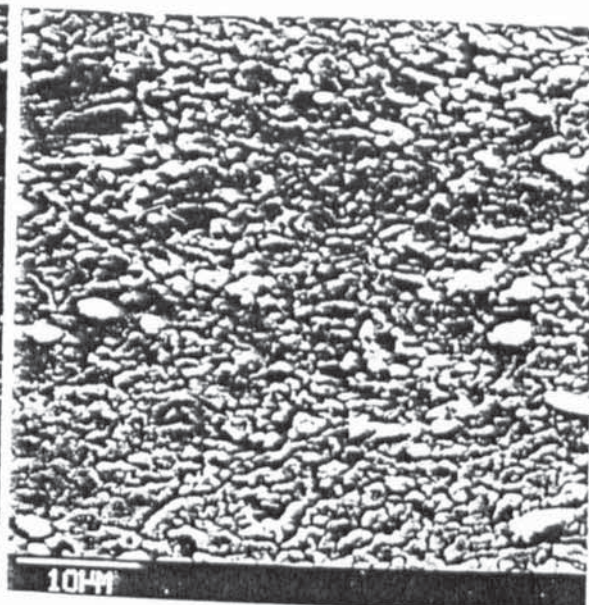
120 Seconds

Figure 6.5 Scanning electron micrographs showing the appearance of coatings formed on (a) electroplated, (b) HDC, (c) HDB and (d) sprayed samples in 0.12M/l  $\text{CrO}_3$  + 0.3M/l NaCl solution (L1) at 25°C and degassed at 220°C for 20 minutes

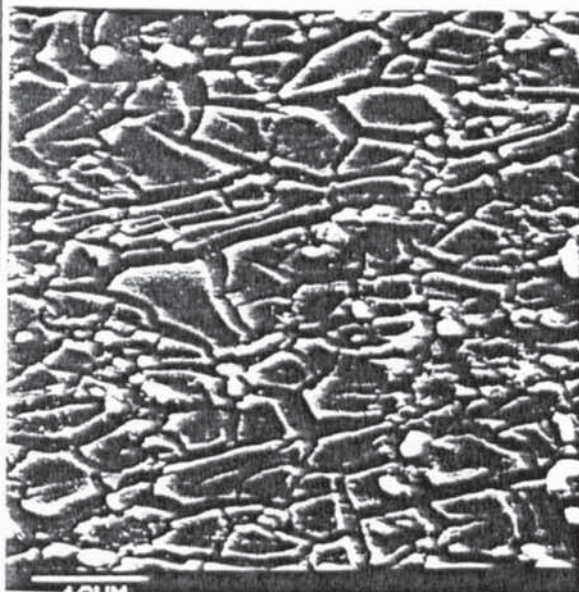
(b)



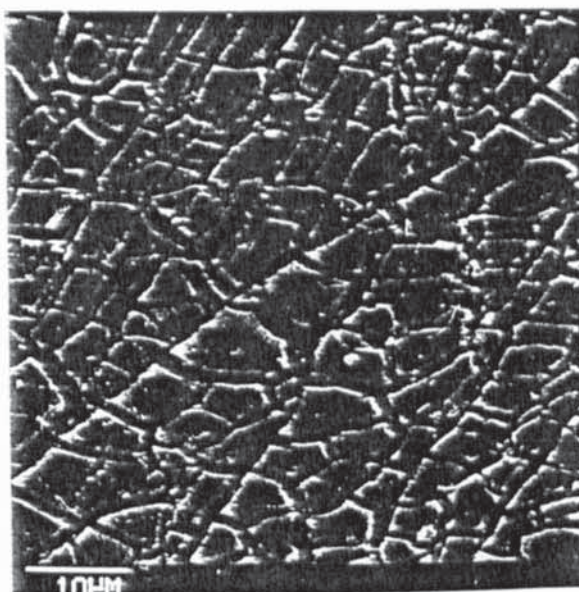
15 Seconds



30 Seconds



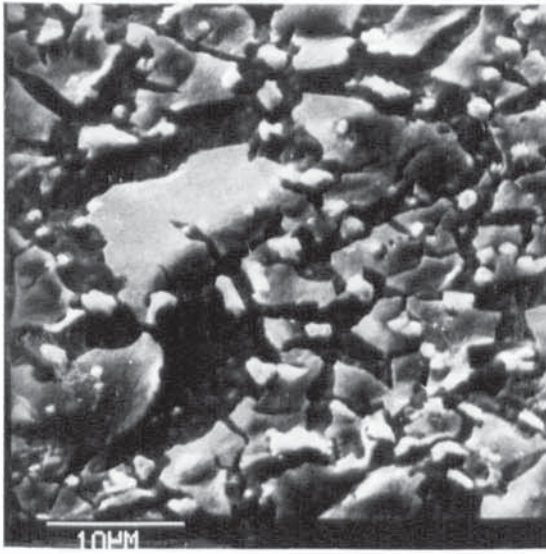
60 Seconds



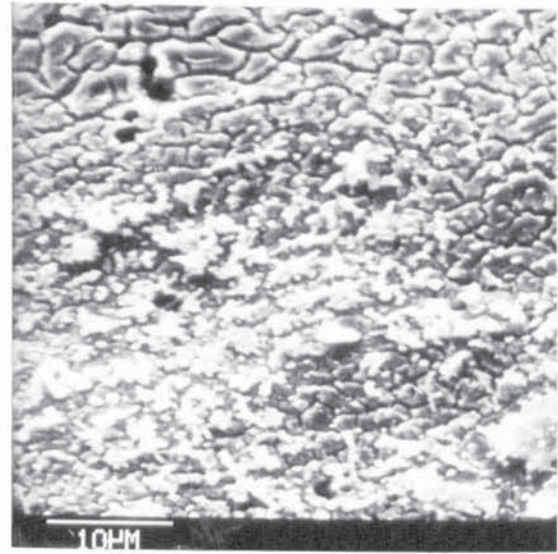
120 Seconds

Figure 6.5 continued

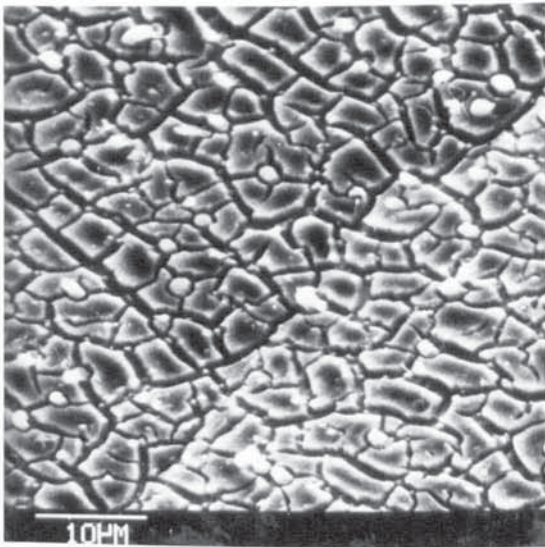
(c)



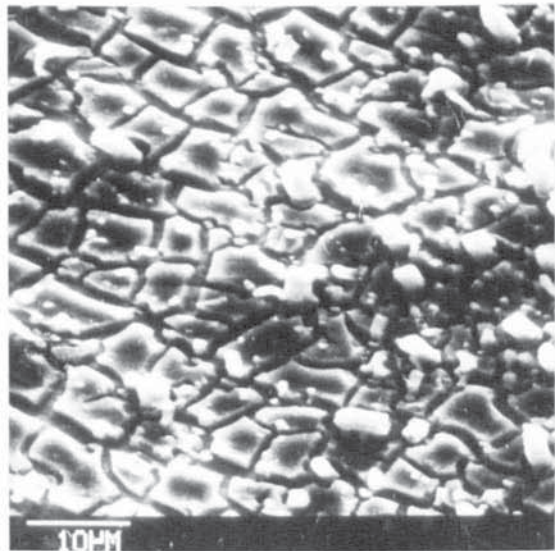
15 Seconds



30 Seconds



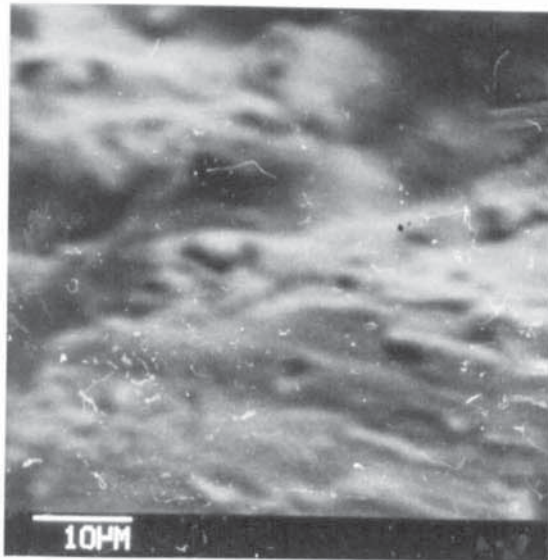
60 Seconds



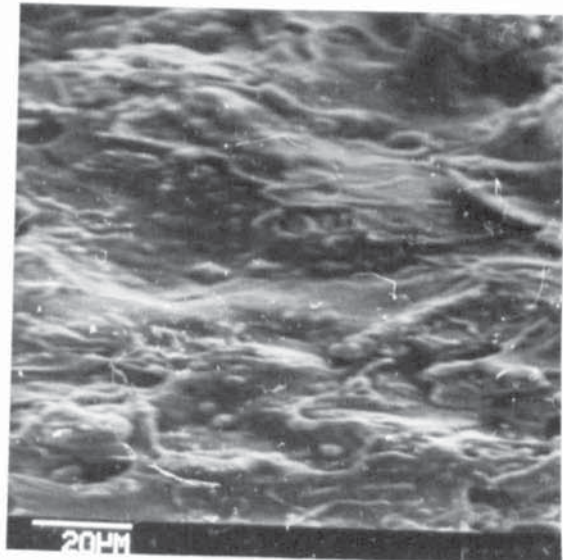
120 Seconds

Figure 6.5 continued

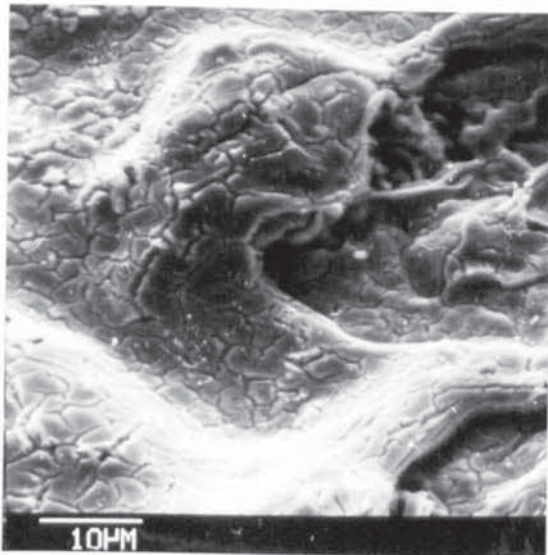
(d)



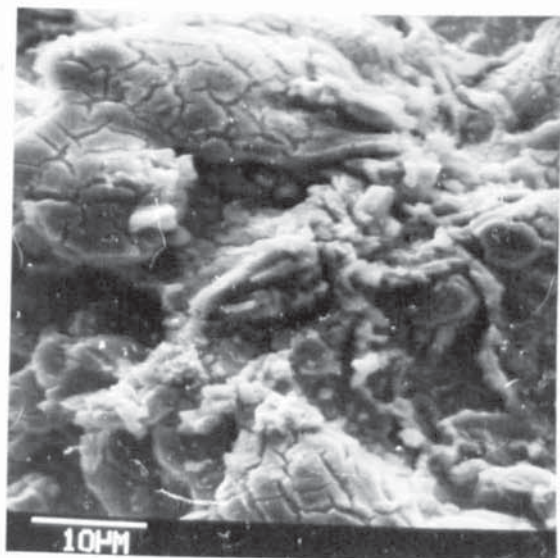
15 Seconds



30 Seconds



60 Seconds



120 Seconds

Figure 6.5 continued

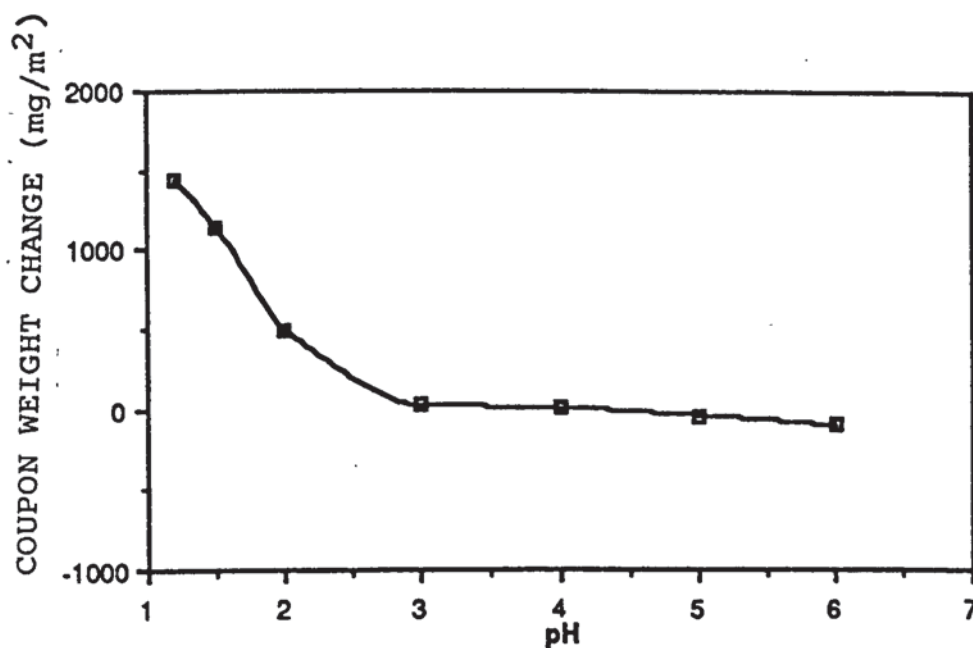


Figure 6.6 (a) Effect of variation of 0.12M/l  $\text{CrO}_3$  + 0.3M/l NaCl solution (L1) pH on coupon weight change of HDC samples treated for 120s

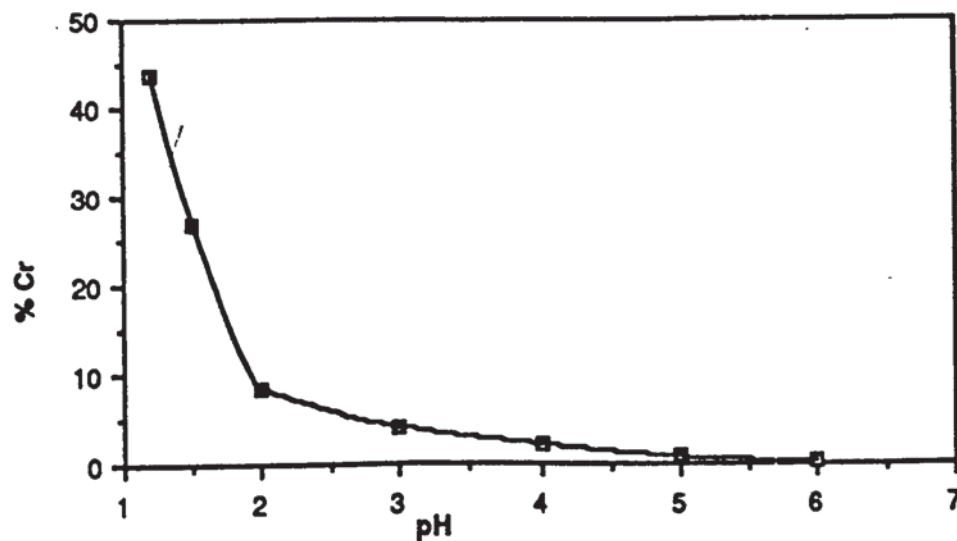
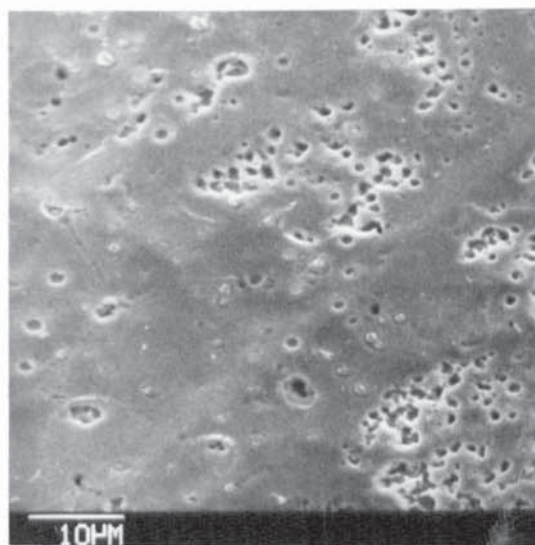


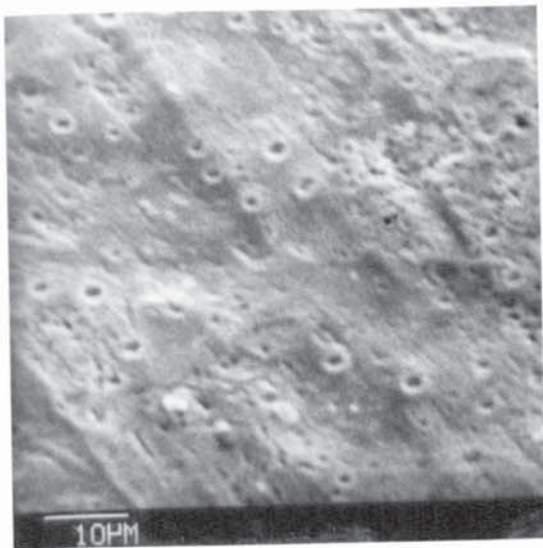
Figure 6.6 (b) Effect of variation of 0.12M/l  $\text{CrO}_3$  + 0.3M/l NaCl solution (L1) pH on at.% Cr content of conversion coating formed on HDC samples treated for 120s



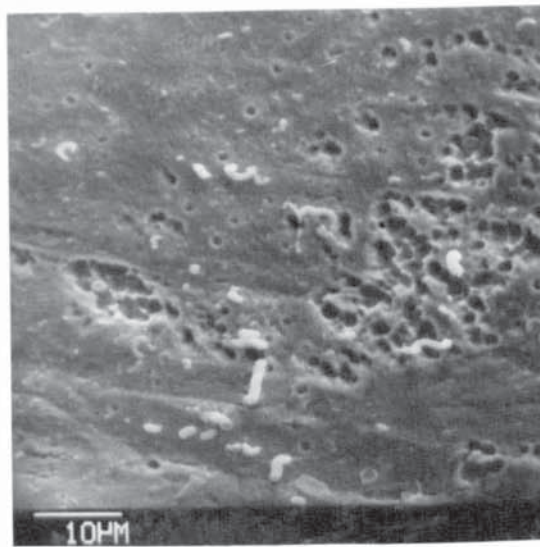
pH = 1.5



pH = 2.0



pH = 4.0



pH = 6.0

Figure 6.7 Scanning electron micrographs showing the appearance of conversion coatings formed on HDC samples treated for 120s in 0.12M/l  $\text{CrO}_3$  + 0.3M/l NaCl (L1) solution at different pH values

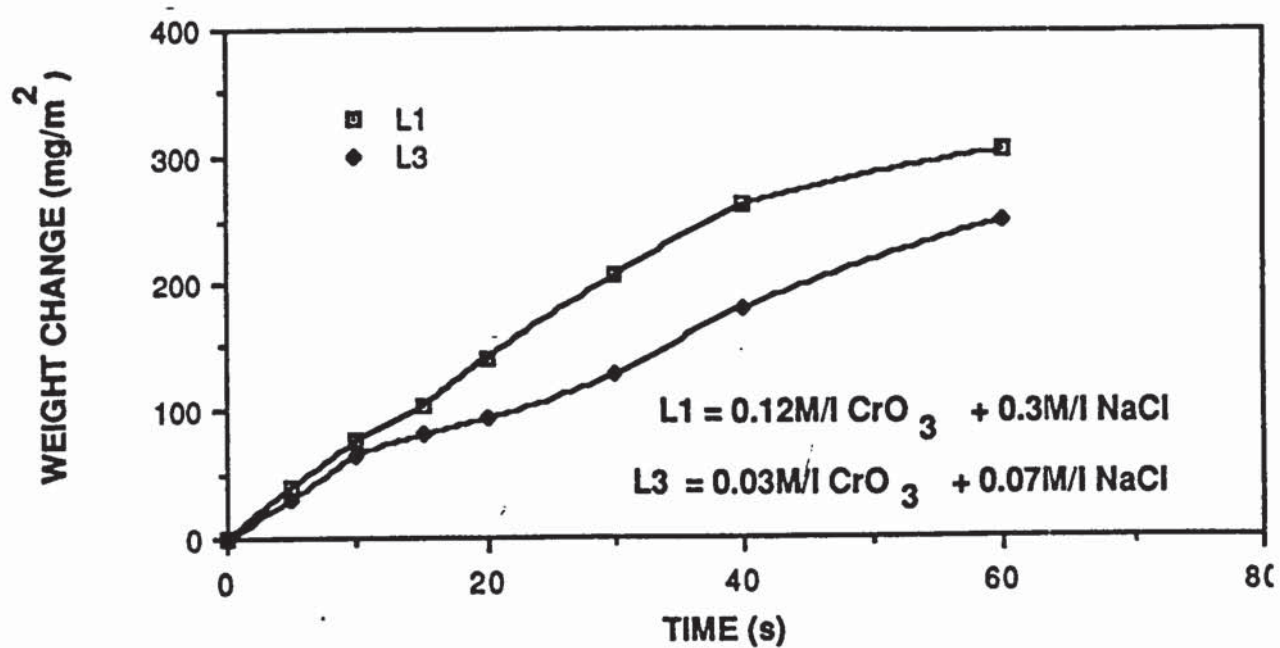
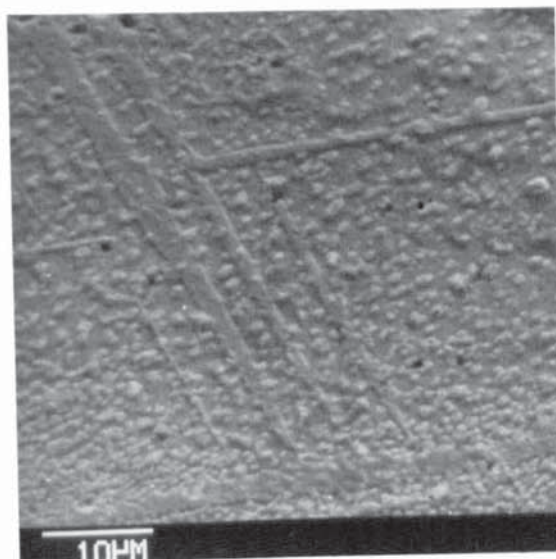
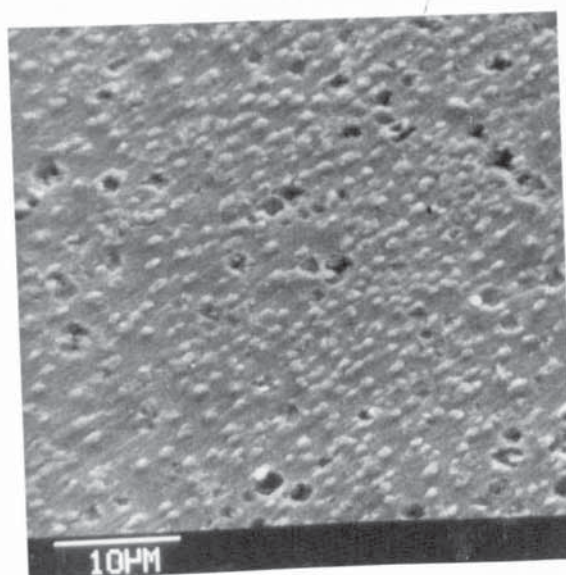


Figure 6.8 Coupon weight change of HDB vs time of immersion in L1 and L3

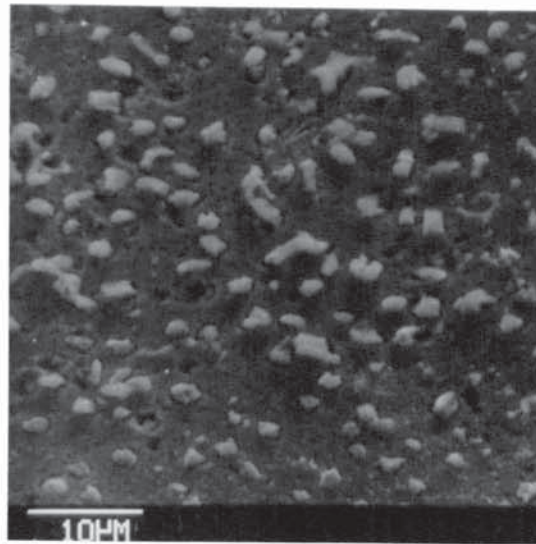


(a) 15 seconds

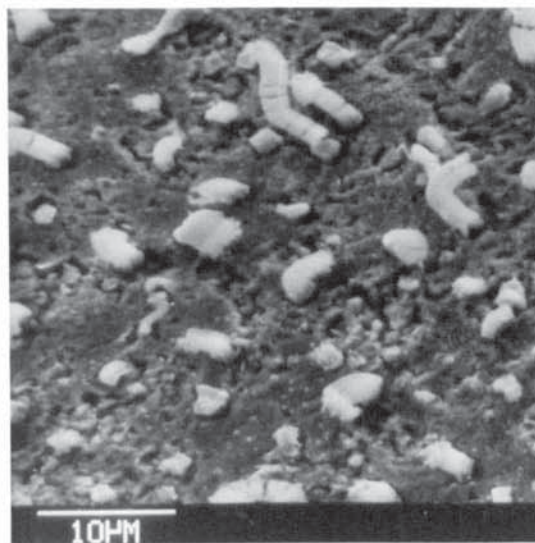


(b) 30 seconds

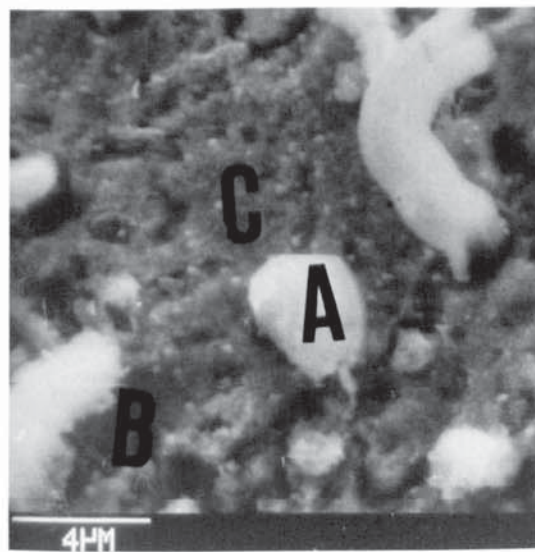
Figure 6.9 Scanning electron micrographs showing the appearance of conversion coatings formed on HDB in 0.03M/l  $\text{CrO}_3$  + 0.07M/l NaCl (L3) solution



(c) 60. seconds



(d) 120 seconds



(e) 120 seconds

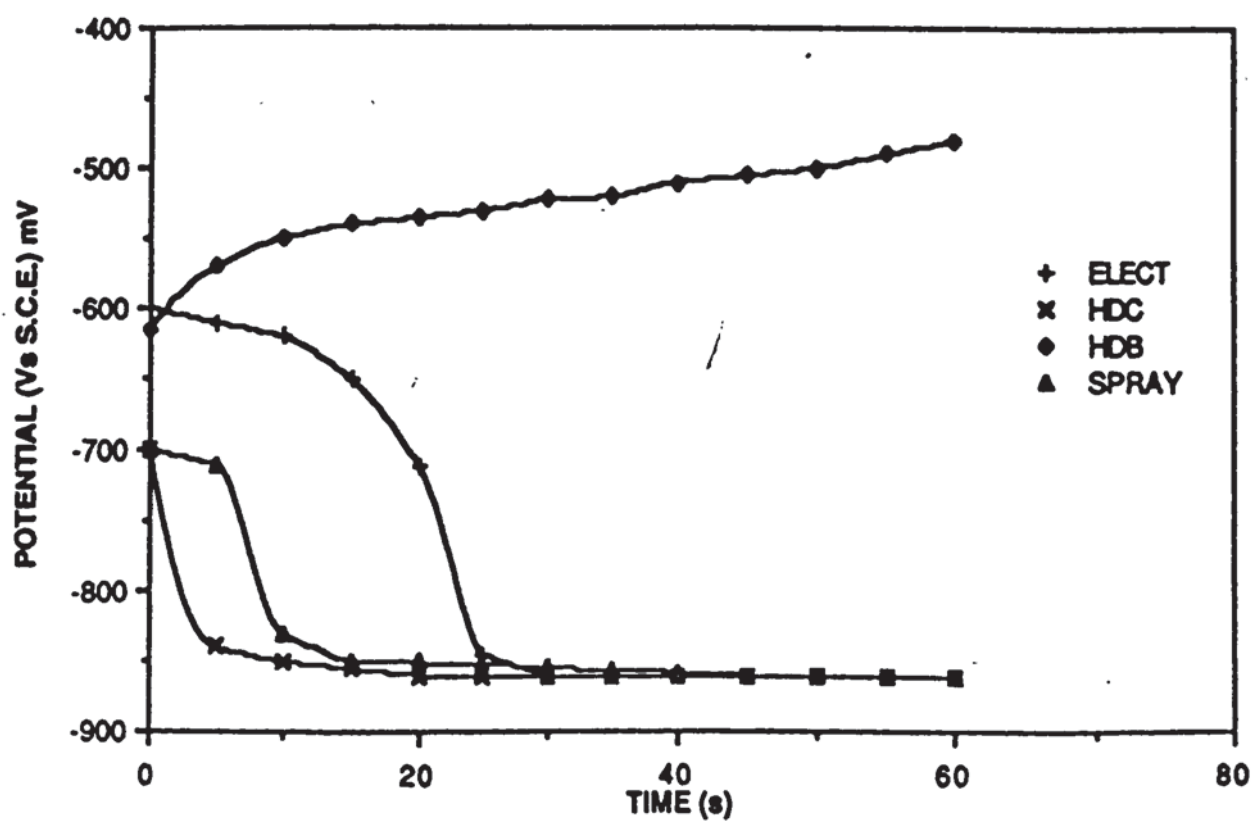
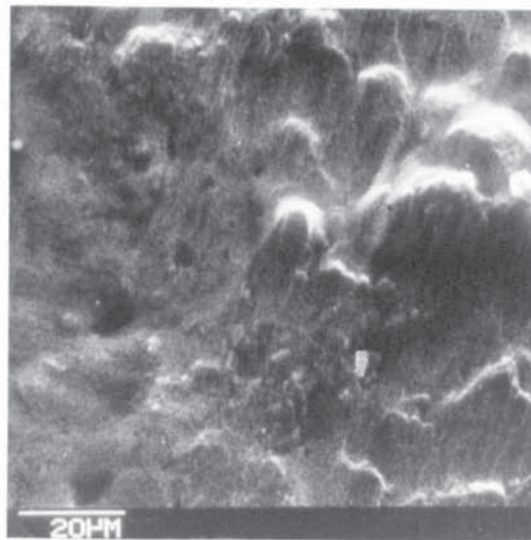
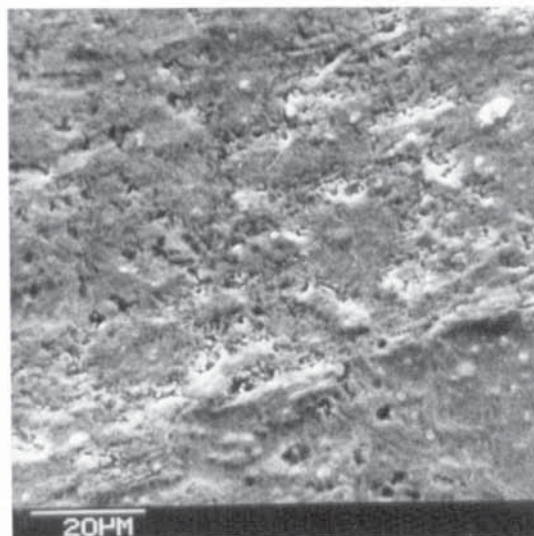


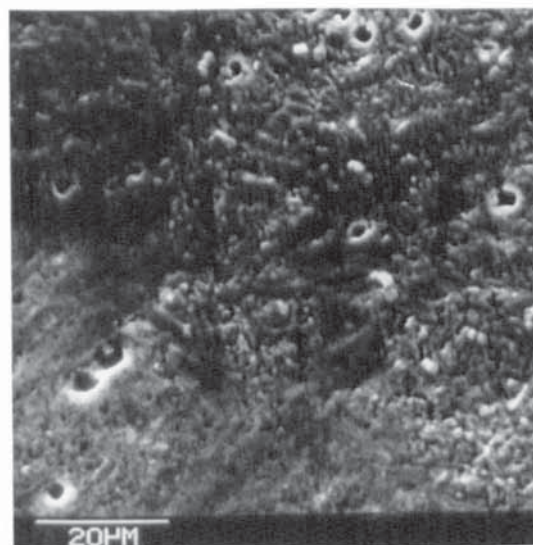
Figure 6.10 Rest potential vs immersion time in 0.12M/l  $\text{CrO}_3$  + 0.1M/l NaF (L2) solution



(60 seconds)



(120 seconds)



(300 seconds)

Figure 6.11 Scanning electron micrographs showing the appearance of conversion coatings formed on HDC in 0.12M/l  $\text{CrO}_3$  + 0.1M/l NaF (L2) solution

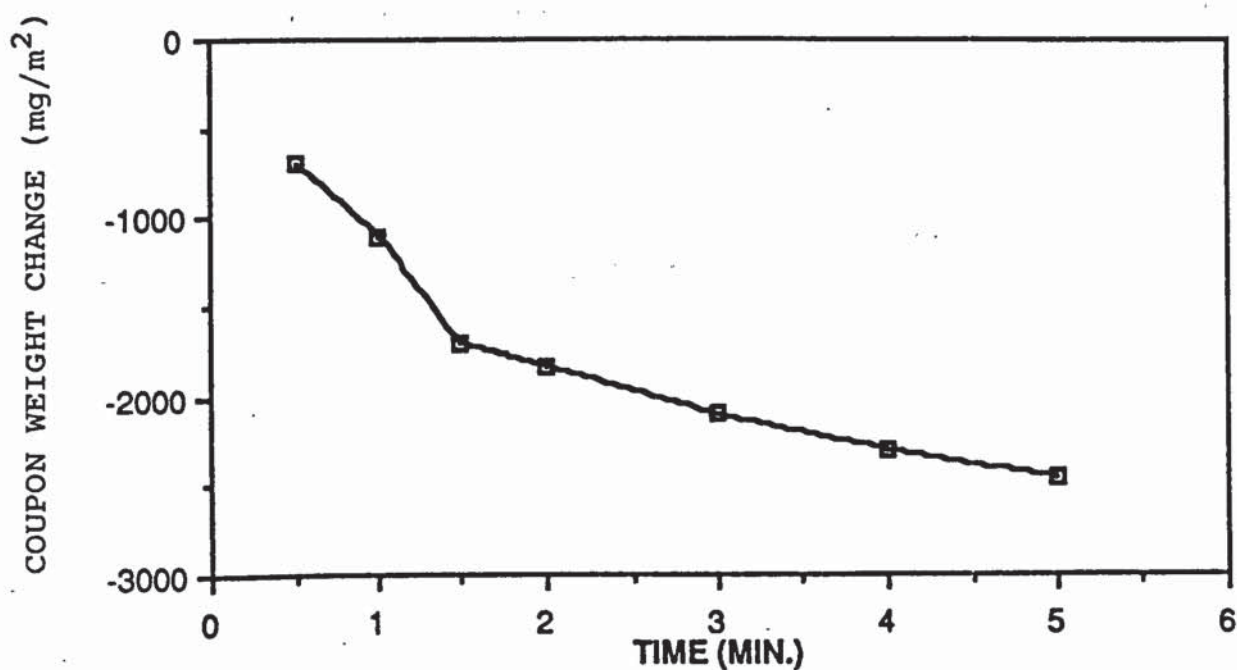


Figure 6.12(a) Coupon weight change vs immersion time in 0.12M/l  $\text{CrO}_3$  + 0.1M/l NaF (L2) solution

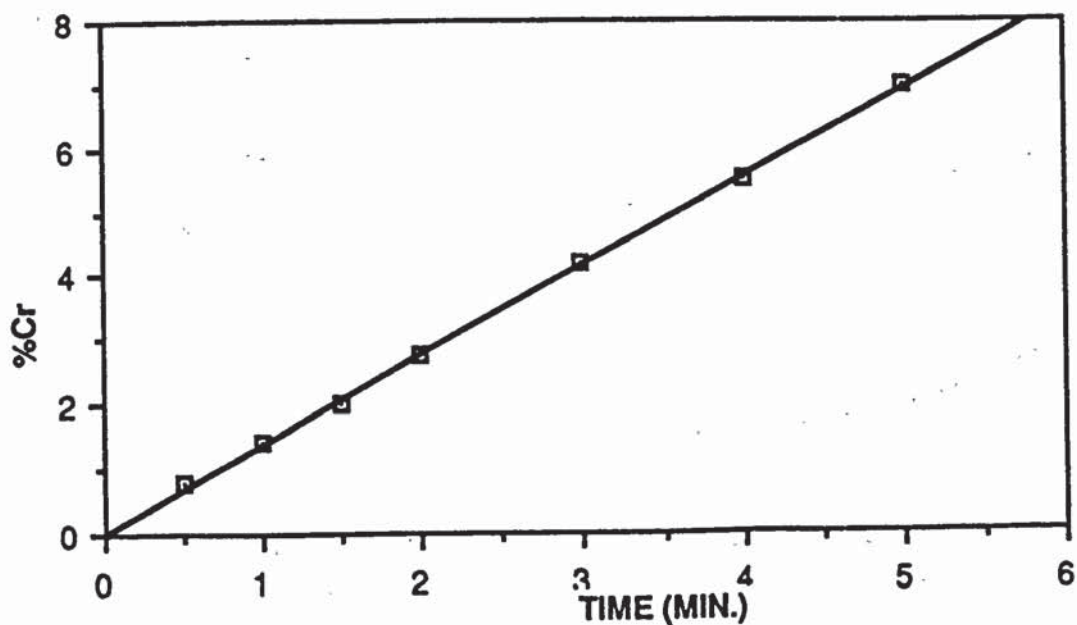


Figure 6.12(b) At. % Cr vs immersion time of HDB in 0.12M/l  $\text{CrO}_3$  + 0.1M/l NaF (L2) solution

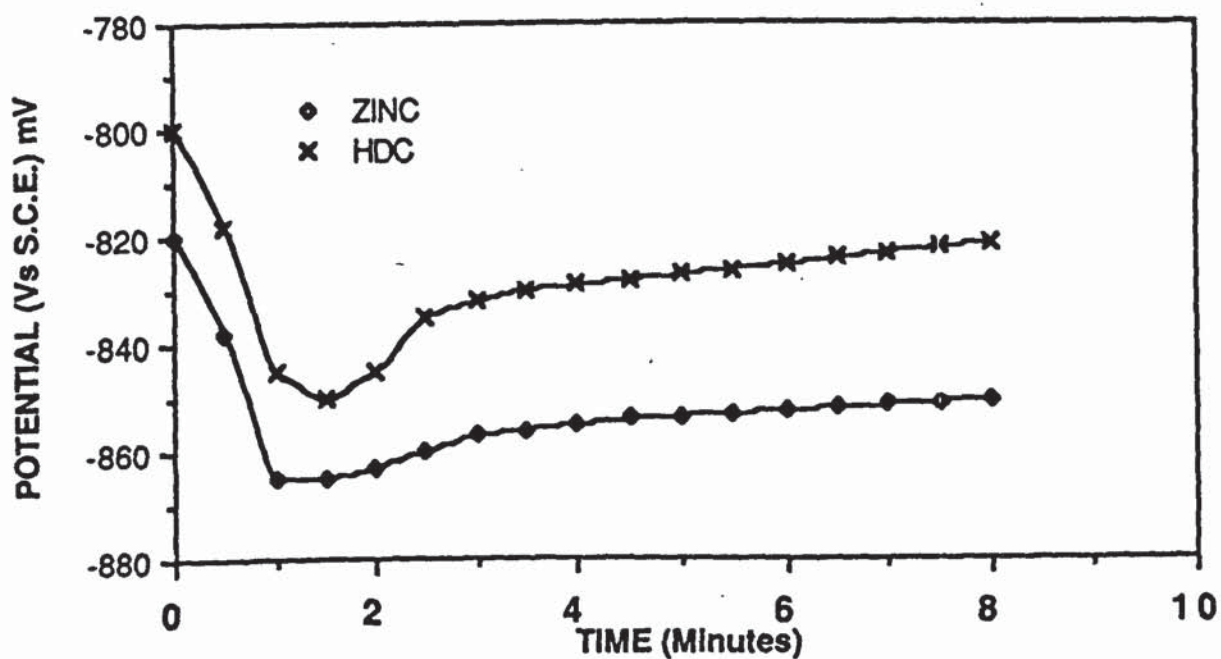


Figure 6.13 Potential vs immersion time in Alocrom 100 solution

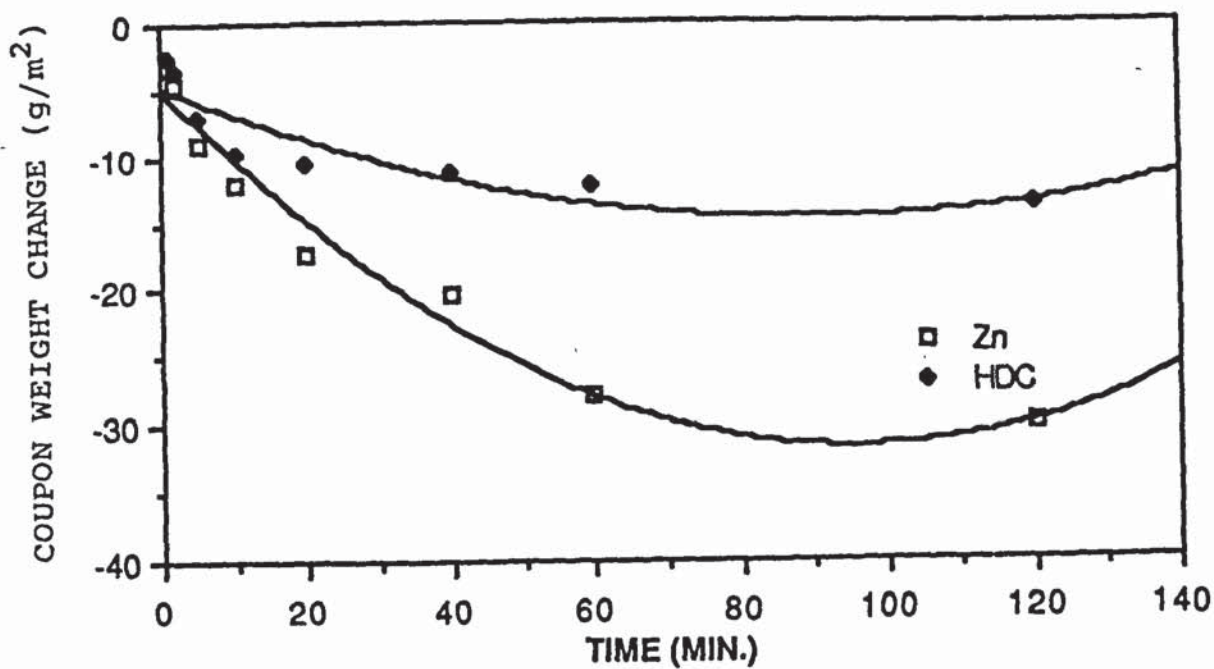


Figure 6.14 Coupon weight change vs immersion time in Alocrom 100 solution

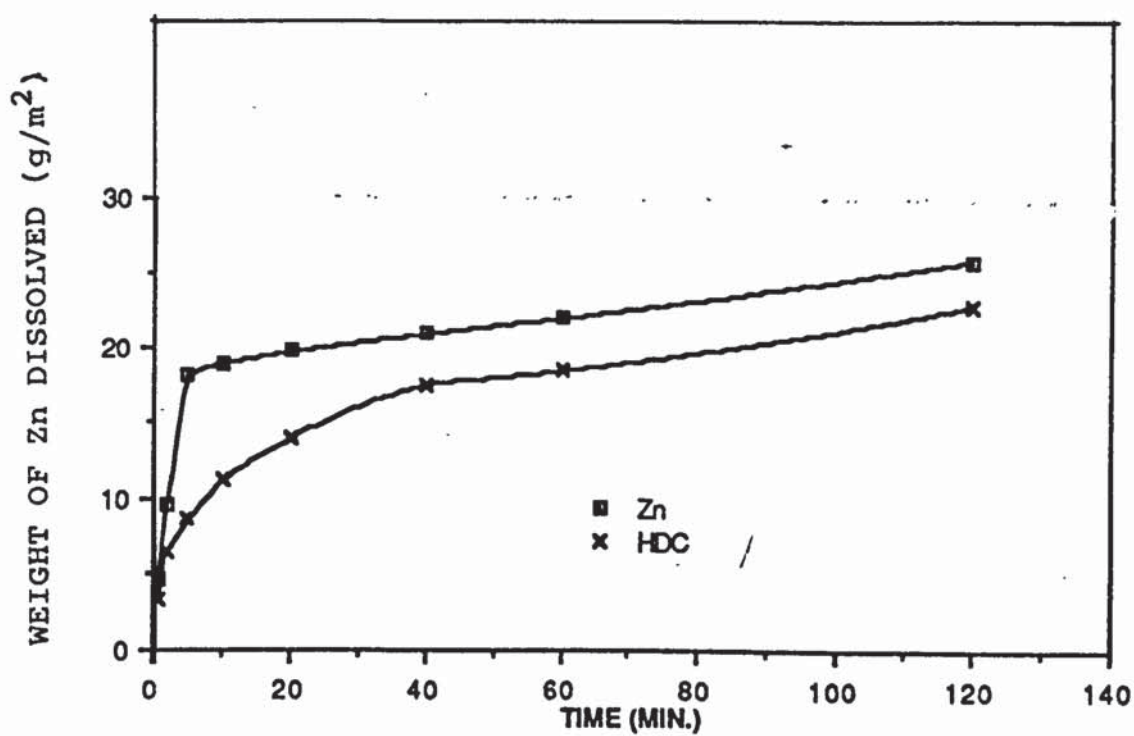
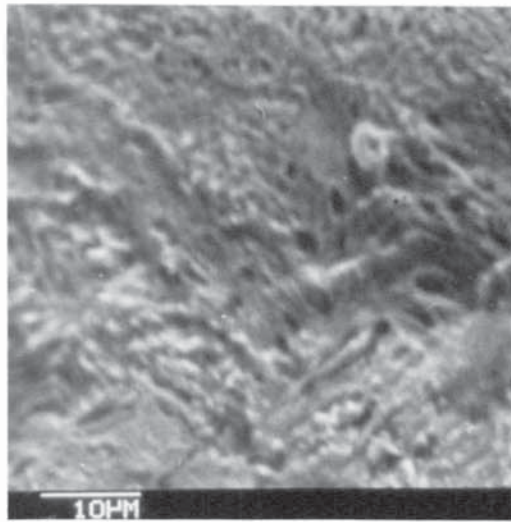
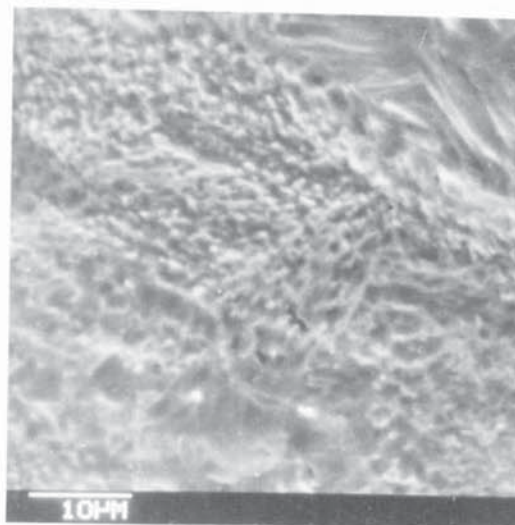


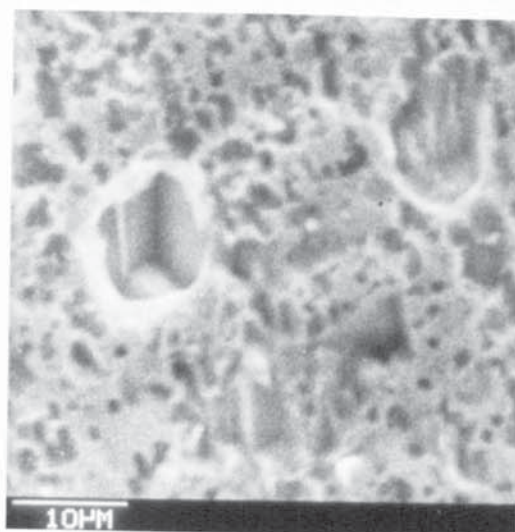
Figure 6.15 Weight of zinc dissolved vs immersion time in Alocrom 100 solution



60 seconds

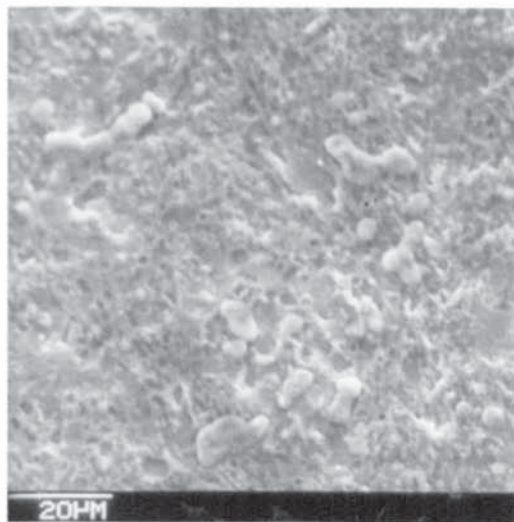


300 seconds

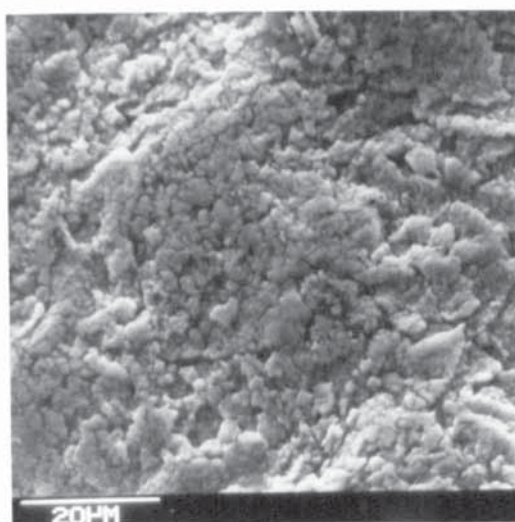


600 seconds

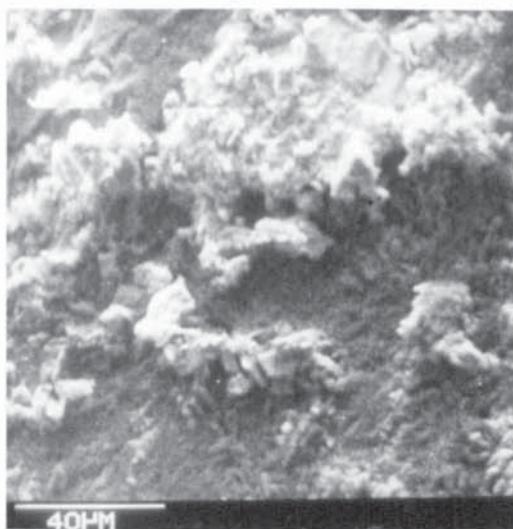
Figure 6.16(a) Scanning electron micrographs showing the appearance of conversion coatings formed on pure Zn samples in Alocrom 100 solution



60 seconds



300 seconds



600 seconds

Figure 6.16(b) Scanning electron micrographs showing the appearance of conversion coatings formed on HDC samples in Alocrom 100 solution

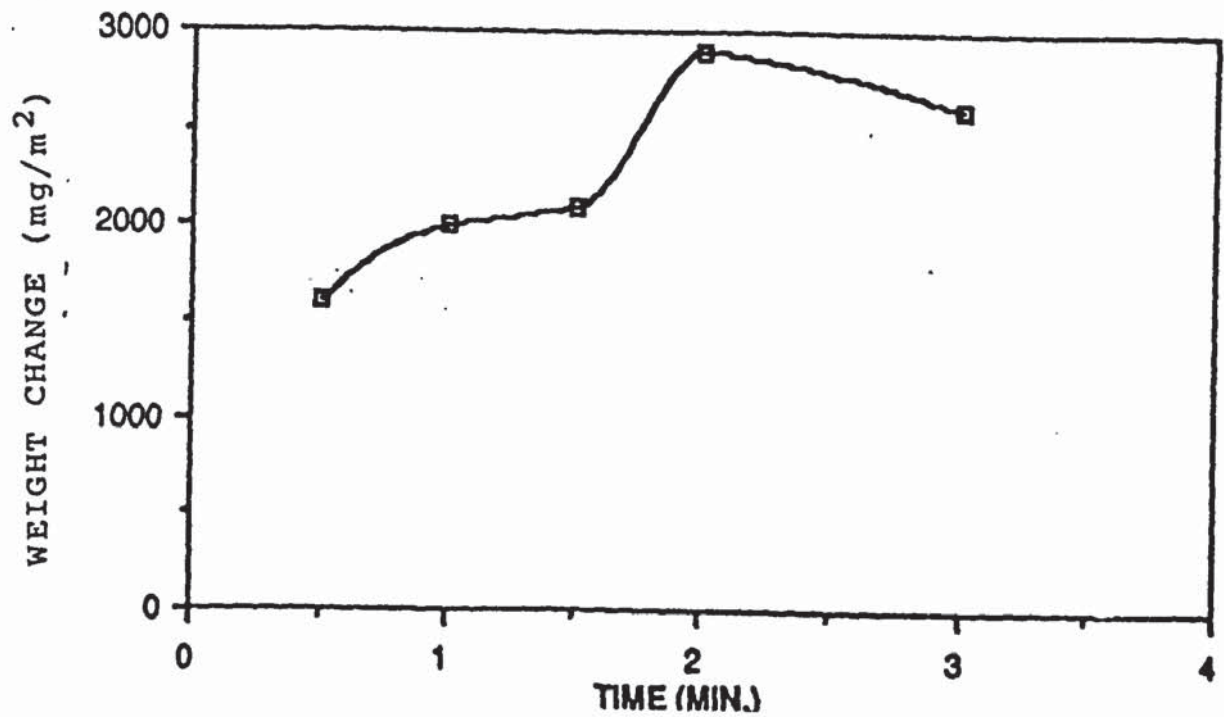


Figure 6.17 (a) Coupon weight change of electroplated sample vs immersion time in Chrometan solution

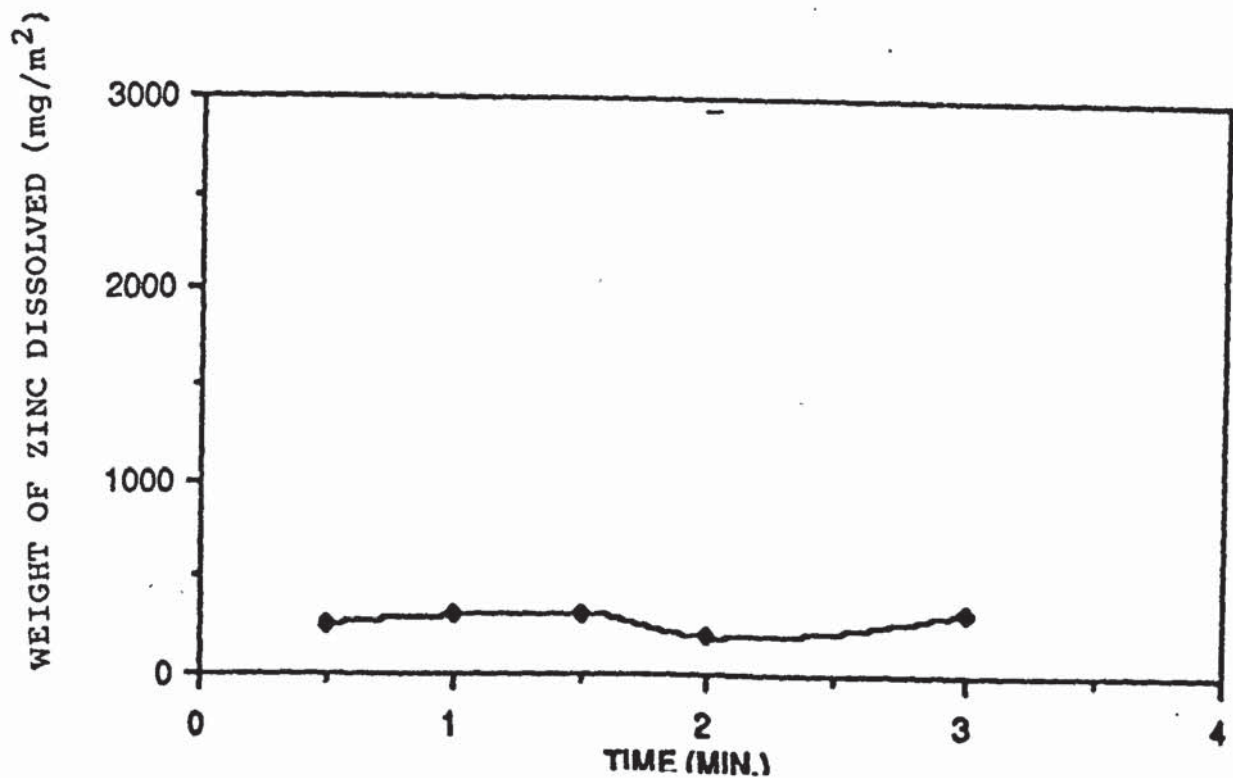
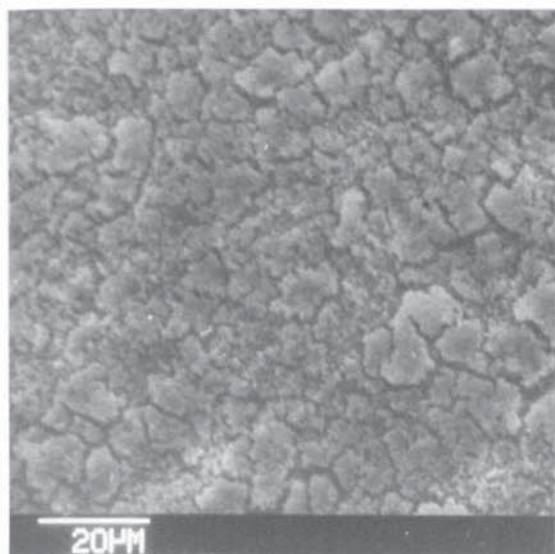
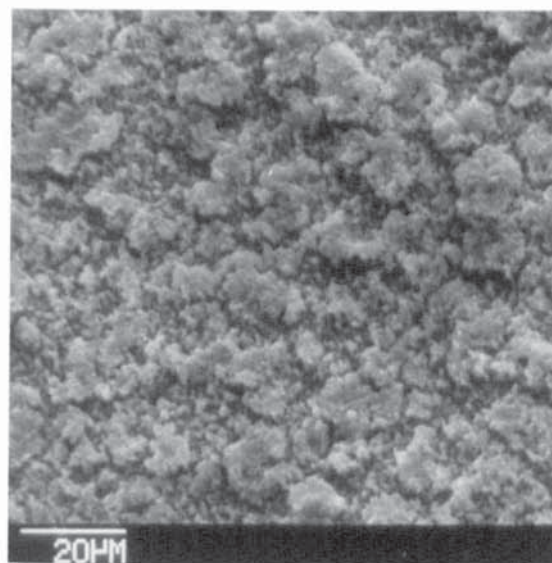


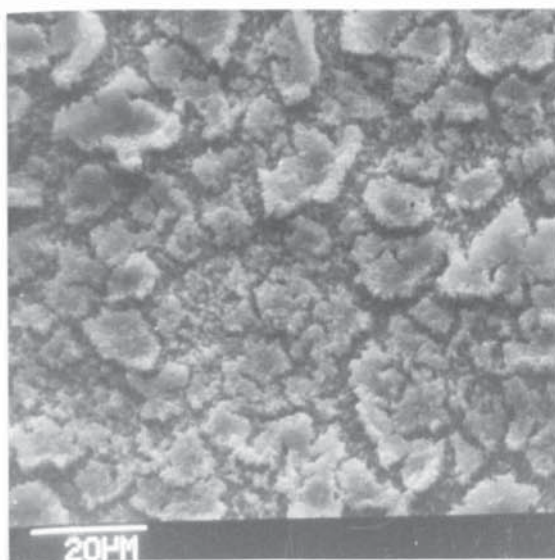
Figure 6.17 (b) Weight of zinc dissolved of electroplated sample vs immersion time in Chrometan solution



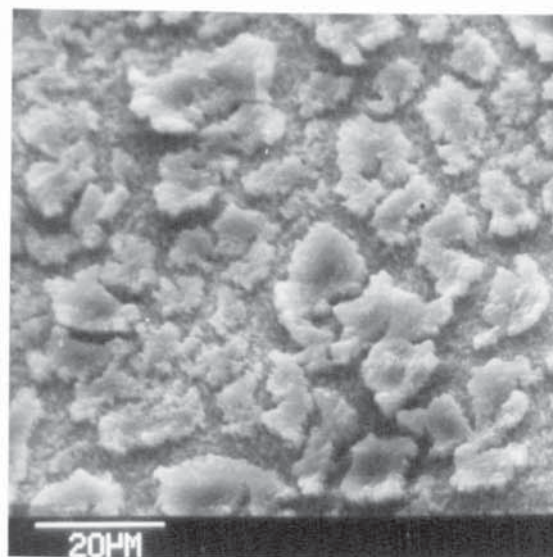
15 Seconds



30 Seconds



60 Seconds



120 Seconds

Figure 6.18 Scanning electron micrographs showing the appearance of conversion coatings formed on electroplated samples in Chrometan solution

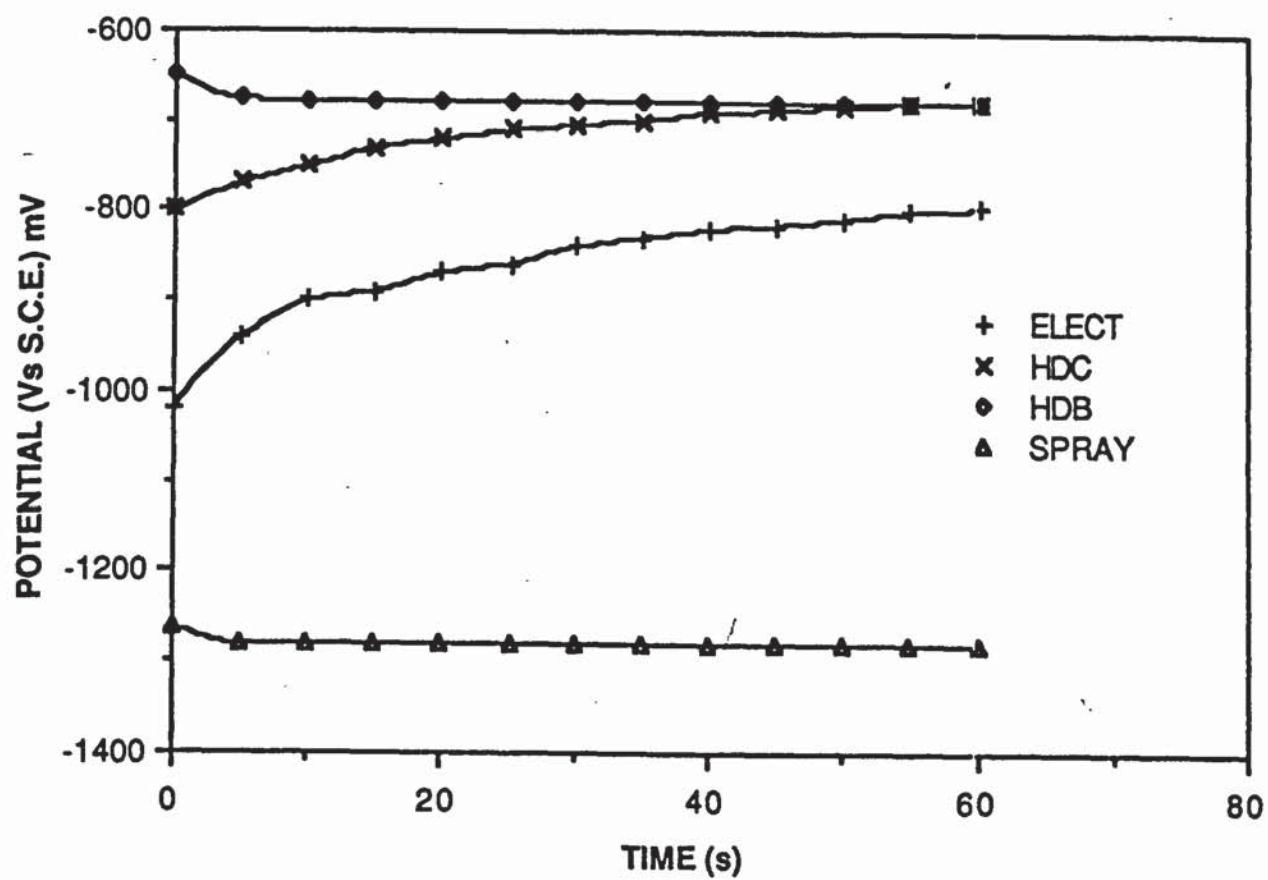


Figure 6.19 Rest potential vs time of immersion in NaOH solution

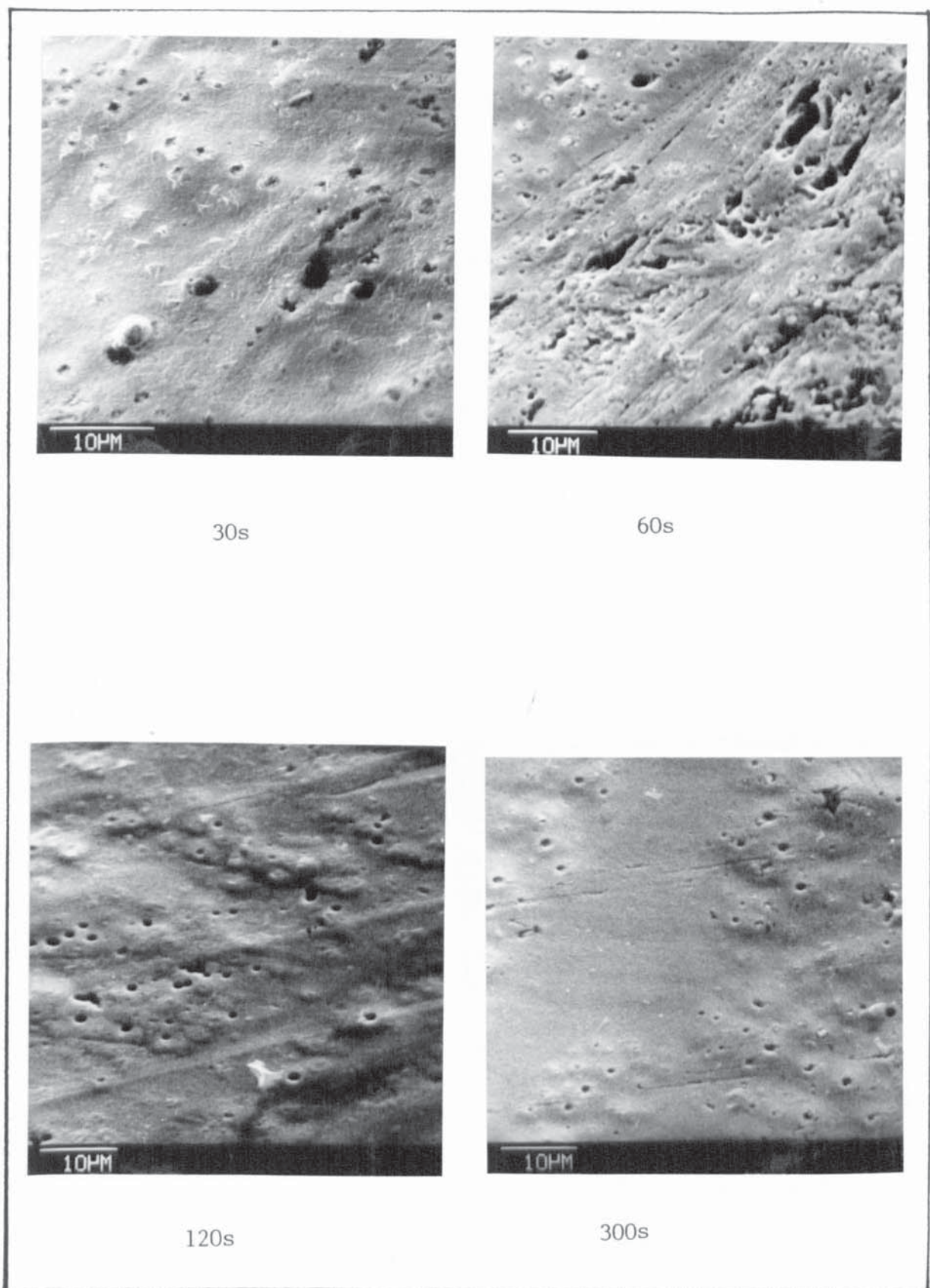


Figure 6.20      Scanning electron micrographs showing the appearance of conversion coatings formed on electroplated samples in NaOH solution

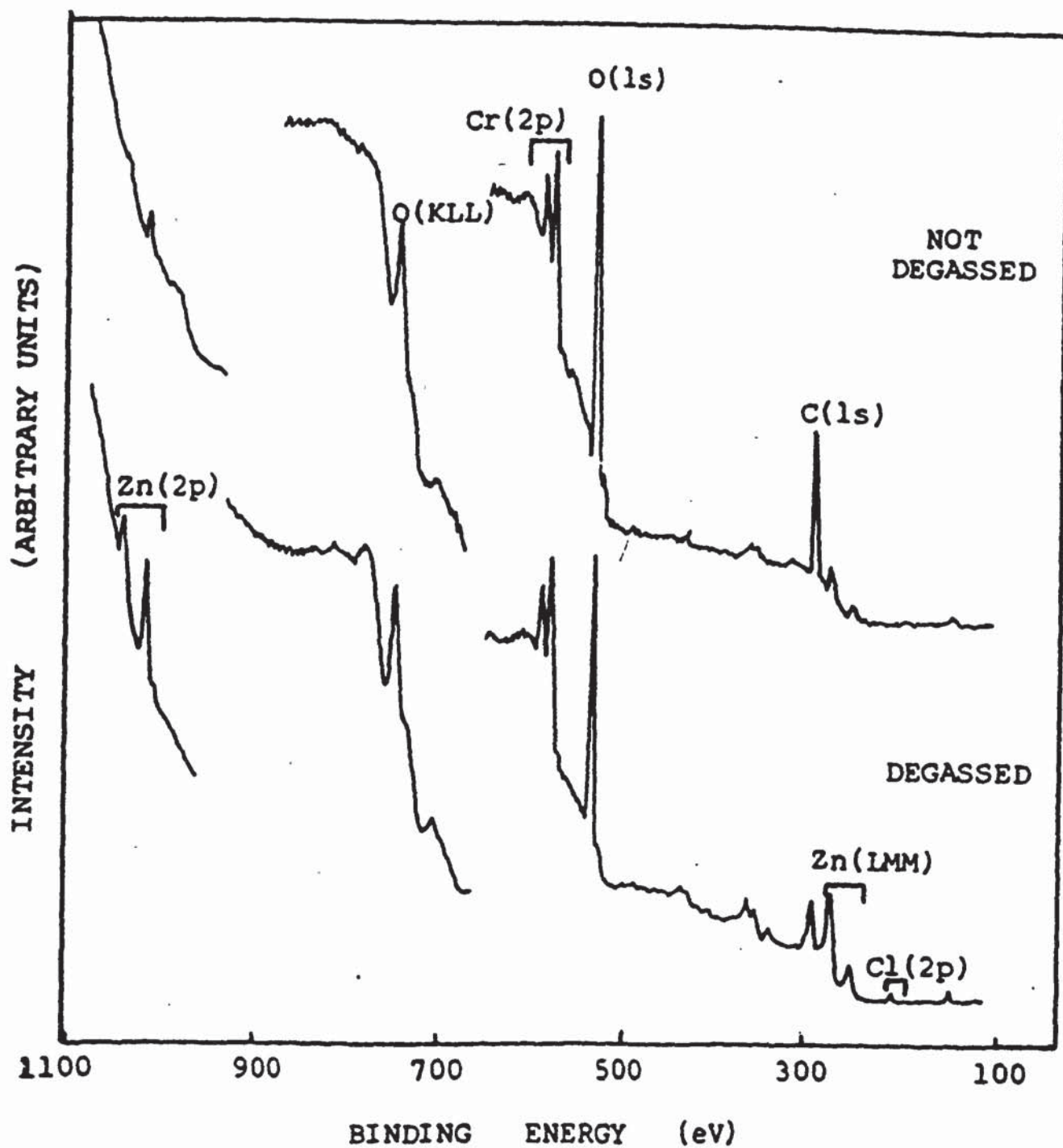


Figure 6.21 XPS survey spectra of chromated electroplated zinc

## 7 ELECTROCHEMICAL BEHAVIOUR OF ZINC COATED STEEL IN CONVERSION COATING SOLUTIONS

### 7.1 INTRODUCTION

Most zinc coating processes such as electroplating (Zintec), continuous hot-dip galvanizing, spraying etc, produce an outer-most-surface layer which is normally nearly pure zinc. However, in the case of batch hot-dip galvanizing the eta (nearly pure zinc) phase is sometimes absent owing to variations in steel composition and galvanizing parameters, leaving the zeta phase exposed at the surface. The aim of this part of the project was to compare the electrochemical behaviour of zinc coatings having an outer most layer of the zinc (eta) phase with zinc coatings possessing an outer most layer of the zeta phase. The effects of solutions having different compositions and pH values were compared. The results were related to the simplified potential - pH diagrams for Zn - H<sub>2</sub>O, Cr - H<sub>2</sub>O, Fe - H<sub>2</sub>O figure 7.1(a-c) and combined diagram, figure 7.1(d)

### 7.2 SAMPLE AND SOLUTION PREPARATION

The materials used in this investigation were as drawn iron rod (main impurities - Mn 0.08, P 0.03, S 0.02, C 0.02 at.-%) and zinc rod (main impurities - Pb 0.03, Cd 0.02, Fe 0.01 at.-%). The iron rod was machined into discs 15 mm diam. x 10 mm thickness. These discs were then galvanized and by careful manipulation of the galva-

nizing parameters (2 hours at 450°C) virtually all the zinc was consumed, leaving a relatively thick layer of the zeta phase (Fe content 6.9 at.-%) which was porosity free<sup>(139)</sup>. The galvanized discs were mounted in resin (CIBA - Giegy, HY932/MY753) and the surface was ground flat to remove any final traces of the eta phase. That the ground surface consisted of the zeta phase was confirmed by microhardness measurements. The surface was then re-ground, degreased in acetone, cleaned in AC51 and rinsed in distilled water. Zinc discs, of similar dimensions, which may be regarded as representing the eta phase, were mounted and polished in the same manner.

The laboratory prepared conversion coating solutions were of the chromate and alkaline types and their chemical composition and pH are given in table 7.1. They are grouped according to similarities in chemical composition

### 7.3 ELECTROCHEMICAL STUDIES

The electrochemical behaviour of the samples (zeta and zinc) were compared using two techniques:

#### (a) Potentiodynamic anodic polarisation.

This technique was used to determine:

- (i) the ability to passivate
- (ii) the potential region over which passivity was maintained ( $E_p$ )
- (iii) the corrosion or dissolution rate when passive (at  $i_p$ )

The detailed procedures were given in section 3.7. A polarisation range of -1.5 V to +1.5 V was chosen so as to cover the whole of the domains shown in figure 7.1 (a-d). Also, polarising from -1.5V, a potential less than the rest potential of zinc or iron in the various solutions used, allowed initial cathodic polarisation which reduced any oxide on the sample surfaces.

#### (b) Potentiostatic anodic polarisation

This technique was used to produce conversion coatings at a constant suitable potential and then assess the protectivity of the film formed by its ability to prevent or reduce further dissolution of the substrate. The log current density measured at a particular time and the rate of current drop with time, were taken as measures of the sample dissolution rate at that particular time and the amount of protection offered by the film formed respectively.

It should be remembered that conversion coatings are considered to be formed by dissolution and precipitation mechanisms. For the chromating process, the dissolution reactions can be written as<sup>(44)</sup>:



and the precipitation reaction as:



The hexavalent chromium complex is frequently termed the

"soluble" portion of the film and it is this that provides resistance to corrosion. However, the compounds which contain soluble hexavalent chromium (chromic acid and chromates) are energy-rich needing highly positive potentials for their formation (figure 7.1). Therefore to obtain the above mentioned conditions, a constant potential of +1.5V was used for the potentiostatic anodic polarisation experiment.

## 7.4 RESULTS & DISCUSSION

### 7.4.1 POTENTIODYNAMIC ANODIC POLARISATION

The curves obtained from the Potentiodynamic polarisation of zeta and zinc samples in the various groups of solutions, Table 7.1, are shown in figure 7.2 (a-h). The curves showed in figure 7.2 (a) were obtained from solutions L1 (0.12 M/l  $\text{CrO}_3$  + 0.30 M/l NaCl), L2 (0.12 M/l  $\text{CrO}_3$  + 0.10 M/l NaF) and L3 (0.03 M/l  $\text{CrO}_3$  + 0.07 M/l NaCl). Table 7.2 gives sample dissolution rate ( $i_{\text{corr}}$ ) in the solutions at a potential of 0.0 V in figure 7.2(a).

It can be seen that the curves for both zeta and zinc have the same profile and no passivity range was obtained. It is known that when the potential of a metal such as zinc is raised anodically beyond its equilibrium potential, a protective film forms on the metal surface, provided the pH of the solution lies within the passivity domain of the Zn- $\text{H}_2\text{O}$  potential versus pH diagram. An attempt to produce a potential versus pH diagram for the

Zn-Cr-Fe-H<sub>2</sub>O system by superimposing Cr- H<sub>2</sub>O and Fe-H<sub>2</sub> diagrams upon Zn-H<sub>2</sub>O diagram is shown in figure 7.1(d). It can be seen from this figure that the pH values of L1, L2 and L3, lie outside of the passivity domain. These pH values are in the corrosion region and the curves in figure 7.2(a) show that dissolution of zeta phase and zinc will occur. Irrespective of many drawbacks associated with potential versus pH diagrams, the potentiodynamic curves obtained from solutions L1, L2 and L3 are in agreement in this instance.

However, the dissolution rates of the samples differ in different solutions as can be seen from the perpendicular dotted lines drawn from the point of intersection of the curves and a horizontal straight dotted line through zero potential in figure 7.2(a). It can be seen that solution L3, which was a diluted version of L1, had a lower dissolution rate compared to L1 and L2, even though the solution (L3) has the same and lower pH compared to L1 and L2 respectively. This highlighted the importance of solution formulation, bath composition and concentration. This is substantiated by the fact that during anodic polarisation, it is known that the rate of metal dissolution depends on the metal exchange current density for the H/H<sup>+</sup> reaction on the particular metal and that the H/H<sup>+</sup> reaction is greatly affected by the type and concentration of the oxidizing reactants and by alloy or impurities in the metal. For example, the presence of halide ions (eg Cl<sup>-</sup> , F<sup>-</sup>) is known to accelerate the corrosion

rate and impedes the mechanisms of protective film formation. Increasing the halide ion concentration in solution led to an increase in the oxidizing reactants in the solution. Also, it is known that increasing the  $\text{Cl}^-$  ion concentration moves the onset of pitting corrosion potential to a lower potential. All these facts are shown in figure 7.2(a). Bengough, Lee and Wormovell<sup>(140)</sup> have shown that when zinc and iron were fully immersed in chloride (KCl) solution, the rate of attack increased with increasing KCl concentration. Also, when Borgmann and Evans<sup>(141)</sup> studied the corrosion of zinc in chloride solution, they found that the rate of dissolution increased with increasing concentration of chloride when zinc was partially immersed in the solution. The later authors attributed this increase in dissolution rate to an increase in conductivity of the solution as a result of the increase in concentration.

Another interesting point revealed in figure 7.2(a), was that at a given potential, the zeta phase sample had a lower dissolution rate (log current density) for the three solutions. The mechanism responsible for this difference is not fully understood. Patterson<sup>(142)</sup> indicated that iron, when added to zinc as impurity, provided a protective action when fully immersed. Borgmann and Evans<sup>(141)</sup> reported a slight increase in attack on partially immersed zinc alloyed with iron (0.05%) in 0.1M of KCl solution whilst Vondracek<sup>(143)</sup> reported a considerable increase of attack in sulphuric acid (0.5M) for the

same alloy. The two later claims were supported by the observation that pure zinc corrodes slowly in dilute acid solution since the hydrogen evolution reaction on zinc is highly polarised. When impurity is present in zinc, hydrogen evolution can proceed more readily on these impurities and the corrosion rate is increased. The present work is different from the above since the solutions are chromic acid based and were either activated with NaCl or NaF. Zeta phase is an alloy of zinc and iron and the higher initial potential of zeta compared to that of zinc (figure 7.2(a)) was due to the more noble potential of this alloy as compared to zinc. In a chromate solution, the two major reactions are the dissolution and precipitation reactions. In the case of zinc immersion in chromate solution, these reactions and their products are as those shown in section 7.3, equations 7.1 - 7.3.

In acidic solution, the cathodic reactions would include hydrogen reduction,



followed by



and in the presence of oxygen, the reaction could proceed to form Hydroxide,



Since the solution contains NaCl there would be a probability of forming both zinc hydroxide ( $\text{Zn}(\text{OH})_2$ ) and zinc chloride ( $\text{ZnCl}_2$ ). These products have been reported to

be sparingly soluble and cannot prevent attack on zinc.

In the case of the zeta samples, apart from all the reactions and products mentioned above, anodic dissolution of iron would produce ferrous ions. These would then be oxidised to ferric as shown in equation (7.7)



The precipitation of ferrous chromate and/or ferric hydroxide follows and this is likely to occur within the pores of the zinc chromate film. The inhibiting power of chromate ions on iron corrosion is well known, and is almost certainly due to their oxidizing power. The ferric compounds produced in the film pores have much smaller solubility products and tend to give film repair at the pores causing the corrosion potential of zeta to become more noble. This is confirmed by the slower dissolution rates of zeta samples (fig. 7.2(a) and table 7.2).

In order to study the detailed effect of pH on solution L3, both with and without activator (NaCl), solutions L4 (0.03 M/l  $\text{CrO}_3$  + 0.07 M/l NaCl + 0.03 M/l NaOH), and L5 (0.03 M/l  $\text{CrO}_3$  + 0.03 M/l NaOH) were prepared. The depassivating effect of  $\text{Cl}^-$  was clearly revealed from the potentiodynamic anodic polarisation curves obtained for zeta and zinc in these solutions. A narrow passive range of 0.1V and 0.08V was obtained for zeta and zinc respectively in solution L4. Passivation starts at about -0.5V, about the same potential as that at which the

risation enters the passivation domain of the Cr-H<sub>2</sub>O potential versus pH diagram. The adsorption of chloride ions(Cl<sup>-</sup>) led to the breakdown of the protective film. Also, with chloride present, self healing of the damaged film would not be possible and intense local attack would then occur. These processes were exemplified by the curves for L4 shown in figure 7.2(b). The curves for zeta and zinc in L4 solution have the same shape although  $i_{\text{passive}}$  for the zeta phase was very much smaller and in the case of L5, a solution without activator, a wider passivation range was obtained for zinc. Since this solution formed a better passive film, it would be unlikely that it would be possible to form conversion coatings in this solution since a high rate of zinc dissolution is necessary as the solubility limit must be reached before precipitation begins.

The solutions in group 3, L6 (0.12 M/l CrO<sub>3</sub> + 0.30 M/l NaOH) and L7 (0.12 M/l CrO<sub>3</sub> + 0.3M/l NaCl + 0.12M/l NaOH) were formulated in an attempt to study the effect of pH and the presence of NaCl in solutions of a higher concentration version of L5 and L4 respectively. The potentiodynamic anodic polarisation curves obtained from these solutions are shown in figure 7.2(c). It can be seen that the absence of NaCl in the solution L6, allowed a passive film to be formed at pH of 5.4 which is inside the passivation region of Cr-H<sub>2</sub>O potential versus pH diagram. Compared with L5 (fig 7.2(b)) a narrower  $E_p$  and lower  $i_p$  were obtained for both zeta and zinc in this

solution (L6). This can be considered to have resulted from higher concentrations of  $\text{CrO}_3$  and  $\text{NaOH}$ .

The addition of  $\text{NaCl}$  into the solution (L7) simply accelerated the dissolution rate as shown in figure 7.2(c). Generally, both zeta and zinc samples were affected equally by these solutions.

The formulations in group 4 were made to verify the effect of chromate solutions, having pH values larger than those for the passivation domain of the  $\text{Zn-H}_2\text{O}$  potential - pH diagram, on zeta and zinc. Three solutions, L8 (0.6 M/l  $\text{CrO}_3$  + 1.25 M/l  $\text{NaOH}$ ), L9 (0.6 M/l  $\text{CrO}_3$  + 1.25 M/l  $\text{NaOH}$  + 0.20 M/l  $\text{NaCl}$ ) and L10 (0.6 M/l + 1.25 M/l  $\text{NaOH}$  + 0.1 M/l  $\text{NaF}$ ), all pH 13, were formulated. L9 and L10 solutions were formulated in order to study the effect of the activator ions on the samples in this domain of the potential versus pH diagram.

The potentiodynamic anodic polarisation curves are shown in figure 7.2(d). It was interesting to find that at this pH, the zinc samples were more favourably affected and that the addition of halide ions provided an advantageous effect by extending the passive range ( $E_p$ ). The curves for zeta samples in L8 solution showed no critical potential (active to passive potential). A closer look at the other curves in figure 7.2(d) revealed that their critical potential is well below -1.0 V compared with other curves in figures 6.2 (b&c) which have critical potentials of -1.0 V. Curves obtained from L9 and L10

for both samples have comparatively wider passive range (see table 7.2).

Theories on passivation to-date have indicated that passivity can be provided by many different compounds depending on the solution composition, concentration, and pH. In the cases of zinc treated in L9 and L10 solutions, the compounds likely to form at pH 13, would probably be  $\text{ZnCrO}_4 \cdot 4\text{Zn(OH)}_2$ ,  $\text{ZnCl}_2 \cdot 6\text{Zn(OH)}_2$  and  $\text{ZnCl}_2 \cdot 4\text{Zn(OH)}_2$ .

The first compound is zinc tetroxychromate and is an important constituent of inhibitive paints. The later two basic zinc salts, and the crystalline zinc hydroxides, have been found<sup>(144)</sup> to have layer structures similar in general to the layer structure attributed to the basic zinc carbonate which forms dense adherent films and appears to play such an important role in the corrosion resistance of zinc against the atmosphere. It would be because of the formation of these corrosion resistant basic zinc salts that the presence of the halide ions widen the passivity range of the curves obtained from solutions L9 and L10.

The solutions in group 5 were L11 (1.0 M/l  $\text{CrO}_3$  + 1.0 M/l NaOH), L12 (1.0 M/l  $\text{CrO}_3$  + 1.25 M/l NaOH) and L13 (1.0 M/l  $\text{CrO}_3$  + 2.0 M/l NaOH). The pH values for the solutions were 5.5, 7.0 and 10.0 respectively. These solutions were formulated in order to compare the effect of a neutral solution (pH 7) with acidic and alkaline solutions. Notice also that pH 10 lies within the reinfor-

ced passivity region of the superimposed potential - pH diagram (figure 7.1 (d)). The potentiodynamic curves obtained in these solutions for both zeta and zinc samples are shown in figure 7.2(e). The curves showed that the reactions of zinc in the three solutions were the same. The same thing can be said of zeta samples but the curves for zinc samples are generally different from those of zeta. Well defined  $E_p$  and  $i_p$  were observed only in the case of zinc samples.

Bijimi and Gabe<sup>(145)</sup> have studied the behaviour of zinc in solutions of sodium chromate, molybdate and tungstate and discussed their results in terms of superimposed potential - pH diagrams. In the case of Sodium chromate, they defined a strong or reinforced passive region as that where both metal and oxyanion passivity coincide. This was given as the region within the pH 8.5 - 10.5, and + 0.4V to -1.0V (SHE) and was associated with the optimum process conditions. In this work, the variation of pH of 1.0 M/l  $CrO_3$  solution did not appear to have a marked effect on the potentiodynamic curves as obtained by the above authors. If figure 7.2(d) is compared with figure 7.2(e), it is obvious that passivation started at a much lower potential for those solutions having pH 13.0 (fig 7.2(d)) than the solution L13 ( pH = 10) whose pH lie within the reinforced passivity region (fig 7.2(e)) and wider passivation range ( $E_p$ ) were obtained for the formal group (4) of solutions. A thorough examination of figure 7.2 (a-e) would tend to suggest that the predomi-

nant factor for better anodic passivation treatment in chromate solutions would be for the pH of the solutions to lie within the passivation region of Cr-H<sub>2</sub>O potential - pH diagram, not necessarily only within the so called reinforced region.

The solutions in group 6, 7, and 8 are sodium hydroxide solutions with pH range of 8 to 14. The potentiodynamic anodic polarisation curves for solutions having pH of 8 (L14), 9 (L15) and 10 (L16) are shown in figure 7.2(f) and those of pH 11 (L17) and 12 (L18) in figure 7.2(g), whilst those for pH 13 (L19) and pH 14 (L20) are depicted in figure 7.2(h).

The potentiodynamic curves obtained from L14, L15 and L16 were identical for both samples. There was no active to passive, passive to transpassive "S" shaped curve. There are two possible explanations for the shape of these curves:

- (a) Either no passive film formed and dissolution of the samples occurred at all potentials, or
- (b) The samples were spontaneously passivated.

A careful examination of the curves revealed that the log current density at the termination of polarisation, especially for solutions L14 and L15, were lower than the passive log current density ( $i_p$ ) obtained from most other solutions for the respective samples. The slope of the curves and the low current density (at all potentials) of the curves, tends to agree with the explanation (b)

above. From the literature<sup>(144)</sup>, it is known that attack on zinc is much slower in solutions having the intermediate range of pH as can be seen from figure 7.3. Figure (7.3) shows how the corrosion rate of zinc varies with the pH<sup>(144)</sup>, and it can be seen from this that the attack is most severe at pH values below 6 and above 12.5, while within this range, the corrosion is very slow. The indications of the potentiodynamic anodic polarisation curves shown in figure 7.2 (a-h) agreed with figure 7.3 to a certain degree. The curve in figure 7.3 suggested that zinc is attacked least at a pH of about 12, a fact which the author doubts on the basis of his results in which the lowest dissolution rate was obtained from NaOH solutions having pH values of 8 and 9 for both zeta and zinc samples. The absence of the peak shaped active to passive transition in the curves obtained from these solutions could mean that the critical anodic currents were relatively low so that the intersection of the cathodic reduction and anodic oxidation curves occurred in the passive region as depicted in figure 7.4.

From figure 7.2(g) and table 7.3, it can be seen that the solution having pH 11 (L17) had a much lower passive current ( $i_p$ ) than the solution with pH 12 (L18) for both samples, although zinc has a lower passive current ( $i_p$ ) in both solutions. On the contrary, the zeta samples have lower  $i_p$  for solutions L19 and L20 as evidenced from table 7.3. This lower dissolution rate can be linked with the presence of iron in the zeta sample. Except at

high temperature, the attack on iron in strong alkali solution is relatively slower than the attack on zinc. If the attack on iron is fast then this will lead to sufficient formation of  $\text{Fe}^{++}$  and  $\text{Fe}^{+++}$  to exceed the solubility product of magnetite and thereby give a protective film of magnetite.

#### 7.4.2 POTENTIOSTATIC POLARISATION

The log current density ( $\text{mA}/\text{cm}^2$ ) versus time curves obtained from potentiostatic anodic polarisation at a constant potential of +1.5 V in all the various solutions detailed in Table 7.1 are shown in figures 7.5 (a-h). The initial and final dissolution rates ( $i_{\text{corr}}$ ) are shown in table 7.4 and these are plotted against the pH of the sodium hydroxide (NaOH) solution in figure 7.6 (a&b).

From table 7.4 and figure 7.5, it can be seen that all the solutions having pH less than 7 show generally the same trend. There was continuous dissolution, at the same rate, from the beginning to the end of polarisation. Although a continuous reduction in the dissolution rate of the zinc sample was noticed in solution L1, which could be due to a very thick gel-like yellow precipitate on the sample surface, its rate of dissolution was still very much higher than the zeta sample in the same solution at all times of polarisation. Generally in solutions with pH less than 7, the zeta samples had a lower dissolution rate than the zinc samples.

The dissolution rate of both samples in chromate solutions showed no particular relationship with the solution pH as might be expected from figure 7.3. For example, solution L1 had the same pH value as L3, and L8, L9 and L10 have the same pH value but in each case, all have different dissolution rates for both samples. This means that the ability of a film to resist the dissolution of the underlying substrate in a chromate bath depends on the bath's formulation, composition and concentration as well as pH. For example, the author has found that the Alocrom 100 solution which has pH of 3.3 does not form a conversion coating film on zinc whilst solution L1 of pH 1.2 and Chrometan (non chromate process) of pH 5 easily formed conversion coatings on zinc.

Another interesting point showed in both figure 7.5 and table 7.4 was that in all cases where a reduction in log current density (dissolution rate) occurred, the zinc samples always had a higher relative reduction. In these cases where decreasing log current density was obtained, the films formed in layers. For zinc samples treated in chromate solution dense adherent yellow chromate coatings were formed beneath a thick gel-like porous yellow chromate precipitate while in the case of zeta samples, black or blue-black dense adherent coatings were formed beneath the porous chromate precipitate. It was noticed during the experiment that film cracking and consequently peeling off and film reforming occurred in some solutions and these times of cracking and reforming of film coin-

cided with the time of rise and fall in some of the curves eg for L8 and L13.

It can be seen from figure 7.6 (a) and (b) and also from table 7.4 that, contrary to the case of chromate solutions, a near linear relationship was found between dissolution rate and solution pH value. The log current density increased with increasing solution pH. The line or relationship for the zeta samples was much better than for the zinc samples particularly between pH values of 11 to 14.

#### 7.5 CONCLUSIONS

(1) The dissolution rates of the zeta samples were less than those of the zinc samples in chromate solutions with a pH less than 7 and in sodium hydroxide solutions with pH greater than 12. The opposite was true in the pH range of 7 to 12.

(2) In chromate solutions, passivity does not occur in solutions having pH outside the passivation region of Cr-H<sub>2</sub>O potential versus pH diagram.

(3) There was no evidence of any marked effect of the so-called reinforced passivation region of the superimposed Zn-Cr-Fe-H<sub>2</sub>O Potential Versus pH diagrams. The predominant factors were the passivation region of the Cr-H<sub>2</sub>O potential versus pH diagram, and solution formulation with respect to composition and concentration.

**Table 7.1 Laboratory prepared conversion coating solutions (repeat of TABLE 3.1)**

Code	Composition M/l	pH	Group
L1	CrO <sub>3</sub> 0.12, NaCl 0.30	1.2	1
L2	CrO <sub>3</sub> 0.12, NaF 0.10	3.4	
L3	CrO <sub>3</sub> 0.03, NaCl 0.07	1.2	
L4	CrO <sub>3</sub> 0.03, NaCl 0.07, NaOH 0.03	5.5	2
L5	CrO <sub>3</sub> 0.03, NaOH 0.03	6.1	
L6	CrO <sub>3</sub> 0.12, NaCl 0.30	5.5	3
L7	CrO <sub>3</sub> 0.12, NaCl 0.30, NaOH 0.12	5.8	
L8	CrO <sub>3</sub> 0.6, NaOH 1.25	13.0	4
L9	CrO <sub>3</sub> 0.6, NaOH 1.25, NaCl 0.30	13.0	
L10	CrO <sub>3</sub> 0.6, NaOH 1.25, NaF 0.1	13.0	
L11	CrO <sub>3</sub> 1.0, NaOH 1.0	5.5	5
L12	CrO <sub>3</sub> 1.0, NaOH 1.25	7.0	
L13	CrO <sub>3</sub> 1.0, NaOH 2.0	10.0	
L14	NaOH 0.000001	8.0	6
L15	NaOH 0.00001	9.0	
L16	NaOH 0.0001	10.0	
L17	NaOH 0.001	11.0	7
L18	NaOH 0.01	12.0	
L19	NaOH 0.1	13.0	8
L20	NaOH 1.0	14.00	

**TABLE 7.2** Dissolution rate ( $i_{\text{corr}}$ ) of zeta and zinc in solutions L1, L2, and L3 at a constant potential of 0.0 V during potentiodynamic anodic polarisation from -1.5 V to +1.5 V.

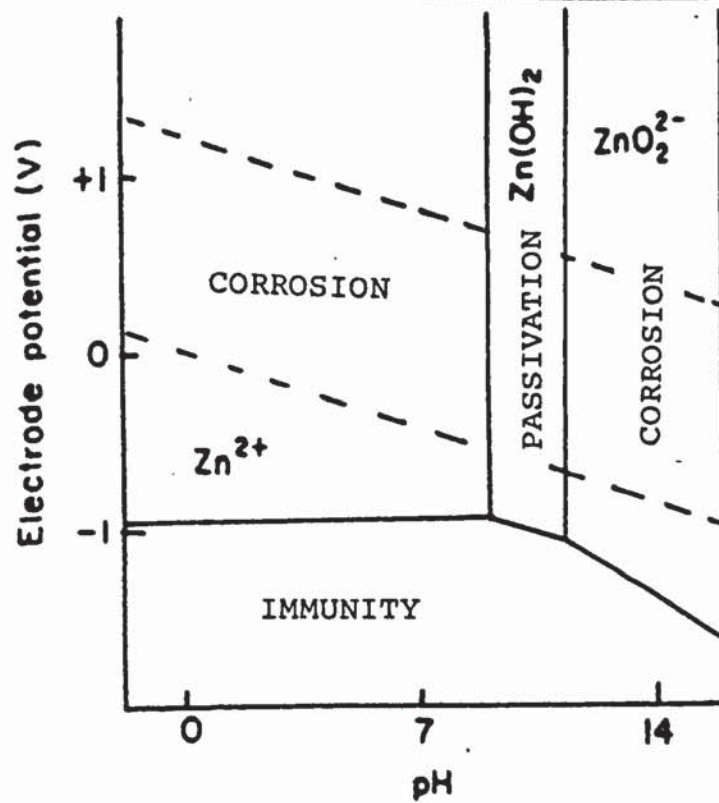
Solution	Dissolution Rate $i_{\text{corr}}$ (mA/cm <sup>2</sup> )	
	Zeta	Zinc
L1	45	150
L2	14	18
L3	6	12

**TABLE 7.3** Range of passive potential ( $E_p$ ) and passive log current density ( $i_p$ ) of zeta and zinc in different conversion coating solutions

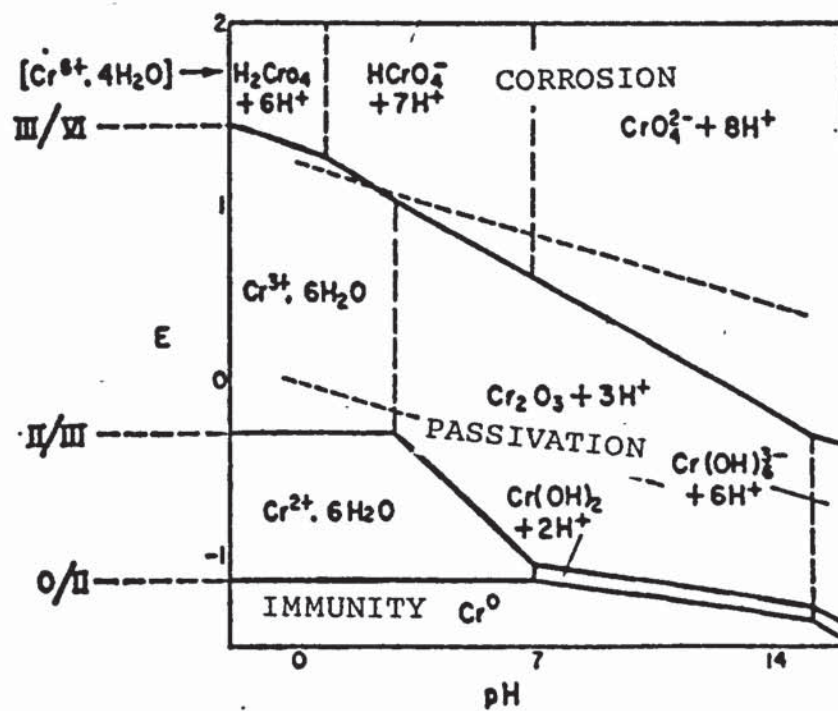
Solution	Range of passive potential $E_p$ (V)		Passive Log Current density $i_p$ (mA/cm <sup>2</sup> )	
	Zeta	Zinc	Zeta	Zinc
L1	-	-	-	-
L2	-	-	-	-
L3	-	-	-	-
L4	0.10	0.08	0.02	0.10
L5	1.00	1.25	0.16	0.09
L6	0.60	1.00	0.08	0.07
L7	-	-	-	-
L8	-	0.80	-	0.08
L9	2.15	2.20	0.14	0.08
L10	1.30	1.85	0.31	0.13
L11	0.75	0.85	0.11	0.07
L12	0.70	1.00	0.15	0.06
L13	0.40	1.20	0.11	0.06
L14	-	-	-	-
L15	-	-	-	-
L16	-	-	-	-
L17	1.60	1.85	0.14	0.05
L18	2.00	2.00	0.17	0.12
L19	1.95	2.10	0.26	0.30
L20	1.20	0.10	3.00	4.00

TABLE 7.4 The initial and final log current density ( $\text{mA}/\text{cm}^2$ ) of zeta and zinc in various solutions during potentiostatic anodic polarisation at a constant potential of +1.5 V.

Solution	pH	Initial Log current Density $\text{mA}/\text{cm}^2$		Final Log Current density $\text{mA}/\text{cm}^2$	
		Zeta	Zn	Zeta	Zn
L1	1.2	143.00	444.00	144.00	324.00
L2	3.4	86.00	104.00	67.60	104.00
L3	1.2	19.70	33.30	19.70	33.00
L4	5.5	19.20	48.00	19.10	50.00
L5	6.1	9.40	9.00	9.20	8.60
L6	5.0	19.00	15.00	19.00	14.10
L7	5.8	67.00	60.00	70.00	60.00
L8	13.0	190.00	280.00	77.00	72.00
L9	13.0	28.00	52.00	5.90	4.00
L10	13.0	29.00	54.00	4.60	4.00
L11	5.3	60.00	141.00	61.00	142.00
L12	7.0	70.00	110.00	39.00	37.00
L13	10.0	19.00	108.00	13.00	11.00
L14	8.0	0.02	0.01	0.02	0.01
L15	9.0	0.04	0.10	0.05	0.09
L16	10.0	0.12	0.17	0.10	0.13
L17	11.0	0.60	0.16	0.13	0.01
L18	12.0	0.90	0.19	0.69	0.06
L19	13.0	1.33	0.36	1.61	0.13
L20	14.0	19.00	2.20	17.6	1.43



(a)



(b)

Figure 7.1 Simplified potential - pH diagrams

- (a) Zn-H<sub>2</sub>O
- (b) Cr-H<sub>2</sub>O
- (c) Fe-H<sub>2</sub>O
- (d) a, b & c combined

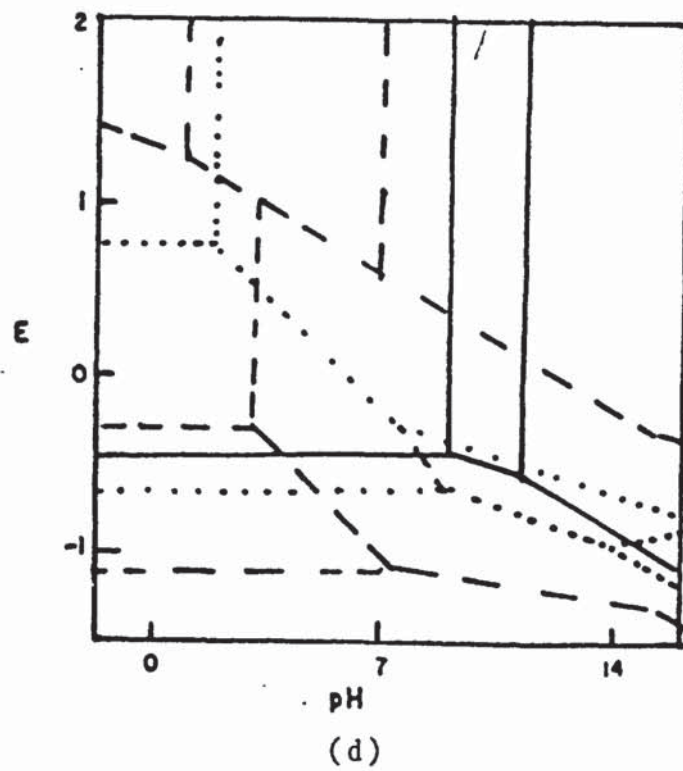
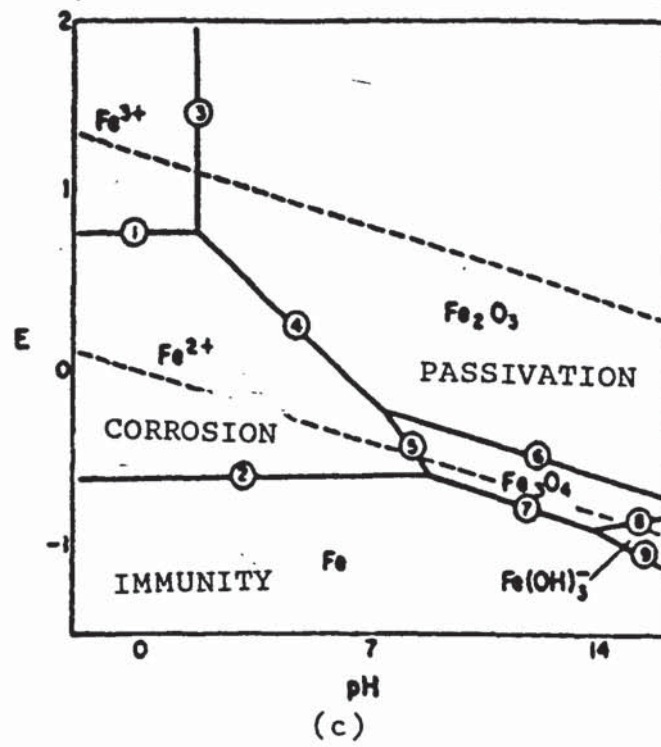


Figure 7.1 Continued  
 FOR (d): continuous line is for Zn-H<sub>2</sub>O  
 broken line is for Cr-H<sub>2</sub>O  
 dotted line is for Fe-H<sub>2</sub>O

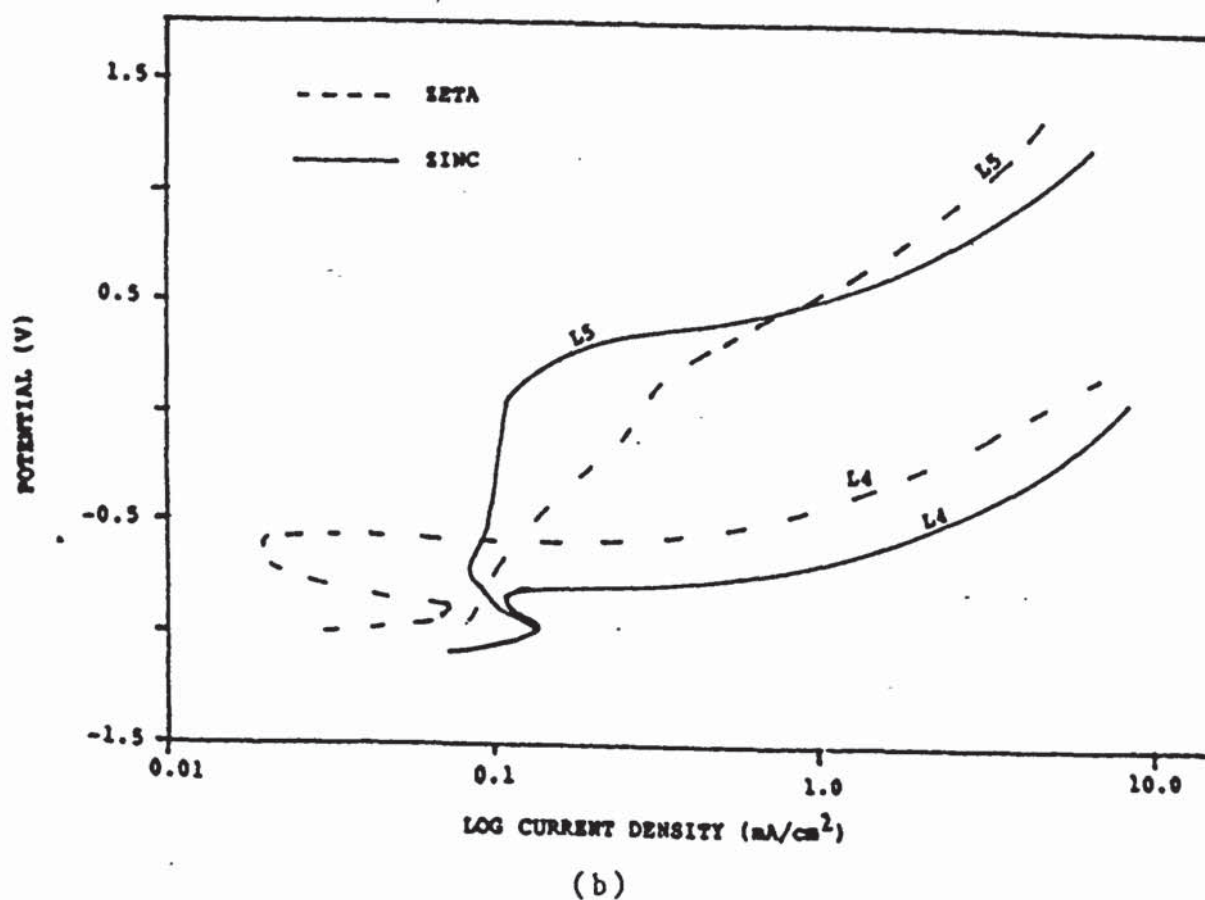
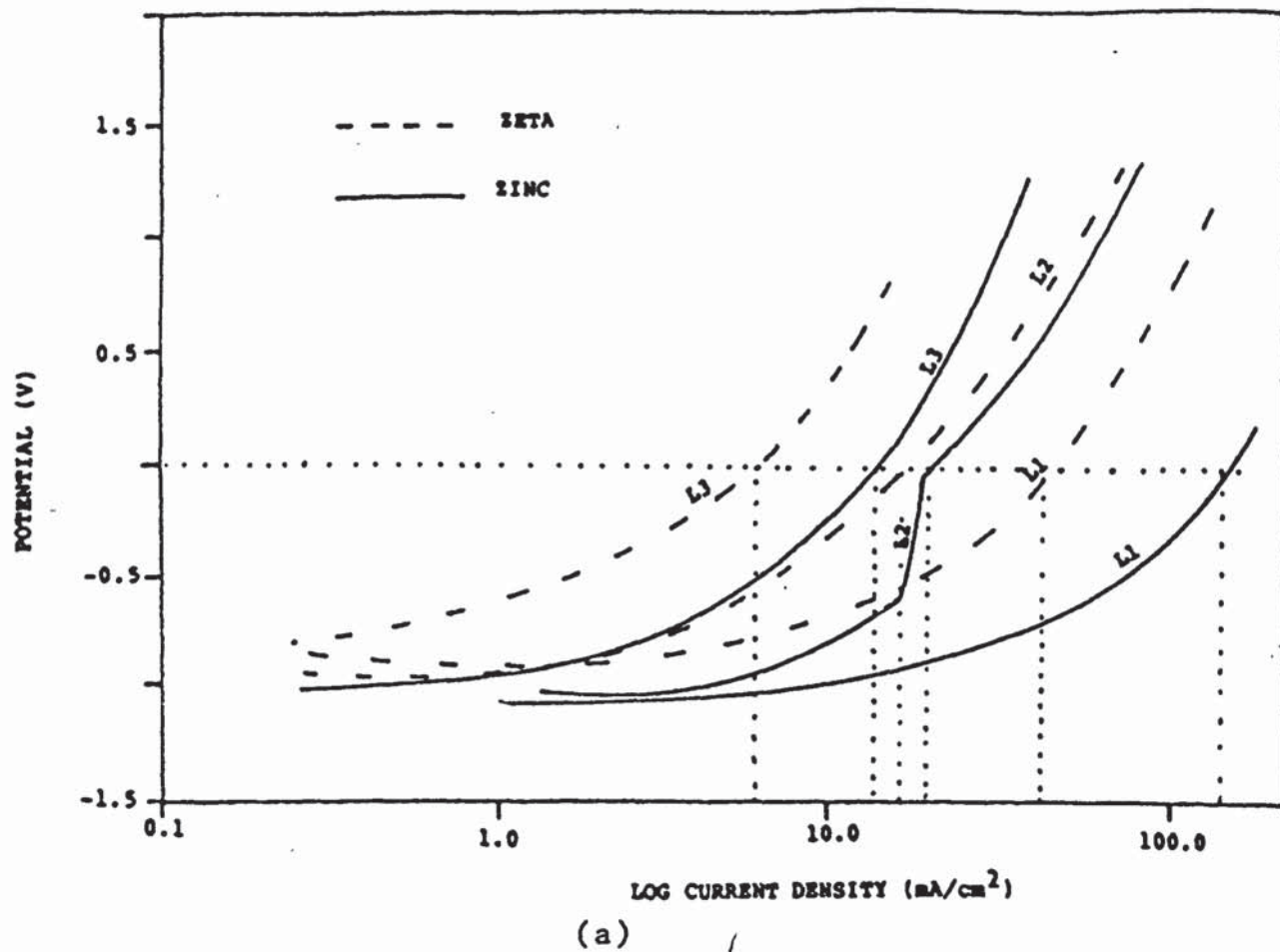
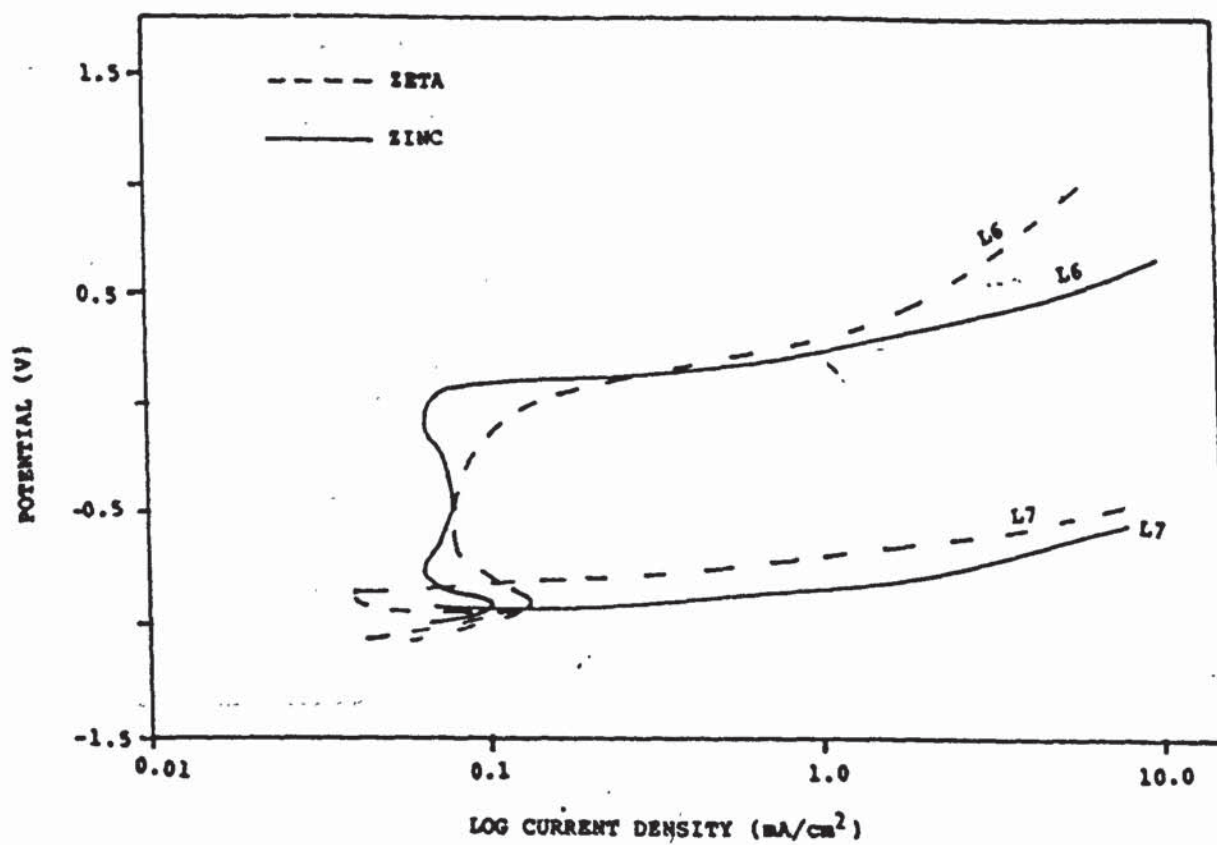
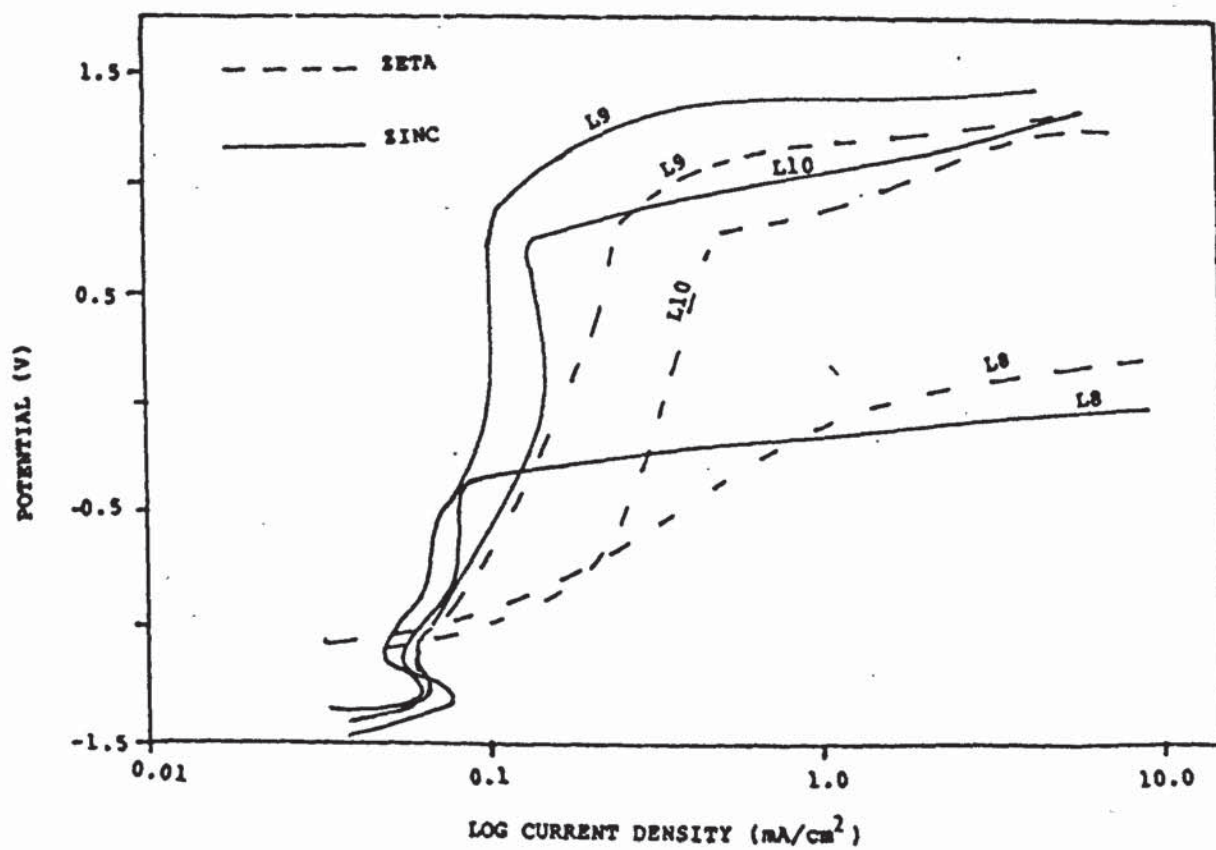


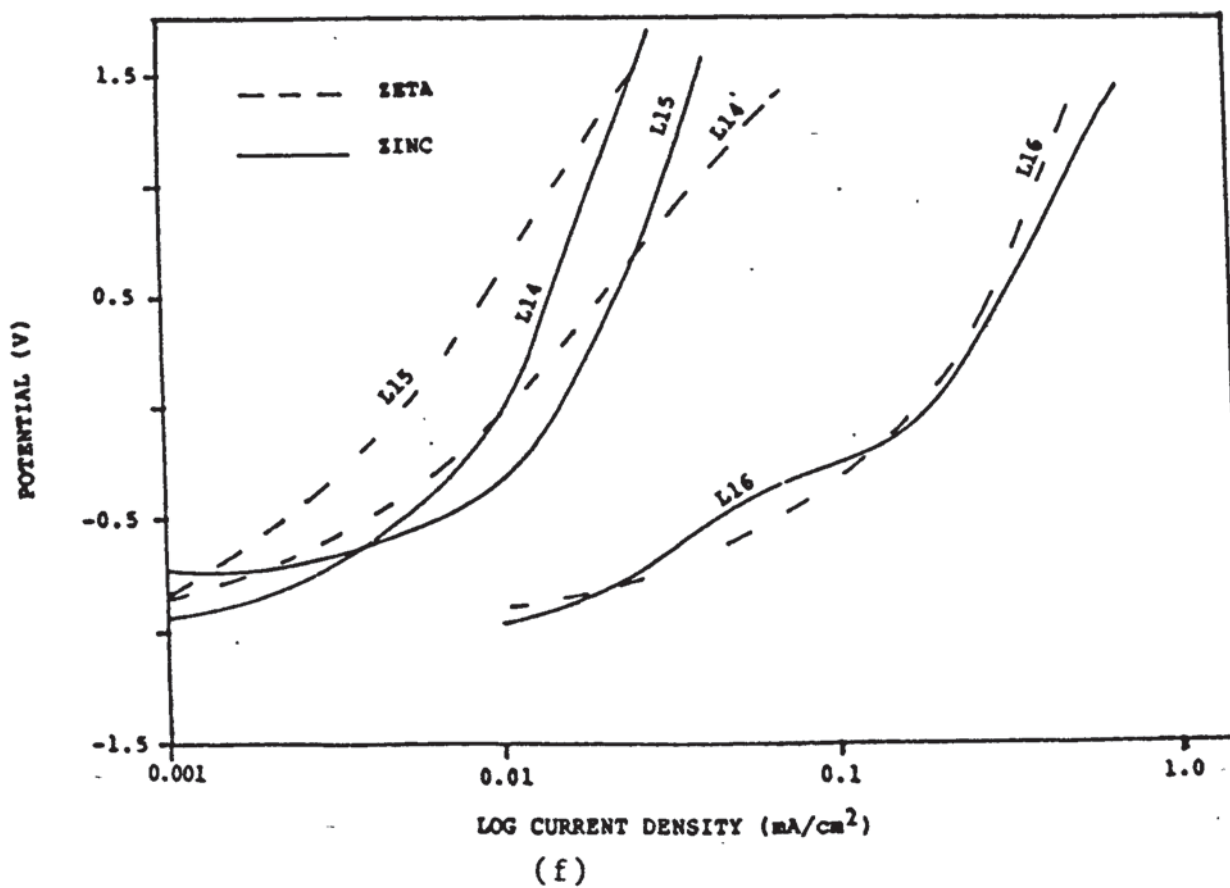
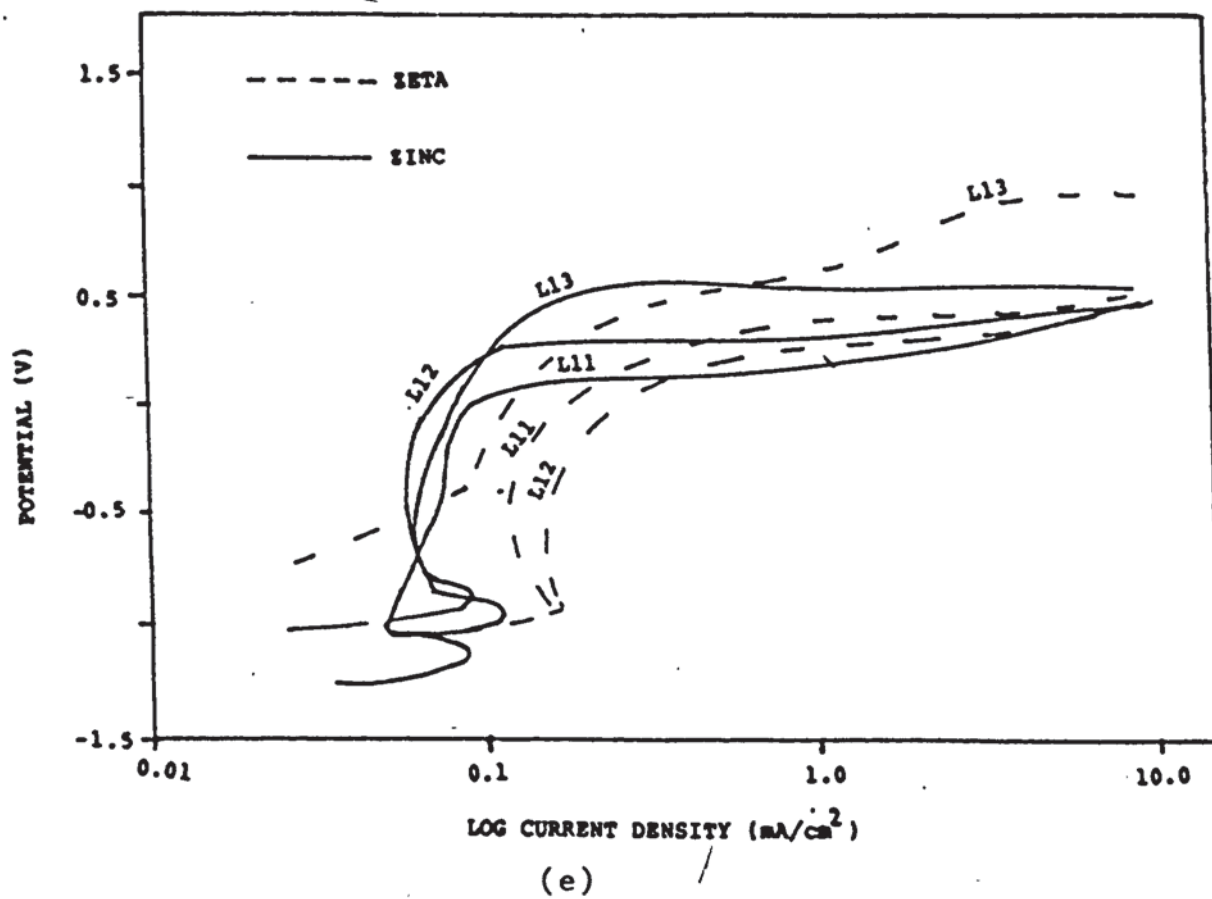
Figure 7.2 (a -h) Groups of potentiodynamic polarisation curves of zeta and zinc in various solutions shown in TABLE 7.1

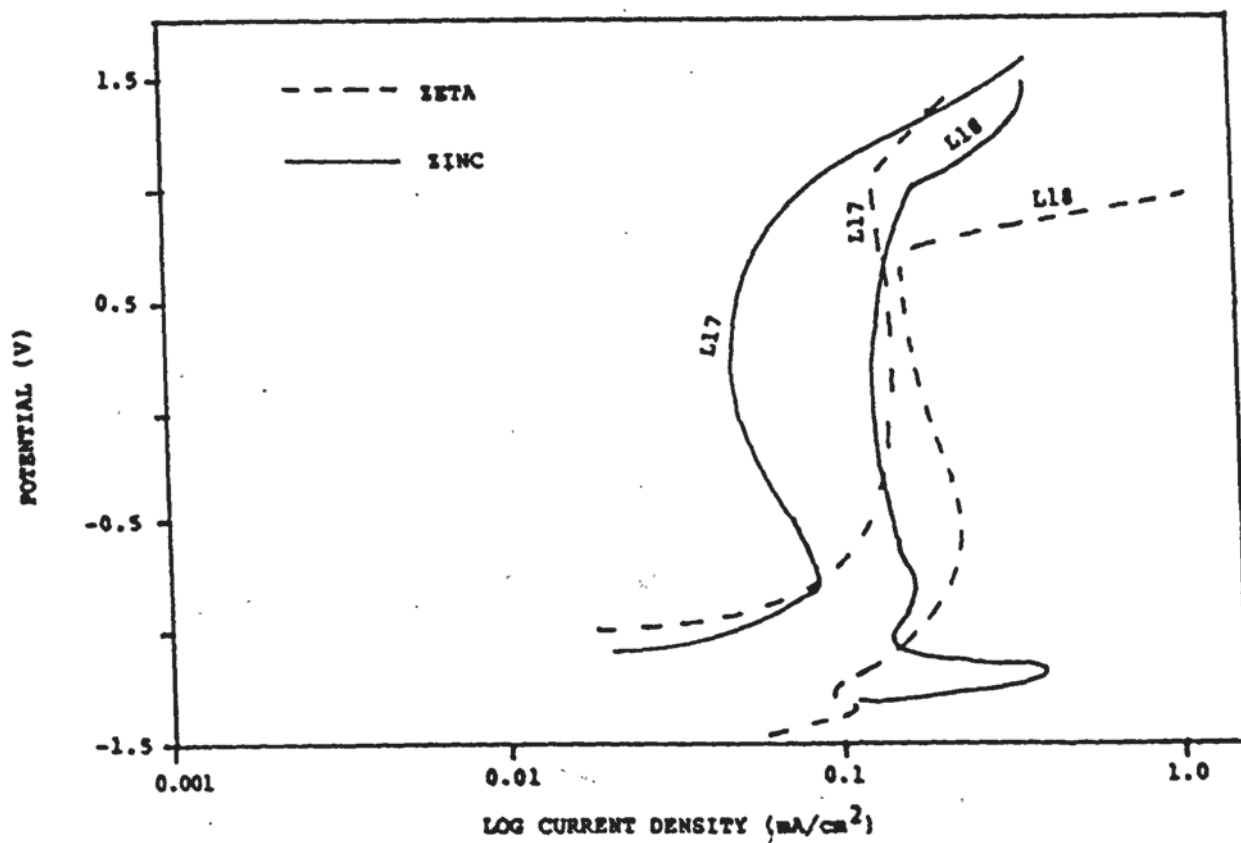


(c)

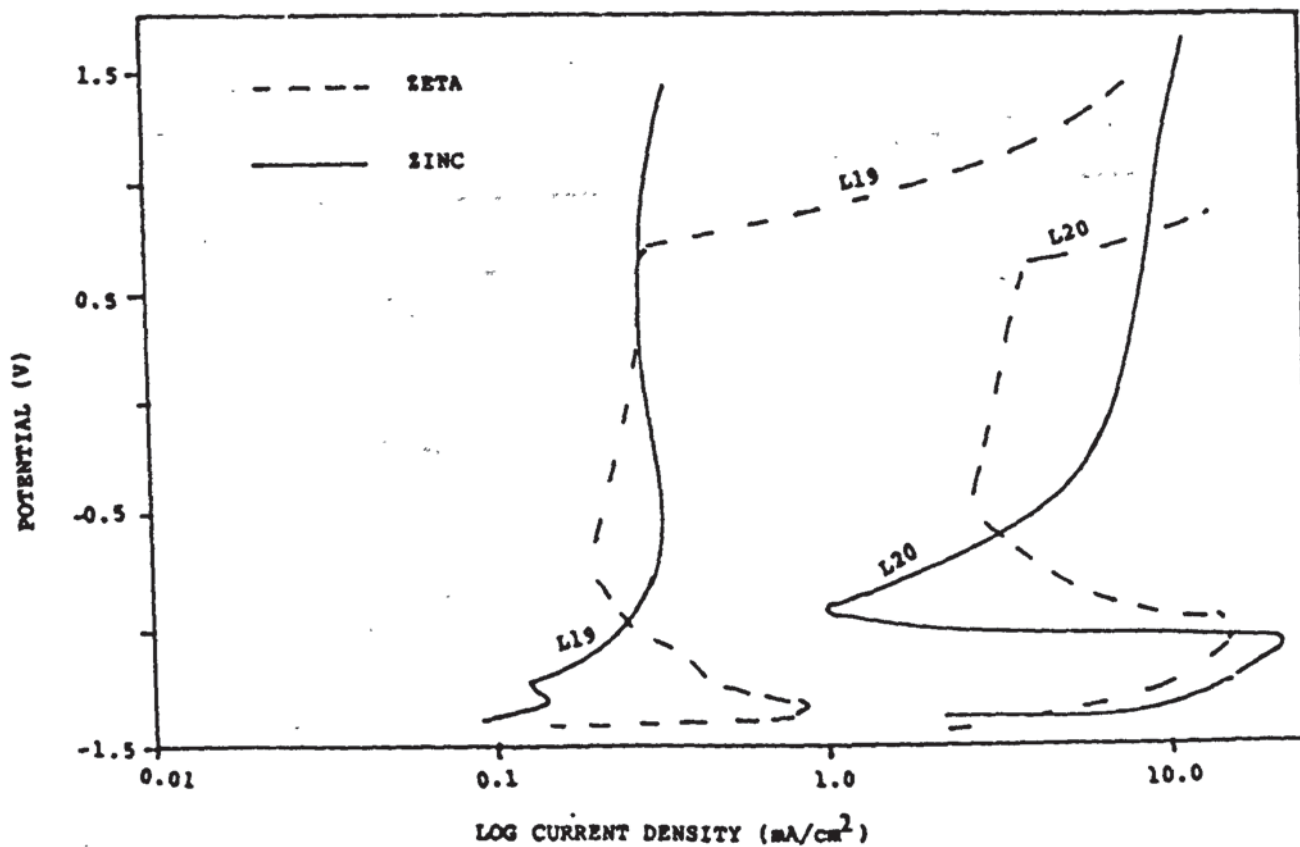


(d)





(g)



(h)

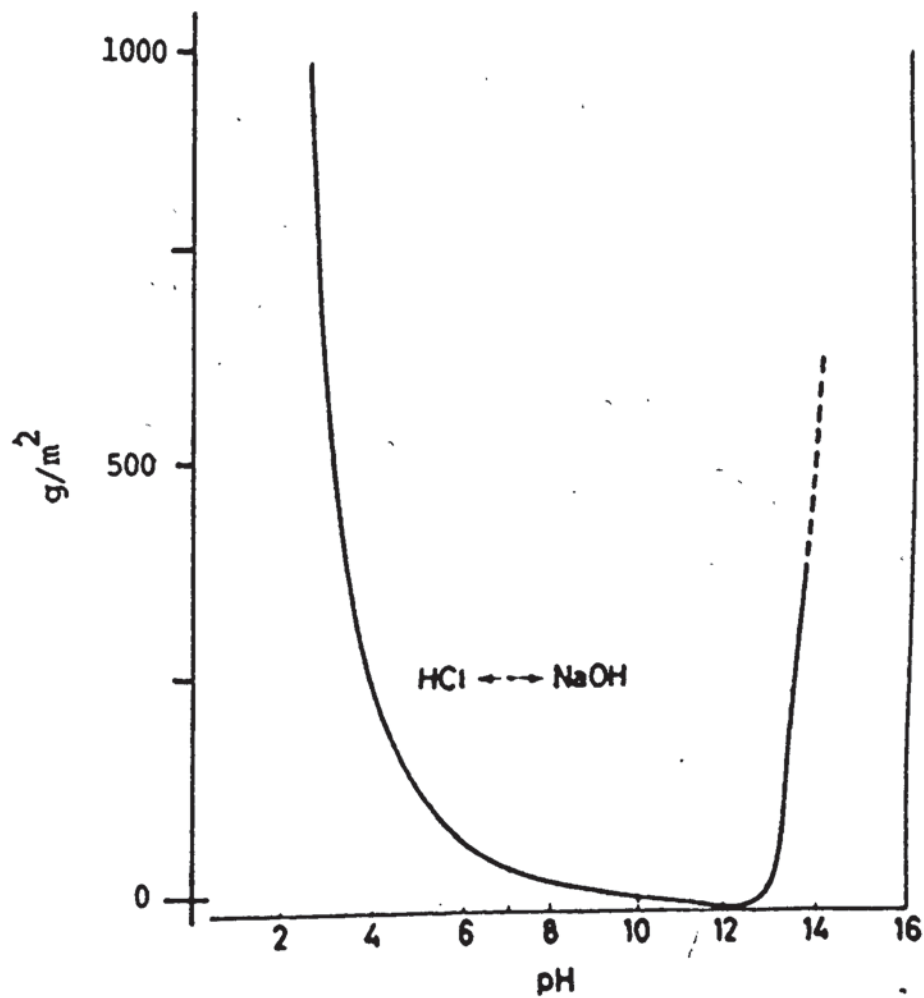


Figure 7.3 Effect of pH on the rate of corrosion of zinc<sup>(139)</sup>

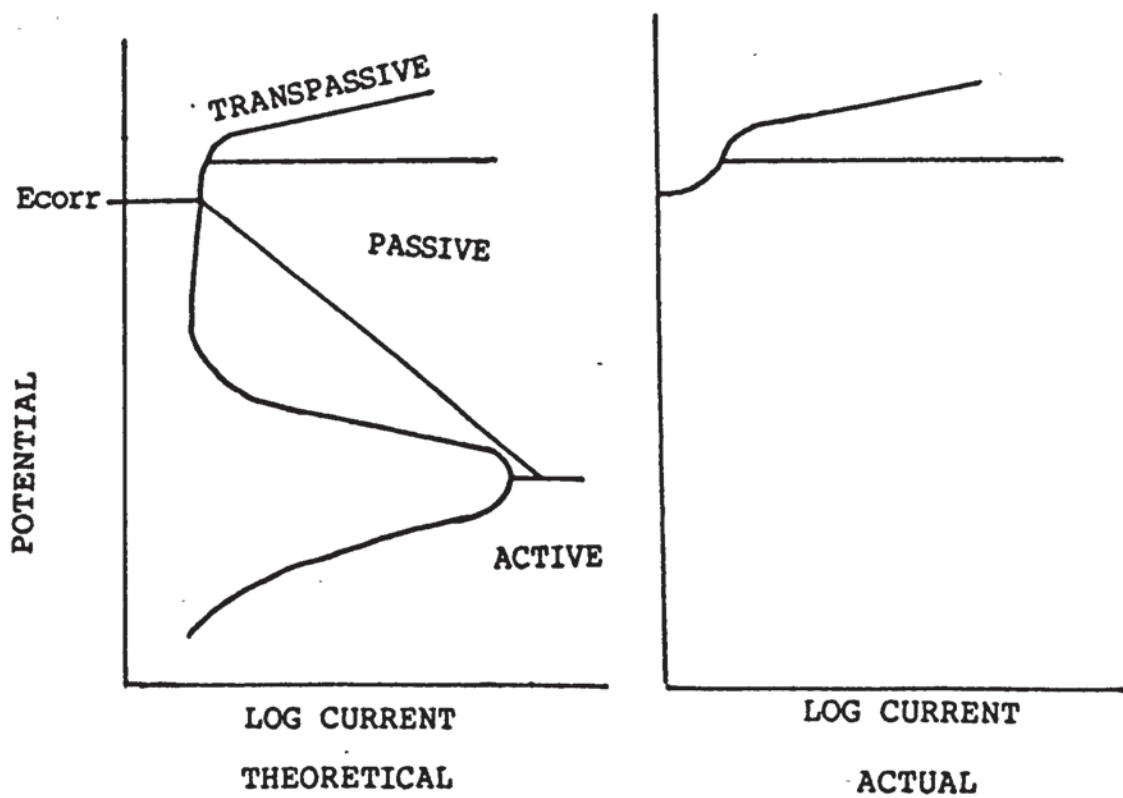


Figure 7.4 Theoretical and actual potentiodynamic polarisation plots of active - passive metals

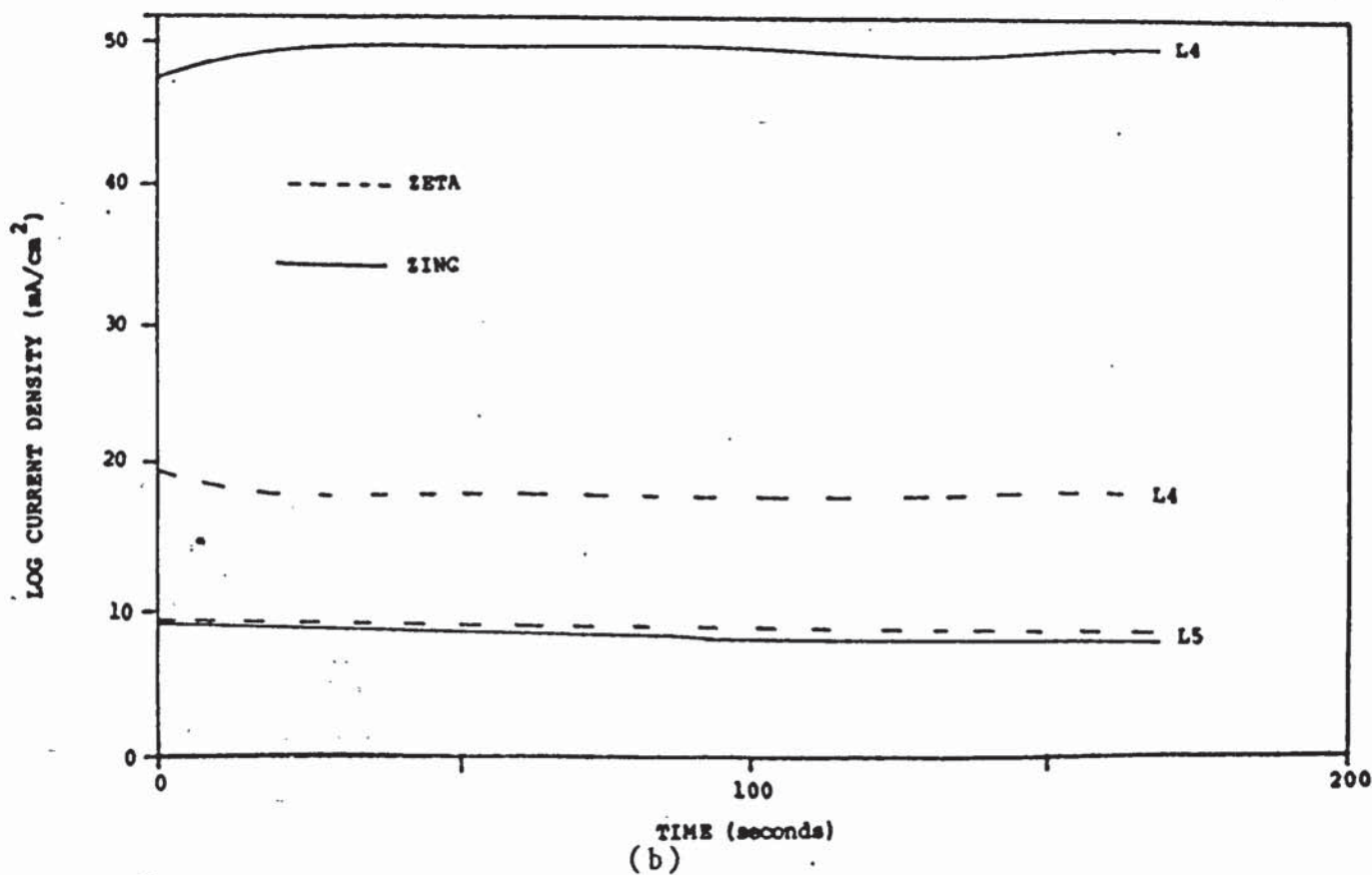
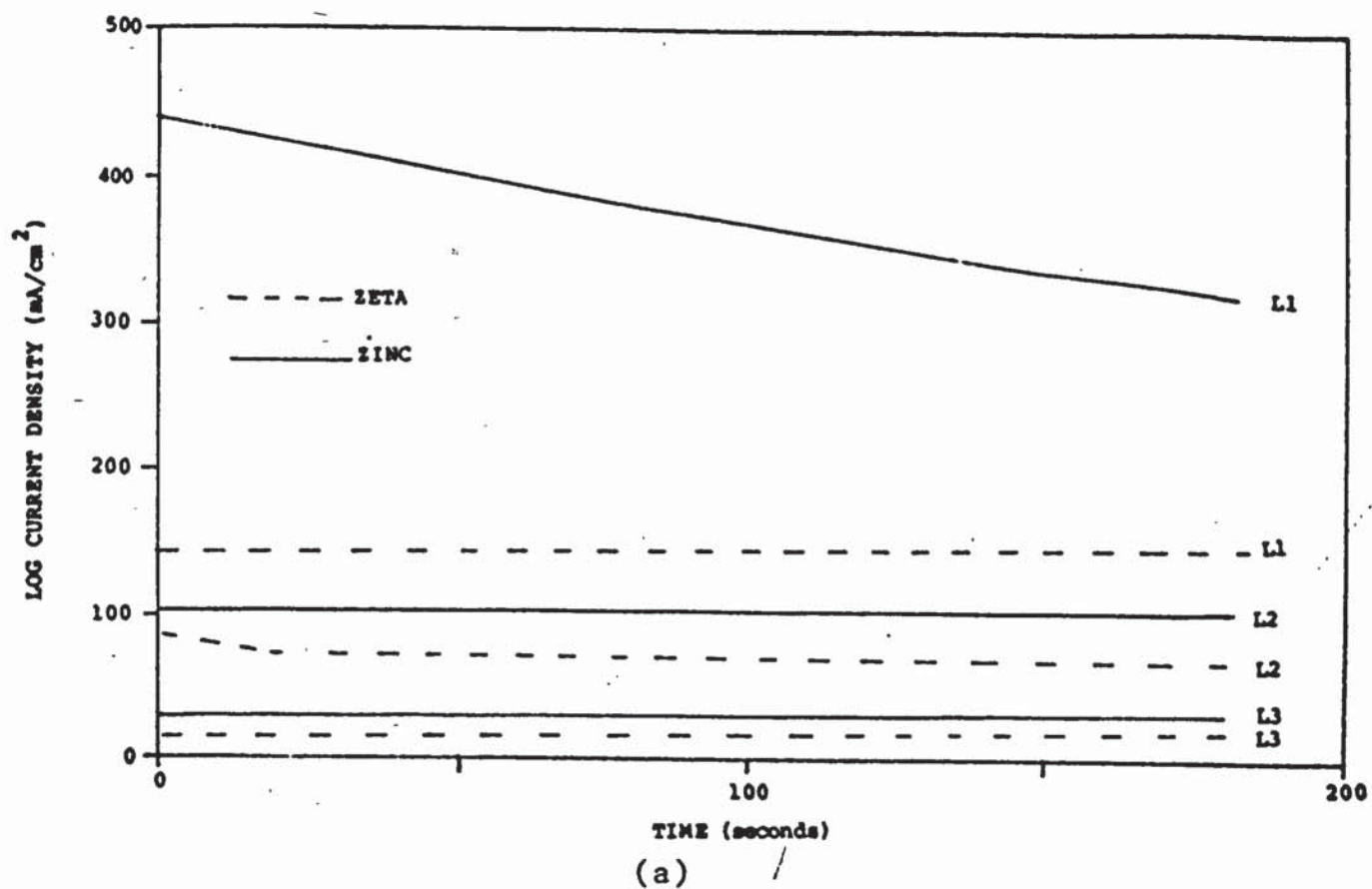
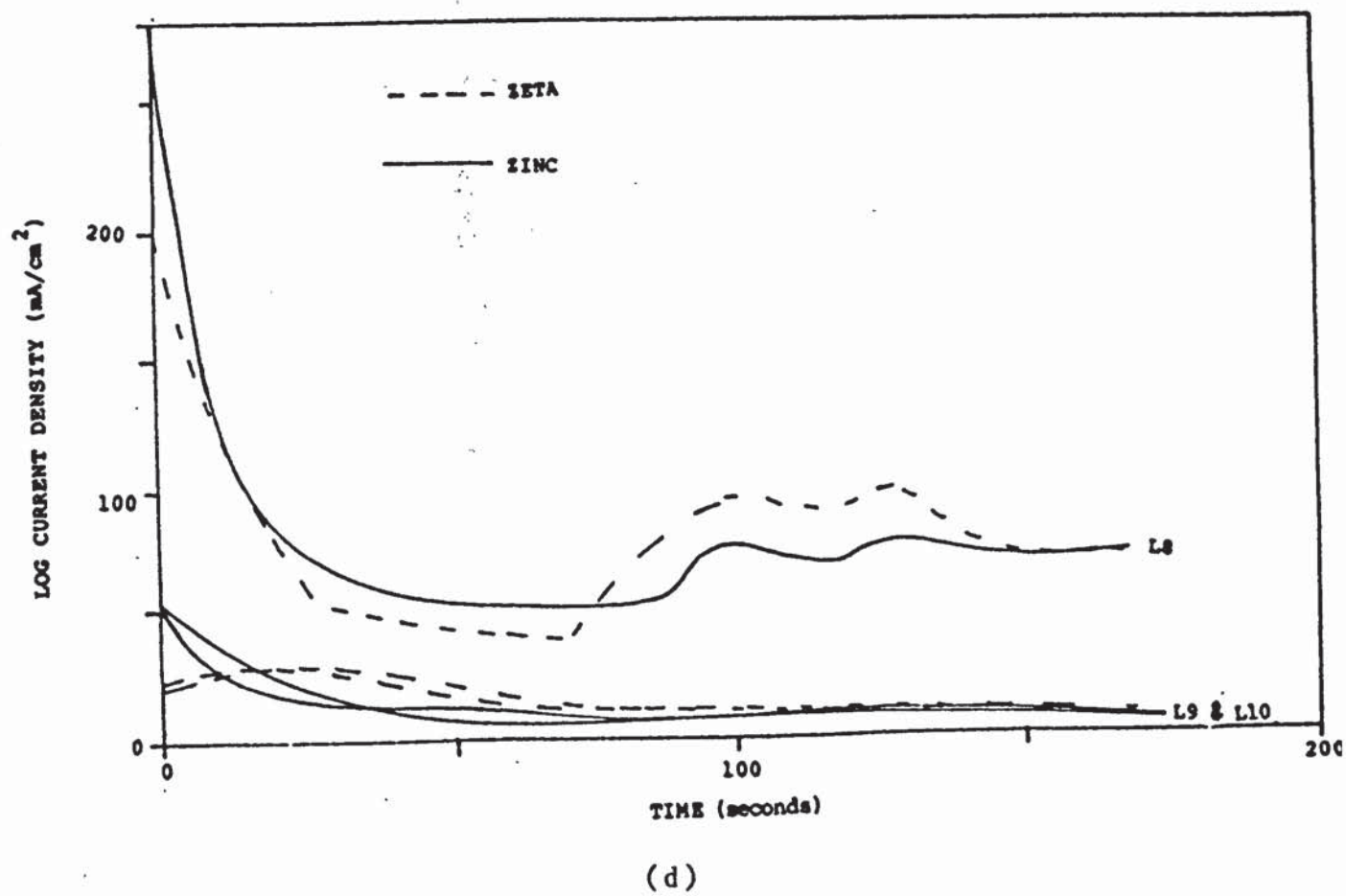
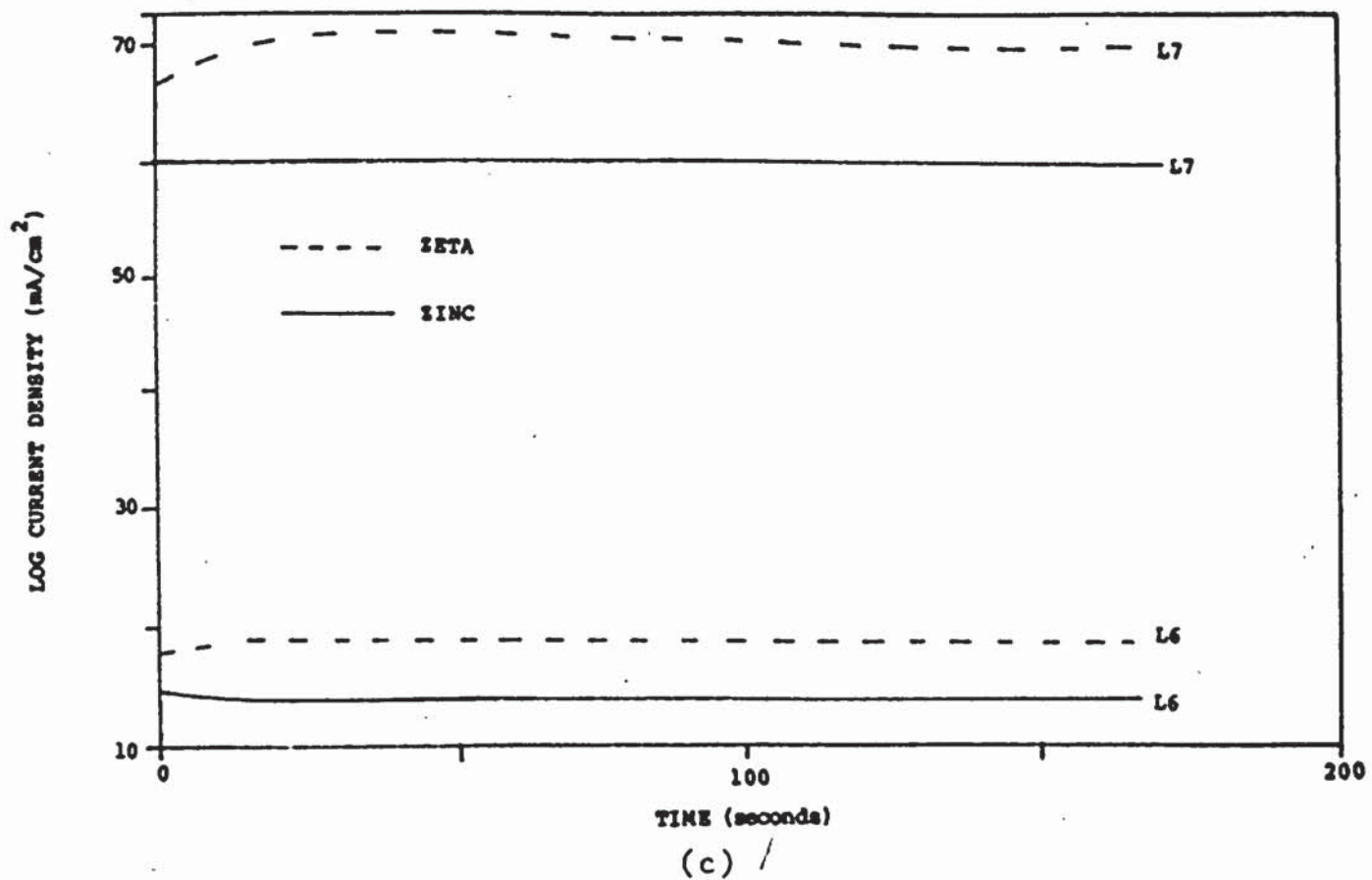
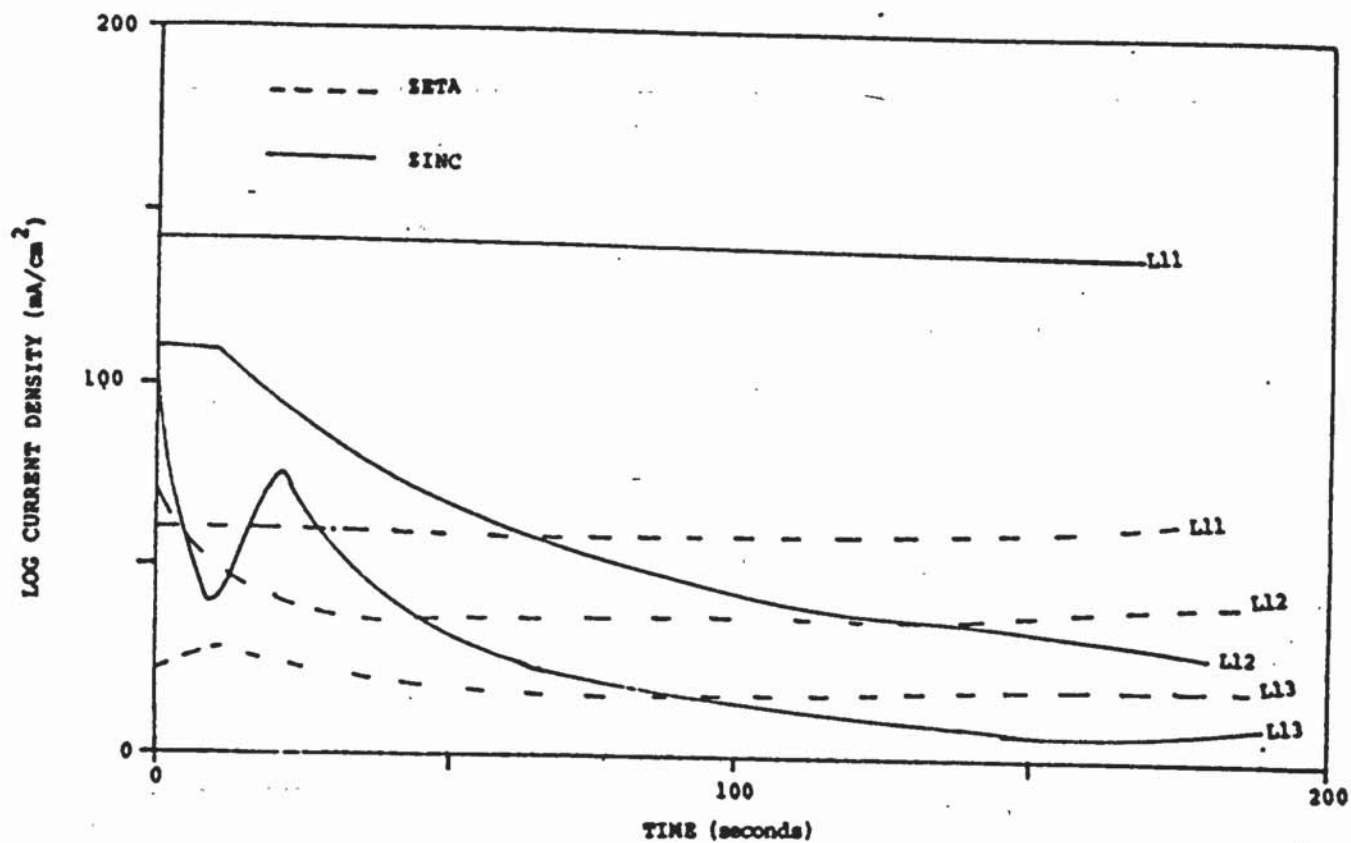
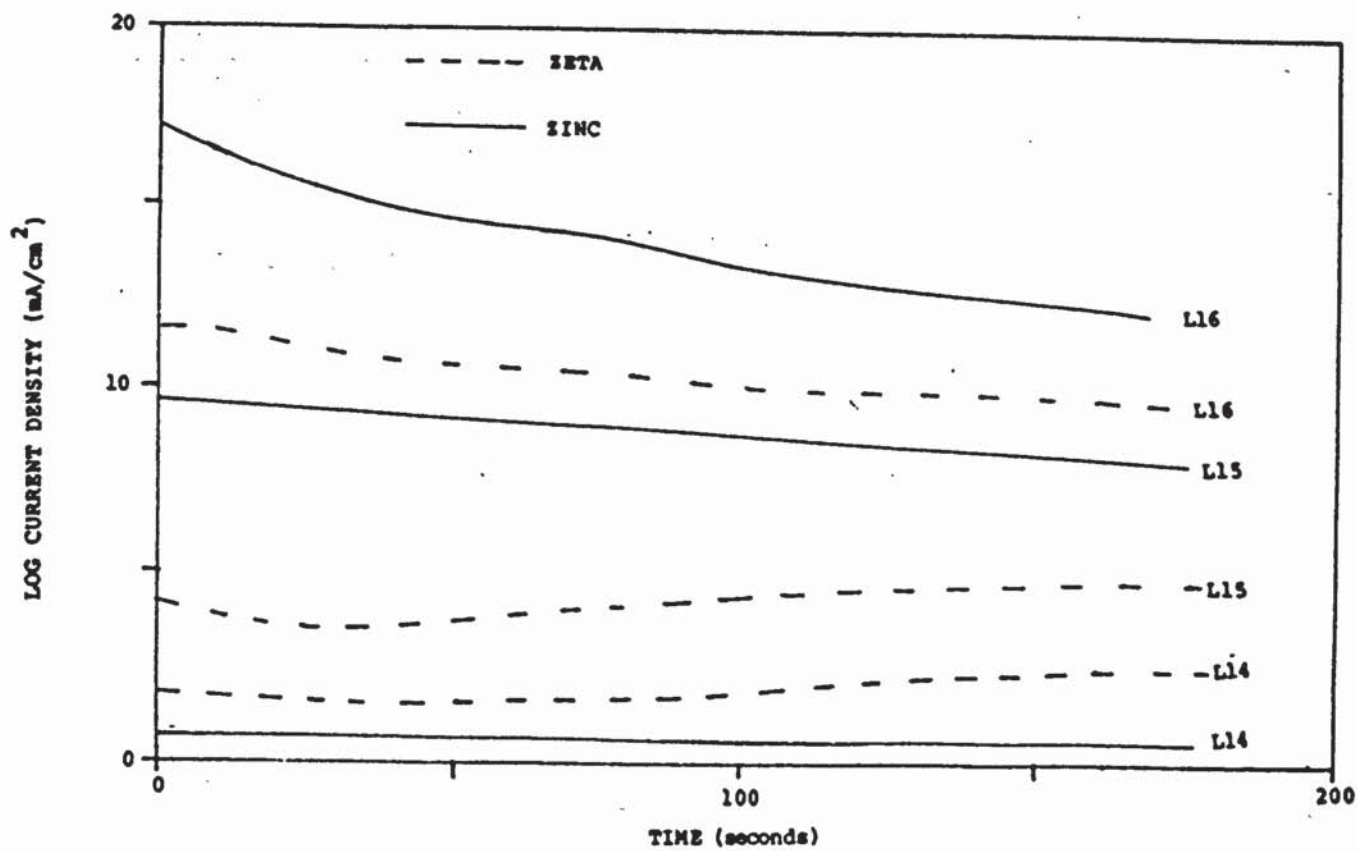


Figure 7.5 (a - h) Groups of potentiostatic polarisation curves of zeta and zinc in the various solutions shown in TABLE 7.1

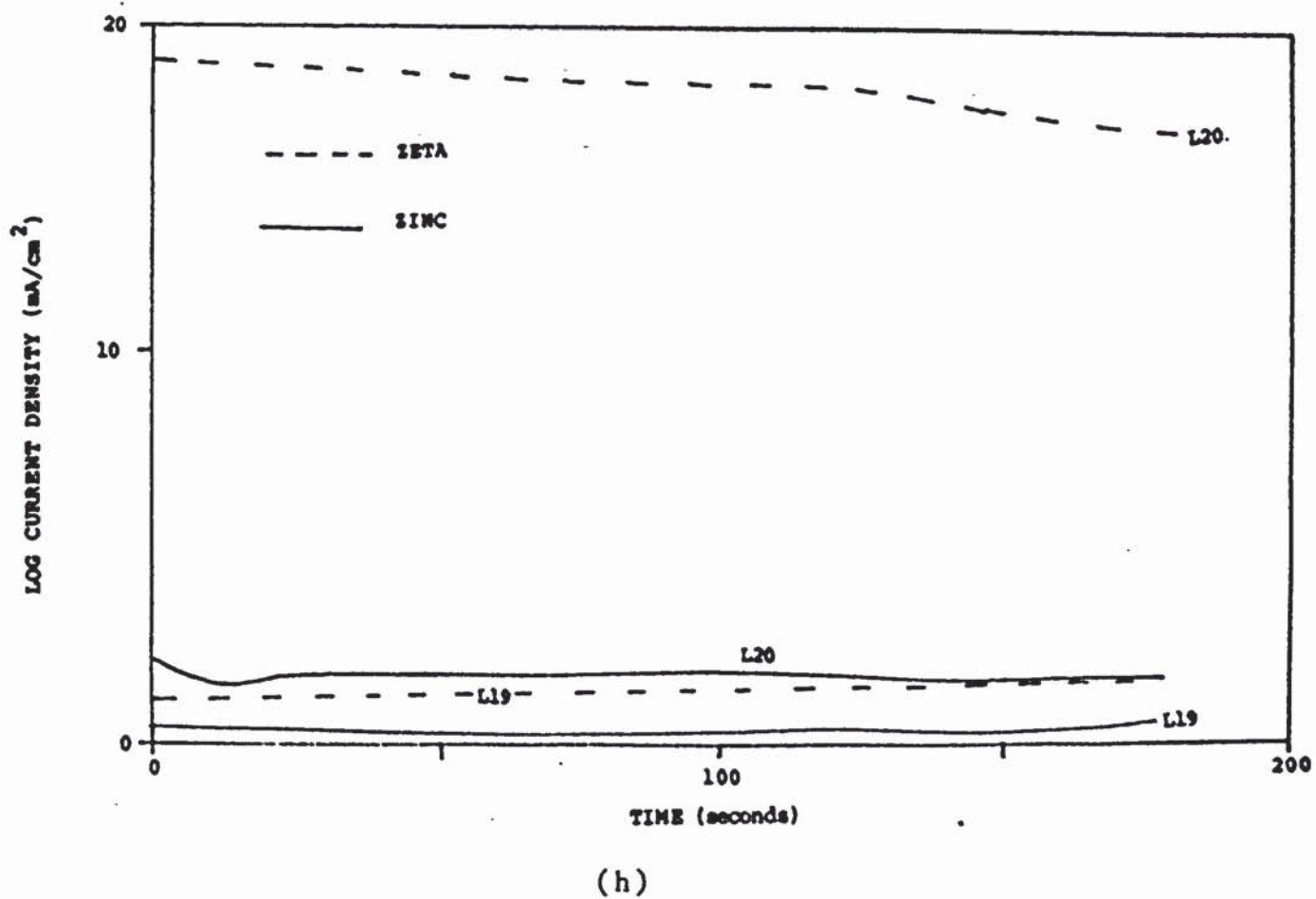
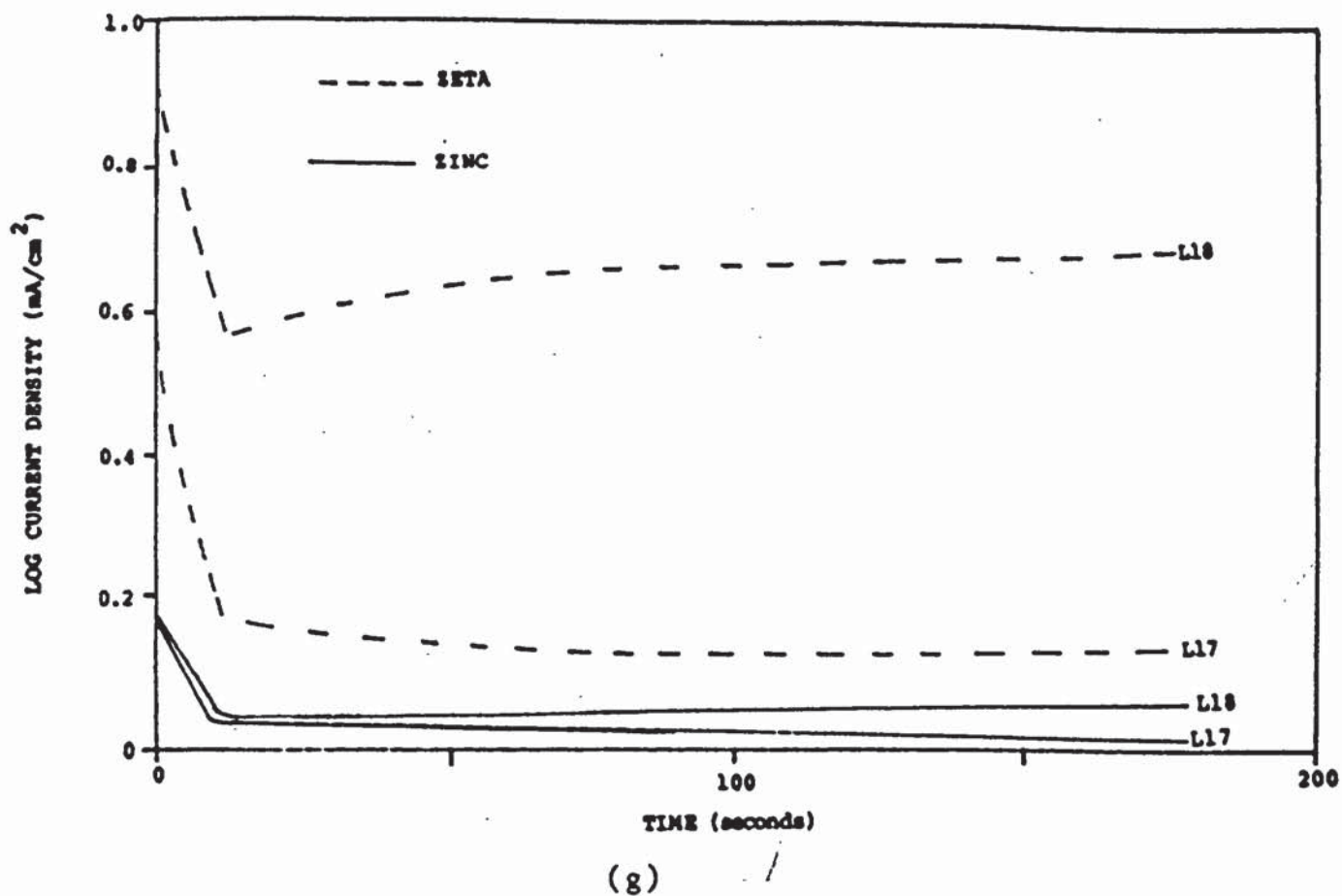




(e)



(f)



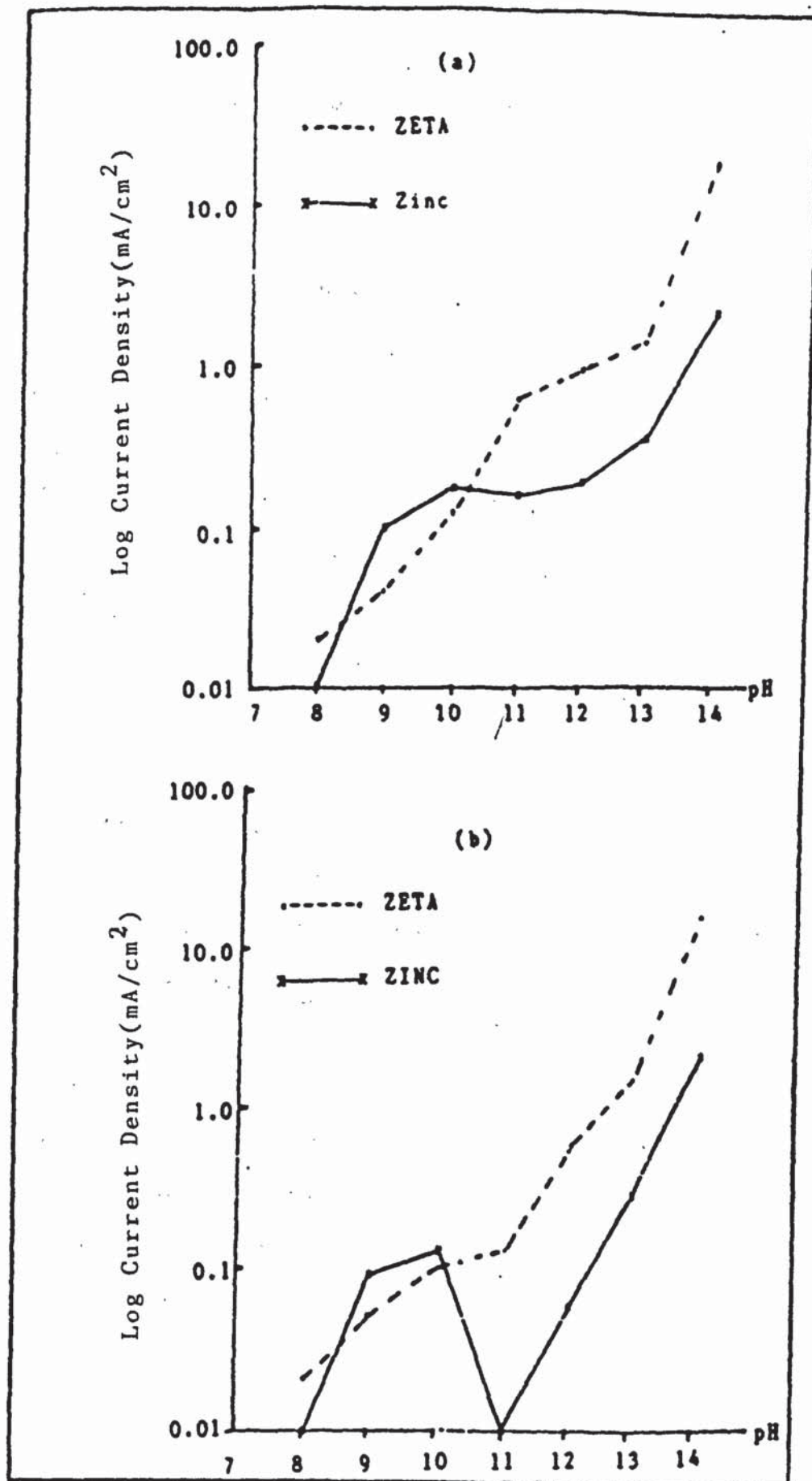


Figure 7.6 (a) Instantaneous current vs solution pH of zeta and zinc in NaOH  
 (b) Final current of zeta and zinc in NaOH solution vs pH of the solution

## 8. POLYESTER POWDER FLOW STUDIES

### 8.1 INTRODUCTION

The study of flow characteristics of organic powder on a substrate surface is of importance because it may affect the quality and performance of the finished product. For example, Gokemre and Dennis reported<sup>(110)</sup> that powders which exhibited the best flow, also provided the best corrosion protection. Nix and Dodge<sup>(102)</sup>, when they examined the flow of individual particles and clusters of particles, stated that the poor flow of clusters resulted in "orange peel". In this chapter, the flow characteristics of polyester powder on different zinc coating surfaces has been studied. The effect of different pretreatments have also been studied. The experiment was carried out as detailed in chapter 3, section 3.10.

### 8.2 RESULTS

Polyester powder was chosen for this work because it has good weathering properties and it was used in the rest of the project. To facilitate presentation, the five different pretreatments to the surface of respective specimens were coded as follows:

(A) Cleaned only

(B) Cleaned, pretreated in 0.12M/l  $\text{CrO}_3$  + 0.3M/l NaCl

(L1) solution for 30 seconds

- (C) Cleaned, pretreated in 0.12M/l  $\text{CrO}_3$  + 0.3M/l NaCl (L1) solution for 120 seconds
- (D) As C but degassed after treatment
- (E) Cleaned, pretreated in NaOH solution of pH 11 for 120 seconds.

The flow curves obtained have been arranged into nine figures, 8.1 - 8.9. Figure 8.1 shows the effect that the type of zinc coating (as cleaned), has on powder flow. Figure 8.2 shows the effect of a short chromating time (30 seconds) on powder flow. Figure 8.3 depicts the effect of a long chromate pretreatment time (120 seconds) on powder flow whilst figure 8.4 shows that degassing after pretreatment affects the powder flow on all the four specimens. Figure 8.5 shows the effect of alkali pretreatment for 120 seconds on powder flow. Figures 8.6 - 8.9 compare the effect of different surface pretreatments on electroplated (Zintech), hot-dip continuous galvanized steel sheets, hot-dip batch galvanized steel sheet and sprayed specimens respectively. Table 8.1 shows the final coverage while figure 8.10 is the comparison of the final coverage of powder on all samples. Table 8.2 shows the flow temperature ranges for the four specimens after five different surface pretreatments.

### 8.3 DISCUSSION

Generally, it can be seen that the melt stage of the curing cycle is accompanied by a decrease in area covered followed by an increase in area covered during

flow. There is no further change in area as the gel stage is reached at which cross-linking reactions start to occur. A second increase in flow (for example, as seen for the spray sample curves in figures 8.2 and 8.4) could be due to late melting of some powder clusters. The decrease in area in the melt stage can be related to powder particle characteristics, since at the room temperature the particles are angular and irregularly-shaped, and may contain some porosity. As the particles melt they assume a spherical shape and occupy a minimum area on the metal surface. Variation from this general behaviour are attributable to variation in experimental conditions.

It can be seen from figure 8.1 that the electroplated sample allowed a better powder flow and had the greatest area coverage (85-95%) compared with the rest of the samples which were all about the same (40%). Since there is a greater proportion of area covered on the electroplated samples, it is tempting to conclude that the smoother the surface, the better the powder flow on it, but the flow curves for the samples and the histogram of the final percentage area covered shown in figure 8.10 did not generally follow this hypothesis. The HDC is smoother than both HDB and sprayed samples but the final powder coverage was less. However, the spray samples which had the roughest surface, did show the least percentage area covered at all surface conditions. Pretreatment "D", as can be seen from figure 8.4 and

8.10, did actually tend to obey the hypothesis; the smoother the substrate surface the better the powder flow on it. However, the extent of surface modification provided by the pretreatment and subsequent degassing to the respective samples were not measured. Therefore the flow characteristics on the as-cleaned electroplated, HDC, HDB and sprayed samples cannot be explained by surface topography alone.

In studies by Gokemre and Dennis, and Ford<sup>(135,146)</sup> on the effect of pretreatment on epoxy powder flow on steel and aluminium, it was found that there was a difference in the flow characteristics on the as-received mild steel compared to the aluminium. The as-received aluminium was smoother than the as-received mild steel but there was still less flow on the former. They attributed this difference to the nature of the oxide film on aluminium. Similarly flow on the samples used in this investigation may well depend on the chemical nature of the surface after cleaning, conversion coating etc as well as as surface roughness.

The effect of chromate pretreatment for 120 seconds (C) can be seen easily from figure 8.3. The flow on all the sample surfaces was reduced compared to that on the as cleaned samples. It is interesting to note that for the electroplated sample the reduction in powder flow was more than 50 %. The HDB and the electroplated sample appeared to have the same and highest percentage

area covered, followed by HDC and lastly, the sprayed samples. It is also interesting that the sprayed sample which has the highest coupon weight change after chromate pretreatment for 120 seconds (figure 6.2) now has the least powder flow whilst the HDB which has a lower coupon weight change than sprayed now has the highest powder flow. This would be expected since the thicker the gel-like chromate film (see figure 6.4 a-d) the deeper the 'mud' cracks and hence the rougher the surface, when the film dried. The difference in surface chemistry, together with variation in surface topography, have accounted for the different flow characteristics on the samples. Initially, the surface topography of the sprayed samples was very rough and was not improved by the chromate treatment.

Gokemre and Dennis reported<sup>(146)</sup> that chromating had the effect of increasing the powder flow on aluminium, the effect being greater with more concentrated solution, a condition which would produce thicker chromate films. Sliwinski<sup>(69)</sup> however, reported that a longer pretreatment time which resulted in deeper 'mud' cracks, due to the greater thickness of the chromate-phosphate film showed a poorer powder flow as compared with the shorter pretreatment time which shows a better flow. A lot of other literature has been published on mechanisms of powder flow in relation to the roles played by viscosity, surface tension, stoving temperature, stoving time, flow additives, particle size and

pigment loading (section 2.3.6). All these studies assumed that the powder was flowing on a smooth surface. No account had been taken of the roughness and chemistry of the surface on which the powder was flowing. A recent investigation<sup>(47,)</sup> has shown that rough surfaces and pits or deep cracks on the surface led to poor powder coverage.

It can be seen from figure 8.4 and table 8.1 that degassing after chromate pretreatment for 120 seconds (D) improved the flow on the electroplated and HDC but made the flow on HDB and sprayed samples worse. However, shorter pretreatment time (B) (figure 8.2), improved flow remarkably on all samples, as compared with longer pretreatment time (C). This improvement can be linked with the reduced surface roughness. This agreed with Sliwinski's work mentioned earlier<sup>(69)</sup>.

The effect of alkali pretreatment (E) is shown in figure 8.5. Again, it can be seen that the best flow was obtained on electroplated sample where 100% area coverage was obtained. Except for shorter chromate pretreatment time (B), the alkali pretreatment (E) gave improved flow over other surface conditions, on the HDC and HDB samples. The alkali pretreatment (B) permits the best powder flow on electroplated and sprayed samples compared with all other surface conditions studied. Again, these improvements could be

linked with the combined effect of the type of surface oxide and topography.

Figure 8.6 shows the effect of different surface pretreatments on the powder flow on electroplated samples. Apart from alkali pretreatment (E), all the other pretreatments provide the same powder melt temperature of about  $55^{\circ}\text{C}$  and flow continued to about  $200\text{--}215^{\circ}\text{C}$ . The flow curves show that the as cleaned surface (A) and the alkali treated (E) (which also acts as cleaning solution) surface provide better powder flow. The best flow, which was obtained from the Alkali treated surface, suggested the recommendation of a double cleaning operation as a means of improving powder flow on electroplated substrates.

One of the reasons for chromating the surface before powder coating is to improve the adhesion of the organic powder coating to the substrate. This would not be done successfully if chromating led to inferior powder flow. Evidence is now available which links cratering (section 2.2. and chapter 4) with powder not able to flow over the surface. Corrosion resistance will increase with chromate film thickness but this will not be achieved if the thick chromate film leads to defective powder coating. However, thinner chromate films as can be seen from figure 8.6, do improve powder flow as compared with thicker ones.

Although it is not known how the topography of the pret-

reated surface affects powder organic coating adhesion, Treverton<sup>(147)</sup> found bonding was as good after 3 seconds treatment in a chromate solution as after 30 seconds treatment. Thick chromate coatings are mechanically weak and prone to cracking and flaking so it is likely that powder flow can give a good indication of the mechanical or physical characteristics of the combined pretreatment and powder coating.

A comparison of effects of different pretreatments on powder flow or HDC is shown in figure 8.7. Here, the most effective pretreatment on powder flow was the shorter pretreatment time (B) and the flow was poorest when the surface was chromated for 120s (C). Also, it can be seen that the best pretreatment for good powder flow on HDB was the chromate pretreatment for shorter time (B) while that for the sprayed sample were alkaline pretreatment (E) and shorter chromated time (B) as shown in figure 8.9. As mentioned earlier, the irregularities in the curves in this figure suggested the tendencies for the powder to cluster on rough surfaces since the dips along the curves are indications of melting of the clusters which probably gather at the bottom of the valleys on the sample surface. A summary of the effects of different pretreatments on powder flow on different zinc coatings surfaces is shown in tables 8.1 and 8.2 and in figure 8.10. If a substrate is to be powder coated, it is recommended to apply pretreatment 'B'(chromate for 30 seconds) so as to achieve both

good powder coverage and corrosion resistance.

#### 8.4 CONCLUSIONS

- (1) The electroplated zinc surface allowed the best powder flow for all the five surface conditions.
- (2) The as cleaned (A) and alkali pretreatment (E) were equally effective on powder flow rate. Therefore, for relatively thick zinc coating, a double cleaning operation would be recommended as this will improve powder flow rate on the surface.
- (3) The roughness of a surface is one of the factors affecting the powder coverage of the surface.
- (4) The chromate conversion coating pretreatment reduces powder flow rate as it increases the roughness of a surface.
- (5) The reduction in flow rate in (4) above can be reduced by degassing after pretreatment and/or shorter pretreatment time.
- (6) There was more likelihood of powder cluster formation on a rough surface.
- (7) The powder flow rate was affected by both substrate surface chemistry and topography.

TABLE 8.1 Final powder coverage

Surface condition	Final Coverage (%)			
	Elect	HDC	HDB	Spray
A	95	40	45	42
B	72	51	52	35
C	40	32	40	29
D	59	41	36	30
E	100	48	48	42

Table 8.2 Flow temperature ranges

Surface condition	Flow temperature range							
	Elect		HDC		HDB		Spray	
	St	End	St	End	St	End	St	End
A	55	190	45	140	45	180	40	200
B	55	215	55	215	58	215	55	215
C	55	200	70	215	45	200	60	210
D	55	215	55	215	58	215	70	215
E	35	160	45	215	70	190	30	190

(St stand for start).

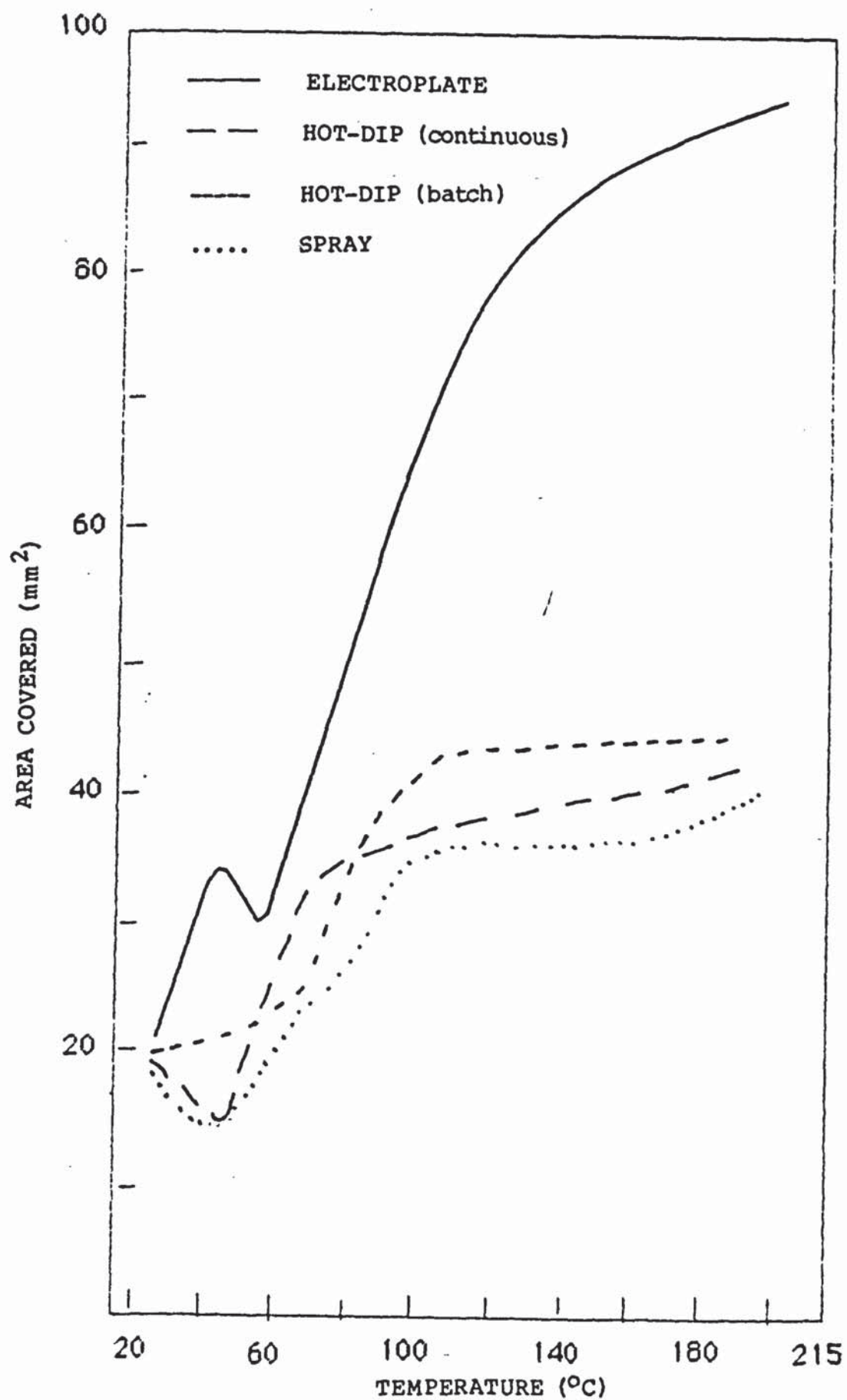


Figure 8.1 The effect of type of zinc coating as cleaned on powder flow

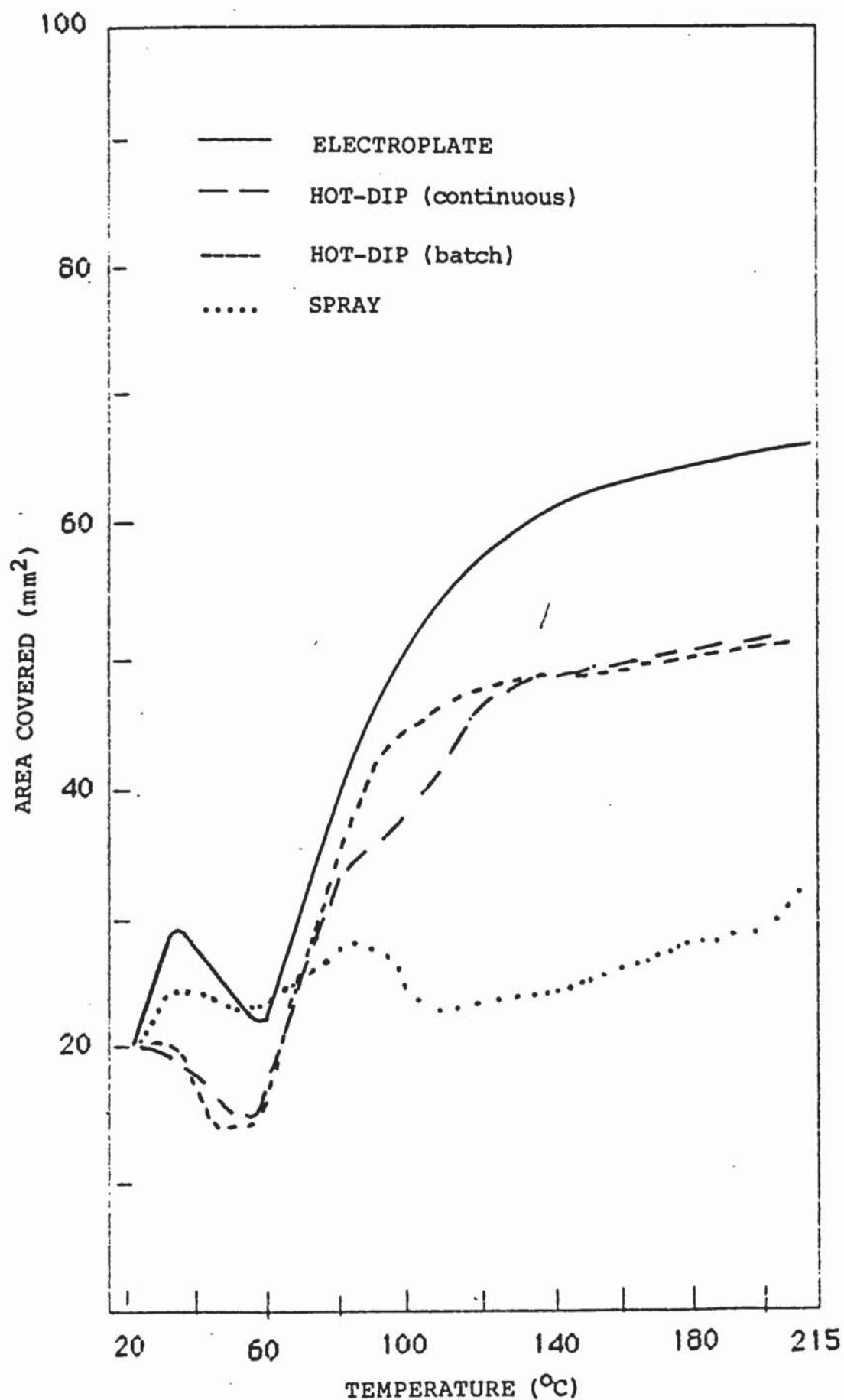


Figure 8.2 The effect of short chromating time (30s) on powder flow

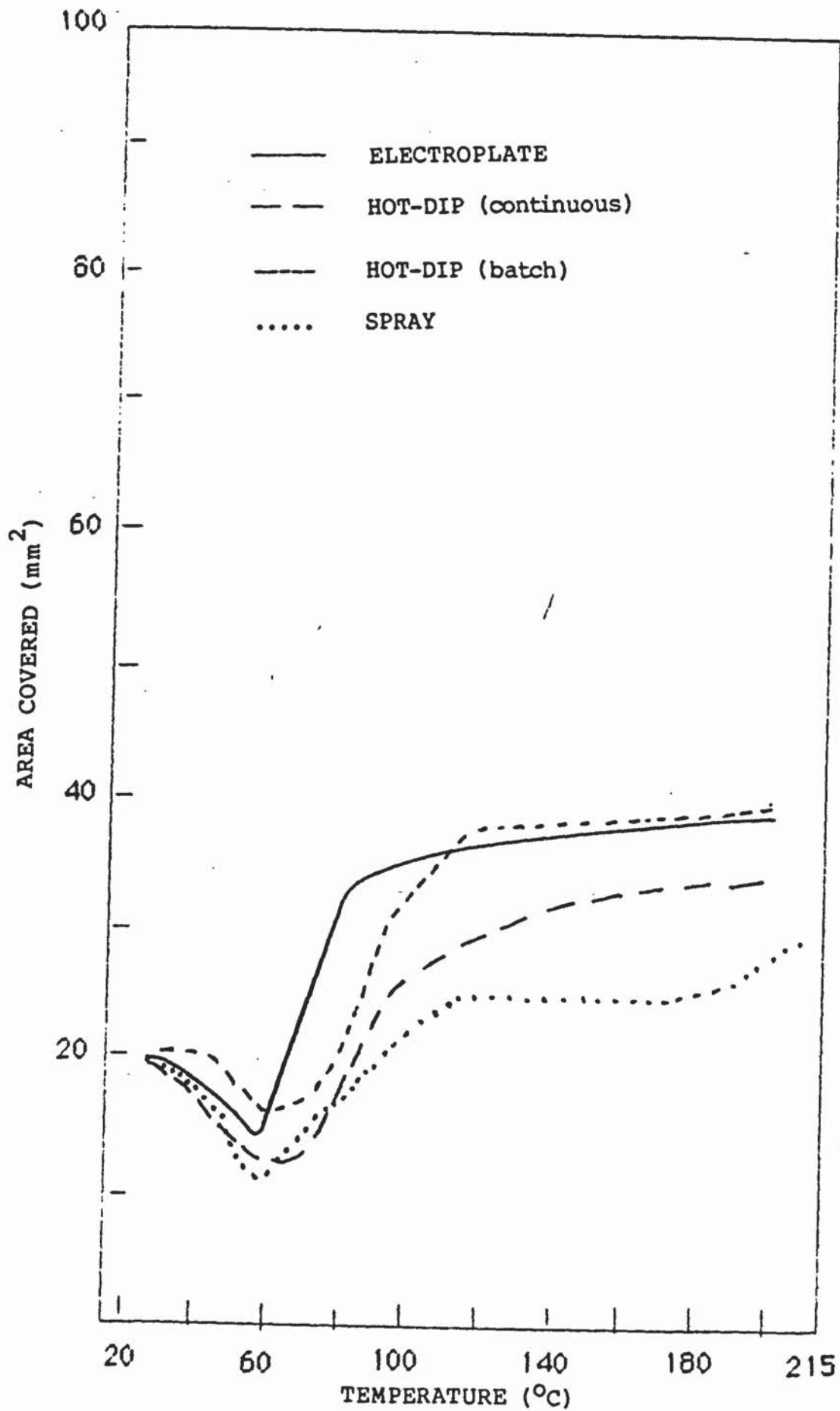


Figure 8.3 The effect of chromate pretreatment (120s) on powder flow

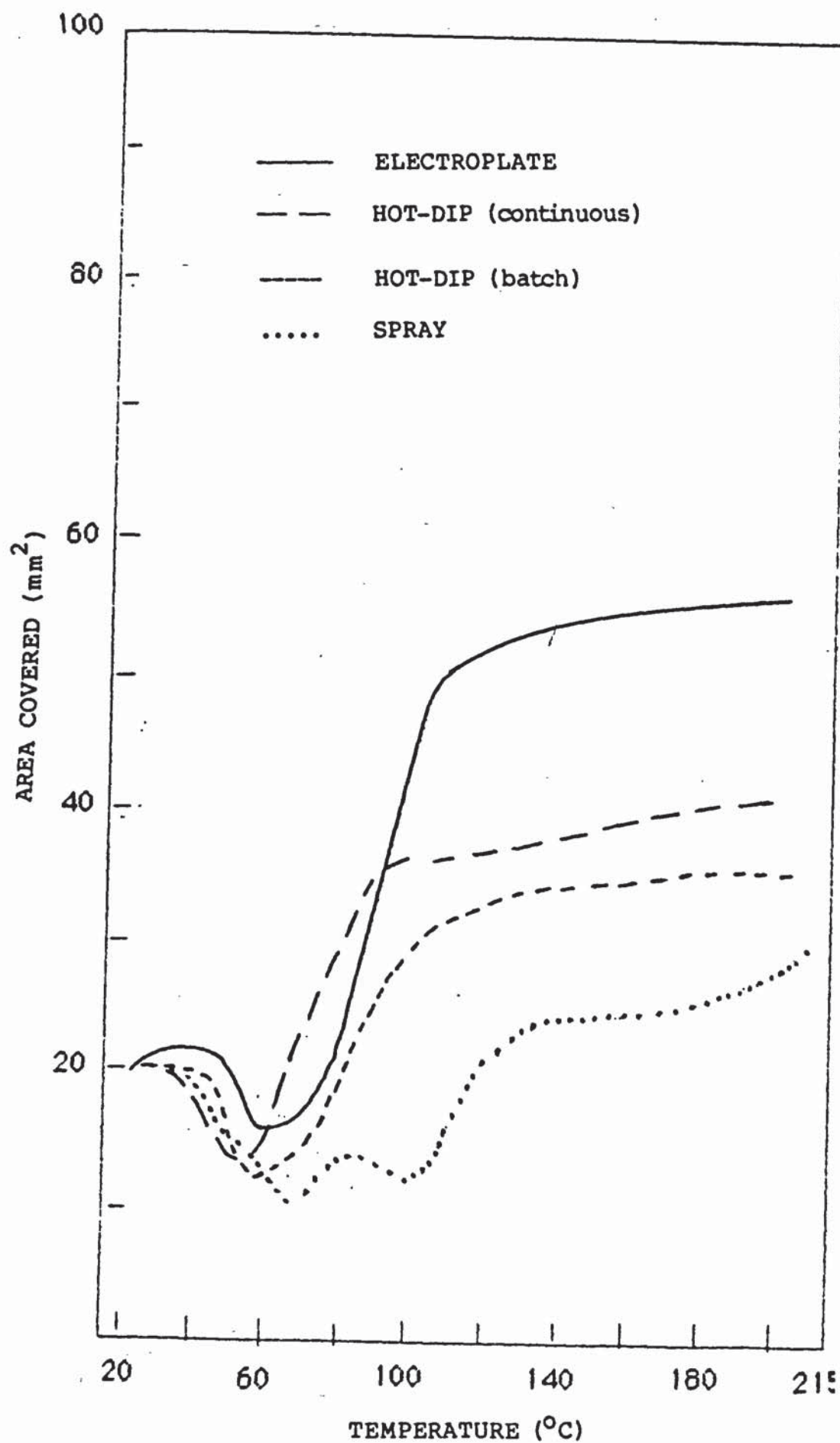


Figure 8.4 The effect of degassing after pretreatment (120s) on powder flow

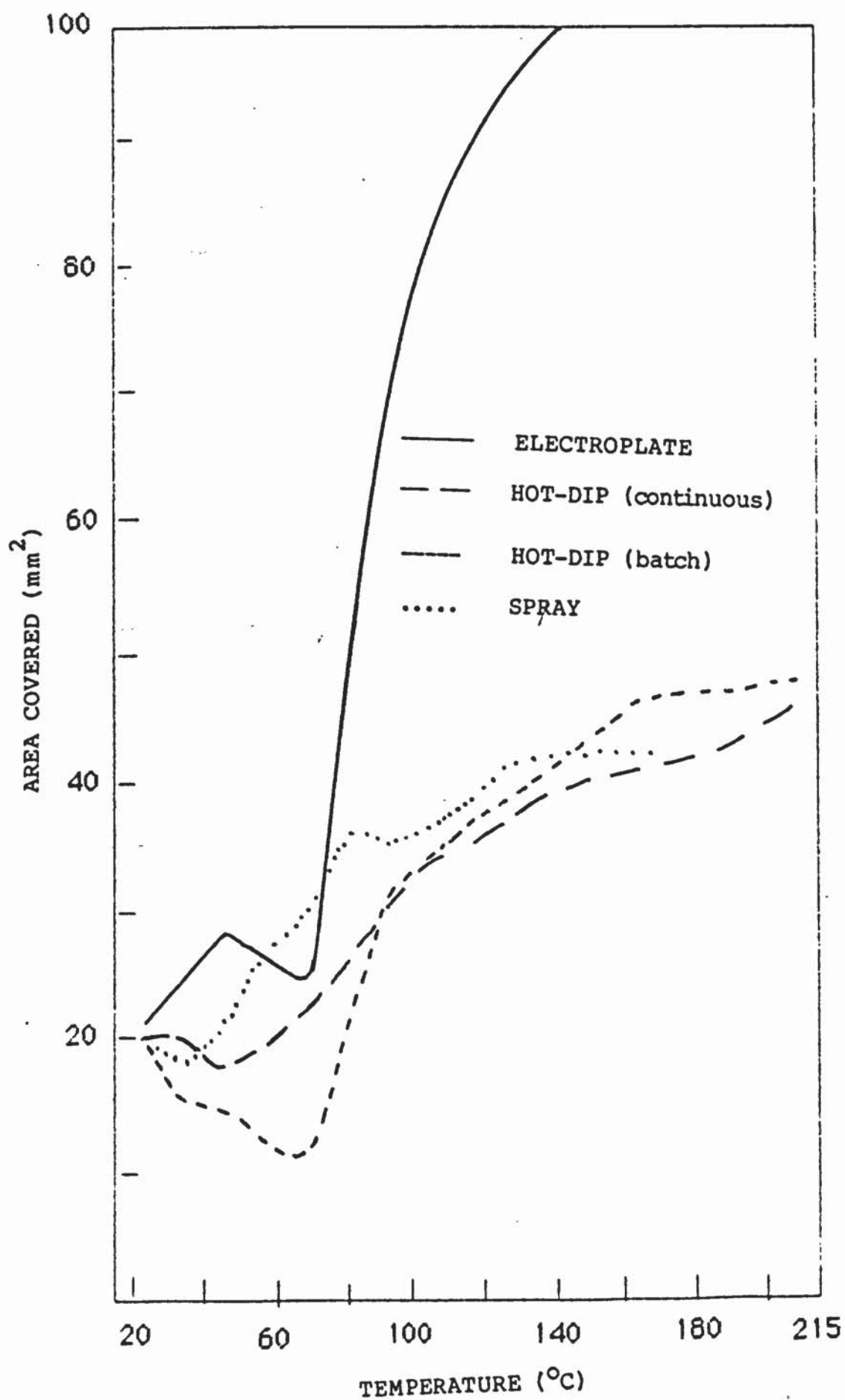


Figure 8.5 The effect of alkali pretreatment on powder flow

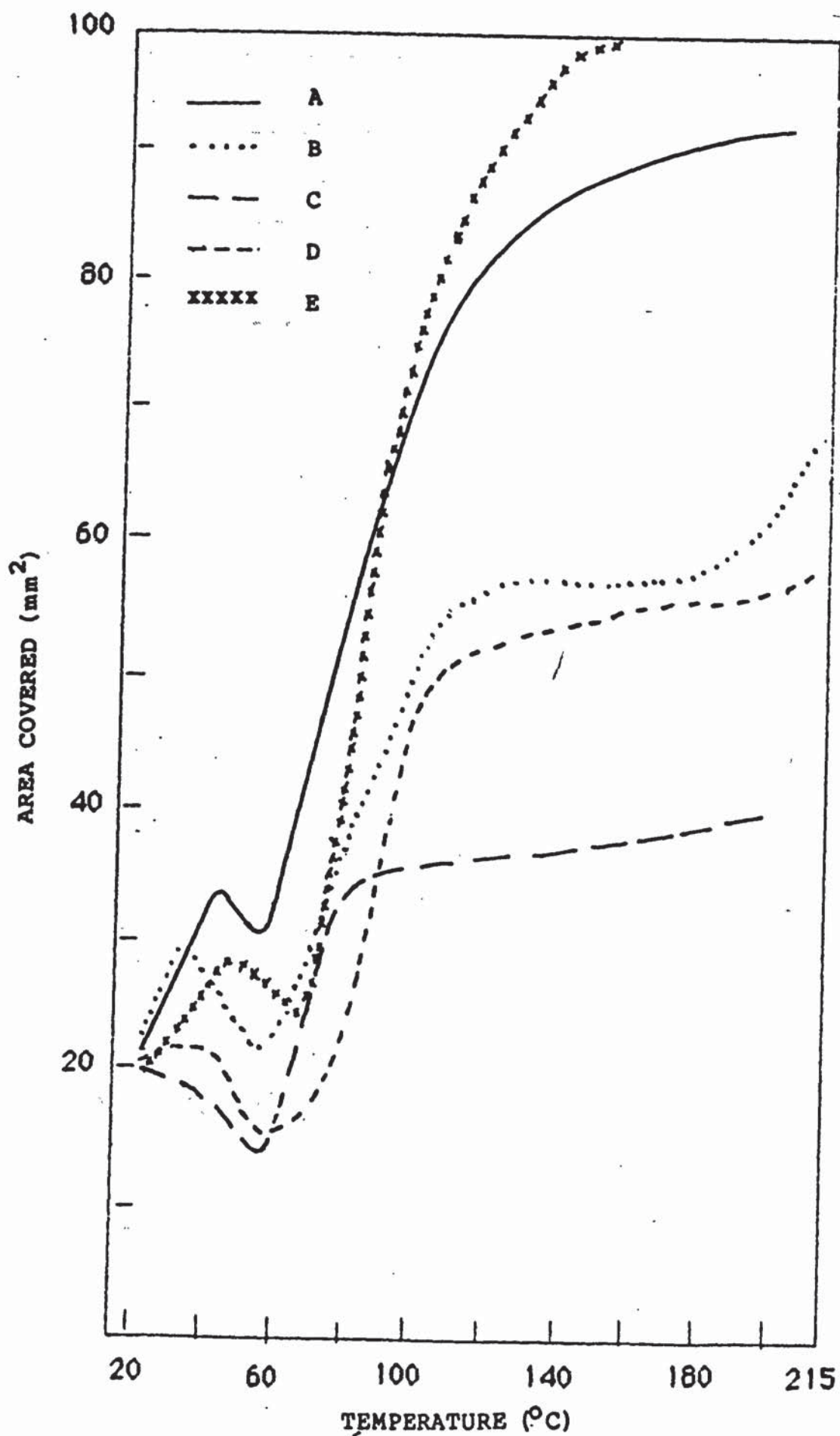


Figure 8.6 The effect of different pretreatments on the powder flow on electroplated samples

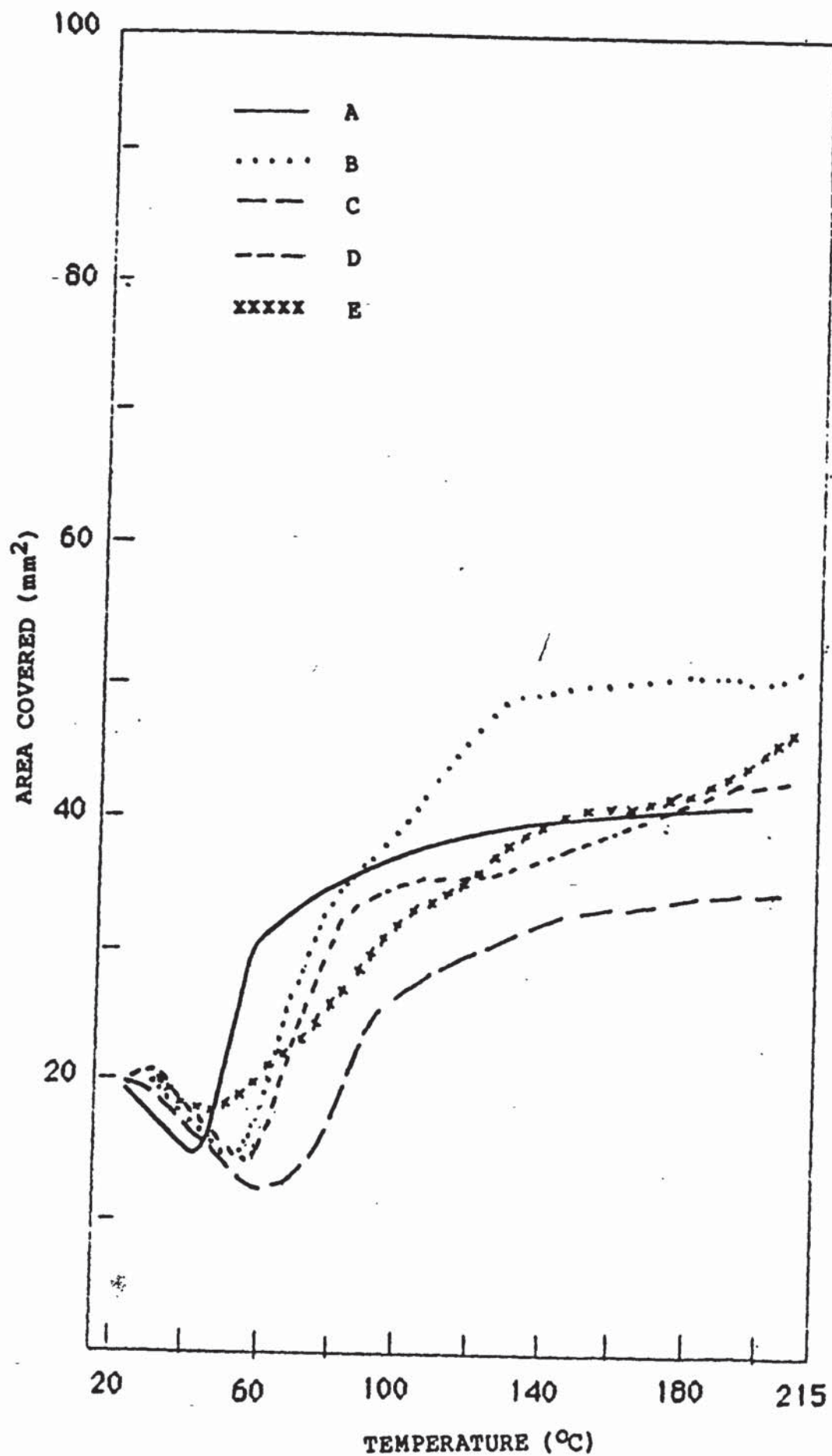


Figure 8.7 The effect of different pretreatments on the powder flow on continuous hot-dip samples

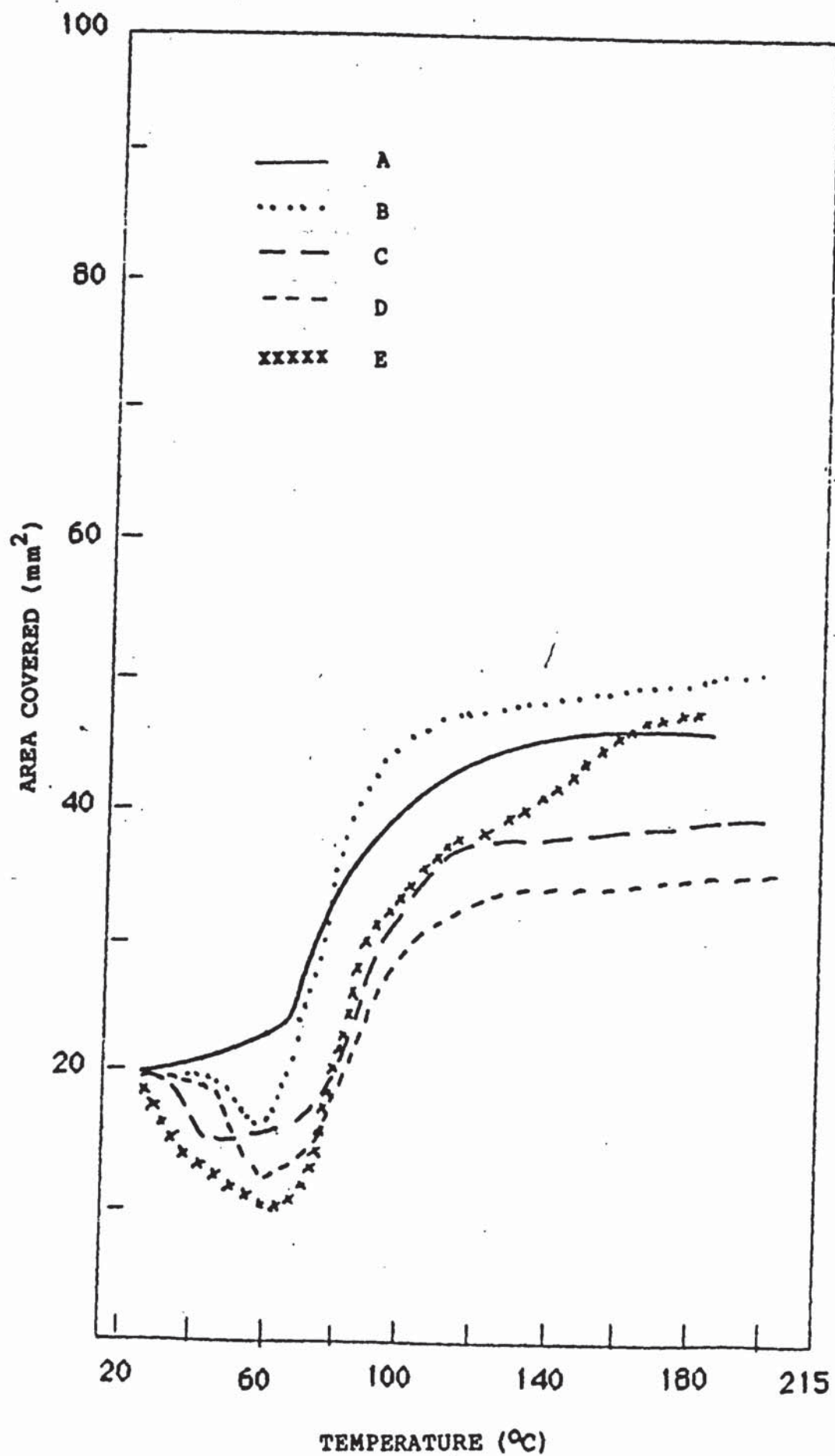


Figure 8.8 The effect of different pretreatments on the powder flow on batch hot-dip samples

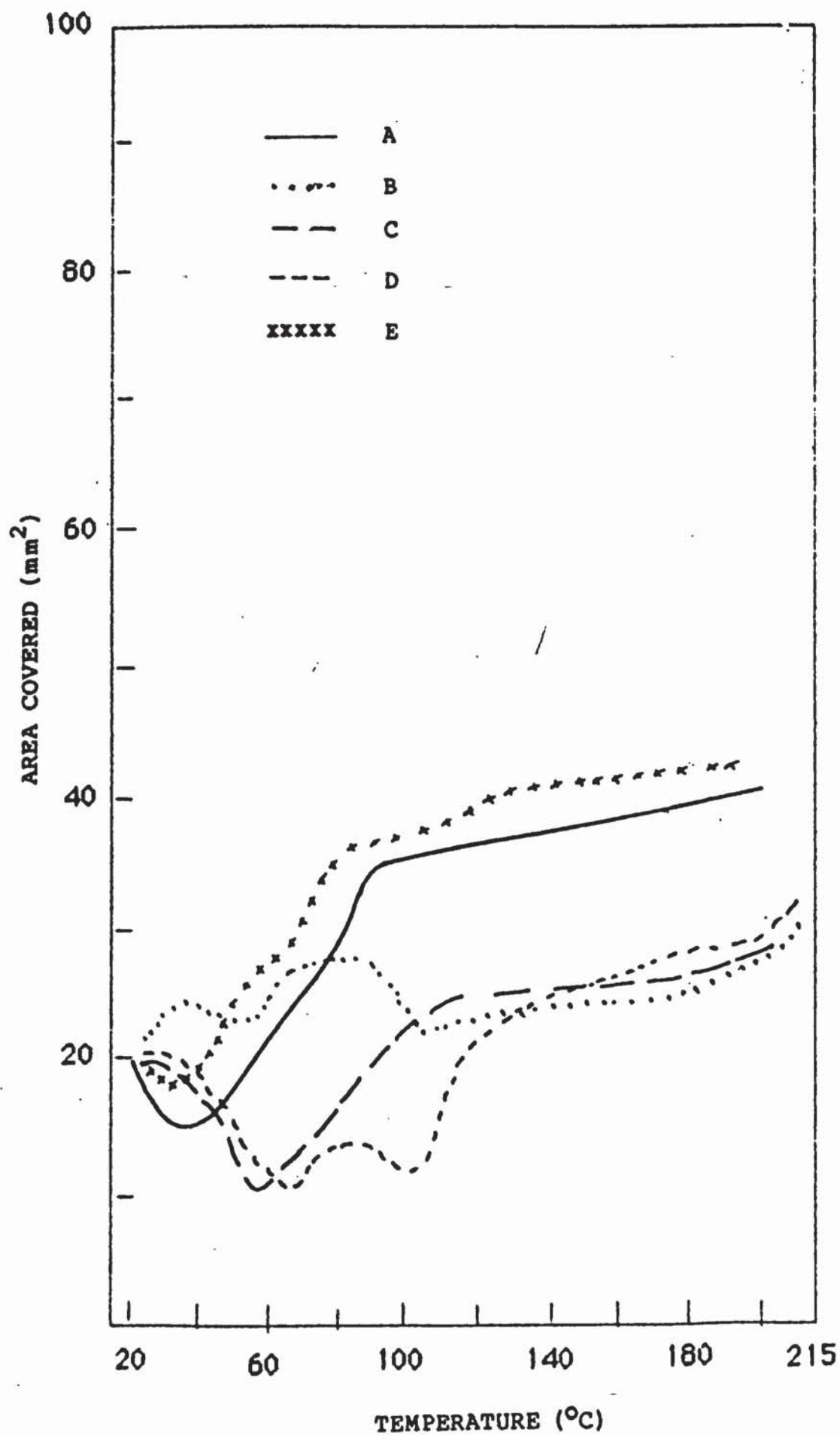


Figure 8.9 The effect of different pretreatments on the powder flow on sprayed zinc samples

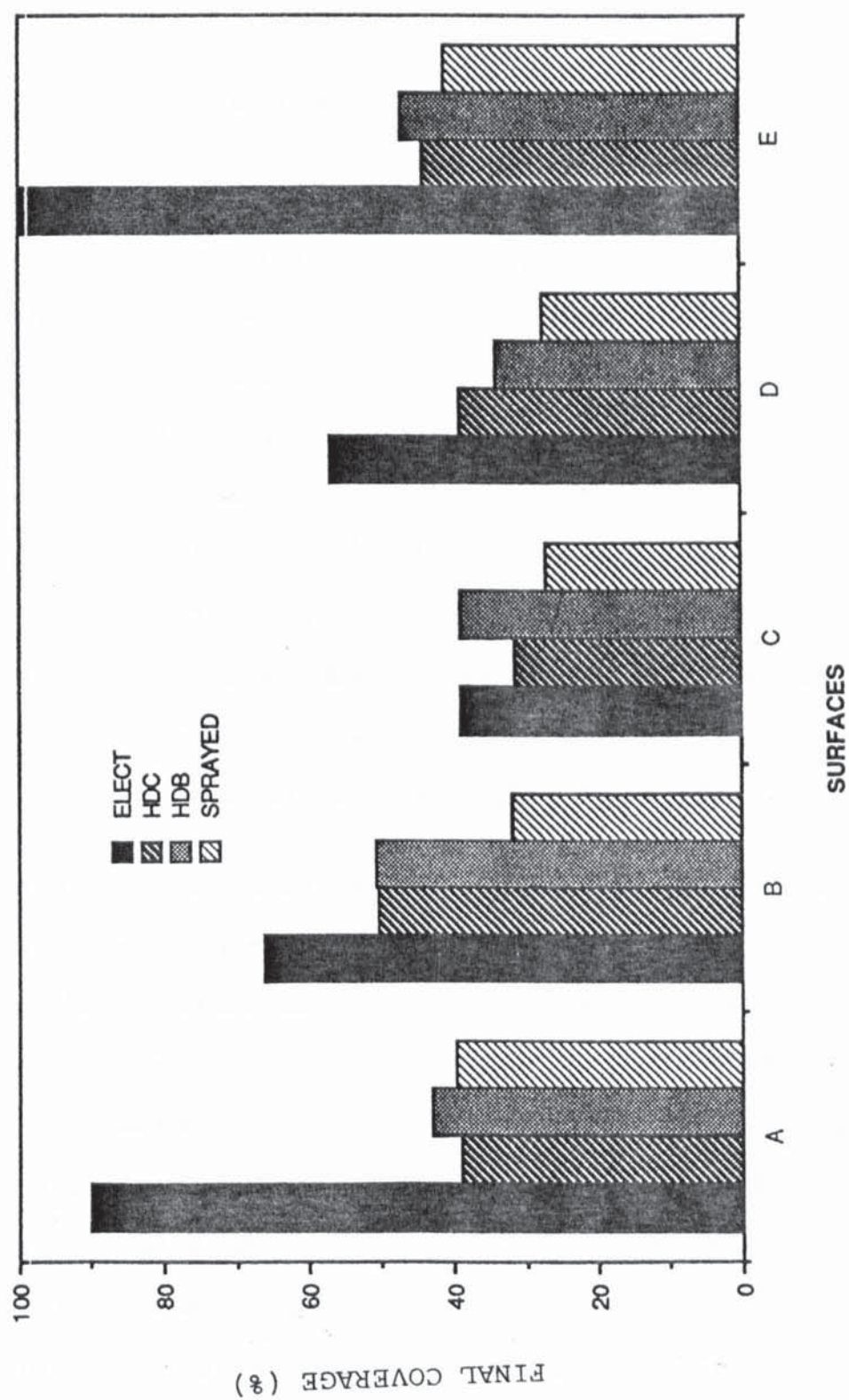


Figure 8.10 Comparison of final coverage on different pretreatment surfaces

## 9 ADHESION CHARACTERISTICS OF DUPLEX POLYESTER POWDER - ZINC COATED STEEL SUBSTRATES

### 9.1 INTRODUCTION

Thin films, thick films and duplex or bulk coatings are used for a variety of purposes in diversified applications in many technologies. Whatever their intended purpose - functional, decorative, or protective, the properties, structures, functional characteristics, and performance all depend on good adhesion between the adherate and adherend<sup>(148)</sup>. In the organic powder coating or painting industry, adhesion is very important. If the adhesion is poor, the extent of deterioration of the substrate by environmental factors (humidity, corrosive gases, liquid etc) is greatly accelerated.

There are essentially two aspects of adhesion covered in the present investigation:

- (a) the measurement of adhesion strength and
  - (b) an understanding of the factors affecting adhesion between polyester films and zinc coated substrates, leading to an improvement of adhesion strength.
- The second aspect will be dealt with in chapter 10 whilst this chapter is concerned with the measurement of adhesion of the polymer film.

The measurement of adhesion is important for a variety of reasons:

- (a) to assess the efficacy of changes in the process

variables, and there-by to optimize the conditions which yield the required adhesion strength;

(b) to discriminate parts or products which have poor adhesion strength from those which are acceptable;

(c) to gain fundamental insight into the mechanism of adhesion.

Thus there is a need for reliable, reproducible, and quantitative methods for measuring the adhesion. There are many techniques for determining adhesion strength of coatings as described in the literature and cross-cut/peel<sup>(149)</sup>, pull-off<sup>(150)</sup> and indentation debonding tests were the techniques used in this work.

## 9.2 CROSS-CUT/PEEL TEST

Eleven diagonal intersecting parallel cuts with spacing of approximately 2 mm between each other were scored on the surface of the test pannels. Two pannels, one degassed and one not degassed, from the different types of specimens, chromated for 30s, 60s and 120s respectively, were tested. Adhesive tape (sellotape type 1101) was applied firmly to the cut areas and then removed swiftly, by pulling at right angles to the test pannel.

## 9.3 PULL-OFF TEST

This is a static load test where an attachment is made to the surface of the film so that a pull-off tension can be applied to the film/substrate interface.

The precursors of the direct pull-off technique were methods in which a metal rod or woven mesh, were embedded in the drying paint film and were then pulled away, hopefully to detach the film. The development of this technique passed through many stages to get to its present stage when Eastman Kodak<sup>(72)</sup> introduced an extremely quick-setting cyanoacrylate adhesive, supplied as a low viscosity monomer which polymerises rapidly when a thin film is squeezed between plane surfaces. The polymer forms a tough film and is an effective adhesive for a wide range of substrates, including most types of paint. It is, of course, extremely difficult to be sure that the adhesive does not affect the paint film.

#### Experimental procedure:

Two rods (with mushroom shaped ends measuring 2 cm diameter and 3 mm thick) were glued to the test pannel in each case. Care was taken to ensure that they were in alignment, for if a very slight bending moment is applied to the adhesive joint, it will result in uneven stressing and propagation of a peeling fracture across the surface. Using a very sharp scriber, a cut was made round one of the mushroom ends in each case. Tension was then applied using a Hounsfield Tensometer. The breaking strength, in MPa for each test assembly is given by the formula  $4F/d^2$ , where F is the breaking force in Newtons and d is the diameter in mm.

#### 9.4 INDENTATION DEBONDING

In many cases, the qualitative adhesion tests, such as the cross-cut/peel test, are not really adequate, and if possible should be replaced with tests that produce quantitative data. One of these methods is the indentation debonding test. Indentation debonding is a test developed for checking the adherence of thin polymer films to hard substrates (e.g. Cu, Zn, Fe, etc). A small pointed indenter is pressed into the surface of the sample in the normal direction. The tensile stresses arising in the bond outside the contact area may exceed the limiting value and debonding will then take place. When the film is transparent observation of this phenomenon is often facilitated by the appearance of Newton's rings created by the diffraction of light passed through and reflected from the debonded film Figure 9.1(a). Mechanical analysis of the deforming polymer film, is based on the computation of displacements of thin plate segments<sup>(151)</sup> confined between the rim of the indentation and the edge of the debonded area. The magnitude of the radius and hence the radial bending strain in the film determines the onset of "peeling" (see fig. 9.1(b). The maximum bending strain at  $r=b$  is computed from the radial bending moment.

It has been shown<sup>(151)</sup> that as long as the material of

the film and substrates stay constant with the same kind of adhesive bond prevailing between them the maximum radial bending strain at the point of anchorage ( $r=b$ ) is fairly constant. Thus radial strain offers itself as a "peeling parameter" setting the limit of adhesion between a specific combination of substrate and bonded polymer layer. Using a computer program, the bending strain (radial strain) was calculated.

#### **Experimental procedure:**

All the samples were powder coated, and tested before and after corrosion test cycles. Six impressions were made on each pannel using conical indenter on a Wilson Rockwell Hardness Tester at a constant load of 15 kg. Although the polyester films are opaque disbonded regions are quite evident figure 9.2. With the aid of a Nikon Linear Transverse measurescope, the radius of the indentation "a" (since this indenter is conical one and there were variations of the depth of indenter due to variation of hardness across the surface of the different specimens) and the width between the indenter and the edge of the debonded area "b" were measured. In each case, the average of the measurements obtained from the six impressions was calculated. The indenter had an included angle of 120 degrees.

## 9.5 RESULTS

For the purpose of presentation of the results the following codes were used:

- 1 for electroplated samples
- 2 for HDC galvanized samples
- 3 for HDB galvanized samples
- 4 for sprayed samples

For indentation debonded results:

B refers to samples pretreated in 0.12M/l  $\text{CrO}_3$  + 0.3M/l NaCl (L1), not degassed, before powder organic coating.

For example:

1B/30 means electroplated, pretreated in 0.12M/l  $\text{CrO}_3$  + 0.3M/l NaCl (L1), for 30 secs, before powder coating.

C refers to samples treated as B but degassed after pretreatment.

The classification of the cross-cut/peel test results is shown in table 9.1<sup>(149)</sup> while the experimental results based on this classification are shown in table 9.2. Table 9.3<sup>(150)</sup> is a classification of the nature of failures in pull-off adhesion tests and the experimental results based on this classification are shown in table 9.4. The indentation debonding test results are shown in tables 9.5 - 9.8, and figures 9.3 - 9.7 while the cross section of thin and thick powder organic coatings on zinc sprayed samples are shown in figure 9.8 (a & b).

## 9.6 DISCUSSION

It is generally accepted that chromate conversion coatings improve adhesion of organic coatings to substrates such as zinc. The reason for the improved adhesion have been under debate for some time. Murphy<sup>(152)</sup> attributed this property to chromate inhibition of corrosion of the underlining substrate which would otherwise undermine the paint and give loss of adhesion in service. Others<sup>(153)</sup> suggested that adhesion between conversion and organic coatings was somehow dependent upon the surface area of the small spherical particles which were thought to be present in the chromate films. It would be reasonable to suggest that these properties will increase with increasing conversion coating thickness (increasing immersion time), although only to a certain degree since prolonged immersion sometimes resulted (depending on the process) in flakes of the coating becoming detached.

### 9.6.1 CROSS-CUT/PEEL TEST

Results given in table 9.2 tend to suggest that sprayed samples have the best adhesion compared with the other three sets of samples. Surface pretreatment time whether short or long as well as degassing after pretreatment appeared to have no influence on the zinc sprayed samples' adhesion characteristics. Table (9.2) also shows that the hot-dip continuous galvanized samples have the poorest adhesion, especially the

samples pretreated for 30 seconds. Generally, there is no noticeable difference between degassed and not-degassed samples, and table (9.2) presents a general impression of better adhesion for samples pretreated for longer than 30 seconds. The good performance of spray samples could be related to the mechanical keying due to the surface roughness of this specimen. However, hot-dip batch, which also has a rough surface, has a comparatively poor adhesion.

#### 9.6.2 PULL-OFF TEST

Table 9.4 also indicates good adhesion between the sprayed zinc substrate and the polymer film but weak zinc sprayed coating in that cohesive failure occurred within the zinc coating substrate. The variation of the breaking strength is simply a reflection of the variation of weakness of the zinc coating at different regions in the coating.

A careful study of table 9.4 revealed, as with the cross-cut test, that samples pretreated for 60s have superior adhesion compared to those pretreated for 30s, in terms of breaking strength, for electroplated and hot-dipped samples. Apart from the hot-dipped batch, degassing appeared to make no difference to the results. Generally, the electroplated samples tended to have a comparatively low breaking strength, although the nature of failure was mostly cohesive failure of the adhesive.

An attempt to relate the breaking strength to the nature

of failure revealed the inconsistency of the results. Some samples that have high breaking strength had more adhesive failure between substrate and polymer film (A/B) and less cohesive failure of adhesive (Y) than some other samples that have low breaking strength. This made it more difficult to attribute breaking strength to either the failure between the substrate and the polymer coating or to the failure between the polymer coating and the adhesive. HDB samples, e.g. pretreated for 30 seconds and 120 seconds and not degassed, showed 80% and 50% polymer coating peeled-off with strengths of 13.1 and 16.6 MPa respectively. The counterparts, in the case of the electroplated samples, showed only 15% and 20% of the polymer coating pulled-off with strength of 12.3 and 12.9 MPa respectively. If the assessment is based on the breaking strength, the hot-dipped-batch has a better adhesion, but in terms of % polymer coating peeled-off it appears that the electroplated sample had better adhesion. Equally, it would be reasonable to expect that the % of polymer peeled-off the electroplated samples would increase had the breaking strength increased to the same level as that of HDB and vice versa.

It can also be seen from table 9.4 that the samples with smoothest surface finish, hot-dipped continuous and electroplated, showed mostly adhesive failure between the polymer coating and the adhesive. The results suggest a tendency for samples with rougher

surfaces to have greater adhesive strength (bonding between the mushroom shaped test rod and the sample) than those with smoother surface. This would be likely due to the influence of mechanical keying associated with rough surfaces. The exact effect of the adhesive on the polymer coating bonding strength would be difficult to assess. However, Hoffmann<sup>(154)</sup> reported that the adhesive did not soften the paint film to which it was applied. Although the cyanoacrylate monomer which he used had a strong solvent power for, or miscibility with, many polymers and had been shown<sup>(155)</sup> to diffuse through various paint films. It was suggested that its use in pull-off tests can be justified only if it can be established that polymerisation occurs so rapidly that penetration into the film is negligible.

At the Paint Research Station<sup>(155)</sup>, investigations into various methods of surface preparation showed poor adhesion on contaminated surfaces, whilst good adhesion with little clear adhesion failure, for freshly grit-blasted steel. The adhesive in the present work required about 6 hours to set and the polymer surface for different samples were expected not to be the same since the surface roughnesses of the respective substrates were different (Chap.5) and pinholing occurred to different degrees (few or sometimes none) in the case of HDC and electroplated). These factors made it more difficult to rely on the results in table 9.4.

### 9.6.3 INDENTATION DEBONDING TEST

Figure 9.3 is a histogram of organic coating peeling strain for different samples pretreated in 0.12M/l  $\text{CrO}_3$  + 0.3M/l NaCl (L1) solution for times of 30s, 60s, and 120s. At all three pretreatment times, the sprayed samples had the lowest peeling strain. The electroplated samples had the highest peeling strain at the pretreatment time of 60s. This method of adhesion measurement showed the hot-dip continuous sample to have the highest adhesion at the shortest pretreatment time of 30s. Adhesion decreased with further increase in immersion time. At a short time of immersion, the HDB samples possessed the highest polymer coating peeling strain, as compared with electroplated, HDC and zinc sprayed samples of the same pretreatment. Marginally, the highest peeling strain was at 120 secs. One fact revealed by figure 9.3 was that, other factors being equal, different pretreatment times favour different types of substrate. Figure 9.4 shows the effect of degassing after pretreatment on the peeling strain. If this figure is compared with figure 9.3, it can be seen that degassing after pretreatment has only a marginal effect on the peeling strain (table 9.5).

Zettlemoyer et.al.<sup>(156)</sup> found that the surface area of hydrated chromium oxide particles increased after heating. This was explained as being due to the removal of the water of hydration and the subsequent formation of micropores or gaps between the inorganic polymer

structures. The gaps between the blocks of the inorganic polymer structure of the hydrated chromium oxide particle permit the absorption and diffusion of organic molecules, particularly if the absorbed molecules can chelate chromium ions. Selective absorption was also shown using a range of organic acids.

Results for the corrosion tested samples are shown in table 9.6 and in figure 9.5 for not-degassed samples and figure 9.6 for the degassed samples. The tests were carried out in areas that looked sound (i.e not blistered) after the acetic 5% salt spray test. As would be expected, the peeling strain of all samples was reduced compared with those obtained before corrosion tests, a factor indicating the reliability of this technique of adhesion measurement.

When the chromate film was not degassed, except for hot-dip-batch, the peeling strain appeared to be highest at a chromating time of 120s, as expected, (sect. 2.2.3.3) since the longer the immersion time the thicker the chromate film. The degassed samples also followed the same trend. It can be seen from figure 9.5 and 9.6 that in general, the degassed samples possessed better adhesion. This trend was expected since degassing improved powder flow and reduced the incidence of pinholing, major factors required for improved corrosion resistance of the duplex system.

Another factor responsible for this improved adhesion was

that degassing dehydrated the chromate film and led to conversion of soluble into insoluble chromium compounds. This provided a surface which enabled easy selective absorption of corrosion inhibitors and adhesion promoters from the organic coating into the conversion coating. Pope et. al<sup>(111)</sup>. also observed that precipitated chromate spherical particles had relatively high surface areas and were useful absorbents.

In order to investigate the effect of polymer coating thickness on the debonding strain and hence on the adhesion, samples pretreated in 0.12M/l  $\text{CrO}_3$  + 0.3M/l NaCl (L1) were powder coated to thicknesses of 55-65  $\mu\text{m}$  and 80-100  $\mu\text{m}$ . The results obtained from indentation debonding tests are shown in table 9.6 and figure 9.7. It can be seen from this figure that the thin coating (55-65  $\mu\text{m}$ ) is better bonded to the electrop- lated and hot-dip continuous galvanized samples when they are degassed after pretreatment. It is interesting to note in figure 9.7 that the sprayed sample which had the roughest surface showed an increased debonding strain with the thicker (80-100  $\mu\text{m}$ ) polymer coatings. A possible reason for this may be that due to the thickness of the polymer film, the peaks and valleys of the rough surface were covered adequately to provide a smooth continuous film surface (see figure 9.8). This smoothed continuous surface coupled with the degassing operation reduced or eliminated the possible weak points at the coating substrate

interface. However, the sprayed samples had a comparatively, low debonding strain. Surprisingly, the mechanical keying effect expected to be seen with the sprayed sample results did not occur. However it may be, as in the case of pull-off test, that the weakness of the sprayed zinc coating is responsible for the low bonding strain being obtained.

## 9.7 CONCLUSIONS

- (1) Results obtained from the three methods of adhesion test used were not directly comparable.
- (2) The indentation debonding test appears to give more reliable results.
- (3) The following deductions were made from the various tests:

### Cross-cut/peel test

- (i) There was no noticeable difference in adhesion between not-degassed and degassed samples.
- (ii) There was some evidence to suggest that shorter pretreatment times led to poorer adhesion.
- (iii) Adhesion decreased in the following order Spray, Electroplated, HDB, HDC.

### Pull-off test

- (i) For spray samples, failure occurred within the zinc coating.

(ii) The electroplated and HDC samples failed mostly at the glue/polymer interface.

(iii) Interpretation of the results was very difficult.

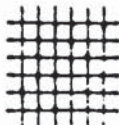
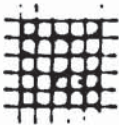


#### Indentation Debonding Test

(i) For a given substrate, the time of pretreatment and degassing after pretreatment only have a marginal effect on the peeling strain.

(ii) On average, the performance of the electroplated, HDC and HDB samples appeared to be the same whilst spray samples were significantly worse.

(iii) After the corrosion test, the peeling strain was smaller for all samples, and there was some evidence to indicate that samples degassed after pretreatment had marginally higher peeling strains.

TABLE 9.1 Classification of cross-cut/peel test results

Code	Description	Appearance of surface of cross-cut area from which flaking has occurred (example for six parallel cuts)
0	The edges of the cut are completely smooth; none of the squares of the lattice is detached.	
1	Detachment of small flakes of the coating at the inter-sections of the cuts. A cross-cut area not distinctly greater than 5% is affected.	
2	The coating has flaked along the edges and/or at the inter-sections of the cuts. A cross-cut area distinctly greater than 5%, but not distinctly greater than 15% is affected.	
3	The coating has flaked along the edges of the cuts partly or wholly in large ribbons, and/or it has flaked partly or wholly on different parts of the squares. A cross-cut area distinctly greater than 15%, but not distinctly greater than 35% is affected.	
4	The coating has flaked along the edges of the cuts in large ribbons and/or some squares have detached partly or wholly. A cross-cut area distinctly greater than 35%, but not distinctly greater than 65% is affected.	
5	Any degree of flaking that cannot even be classified by classification 4.	

**TABLE 9.2 Cross-cut tests**

Sample/pretreatment times	Classification of Results using code in TABLE 9.1	
	Not Degassed	Degassed
1/30	1	0
1/60	0	0
1/120	0	0
2/30	3	3
2/60	1	1
2/120	1	1
3/30	1	2
3/60	0	0
3/120	1	1
4/30	0	0
4/60	0	0
4/120	0	0

**TABLE 9.3 Classification of the nature of failure of pull-off adhesion test**

A	= Cohesive failure of substrate
A/B	= Adhesive failure between substrate and first coat
B	= Cohesive failure of first coat
B/C	= Adhesive failure between first and second coats
-/Y	= Adhesive failure between final coat and adhesive
Y	= Cohesive failure of adhesive

TABLE 9.4 Pull-off adhesion test results

Sample/ Classification using TABLE 9.3  
Time

	Not degassed		Degassed	
	Breaking Strength	Nature of Failure	Breaking Strength	Nature of Failure
	(MPa)	(%)	(MPa)	(%)
1/30	12.3	15 A/B, 85-/Y	13.4	20 A/B, 80-/Y
1/60	13.6	10 A/B, 90-/Y	14.1	15 A/B, 85-/Y
1/120	12.9	20 A/B, 80-/Y	11.5	25 A/B, 75-/Y
2/30	17.4	20 A/B, 80-/Y	18.7	30 A/B, 70-/Y
2/60	21.7	100 -/Y	21.3	100 -/Y
2/120	14.6	20 B, 80-/Y	19.4	2 A/B, 98 -/Y
3/30	13.1	80 A/B, 20-/Y	20.1	10 A/B, 90 -/Y
3/60	18.5	10 A/B, 80-/Y	25.5	70 A/B, 30 -/Y
3/120	16.6	50 A/B, 50-/Y	18.0	5 A/B, 95 -/Y
4/30	21.0	100 A	14.7	100 A
4/60	20.3	100 A	18.6	100 A
4/120	18.9	100 A	19.8	100 A

**TABLE 9.5 Indentation debonding test results before corrosion test**

Sample	a (mm)	b (mm)	Strain
1B/30	0.15	0.40	2.58
1B/60	0.16	0.36	3.51
1B/120	0.15	0.36	3.24
1C/30	0.16	0.40	2.77
1C/60	0.14	0.41	2.28
1C/120	0.17	0.38	3.85
2B/30	0.18	0.42	2.87
2B/60	0.16	0.41	2.63
2B/120	0.15	0.41	2.45
2C/30	0.15	0.39	2.72
2C/60	0.15	0.38	2.88
2C/120	0.16	0.38	3.10
3B/30	0.17	0.39	3.16
3B/60	0.16	0.39	2.93
3B/120	0.17	0.38	3.35
3C/30	0.18	0.42	2.87
3C/60	0.15	0.39	2.72
3C/120	0.18	0.39	3.40
4B/30	0.13	0.50	1.45
4B/60	0.15	0.51	1.59
4B/120	0.16	0.50	1.75
4C/30	0.19	0.52	1.93
4C/60	0.16	0.51	1.69
4C/120	0.15	0.50	1.65

**TABLE 9.6 Indentation debonding test after corrosion test**

Sample	a (mm)	b (mm)	Strain
1B/30	0.17	0.49	1.94
1B/60	0.15	0.46	1.94
1B/120	0.14	0.44	1.98
1C/30	0.15	0.48	1.79
1C/60	0.14	0.47	1.74
1C/120	0.17	0.42	2.68
2B/30	0.13	0.47	1.63
2B/60	0.14	0.46	1.82
2B/120	6.13	6.41	2.12
2C/30	0.14	0.44	1.98
2C/60	0.14	0.44	1.98
2C/120	0.16	0.44	2.67
3B/30	0.15	0.52	1.53
3B/60	0.15	0.39	2.72
3B/120	6.14	0.40	2.40
3C/30	0.15	0.39	2.72
3C/60	0.15	0.39	2.72
3C/120	0.14	0.40	2.40
4B/30	0.15	0.55	1.38
4B/60	0.14	0.54	1.34
4B/120	0.15	0.55	1.38
4C/30	0.15	0.55	1.38
4C/60	0.15	0.55	1.38
4C/120	0.15	0.53	1.48

**TABLE 9.7 Effect of organic powder coating film thickness on peeling strain**

Sample	Peeling strain 55-65 $\mu$		80-100 $\mu$	
	Not degassed	Degassed	Not degassed	Degassed
Elect	3.24	3.85	2.91	2.98
HDC	2.45	3.10	2.95	2.87
HDB	3.35	3.40	2.95	3.54
Sprayed	1.75	1.65	2.04	2.11

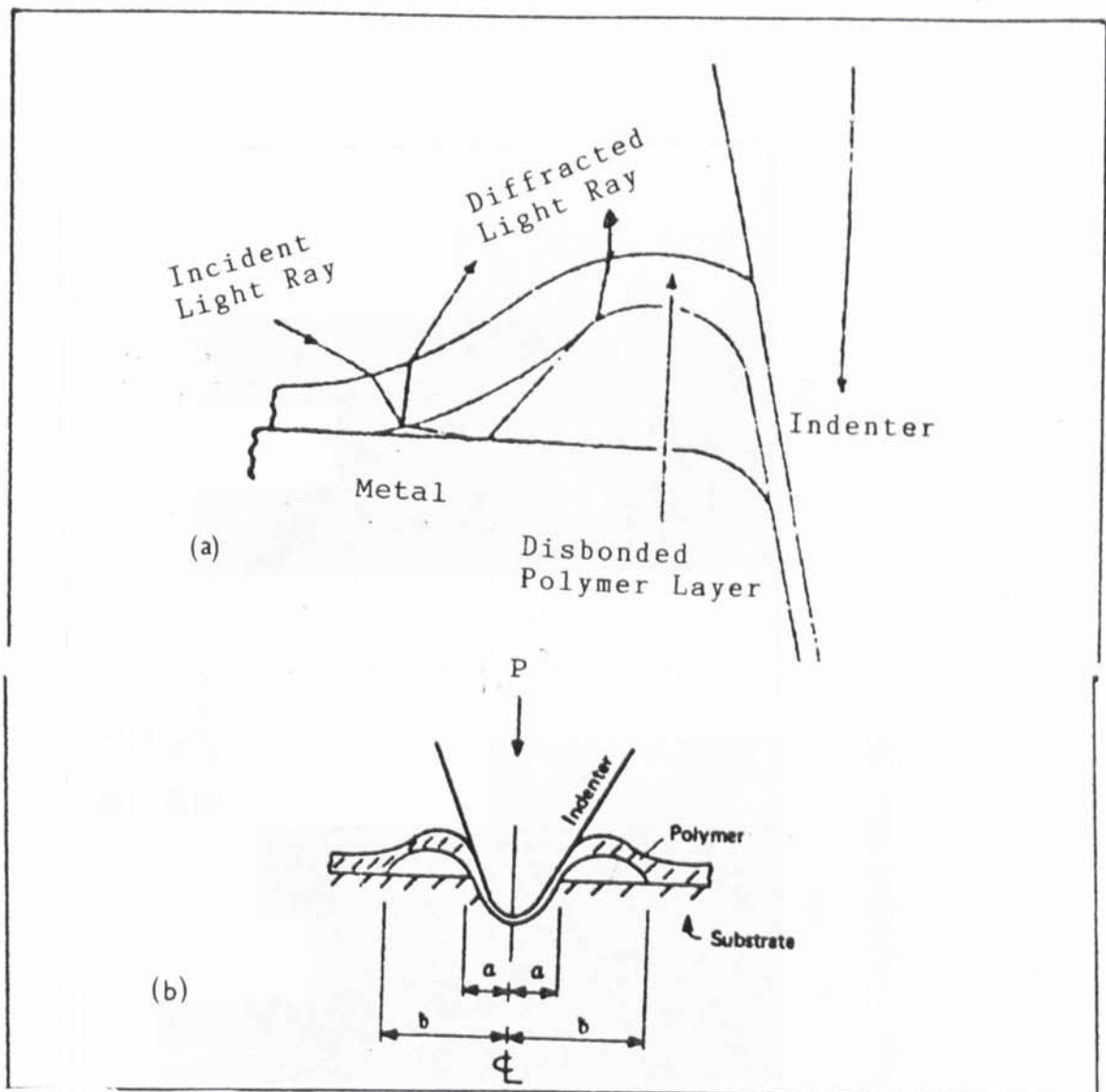


Figure 9.1 (a) Schematic diagram for the case of indentation debonding of a transparent film on metal<sup>151</sup>  
 (b) Illustration of indenter radius ( $a$ ) and debonded radius ( $b$ )

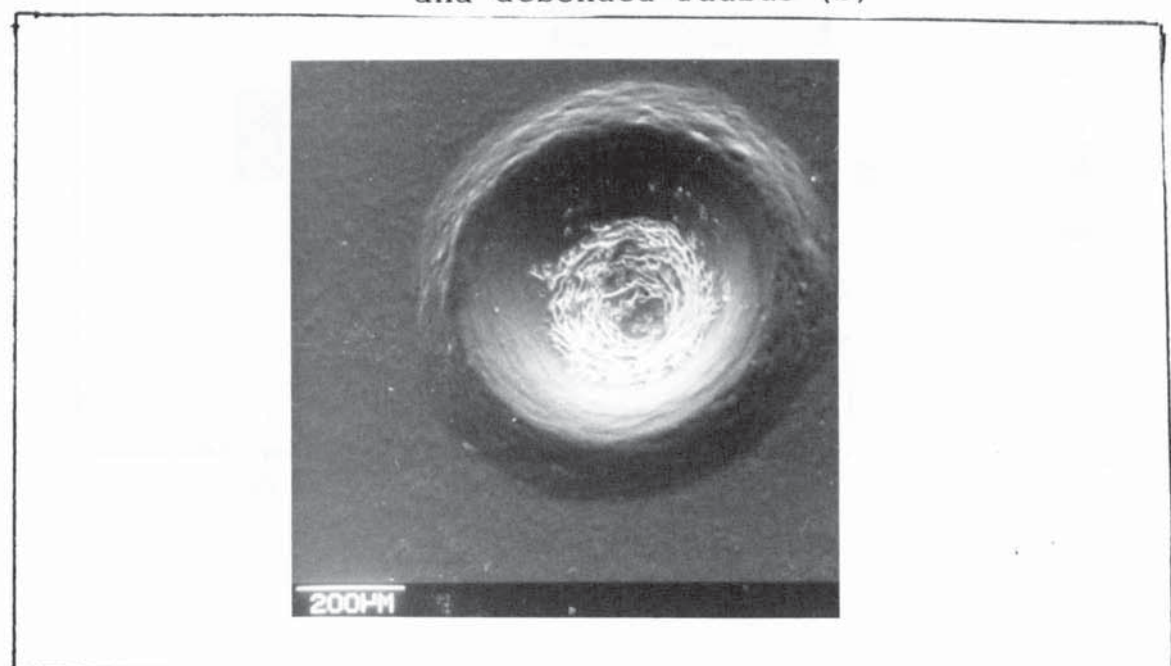


Figure 9.2 Micrograph of an indent produced in polyester film on zinc

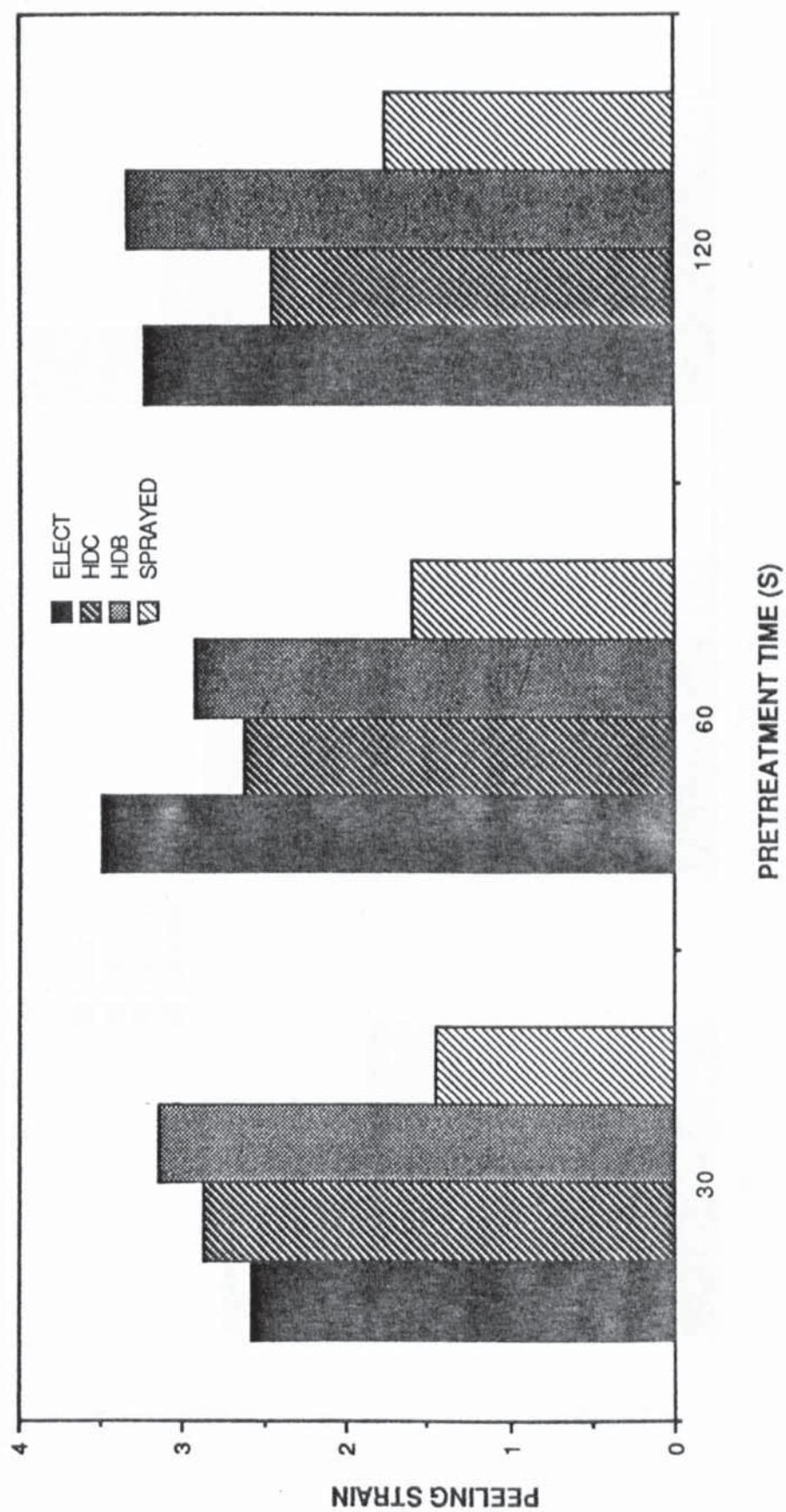


Figure 9.3 peeling strain vs time for samples not degassed

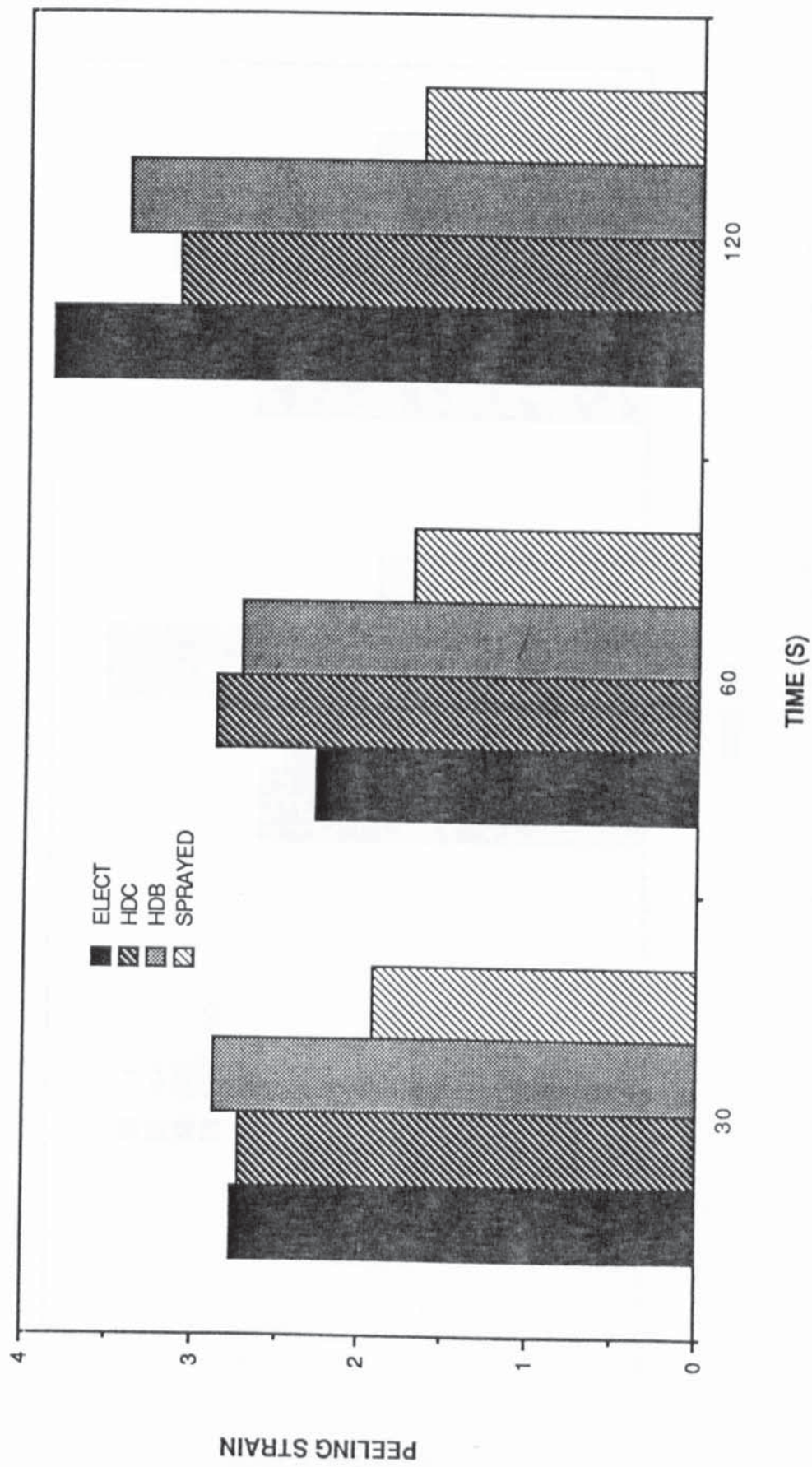


Figure 9.4 Comparison of peeling strain vs time for degassed samples

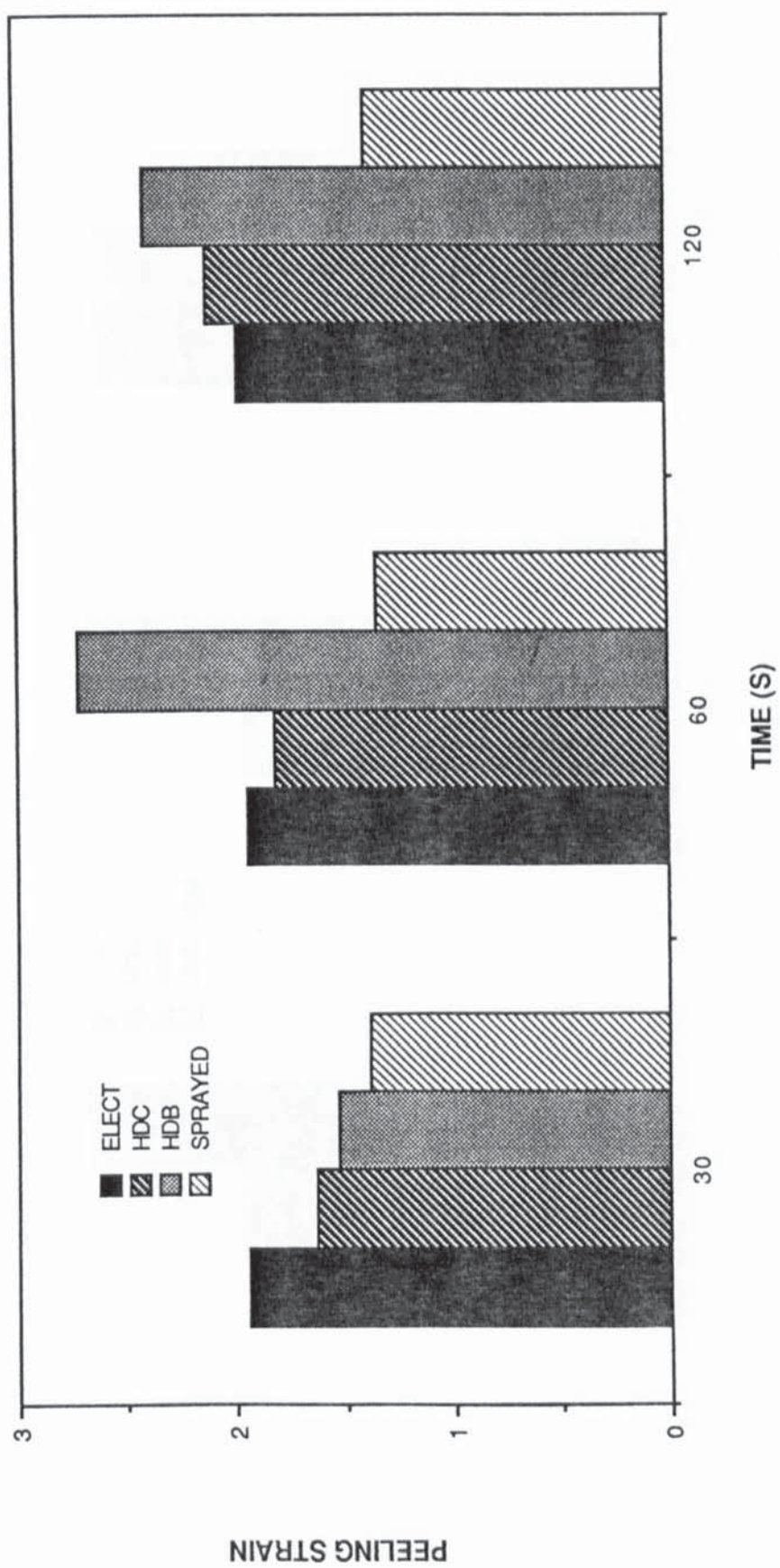


Figure 9.5 Comparison of peeling strain vs time for samples no degassed (Peeled after 700hours in acetic 5% salt spray corrosion test)

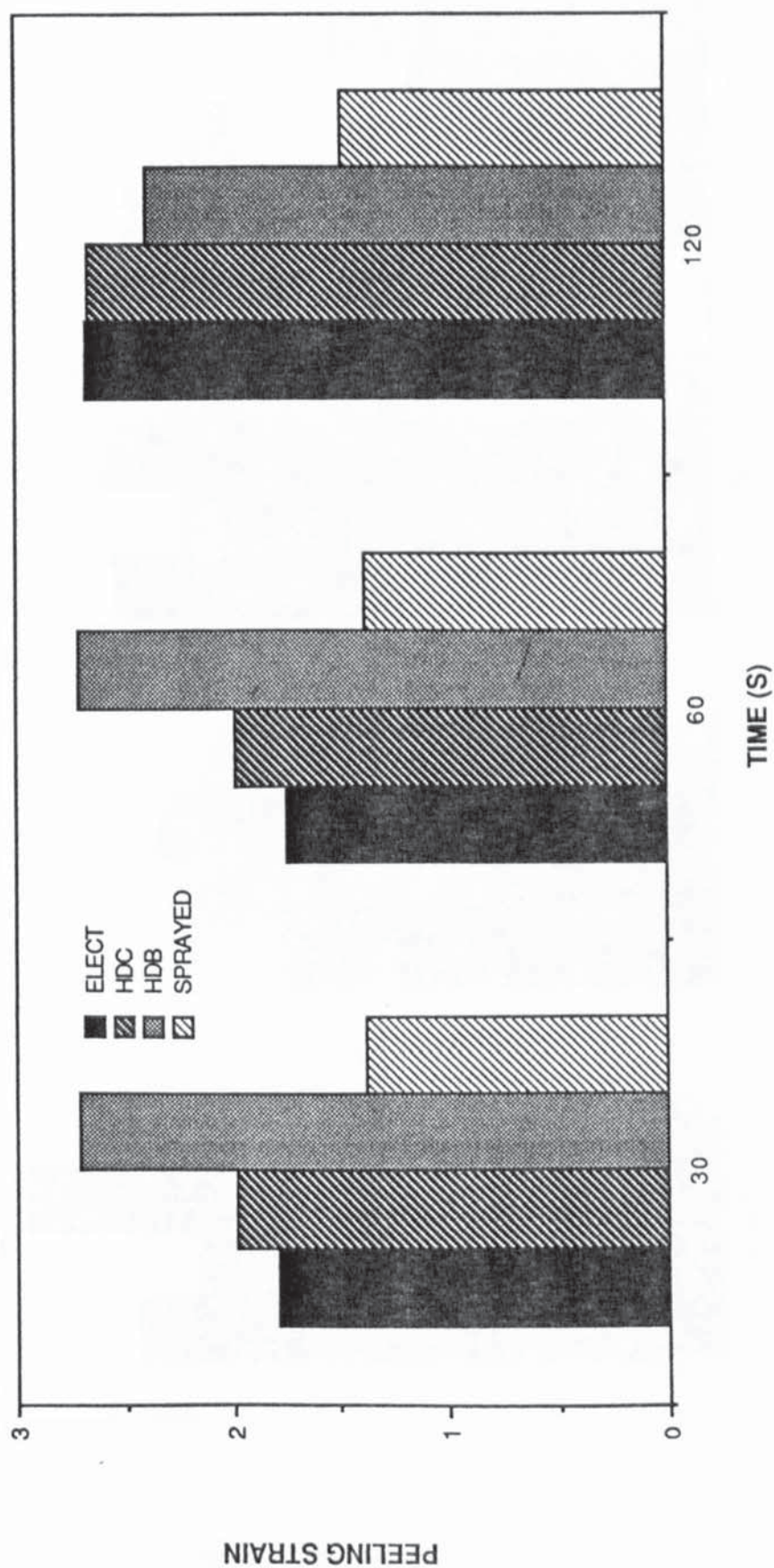


Figure 9.6 Comparison of peeling strain vs time for samples degassed (peeled after 700 hours in acetic 5% salt spray corrosion test)

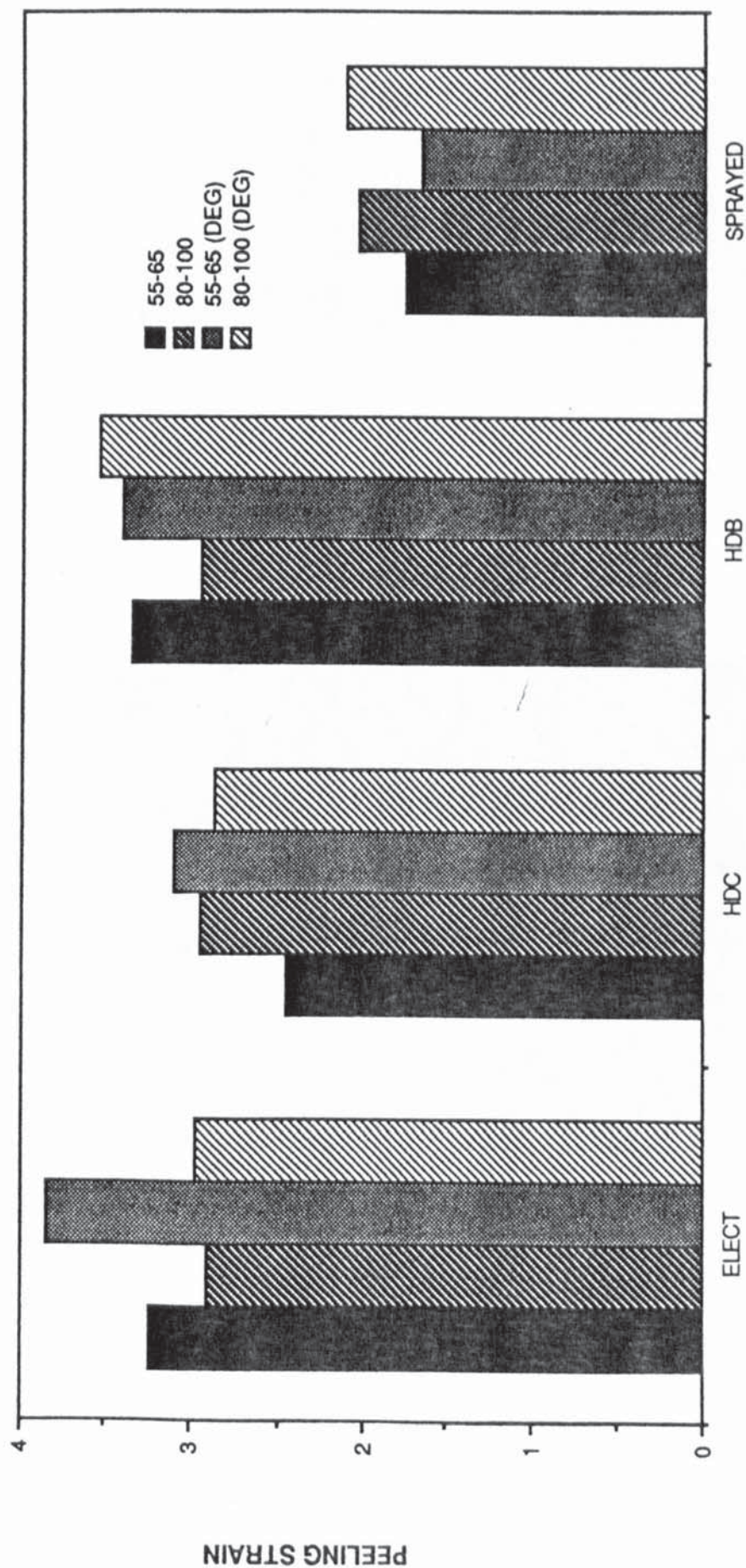
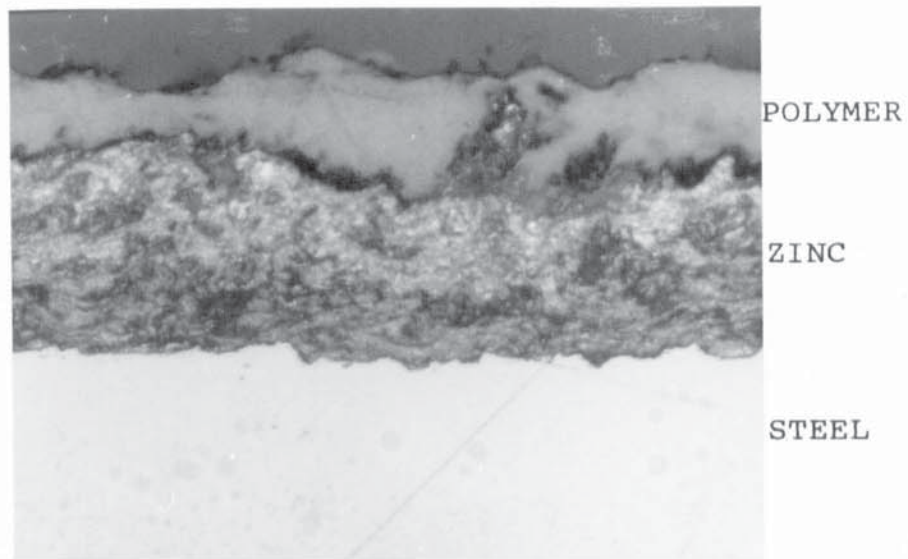
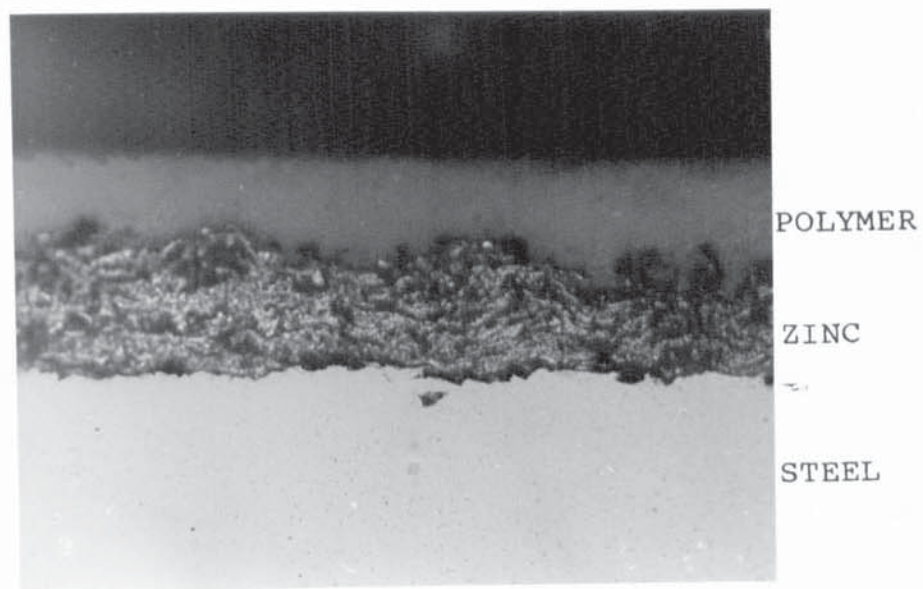


Figure 9.7

Effect of polymer coating thickness on peeling strain (pretreated in 0.12M/l  $\text{CrO}_3$  + 0.3 M/l NaCl solution for 120s and degassed)



(a)



(b)

Figure 9.8 Powder organic coating on zinc sprayed samples  
 (a) Thin film (55 - 65  $\mu$ )  
 (b) Thick film (80-100  $\mu$ )

## 10. CORROSION TESTING OF THE CONVERSION COATED ZINC AND THE DUPLEX POLYMER - ZINC COATINGS ON STEEL

### 10.1 INTRODUCTION

The corrosion resistance of the duplex zinc - polymer coatings on steel depends not only on the properties and thickness of the zinc and polymer coatings but also on the zinc coating surface preparation .

It is known that zinc coatings can be made more corrosion resistant by treatment in a chromic acid solution, thus forming a chromate conversion coating on the zinc surface. Depending on the chromating process used, this leads to retention of the decorative appearance over long periods of time and significantly increases corrosion resistance compared with untreated zinc coatings. However, this is achieved only if the formulations used for chromating are tailored precisely to the type of zinc coating, and their compositions are kept constant<sup>(157)</sup>. The effect of individual bath parameters on corrosion protection properties has not yet been defined exhaustively, but pH value and chromate content are among the most important limiting variables.

To enhance the corrosion resistance of the duplex Zn - polymer coatings on steel, the zinc coating is usually conversion coated before applying the powder coating. However, the mechanism of corrosion protection by different chromate films on various zinc coatings is yet

to be documented. It was decided to study, electrochemically, the corrosion rate of conversion coated samples and to evaluate the corrosion resistance of both conversion coated and powder coated samples using accelerated, acetic acid, 5% salt spray test.

## 10.2 CORROSION RATE STUDIES OF CONVERSION COATED SAMPLES

The corrosion rates of electroplated (1), hot-dip continuous (2) and hot-dip batch (3) galvanized and zinc sprayed steel (4) samples conversion coated using Alocrom 100 (C1), chrometan (C2), 0.12M/l  $\text{CrO}_3$  + 0.3/1 NaCl (L1), and NaOH (L17) pretreatment solutions were determined electrochemically in acetic acid, 5% salt solution. This was done by using the linear polarisation technique. The corrosion resistance of chromated (0.12M/l  $\text{CrO}_3$  + 0.3M/l NaCl (L1)) and alkaline treated (NaOH L17)) samples was compared using the accelerated acetic acid, salt spray technique.

The results of the electrochemical corrosion rate tests for the conversion coated samples are shown in table 10.1 and figures 10.1 (a) and (b) and 10.2. Figures 10.1 (a) and (b) are histograms of the corrosion rate ( $i_{\text{corr}}$ ) and corrosion in mm/year, respectively, for the different samples, in acetic acid, 5% salt solution. Figure 10.2 shows the corresponding polarization resistance ( $R_p$ ) values. Table 10.2 is a summary of the results obtained for the same set of samples when

subjected to the accelerated acetic acid 5% salt spray test.

### 10.3 CORROSION TESTING OF DUPLEX SAMPLES

The salt spray tests and rest potential measurements, on powder coated samples, were carried out as described in chapter 3. The samples for rest potential measurements were cut to measure 5 cm x 2.5 cm, pretreated in 0.12M/l  $\text{CrO}_3$  + 0.3M/l NaCl (L1) and powder coated.

The results of the open-potential measurement are shown in table 10.3. Optical macrographs of the accelerated acetic acid 5% salt spray tested samples and the cross-section of sprayed samples, before and after testing, are shown in figures 10.3 and 10.4 respectively. The estimated extent of blistering noticed on samples, pretreated in 0.12M/l  $\text{CrO}_3$  + 0.3M/l NaCl (L1) and powder coated, after the accelerated test are shown in figure 10.5.

### 10.4 OBSERVATIONS DURING THE ACETIC ACID 5% SALT SPRAY TEST OF THE DUPLEX SAMPLES

(a) After about 112 hours of test, a few red rust spots were noticed on the face of electroplated pannels and significant amounts of zinc corrosion products were also observed on the hot-dip continuous galvanized pannels.

(b) There were red rust spots all over the electrop-lated samples after about 400 hours of test. There was

severe lateral rust along the diagonal scratches of both degassed and not degassed electroplated pannels chromated for 60 and 120 secs respectively.

(c) White corrosion was not detected until after about 520 hours of test in the case of hot-dip batch and the sprayed samples.

(d) After about 500 hours of test, the extent of rust on the electroplated panels was so bad that they had to be removed from the cabinet.

The results of the final visual examination can be briefly summarised as follows:

(i) The shorter the chromating time, the more corrosion occurred (see figure 10.5).

(ii) For samples chromated for times over 1 min, there were no appreciable differences in the amount of corrosion between the degassed and not degassed pannels, whilst for times less than 1 min and degassed samples were more corroded.

(iii) The four different sets of specimens follow approximately the same trends.

(iv) The types of corrosion observed include:

(a) Red rust and lateral corrosion along the scratch lines; this was mostly associated with the electroplated samples.

(b) Blistering, and anodic undermining, mostly associated with electroplated, HDC and HDB galvanized pannels (see figures 10.3 c & d).

(c) Spot rusting was found on the surfaces of the

HDB and particularly on the sprayed samples (figure 10.3 d & e).

#### 10.4 DISCUSSION

##### 10.4.1 CONVERSION COATED SAMPLES

The corrosion rates, plotted as histogram of  $i_{\text{corr}}$  and mm/year, are shown in figures 10.1 and 10.2. Corrosion resistance of HDB galvanized samples appeared to be the best for all the four pretreatment processes used whilst the sprayed samples were the worst. In the case of sprayed samples, it is thought that the surface roughness is responsible since the conversion coating would not have adequately covered the peaks of the coating, a situation which would lead to very easy formation of local corrosion cells all over the surface.

Disregarding the sprayed sample, generally, Alocrom 100 pretreatment (C1) appeared to be the worst while the rest of the pretreatments (C2, L1, L17) were found to be about the same.

Detailed assessment however tends to suggest that, NaOH solution (L17) is the most effective pretreatment for HDB, 0.12M/l  $\text{CrO}_3$  + 0.3M/l NaCl (L1) the best pretreatment for HDC whilst the chrometan pretreatment (C2) is the best for the electroplated sample. Alocrom 100 (C1) and chrometan (C2) appeared to have given equal protection to the sprayed sample. Assessment in this manner tends to suggest that different zinc coatings have different optimum pretreatment processes.

The results obtained from the salt spray cabinet tests are shown in table 10.2. It can be seen from this table that there is no difference between the samples cleaned only and samples treated in NaOH in the times to notice white rust. This suggests that there is no protective film formed in the NaOH solution. It can be seen that chromate pretreatment (0.12M/l  $\text{CrO}_3$  + 0.3M/l NaCl (L1)) increased the times to notice the white rust by as much as 4. The same is applicable to the times to notice red rust. Generally, the time to notice red rust increased with increased zinc coating thickness.

These results appear to be contradictory to those obtained from the electrochemical tests. Although the occurrence of red-rust would, among other factors, depend on the zinc coating thickness the appearance of white rust would directly depend on the type of the conversion coating. On the basis of these results, it would be necessary to take in to account the method of carrying out the corrosion test before concluding whether a coating is corrosion resistance or not.

However, it is interesting to observe the high improvement in corrosion resistance which 0.12M/l  $\text{CrO}_3$  + 0.3M/l NaCl pretreatment process had provided on all the samples; remembering that passivation was not obtained in this solution when zeta and zinc samples were subjected to potentiodynamic anodic polarisation (see Chapter 6).

This means that chromate conversion coatings do not require the formation of a passive film layer over the substrate in order to reduce corrosion. This would be expected since chromate films contain corrosion inhibitors

#### 10.4.2 CONVERSION AND POWDER COATED (DUPLEX) SAMPLES

The rest potentials of all the samples, as can be seen in table 10.3, move towards a more noble potential with time. The lower noble initial potential of the HDC, HDB and spray compared with electroplated means that the former samples provide more sacrificial corrosion protection to the steel. As the time of immersion increased, corrosion products covered the surface, providing more corrosion resistance hence the movement of the rest potential or corrosion potential in the more noble direction. Alternatively, the movement towards more noble potential could be an indication of an increasing cathodic/anodic surface area ratio and this indicates that oxygen and water are penetrating the polymer coating to the metal/coating interface. This may imply that alkaline conditions as a result of the oxygen reduction reaction are developing locally at the metal/coating interface and delamination may start to take place. This was evidenced by the popping up of the polymer coating around the edges of the samples during the latter part of the test.

Figure 10.5 shows the relative areas of blistering

or disbondment for the samples cleaned only and samples conversion coated in 0.12M/l  $\text{CrO}_3$  + 0.3M/l NaCl (L1) solution for 30s and 120s, after 700 hours in the salt spray cabinet. Assessment of the blistering or disbonded area was made visually, the maximum, in figure. 10.5 representing about 20% of the total area.

The greatest area of disbondment occurred on the samples which had not received a conversion coating treatment. However, the area of disbondment decreased when a chromating treatment was used and decreased further with increased chromating time.

In all three cases the sprayed zinc substrate showed the least disbondment persumably related in some way to the initial roughness of the surface. The continuous hot-dipped sample showed a high area of disbondment with no conversion coating, but this did reduce with chromating. In the case of the batch hot-dipped sample, chromating for 30 secs had little effect, compared to no treatment.

It is known that, an organic coating protects a metal substrate from corroding by two main mechanisms:

- (a) serving as a barrier to the environment and
- (b) serving as a reservoir for corrosion inhibitors that assist the surface in resisting attack. The barrier properties of the coating are improved by increased thickness, by the presence of pigments and fillers that increase the diffusion path for water and

oxygen, and by the ability to resist degradation. The effect of reduced polymer thickness on corrosion resistance is shown in 10.4 (a) and (b). It can be seen that weak points for penetration of corrosion reactants have been created at peaks on the zinc sprayed coating. No doubt, pinholing would aggravate this phenomenon. The pitting that occurred on the HDB samples is thought to be due to both the surface roughness and contamination.

#### 10.5 CONCLUSIONS

- (1) The tendency of the duplex polymer-zinc coating on steel to corrode is a function of:
  - (a) The nature of the substrate eg zinc coating surface roughness, thickness, etc
  - (b) The characteristics of the interfacial region between the coating and the substrate eg type and nature of pretreatment.
  - (c) The nature and thickness of the polymer coating.
- (2) The method of corrosion resistance determination has a major influence on the results obtained.
- (3) The results from the acetic acid, 5% salt spray test show that different types of corrosion were associated with different types of substrate surface eg blistering and anodic undermining with smooth surfaces, and pitting or spot rusting with rough surfaces.
- (4) Chromate pretreatment gives better corrosion resistance than alkali pretreatment.

(5) There is evidence, although not conclusive, to suggest that different zinc coatings require different pretreatments to attain optimum corrosion resistance

TABLE 10.1 Results of electrochemical corrosion rate tests on conversion coated samples

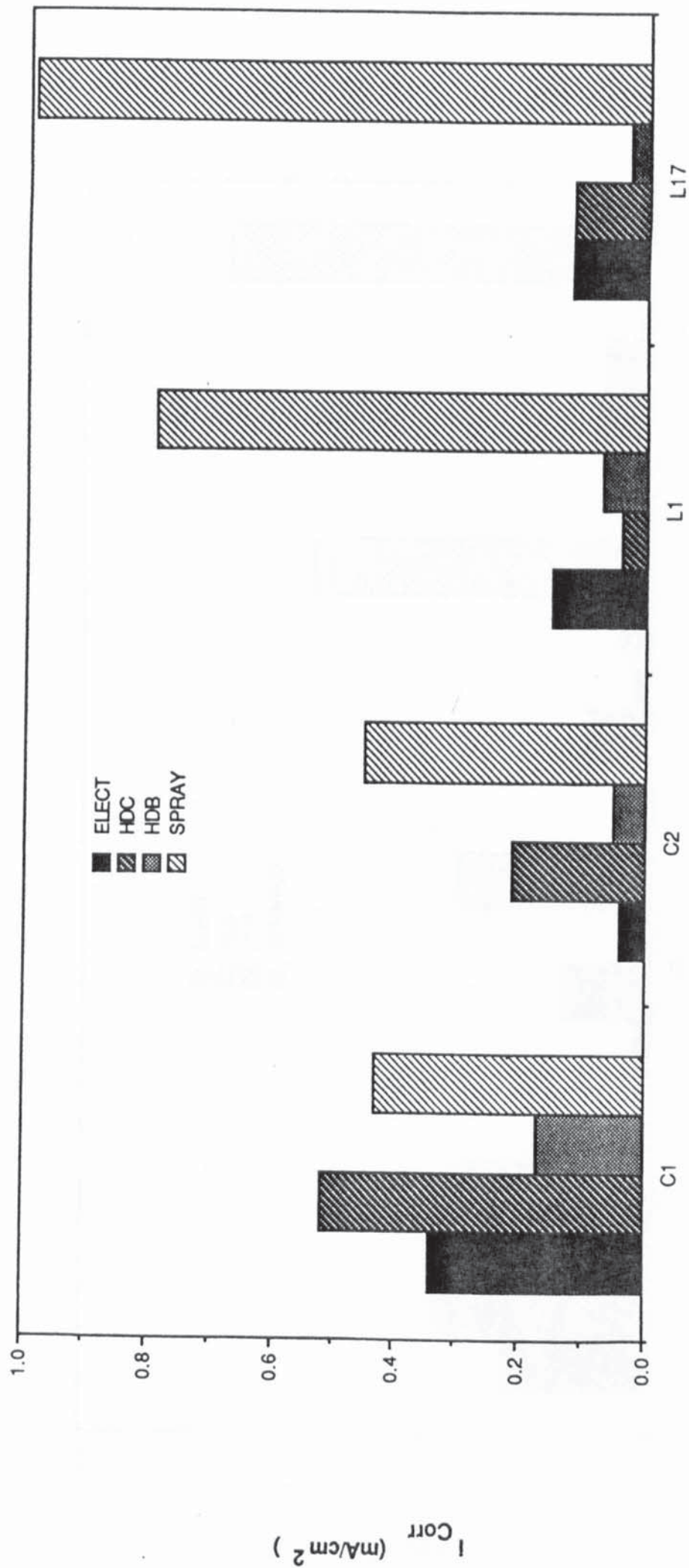
Sample/ solution	RP x 10 <sup>2</sup>	E <sub>Corr</sub> (V)	i <sub>Corr</sub> (mA/cm <sup>2</sup> )	(mm/y)
1/C1	1.27	-1.03	0.34	5.10
1/C2	11.50	-0.98	0.04	0.57
1/L1	2.90	-1.02	0.15	2.24
1/L17	3.45	-1.04	0.12	1.87
2/C1	0.84	-1.03	0.52	7.70
2/C2	2.11	-0.96	0.21	3.10
2/L1	10.35	-1.01	0.04	0.62
2/L17	3.68	-1.00	0.12	1.63
3/C1	4.06	-1.04	0.17	1.59
3/C2	9.14	-0.95	0.05	0.71
3/L1	6.12	-1.02	0.07	1.10
3/L17	13.82	-1.01	0.03	0.47
4/C1	1.02	-1.02	0.43	6.41
4/C2	0.97	-1.02	0.45	6.71
4/L1	0.55	-1.01	0.79	11.88
4/L17	0.44	-1.03	0.99	14.88

TABLE 10.2 Results of acetic 5% salt spray test on conversion coated samples

Sample	Time to notice white rust (hrs)			Time to notice red rust (hrs)		
	cleaned only	treated in NaOH	treated in CrO <sub>3</sub> + NaCl	cleaned only	treated in NaOH	treated in CrO <sub>3</sub> + NaCl
Elect	15	20	41	20	20	114
HDC	40	41	160	161	161	558
HDB	41	41	160	161	165	684
Spray	40	40	165	684	554	700+

TABLE 10.3 Rest potential of powder coated samples  
immersed in 5% NaCl (acetic) solution  
(vs S.C.E)

Time (Days)	Elect		HDC		HDB		Sprayed	
	Not deg	deg	Not deg	deg	Not deg	deg	Not deg	deg
0	0.83	0.92	1.02	0.99	1.0	0.98	1.06	1.06
5	0.83	0.81	1.02	0.99	1.0	0.98	1.05	1.05
10	0.83	0.79	1.00	0.98	0.99	0.99	1.04	1.03
15	0.84	0.83	0.96	0.98	0.99	0.96	1.04	1.03
20	0.82	0.81	0.96	0.97	0.96	0.94	1.03	0.13
25	0.79	0.70	0.96	0.95	0.89	0.90	1.00	1.01
30	0.70	0.68	0.95	0.94	0.86	0.87	0.98	0.98
35	0.59	0.60	0.92	0.93	0.81	0.79	0.96	0.96
40	0.56	0.55	0.85	0.87	0.76	0.72	0.94	0.95



SOLUTION

Figure 10.1 (a) Comparison of corrosion current of samples immersed in acetic acid salt spray solution after treatment in different pretreatment solutions

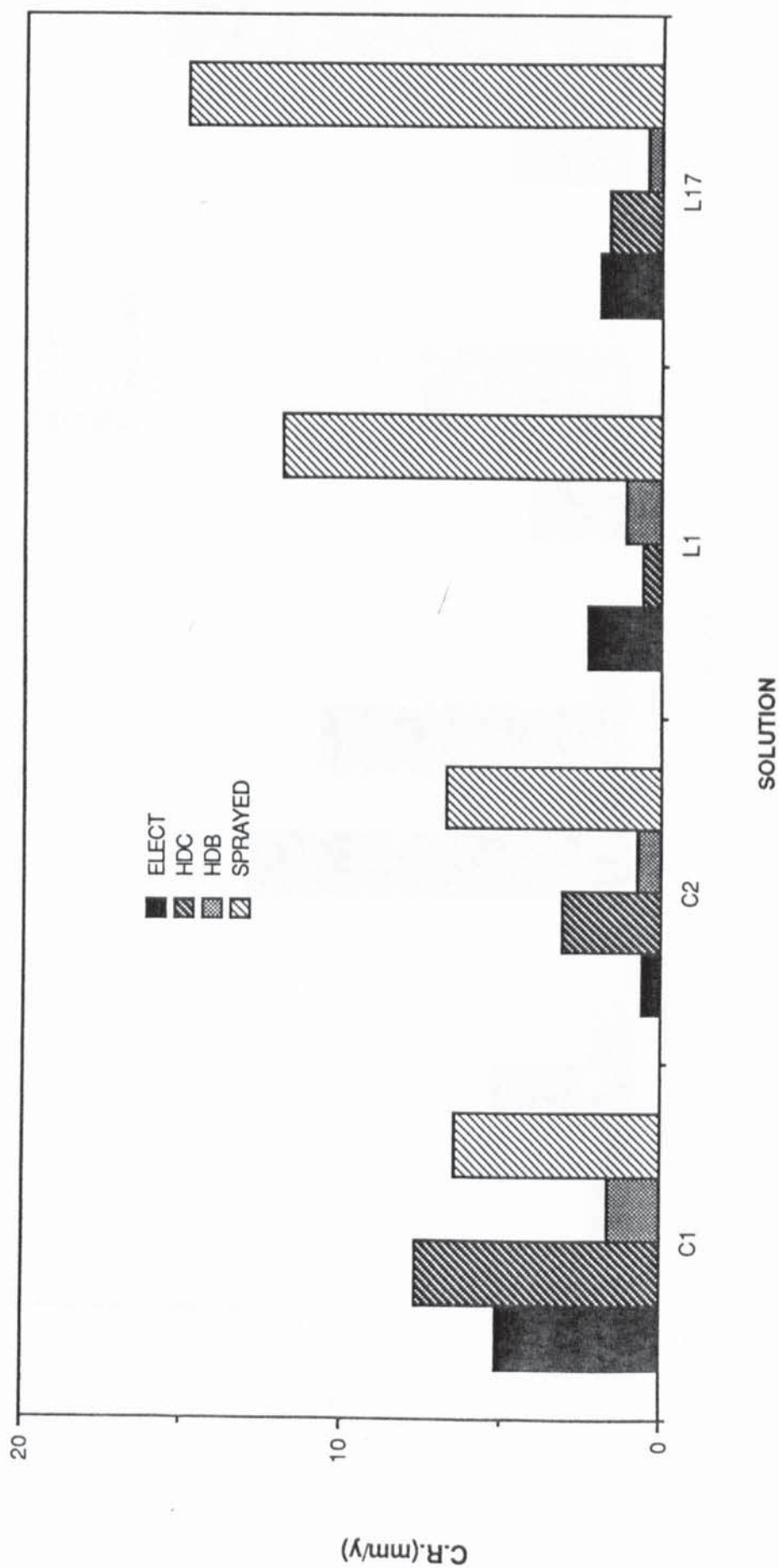


Figure 10.1 (b) Comparison of corrosion rate in mm/yr. of samples immersed in acetic acid salt spray solution after treatment in different pretreatment solutions

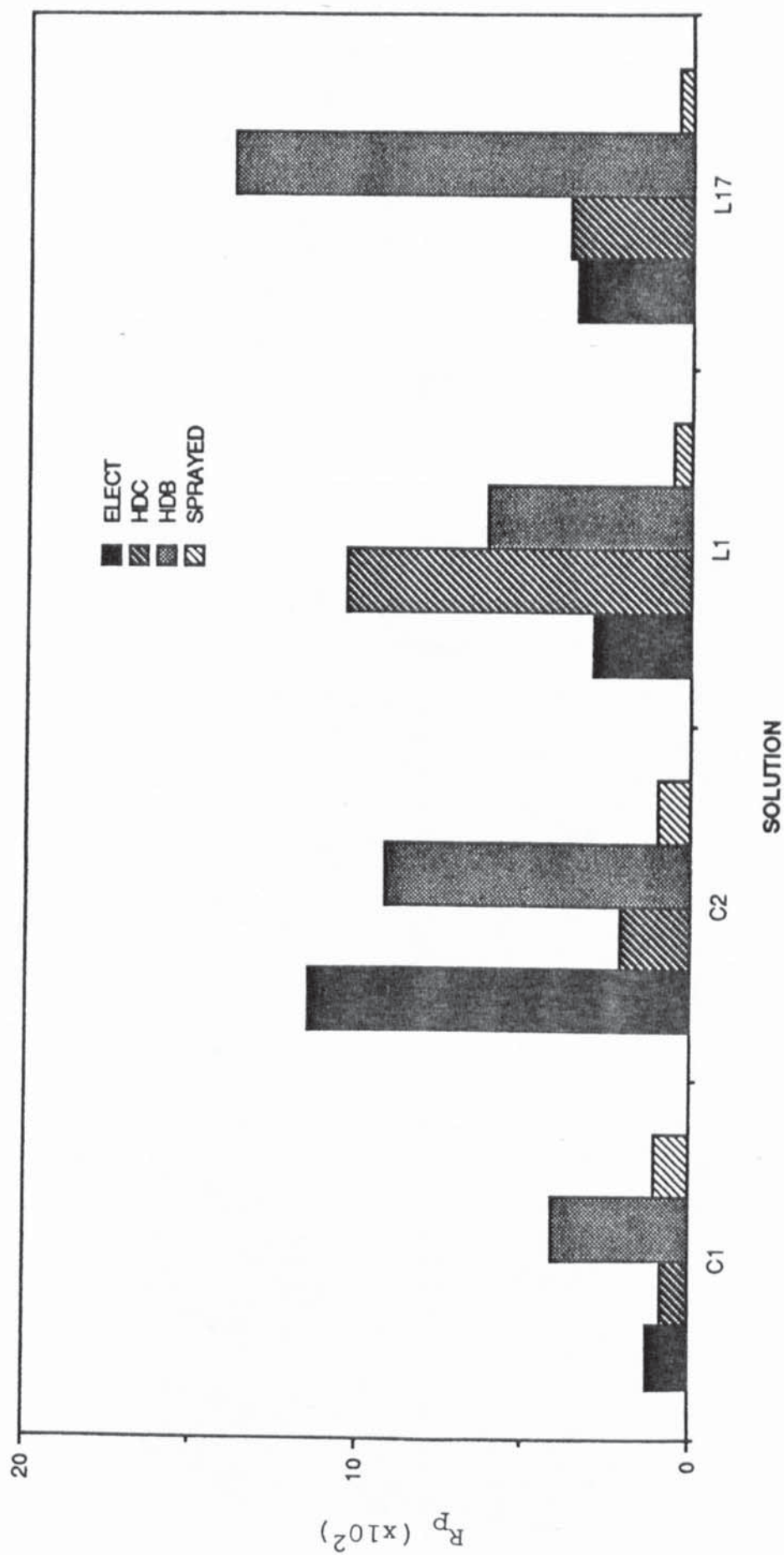
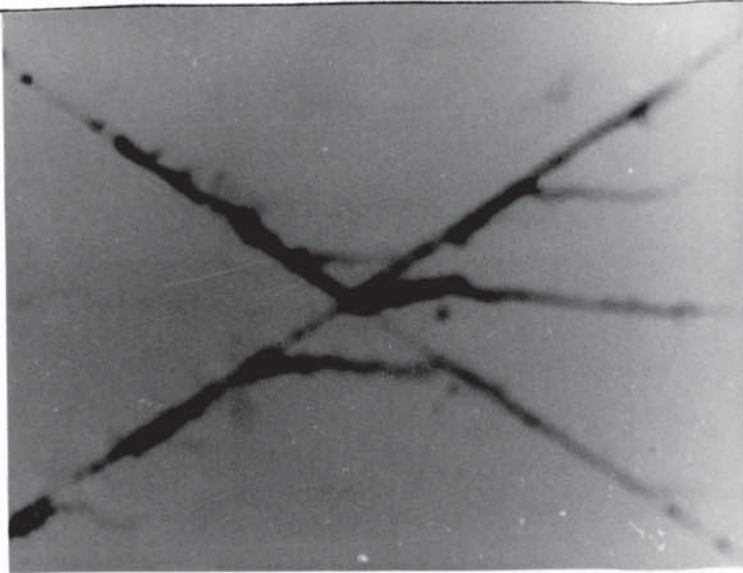
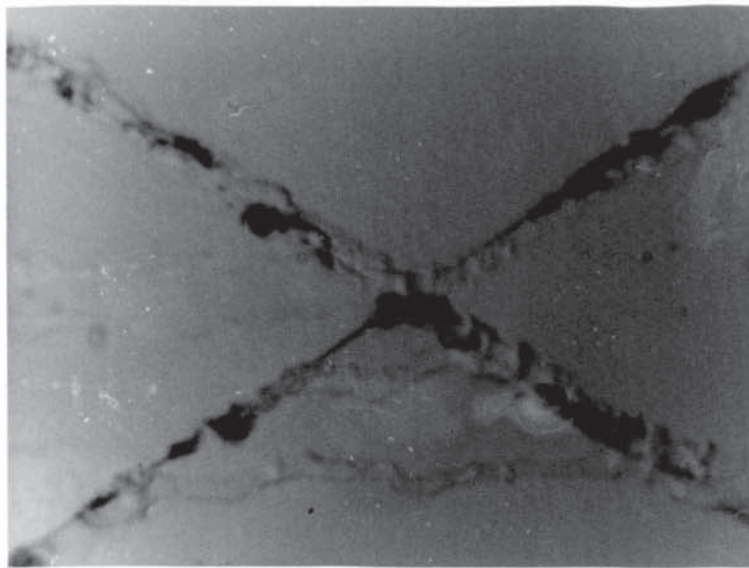


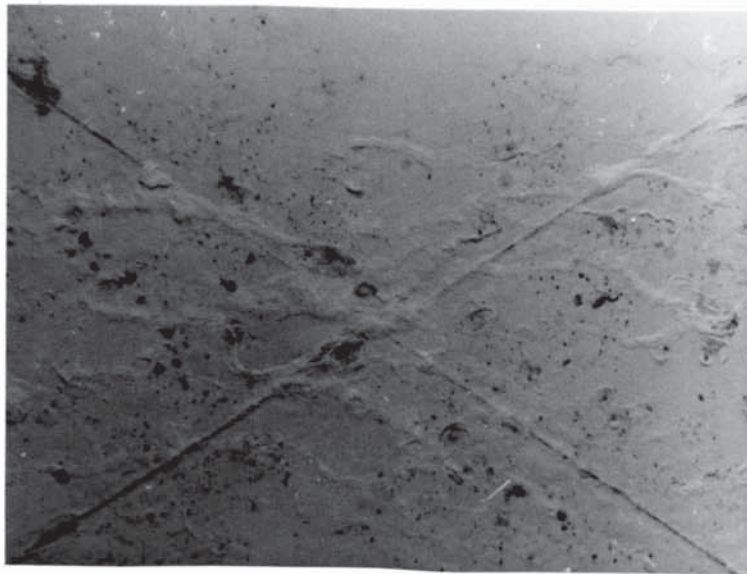
Figure 10.2 Comparison of polarisation resistance ( $R_p$ ) of samples immersed in acetic acid salt spray solution after treatment in different pretreatment solutions



(a) ELECTROPLATE

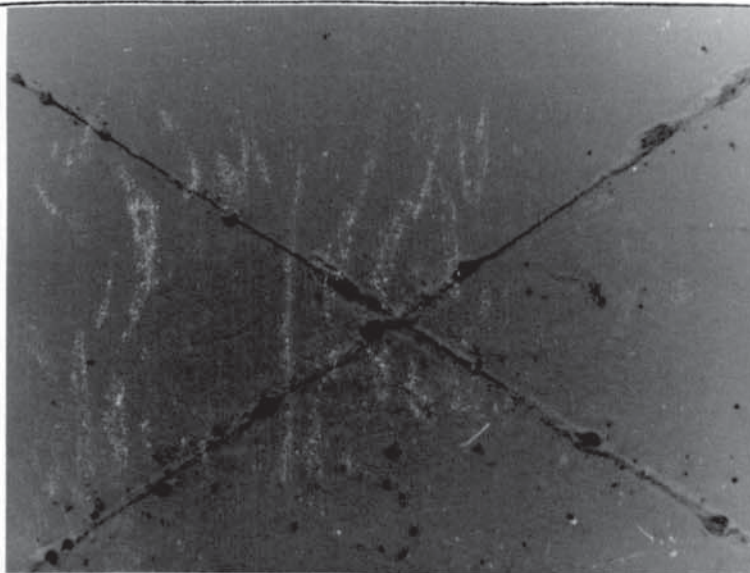


(b) HDC

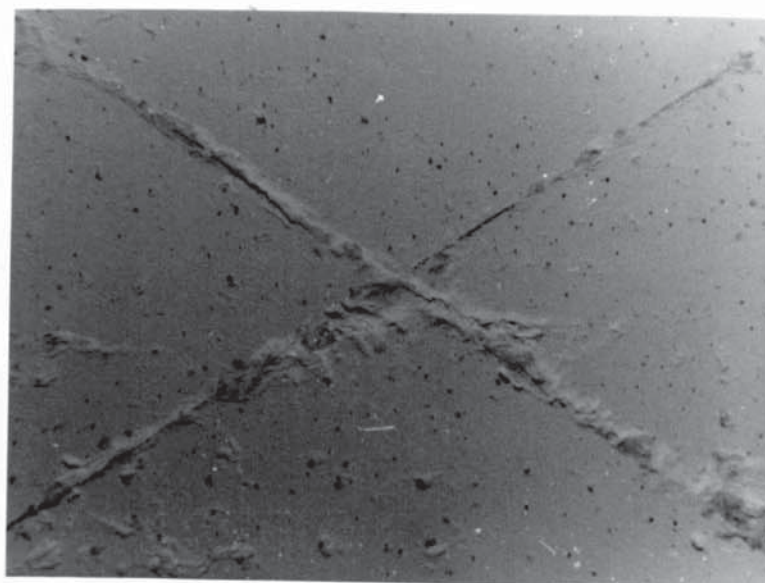


(c) HDB (30 seconds)

Figure 10.3 Optical macrographs showing the appearance of the significant face of the acetic 5% salt spray corrosion tested (for 700 hours) pannels (a - e)

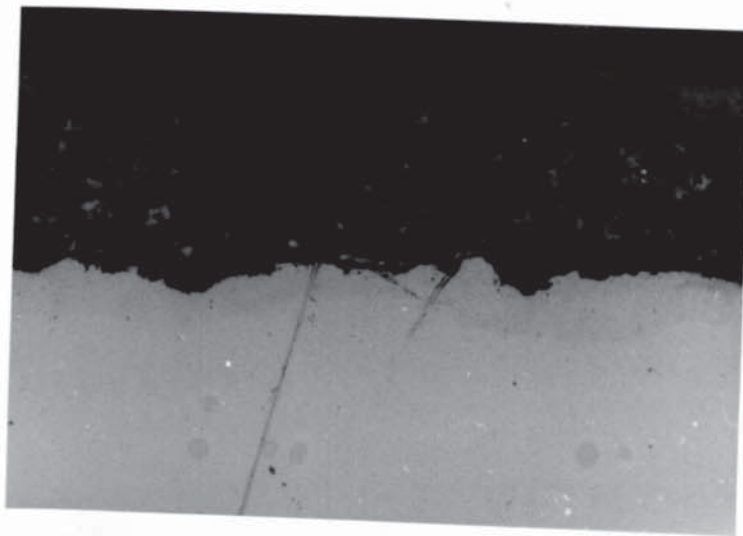


(d) HDB (120 seconds)

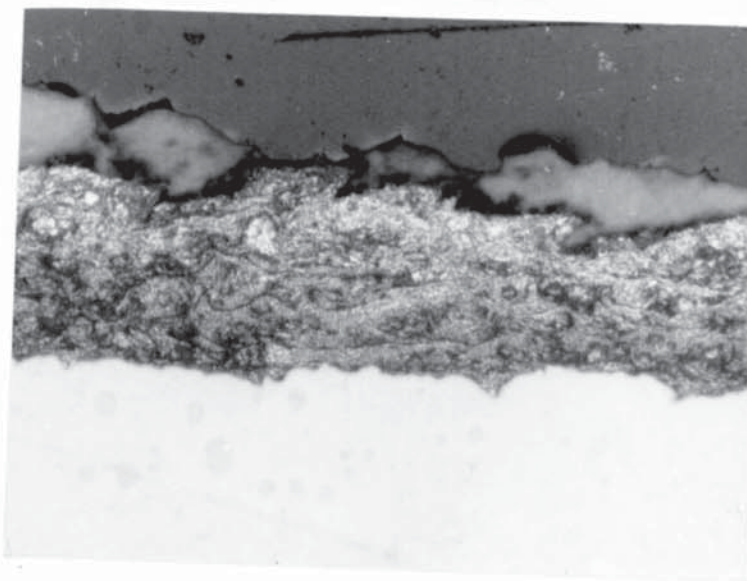


(e) SPRAY)

Figure 10.3 continued



(a)



(b)

Figure 10.4 Optical micrographs showing the appearance of powder coated zinc sprayed sample cross-section before (a) and after (b) corrosion test

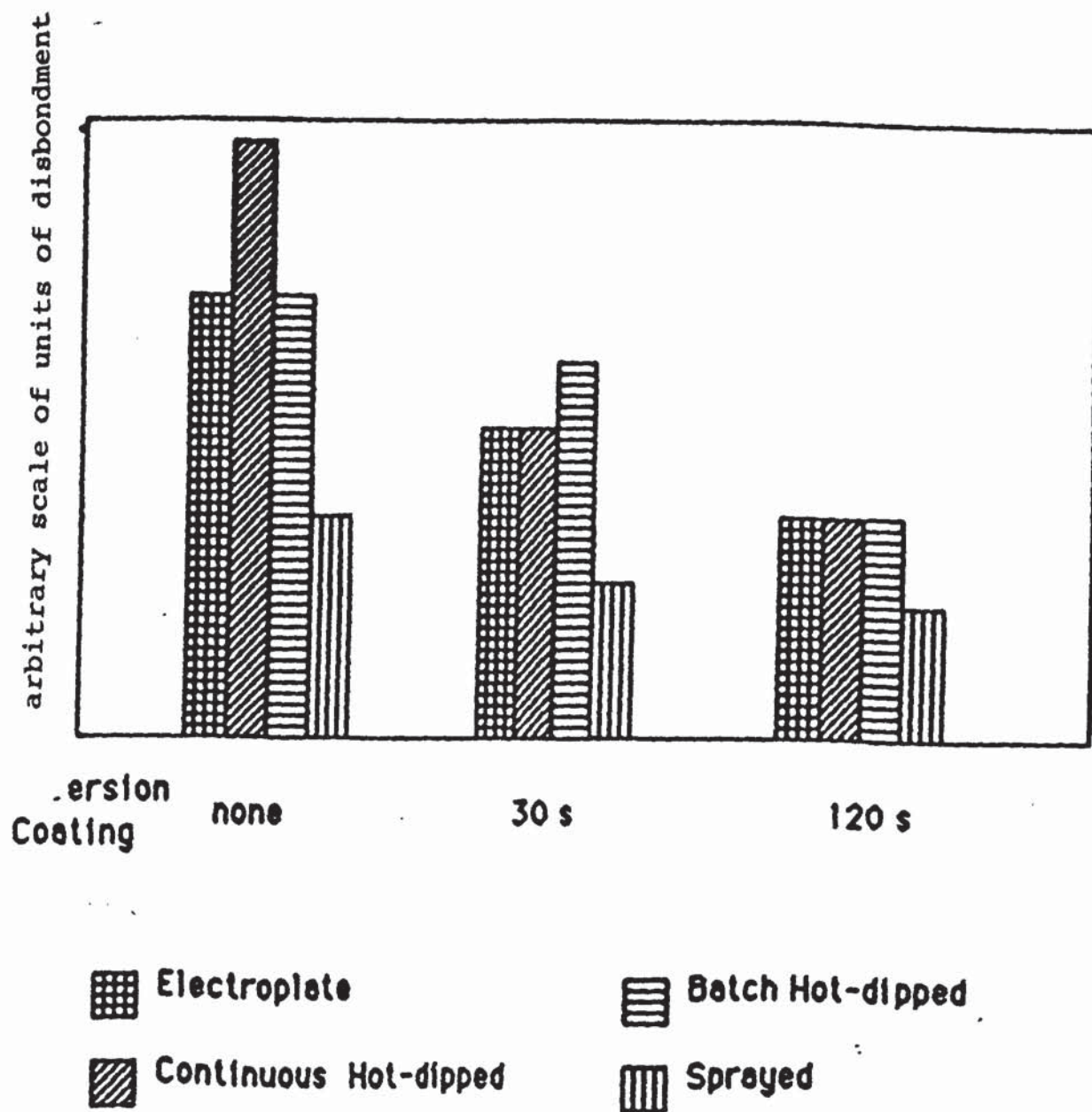


Figure 10.5 Relative disbonded areas of samples cleaned only and samples conversion coated in 0.12M/l  $\text{CrO}_3$  + 0.3M/l NaCl (L1) for 30s and 120s

## 11. LOCUS OF FAILURE OF DUPLEX POLYMER -ZINC COATINGS ON STEEL SUBSTRATES

### 11.1 INTRODUCTION

The determination of the locus of failure is of practical importance in that different measures may be needed to remedy different failure mechanisms, e.g. adhesive or cohesive failure. Furthermore the properties of the interface between a substrate and a coating is of crucial importance in determining the performance of the system. A major advance in the field of adhesion science and technology in recent years has been the chemical definition of surface and interfacial regions. X-ray photoelectron spectroscopy (XPS) and Auger electron spectroscopy (AES) are now well established techniques for the determination of surface and near surface composition of materials.

In the present work the locus of failure was studied using XPS/AES and SEM techniques. Test pannels were cleaned, pretreated in 0.12M/l  $\text{CrO}_3$  + 0.3M/l NaCl (L1) for 120 secs, dried in warm air and then powder coated. A set of these powder coated samples was subjected to acetic acid, 5% salt spray test for 700 hrs to obtain corrosion induced failure whilst another set was used to induce failure by bending

## 11.2 RESULTS AND DISCUSSION

### 11.2.1 CORROSION INDUCED FAILURE

The elements detected on the surfaces of the metal substrate and the polymer film for the corrosion induced disbonded samples are given in Table 11.1. There was no difference in the elements detected between samples which had been degassed and those which had not.

It is evident from Table 11.1 that there are differences in the elements detected when using SEM or XPS. This is due to the range of elements detected and relative depths analysed (SEM in the region of  $\mu$ , XPS in the region of nm) by the two techniques. The XPS spectra always exhibit peaks due to oxygen and carbon and in the case of thin electroplated coatings SEM is capable of detecting iron below the zinc.

In general, both techniques detected chloride on the failure surfaces of both the substrate and the polymer. It is present presumably as corrosion products of zinc, and/or iron in the case of the electroplated sample, or possibly from the pretreatment.

The titanium detected on the polymer failure surface, when using SEM, is from the pigment ( $\text{TiO}_2$ ) used in the white polyester.

That iron is detected on the substrate face of the electrodeposited and continuous hot dipped samples, is interesting, in that it suggests that most

of the zinc has been consumed, although this was not so in the case of the batch hot-dipped sample. This suggests that the area of disbondment (see figure 10.5) is not related to zinc consumed in the corrosion reaction.

Of major significance is the fact that chromium is always detected on the underside of the polymer film when using SEM but not when using XPS. Bearing in mind the relative depths analysed by the two techniques, this suggests that the chromate has remained attached to the polymer film during disbondment and is then covered by a layer of zinc corrosion products.

Figure 11.1 shows the scanning electron micrographs of the failure surfaces of both the substrate and the polymer of the electroplated and HDB samples. It can be seen that the polymer faces are not good replica of the substrate faces. This confirmed the results of the analyses (Table 11.1) which suggest the presence of corrosion products on the failing faces.

#### 11.2.2 MECHANICAL INDUCED FAILURE

Table 11.2 shows the elements detected on the failure surfaces of the substrates and the polymer film for the mechanically disbonded samples. The sprayed sample was not included since it was obvious from pull-off test results (see Chapter 9) that failure occurred within the zinc. Again, there are differences between the SEM

and XPS/AES results. Comparing results given in tables 11.1 and 11.2, it can be seen that differences exist between the corrosion induced and mechanically induced failures. For example, in the latter case no chloride is detected either by SEM or XPS on the substrate face. This was not surprising since no corrosion would have taken place and the Cl found on the polymer side of the interface would be that associated with the pretreatment. Fe was detected from the substrate face of the HDB sample when using SEM possibly due to fracture of the zinc coating which exposed the Zn-Fe alloy. SEM examination of the polymer side of the failing interface revealed the presence of Al which was not detected from the corrosion induced samples. The Al could have come from pigment in the polymer film.

Figure 11.2 shows the scanning electron micrographs of the failure faces of both substrate and polymer of mechanically induced failures of electroplated and hot-dipped batch galvanized samples respectively. In both cases, initial visual examination of the polymer face of the disbonded interface tends to suggest that disbonding occurred due to adhesive failure between the chromate conversion coating and the zinc because the cracked nature of the chromate film can be seen easily. However, the metal substrate face illustrate a different and possibly, the correct picture. There are differences between the failure face of the substrate of the mechanical induced failure (Fig 11.2 (a & c)) and corrosion

induced failure (Fig 11.1 (a &c)) due to the force which was applied during the mechanical disbondment.

Figure 11.3 (a) is a schematic diagram of the polymer coating on zinc. Notice that the conversion coating pretreatment is sandwiched between the polymer and zinc. Good<sup>(158)</sup> used a model shown in figure 11.3(b), to define the five possible regions for the locus of failure of a joint. Using this model, Good assumed each phase to be uniform with respect to the composition and molecular orientation. Regions 1 and 5 of figure 11.3(b) are within the respective bulk phases, and are far from the interface.

There is no sharp boundary, but a continuous gradient of properties and behaviour into regions 2 and 4, from region 1 and 5 respectively. He reported that in regions 2 and 4, local mechanical behaviour is influenced appreciably by the presence of the interface and of the other phase.

A model like that of Good applied to this work is shown in figure 11.3 (c). It can be seen that this is more complicated than the situation considered by Good. The cracks in the chromate film can be seen but it is not known whether the cracks are through right to the zinc. Secondly, the author is not sure whether the polymer penetrates cracks to the base and thirdly, there is possibility of formation of several zinc based compounds,

e.g.  $\text{ZnO}$ ,  $\text{Zn(OH)}_2$  or complex  $\text{Zn/Cr}$  compounds at the chromate film / Zn interface.

However this model can be used to suggest the locus of failure of the samples. The locus of failure of the sprayed sample is region 11 and the locus of failure of the rest of the samples -electroplated, HDC, and HDB, are within regions 7 - 9

A theory supporting these suggestions is that reported by Good<sup>(158)</sup>. It was reported that the interface region may be sharp on a molecular scale, or it may be molecularly diffused to an appreciable degree. It was also suggested<sup>(158)</sup> that the mechanical properties may exhibit a "jump", over a dimensional region equivalent to the distance between two atoms or molecules and that certain local properties that are most directly relevant to the strength of the two-phase system (of each joint) may change more gradually, even when the gradient of composition is the steepest possible. Another theory supporting these reasonings, is the Weak Boundary Layer (WBL) doctrine of Bikerman<sup>(159)</sup>. This doctrine states that if a system appears to have failed at a phase boundary, the failure must actually have occurred in an unsuspected layer of material at the interface, which had a low cohesive strength - a weak boundary layer. Such a layer, he said, might be a brittle oxide of a metal, or low-molecular weight polymeric material which migrates to the surface of a high - molecular - weight polymer, or a minor component of one

phase which absorbs at the interface; or it may be contamination, such as foreign matters which should not have been present at all.

Here, the point of interest is the brittle oxide of the zinc. It can be seen from figure 11.2 that the mechanical induced failures are probably of cleavage or brittle type. Also, detailed analysis of the Zn 2p peak on the polymer face of the disbonded interface with the aid of computer attached to XPS, revealed the peak to be of a Zn compound (1021.83 eV) whilst those on the substrate face were Zn (1021.43 eV). Combining all the above discussed facts together, it would be appropriate to suggest that the failure of the duplex system occurred at the interface between zinc and zinc compound layer (region 9 figure 11.3 (c))

**PAGE**

**NUMBERING**

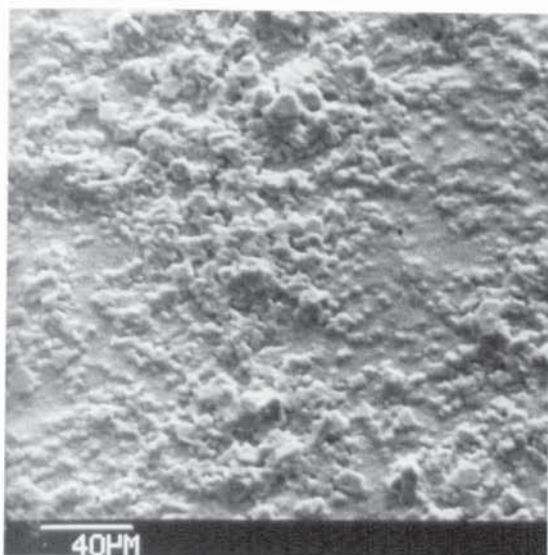
**AS ORIGINAL**

**TABLE 11.1 Surface analysis of the interfaces of samples from corrosion induced disbondment experiments**

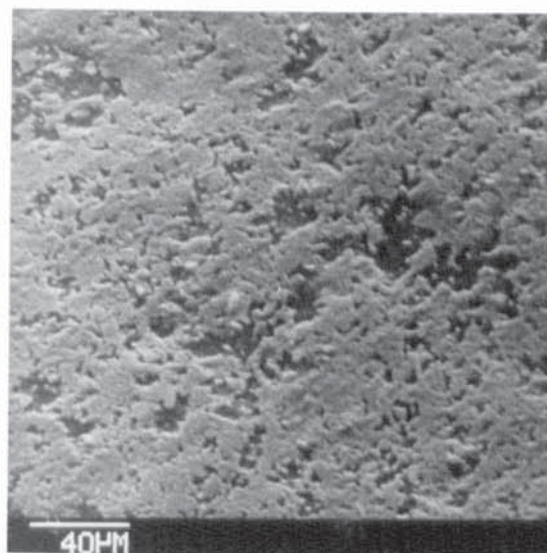
Sample	Technique	Elements Detected at the failed interface	
		Substrate Face	Polymer Face
ELECT.	SEM XPS	Zn, Fe O, C, Zn, Fe, Cl	Cr, Ti, Cl, Zn, O, Zn, C, Fe, Cl
HDC.	SEM XPS	Fe, Zn, Cl O, Zn, C, Cl	Cl, Cr, Zn, Ti, Fe O, Zn, C, Cl
HDB	SEM XPS	Zn, Cl O, Zn, C, Cl	Cl, Cr, Zn, Ti O, Zn, C, Cl
Spray	SEM XPS	Fe, Zn, O, Zn, C, Cl	Cl, Zn, C, Cl O, Zn, C, Cl

**TABLE 11.2 Surface analysis of the interfaces of samples from mechanical induced disbondment experiments**

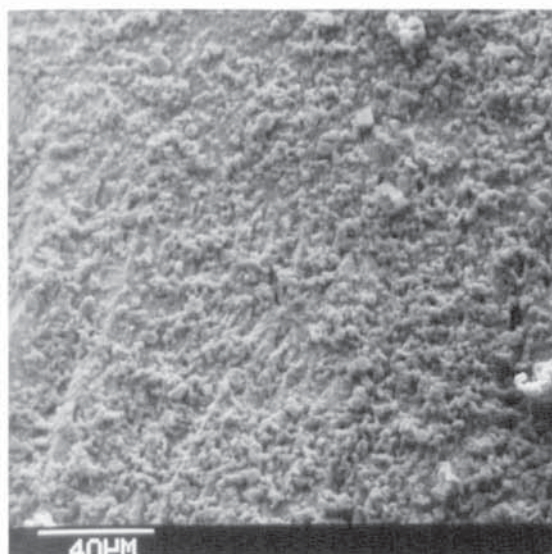
Sample	Technique	Elements detected at the failed interface	
		Substrate face	Polymer face
ELECT	SEM XPS	Zn, Fe Zn, O, C	Cr, Ti, Al, Zn, Cl Zn, O, C
HDC	SEM XPS	Zn, Zn, O, C	Cr, Ti, Zn, Al, Cl Zn, O, C
HDB	SEM XPS	Zn, Fe Zn, O, C	Cr, Ti, Al, Zn, Cl Zn, O, C



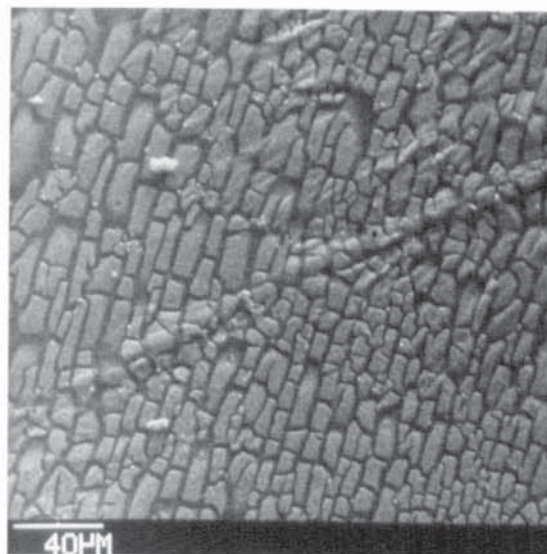
(a)



(b)



(c)



(d)

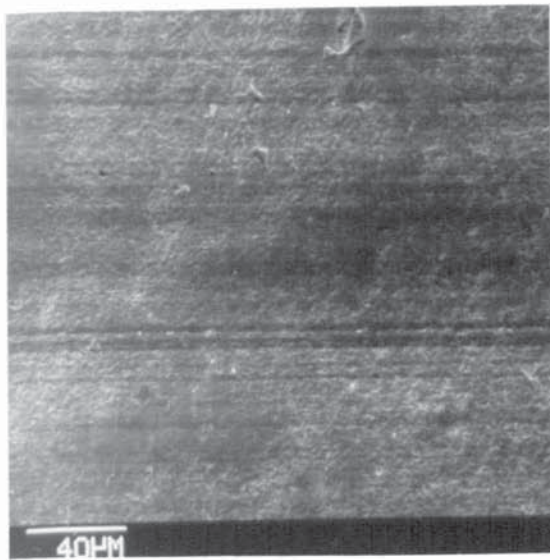
Figure 11.1 Scanning electron micrographs showing the appearance of disbonded interfaces of corrosion induced failure

(a) electroplated sample; metal face

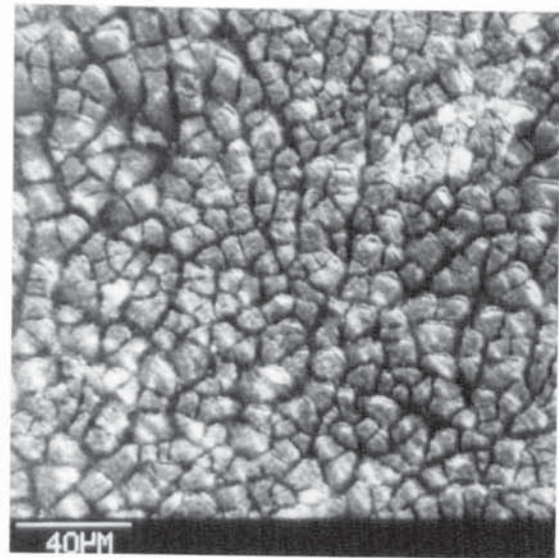
(b) " " polymer face

(c) HDB sample; metal face

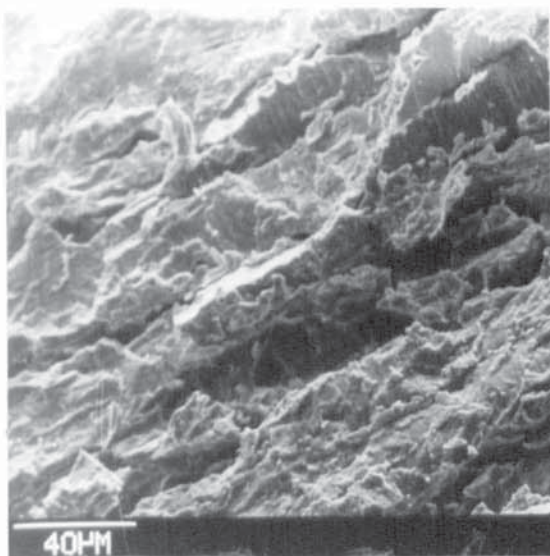
(d) " " polymer face



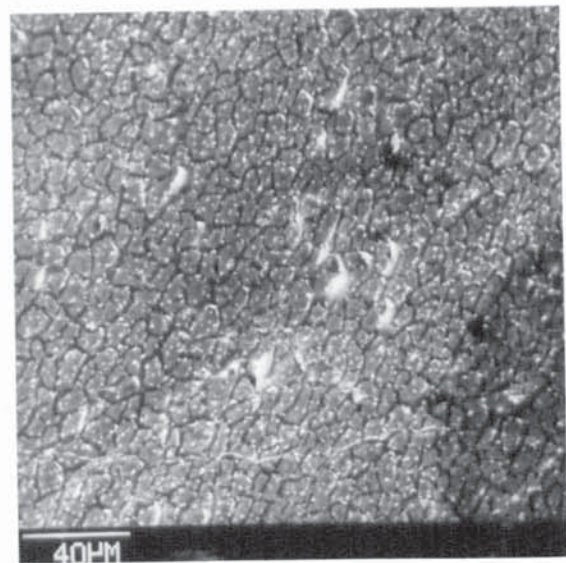
(a)



(b)

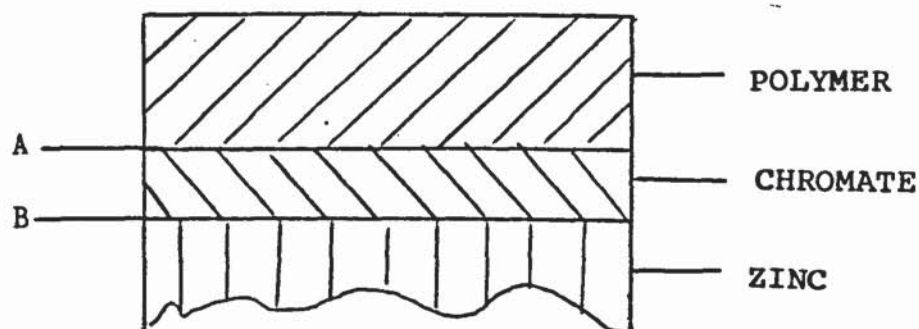


(c)

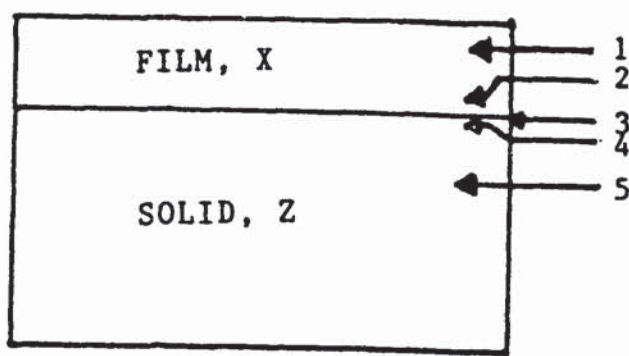


(d)

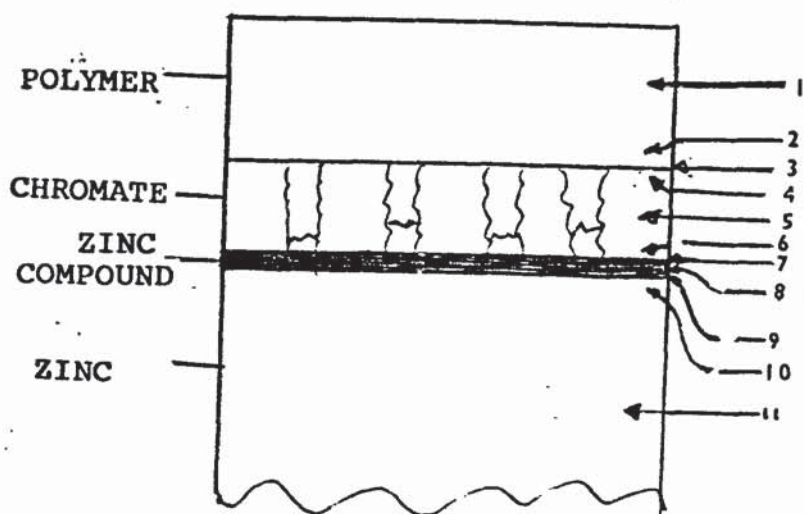
Figure 11.2 Scanning electron micrographs showing the appearance of disbonded interfaces of mechanical induced failure  
 (a) electroplated sample; metal face  
 (b) " " polymer face  
 (c) HDB sample; metal face  
 (d) " " polymer face



(a)



(b)



(c)

Figure 11.3 (a) Schematic illustration of the duplex polymer - zinc coating on steel

(b) Good's model illustrating the five possible regions for the locus of failure of joints A and B ;

(c) Possible regions for the locus of failure of the duplex polymer - zinc coating on steel applying Good's model.

The advantages of powder organic coatings compared with solution paints have led to their increasing use, particularly on aluminium and galvanized steel. In both cases, improved durability and decorative appearance are of importance. However, powder coating of zinc substrates often leads to defects such as pinholing and cratering which distract from appearance and may lead to premature failure . These defects have been linked with back ionisation during electrostatic powder coating, entrapped air or volatile products and lack of flow control agents

In the present work several examples of defects on commercially produced samples were obtained. Careful examination of these showed craters to be present as a result of incomplete spreading of molten powder, due to the presence of corrosion products, dirt, entrapped gases or defects in the galvanized coating. Pinholing is a result of collapsed voids in the organic film. These voids were probably present as a result of trapped air or volatile condensation products which could not escape due to the powder solidifying first at the air interface to form a continuous layer. This work further revealed that these defects are also strongly associated with the nature and surface roughness of the zinc substrate and the type and condition of the conversion coating applied. The adverse

effect of defective galvanized coatings on the finished powder organic coated product was also revealed.

Rougher surfaces increase the chance of air being trapped and hence the occurrence of pinholes on the rough surfaces (sec. 4.5). The voids in the polymer film and consequently the pinholes were associated with depressions or defective areas on the substrate surface.

Entrapped air or vapour will raise viscosity and interfere with powder melt flow. This was clearly evidenced during the powder flow studies, where relatively poor coverage was obtained for samples with rougher surfaces (chapter 8).

The surface roughness also influenced the thickness of the polymer film on the substrate. If adequate coverage of the peaks on the substrate surface was to be obtained and the unsightly early rusting and pitting avoided, then very thick polymer layers were required (chapter 10).

It was evident that the effect of cleaning varied with the nature of the zinc coating thus on electroplate samples there was no effect whilst the surface of hot-dip continuous and hot-dip batch were pitted and etched respectively when cleaned in AC51.

Effective conversion coating treatments should produce an adequate uniform surface upon which the organic powder is deposited so as to obtain good adhesion and consequently extended life span of the duplex coating system. This

work has revealed that, although the conversion coatings formed from most of the solutions investigated were not passive in conversion coating solutions, an improved corrosion resistance was found. It was clear from this work that different pretreatments affect adhesion and corrosion resistance to different degrees. Chromate conversion coatings, whether degassed or not degassed, improved corrosion resistance much more than alkaline (NaOH solution) conversion coatings.

The formation of chromate films on the four sets of samples have been shown to follow a parabolic law. Although the film formation on all the samples obeyed the same type of rate law, the coupon weight change for the samples were different at a given time, the samples that had the highest coupon weight change after a particular time, say 30 seconds immersion, were not the samples that had the highest coupon weight change after 120 seconds immersion. The determining factor here appeared to be the type and nature of the zinc coating (section 6.6). The solution formulation and concentration coupled with the substrate surface chemistry were the major factors dictating the mechanisms, rate of film formation and the compositions of the film.

It was discovered during the investigation of the defects and the characterisation of the samples used for this work that the surface of the hot-dip samples was not always eta (almost pure zinc), but that some parts of the surface consisted of the zeta phase or out-busts of the

zeta phase. The electrochemical behaviour of these phases was studied (chapter 7). The results obtained suggested that the zeta phase was more resistant to dissolution in acidic solutions and in alkaline solutions of pH greater than 12 than pure zinc but the latter performed more favourably in the solutions of the intermediate range of pH (7 - 12).

This work revealed the adverse effect of rough surface finish of the substrate on powder flow. It was found that with samples only cleaned in AC51, powder flow was best on the surface of electroplated samples. Application of the chromate conversion coating reduced the flow on the surfaces of all the samples and brought the final percentage coverage to almost the same value. This reduction of powder flow was reversed by using short chromating time and degassing after the formation of the conversion coating.

Three methods of adhesion measurement were used and produced conflicting results. The indentation debonding method gave the best results and looked promising for monitoring or detecting sample weaknesses during, say, the salt spray test.

Analysis of the chromated sample surfaces before and after degassing using XPS/AES revealed the conversion of hexavalent to trivalent chromium. Some authors have claimed that this conversion leads to a reduction in corrosion resistance since the hexavalent chromium, which

is frequently termed the "soluble" portion of the film, is believed to provide resistance to wet corrosion and also to provide a self-healing mechanism. However, this research work had showed that except for short chromating times, there was no appreciable difference in corrosion resistance of the degassed and not degassed samples. The probable reason for this was, that although degassing reduced the solubility of the chromate film, it provided a surface which enabled easy selective absorption of corrosion inhibitors and adhesion promoters from the organic coating into the film. XPS/AES was also used to study the locus of failure. Compared with results obtained from SEM, XPS/AES results gave a clearer insight into the locus of failure of the duplex system. It was evident from the XPS/AES results that failure occurred within zinc compounds between the zinc coating and chromate film.

### 13 RECOMMENDATION FOR FURTHER WORK

- (1) On some samples pinholes appeared to be oriented in lines suggesting that they are related to zinc spangle boundaries. It is of importance to determine whether this assumption is correct.
- (2) An electrostatic powder spray coating system, using negative corona charging, was used for this work. Further work is required to check the incidence of defects when using positive corona charging and tribocharging systems.
- (3) An investigation is also required to check and compare defects in powder coatings produced using non-electrostatic deposition methods such as the fluidised bed, flock coating and flame spraying.
- (4) During the investigation of defects it was found that the crater type defect was associated with depressions in the zinc substrate. More work is therefore necessary to determine the implication of possible Faraday cage effects on rough galvanized surfaces.
- (5) This work has revealed that the Talysurf gave the same Ra value (CLA) for dissimilar surfaces as identified in the SEM. Further work is required to provide a more detailed analysis.
- (6) Lead is normally added to galvanizing baths to aid drossing. It was found in this work that lead tended to

be segregated at the surfaces of the zinc coatings and influence the formation of the conversion coating . More work is required to substantiate this effect.

(7) Further work is required to ascertain the causes of preferential etching and pitting during the cleaning processes.

(8) Chromate conversion coatings improved considerably the corrosion resistance of all samples. Further work is required to investigate whether any improvement can be made by the addition of other corrosion resistant materials such as Ni, Co or Al.

(9) Degassing has been found to reduce greatly the incidence of the pinholing type of defect. However, the nature or type of gas involved has yet to be ascertained. Further research is required therefore to ascertain this and to find a way of avoiding the production of vapour.

(10) It has been suggested that the locus of failure is within a zinc compound formed between the zinc and the chromate film. More work is required to confirm the precise locus of failure.

(11) The acetic acid salt spray test was used to assess the corrosion resistance of all the samples used in this work. Other corrosion tests such as Prohesion, field exposure sites eg marine industrial and rural environments are required

(12) More adequate tests are still required to determine adhesion levels. This may be achieved by a refined indentation debonding test, Decrimet 'Q' meter or Impedance methods.

(13) The flow characteristics of polyester powder on different zinc coatings were studied using a heating rate of 5°C per minute. Further work is required to investigate the effect of using both higher and lower heating rates.

(14) More work is required to study the degree of cure of the polyester powder using eg Differential Thermal Analysis (DTA), and the Dielectric Spectrometer.

## REFERENCES

- (1) Leidheiser. H., "Corrosion control by Organic Coatings",  
Natl Assoc Corrosion Engs Houston, Texas 1981.
- (2) Leidheiser. H., Jr. "Corrosion of Painted Metals",  
Corrosion, 1982, 38, 7.
- (3) Mittal, K.L., "Adhesion Prospects of Polymeric Coatings",  
Plenum Pub. Corp., 1983.
- (4) Dong. K. Kim and Leidheiser, H., Jr., "A chemical test for identifying the surface of galvanized steel that have orientations approximating (0001) - importance to paint adherence",  
Metallurgical Transactions, 1978, 9B, 581.
- (5) Duncan, J. R., " Electron Spectroscopy of Chromated Galvanized Steel Surfaces",  
Surface Technology, 1982, 16 163.
- (6) Barns, C., Ward, J.J.B., Sehmbhi, T.S. and Carter, V.E., "Non-chromate Passivation treatments for Zinc",  
Trans. IMF, 1982, 60, 45.
- (7) Solomom , D.H. and Hawthorne, D.G., "Chemistry of Pigments and Fillers",  
J, Wiley & Son Inc., USA. 1983.
- (8) BS6497 : 1984, Specification for Powder Organic Coatings for Application and Stoving to Hot-dip Galvanized Steel.
- (9) Zinc Development Association, "Technical notes on zinc coatings", Published by Zinc Development Association, London, 1983.
- (10) Morgan, S.W.K., "Zinc and its alloys and compounds",  
Ellis Harwood Ltd., Chichester, 1985, 192.

- (11) Evans, U.R., "An Introduction to Metallic Corrosion",  
Edward Arnold Ltd., London, 1955.
- (12) Mars, G.F. and Norbert, D.G., "Corrosion Engineering",  
2nd Edition, McGraw - Hill Inc., London, 1983,  
29.
- (13) Mathewson, C.H., "Zinc - The Science and Technology of the metal, its alloys and Compounds",  
Reinhold Publishing Corporation, New York, 1959,  
453.
- (14) Zinc Development Association, "Technical notes on zinc galvanizing",  
Published by Zinc Development Association,  
London, 1982.
- (15) Zinc Development Association, "Galvanizing Guild",  
Published by Zinc Development Association,  
London, 1977.
- (16) Cameron, D.I. and Ormay, Proc. of 6th. International Conference on hot-dip galvanizing, Interlaken, 1961, 1962, London, Zinc Development Association.
- (17) Ghuman, A.R.P., and Goldstein, J.I., "Reaction mechanisms for the coatings formed during the hot dipping of iron in 0 to 10 Pct Al-Zn baths at 450° to 700°C"  
Metall. Trans., 1971, 2, 2903
- (18) Palmer, R.H., Thrers, H.R. and Sebisty, J.J., Proceedings of 9th International Hot-dip Galvanizing conference, Dusseldorf, 1970, 1971, Industrial Newspapers Limited, London.
- (19) Horstmann, D., "Galvanizing of steels", paper presented at 10th. International Hot-dip Galvanizing Conference, Stressa, Italy, Sept. 1973, Zinc Development Association, London.

- (20) Baldwin, A.T., "Electroplating prior to hot galvanizing for improved results"  
Metal Progr., 1953, 64, 76.
- (21) Hughes, M.L., Prod. Finishing, (London), 1953, 6, 49.
- (22) Bablik, H., Iron and Steel, 1939, 13(1), 2,;  
(2), 46.
- (23) Bablik, H., "The reaction of zinc and iron in hot-dip galvanizing"  
Metal Finishing, 1940, 38, 486.
- (24) Zinc Development Association, "Technical notes on zinc spraying",  
Published by Zinc Development Association, London, 1976.
- (25) The Canning Handbook on Electroplating, W. Cannings Limited, Birmingham, 1978, 658.
- (26) Bridger, R.D.E.L., "Pretreatment of galvanized surfaces prior to powder coating",  
Trans. Inst. of Metal Finishing, 1983, 61, 13.
- (27) Freeman, D.B. and Brunt, P.J., "Pretreatment options for rolled and galvanized steels",  
Product Finishing, 1983, 18.
- (28) Wilhelm, E.J., U.S. Patent, 2 035 380 (1936).
- (29) Anderson, E.A., "Chromate conversion coatings",  
Proc. Amer Electroplaters Soc., 1943, 31, 6.
- (30) Williams, L.F.G., "Chromate Conversion Coatings on Zinc",  
Plating, 1972, 59, 931.
- (31) Williams, L.F.G., "The Mechanism of Formation of Chromate Conversion Films on Zinc",  
Surface Technology, 1976, 4, 355.
- (32) Ashdown, R.A., "Chemical conversion treatments for zinc surfaces",  
ibid, 7.

- (33) Halls, E.E., "Chromate passivation of sprayed zinc coatings",  
Metal Treat., 1947, 14, 164.
- (34) Clarke, S.G., and Andrew, J.F., Ist.  
International Congr. on Metallic Corrosion,  
London, 1961.
- (35) Woldt, Von Berlim, G., "Uber die chromatierung  
von Nichteisenmetallen",  
Werkstoffurd Korros., 1961, 12, 486.
- (36) Freeman, D.B and Triggle, A.M., "Studies of the  
surface treatment of aluminium and zinc",  
Trans. Institute of Metal Finishing, 1960, 37,  
56.
- (37) Williams, L.F.G., "Formation and Performance  
of Chromate Conversion Coatings on Zinc",  
Surface Technology, 1977, 5 105.
- (38) Sheir, L.L., "Chromate Treatment".  
Corrosion, 2nd Ed. Newnes-Butterworth, London,  
1976.
- (39) Jenkins, H.A.H., and Freeman, D.B., "Aspect of  
chemical conversion coating processes",  
Trans. Institute of Metal Finishing, 1964, 42,  
163.
- (40) Gabe, D.R., "Oxide conversion coatings",  
Principles of metal surface treatment and  
protection, 2nd. ed., Oxford, Pergamon, 1978.
- (41) McLaren, K.G., Green, J.H. and Kingsbury,  
A.H., "A radiotracer study of the passivation of  
zinc in chromate solutions",  
Corrosion Sci., 1961, 1, 161
- (42) Biestek, T. and Weber, J., "Electrolytic and  
chemical conversion coatings",  
Portcullis Press Ltd., Redhill, 1976.
- (43) Farr, J.P.G. and Kulkarni, S.U., "The chromate  
and dichromate passivation of zinc",  
Trans. Inst. Met. Fin. 1966, 44, 21.

- (44) Van de Leest, R.E., "Yellow Chromate Conversion Coatings on Zinc: Chemical Composition and Kinetics" Trans. IMF, 1978, 56, 51.
- (45) Rekertas, R.V., Shamaytio, R.R. and Matulio, Yu., Proc. 13th Conf., Lithuania Electrochemists, Vilsa, 1975, 230.
- (46) Spencer L.F., "Conversion Coatings", Metal Finishing, 1960, 58, 58.
- (47) Agbonlahor S.O., Short N.R. and Dennis, J.K., "The nature of defects in polyester powder films on zinc coated steel substrated", Trans. Inst. Met. Fin., 1986, 64, 115.
- (48) Finishing Publications Inc., "Metal Finishing Guide book" 1958 ed. Westwood, N.J.
- (49) Perfetti, B.M., "Comparison of pretreatments for prepainted galvanized sheet, Metal Finishing, 1983, 57.
- (50) Pocock, V.E., "A Survey of Chromate Treatments" Metal Finishing, 1954, 52, 48.
- (51) Spencer, L.F., "Conversion Coatings", Metal Finishing, 1959, 57, 64.
- (52) Lorin, G., "Phosphating of Metals", Finishing Publications, 1974.
- (53) Heitzelmann, E. Jr., Organic Finishing, 1957.
- (54) Coslett, T.W., Brit. Pat. 8667, USP 1007069 and 1610362.
- (55) Wusterfield, H., Arch. Metallic, 1949, 3, 223.
- (56) Leidheiser, Tr. and Suzuki, I., "Cobalt and Nickel cations as corrosion inhibitors for galvanized steel", ElectrochemicalSoc., 1981, 128, 142.

- (57) Toft, J.D., "Some thoughts on powder coating development",  
Product Finishing, 1979, 32(8), 10.
- (58) Harris, S.T., "The Technology of powder coatings",  
Portcullis Press Ltd, London, 1976.
- (59) Gormley, E.F., "Paints for metal finishing",  
Plating and Surface Finishing, 1982, 69(5), 78.
- (60) Anon, "Steady growth in powder coatings forseen for EEC",  
Polymer Paint Colour Journal, 1980, 179, 761.
- (61) Anon, "Powder coatings in the EEC",  
Paint Manufacture and resin News, 1980, 50(8), 1.
- (62) Donalds, S.T., "Electrostatic Powder Coating",  
Trans. Inst. Met Fin., 1983, 23.
- (63) Sampuran Singh, "Why use Electrostatic Powder Coating"? Wolfson Electrostatics Advisory Unit, Department of Electrical Engineering, University of Southampton, 1978.
- (64) Gokemre, B., PhD Thesis, University of Aston, 1979.
- (65) Van der Klis, T., "Double-layer, Powder Coatings",  
Metal Finishing; 1985, 15.
- (66) Salvatore, C.L., "Selecting Powder Coatings",  
Metal Finishing, 1984, 43.
- (67) Law, E.F., "Development in electrostatic powder coatings",  
Product Finishing, 1982, 35(8), 12.
- (68) Ribnitz, P., Powder Coatings, 1981, 4(2), 6.

- (69) Sliwinski, P., PhD Thesis, University of Aston, 1985.
- (70) Franz, P. and Bolt, A., Powder Coatings, 1981, 4(1), 3.
- (71) Hardy, G.F., "Role of critical coating thickness in electrostatic powder deposition", J. of Paint Technology, 1974, 46(559), 73.
- (72) Drury, M.J., "Equipment for powder coating", Product Finishing, 1974, 27(11), 37.
- (73) Friberg, G., Powder Coatings, 1981, 4(3), 2.
- (74) Szasz, J., Industrial Finishing, 1970, 22(270), 4.
- (75) Richardson, W.J., "Plastic coating techniques", Surfacing Journal, 1974, 5(3), 10.
- (76) Toff, J.D., "Current developments in electrostatic powder coating", product Finishing, 1976, 29(3), 14.
- (77) Cross, J.A., Industrial Finishing and Surface Coating, 1975, 4,
- (78) Roobol, N.R., "Principle of Powder Coating". Trans. Inst. Met. Fin., 1983, 38.
- (79) Sampuran Singh, "Review of Powder Coating Systems", Wolfson Electrostatics Advisory Unit, Department of Electrical Engineering, Southampton University, Southampton, 1978.
- (80) Cross, J. and Bassett, J.D., "Observation during electrostatic deposition of high resistivity powders", Trans. Inst. Met. Fin., 1974, 112.
- (81) Toff, J.D., "New Electrostatic Developments", Powder Coating Conf. Proceedings, Herts, Technical Conference Organisation, 1973.

- (82) Hughes, J.F., "Electrostatics Powder Coating", Hertfordshire, Research Studies Press Ltd, 1984.
- (83) Sampuran Singh, "Charging characteristic of some powders used in electrostatic coating", IEEE Transactions on Industry Applications, 1981, 1A-17(1).
- (84) Cross, J.A., and Bassett, J.D., "Electrostatic powder coating", Trans. Inst. Met Fin., 1976, 52, 112.
- (85) Sampuran Singh, and Bright, A.W., IEEE, Conf., 1977, Los Angeles, 729.
- (86) Masuda, S. and Hizuno, A., "Electrostatic charging of powder particles", Journal of Electrostatics, 1978, 35.
- (87) Hughes, J.F. and Ting, Y.C., IEEE/IAS 12th. Annual Meeting, Los Angeles, 1977, 906.
- (88) Hughes, J.F., "Future trends in powder coating", Finishing, 1982, 6(11), 17.
- (89) Anon, "Finishing", Wheatland Journals LTD., 1982, 6(12), 21.
- (90) Freshwater, D.C., Proc. 1st Inter. Symp. on Powder Coatings, London, 1968. (14).
- (91) Bright, A.W., Proc. 1st. Inter Symp. on Powder Coatings, London, 1968, (7).
- (92) Hunecke, H., Ind. Lack. Betrieb., 1971, 39(5).
- (93) De Lange, P.G., and Selier, P., "Particle Size Distribution and Properties of Electrostatic Spraying Powders" Farbe u. Lack, 1973, 79(5), 403.
- (94) Oesterle, K.M. and Szasz, I., "Characteristics of electrostatic powder spraying", J.O.C.C.A., 1965, 48, 956.

- (95) Bright, A.W., et al., Proc. Conf. IEE., 1970, (61), 119.
- (96) Lever, R.C., Proc. 2nd Inter. Powder Coatings Conf., London, 1970, (2).
- (97) de Lange, P.G., "Behaviour of the powder fractions on spraying and after stoving" BISITS 12351, 1975, The Metals Society, London.
- (98) Pauthenier, M., Journal Phys. Radium, Ser. No. 7, 1932, 590.
- (99) Hughes, J.F., and Ting, Y.C., 3rd. Inter. Congr. on static Electricity, European Federation of Chemical Engineering, Grenoble, 1977.
- (100) Williams, J.F. Materials Protection and Performance, 1974, 9, 15.
- (101) de Lange, P.G., Film formation and rheology of powder coatings", Journal of Coating Technology, 1984, 56(717), 23.
- (102) Nix, V.G., and Dodge J.S., "Rheology of powder coatings", Journal of Paint Technology, 1973, 45(586), 59.
- (103) Fowkes, F.M., "Attractive forces at interfaces", Ind. Eng. Chem., 1964, 56(12), 40.
- (104) Gabriel, S., "The flow of epoxy based powder coating films in relation to reactivity, rheology and wetting", J.O.C.C.A., 1976, 59(2) 52.
- (105) Simpson, L.A., Proc. XVllth FATIPEC Congress, Lugano, 1984.
- (106) Ghijsels, C.H.J., and Klaren, C.H.J., Xll FATIPEC-Congress, Garmisch - Paetenkirchen, 1974, 269.

- (107) Ghiljadow, S.K., XII FATIPEC-Congress  
Garmisch - Paetenkirchen, 1974, 617.
- (108) Zorll, U., Farbe und Lack, 1974, 80(12), 1273.
- (109) Hoeflaak, M. and Selier, P., Farbe und Lack,  
1973, 70(10), 960.
- (110) Gokemre, B. and Dennis, J.K., "Effect of powder  
storage conditions on the performance of thermo-  
setting powder coatings",  
Trans. Inst. Met. Fin., 1980, 58, 15.
- (111) Pope, M.I. and Judd, M.D., "Differential  
Thermal Analysis", Heyden, London, 1977.
- (112) Brett, C.L., "The effect of state of cure on bond  
performance for an epoxy resin system",  
Journal of Applied Polymer Science, 1976, 20,  
1431.
- (113) Martin, J.K. and Tilley, R.I., "Influence of  
radiation wavelength on photo-oxidation of un-  
stabilized PVC",  
British Polymer Journal, 1971, 3, 36.
- (114) Franians, R.P., Powder Coating, 1980, 3(1), 15.
- (115) Leidheiser, H., Jr. and Kim, D.K.,  
"Crystallographic factors affecting the adher-  
ence of paint to deformed galvanized steel",  
J. Metals, 1976, 28(11), 19.
- (116) Frank, L., Coduti, P., and Smith, D., "Surface  
composition of hot-dip galvanized steel",  
68th. Meeting of the Galvanisers Committee, Zinc  
Institute, Philadelphia, Pennsylvania, 1976.
- (117) Kim, D.K., and Leidheiser, H., Jr., Surface  
Tech., 1977, 5, 379.
- (118) Leidheiser, H., and Kim, D.K., Progress Re-  
ports, numbers 1-8, Int. Lead/Zinc Research Org.  
Inc., on ILZRO Project No. ZE-207, July 1974 to  
Feb. 1977.

- (119) Leidheiser, H., Jr. and Suzuki, I., Progress Report No. 10, ILZRO Project No. ZE-207, American Iron and Steel Institute, Washington, D.C. 20036. Feb 1979.
- (120) Cameron, D.I. and Harvey, G.J., "Solidification and Spangle of Galvanized Coatings", Proc. 8th. Inter. Conf. on hot-dip galvanizing, London, "Intergalva 67", Zinc Development Assoc., London, 1967.
- (121) Cameron, D.I., Harvey, G.J. and Ormay, M.K., "The spangle of galvanized iron", J. Aust. Inst. Metals, 1965, 10(3), 255.
- (122) Sebisty, J.J. and Palmer R.H., Proc. 6th. Inter. hot-dip galvanizing conf., Interlaken, 1961, 215.
- (123) Jaffrey, D., Browne, J.E. and Howard, T.J., "The Cracking of Zinc Spangles on hot-dip Galvanized Steel", Metallurgical Trans. 1980, 11B, 631.
- (124) Barlow, G, and Harvey, G.J., "Spangle Cracking on Galvanized Iron" Lysaght's Central Research Laboratory Report No. 340, John Lysaght (Australia) Ltd., Newcastle, Australia. 1965.
- (125) Bell, R.L. and Cahn, R.W., "The nucleation problem in deformation twinning", Acta Met., 1953, (1) 752.
- (126) Prenyakow, A.A., Duisemalieyev and Mironenko, Yu. P., Tsentyne Met., 1960, 33(11), 79.
- (127) Jaffrey, D., Browne, J.D., and Lock-Lee, L.G., "On the Origin of Spangle Cracking", 11 W-1976-MTC, Annual Conference of the Inter. Inst. of Welding, Sydney, Australia, 1976, Paper 15-21.
- (128) Gourke, M. J., "Formulation of early rust resistant acrylic latex maintenance paints", J. Coatings Technology, 1977, 49(632), 69.

- (129) Gourke, M.J., and Heag, T.H., Resin Rev. 1974, 24,(1).
- (130) Paint Research Association, Newsletter No.7, 1978.
- (131) Leidheiser, H., Jr. and Kending, M.W., "The mechanism of corrosion of polybutadiene coated steel in aerated sodium chloride", Corrosion, 1976, 32, 69.
- (132) Galyer, J., and Shotbolt, C., "measurement of Surface Texture and Roundness" Metrology for Engineers, Fourth Ed., Cassell Ltd, London, 1980.
- (133). Wagner, C.D., Riggs, W.M., Davies, L.E. and Moulder, J.F., Hand Book of X-ray Photoelectron Spectroscopy, Perkin-Elmer Corporation, Physical Electronics Division, Eden Prairie, Minnesota, 1979.
- (134) Hess, M., Hamburg, H.R., and Morgans, W.M., Hess's Paint Film Defects, 3rd Ed., Chapman and Hall, London, 1979.
- (135) Whiting, C.D., and Dennis J.K., "Hot stage microscope technique for the study of thermosetting powder", Trans. IMF, 1978, 56, 32.
- (136) Wagner, C.D., "Sensitivity of Detection of the Elements by Photoelectron Spectrometry", Analytical Chemistry, 1972, 44(6), 1050.
- (137) May, R., "Impingement attack; its causes, and some methods of prevention", Journal Inst. of Metals, 1928, 40, 141.
- (138) Chao, C.Y., Lin, L.F., and MacDonald, Film growth kinetics J. Electrochemical Soc, Electrochemical Science and Technology, 1981, 128(6).
- (139) Sergi, G., Short, N.R., and Page C.L. "Corrosion of Galvanized and galvanized steel in solutions of pH 9.0 - 14.0", NACE, 1985, 272, 1.

- (140) Bengough, G.D., Lee, A.R. and Wormwell, Proc. Roy. Soc. 1931, 131(A), 494.
- (141) Borgmann, C.W. and Evans, U.R., "The corrosion of zinc in chloride solution", Trans. Electrochem. Soc., 1934, 65, 249.
- (142) Patterson, W.S., "The effect of certain impurities in zinc upon its corrosion in acid and oxygenated solutions", J. Soc. Chem. Ind., 1926, 45, 329.
- (143) Vondracek, R., Coll. Czech. Chem. Comm. 1929, 1, 627.
- (144) Shreir, L.L., "Metal/Environment Reactions", Corrosion, Newness-Butterworths, London, 1977 1.
- (145) Bijimi, D., and Gabe, D.R., "Anodic treatment of zinc", Br. Corros. J. 1983, 18(3), 138.
- (146) Ford, P.A., "Electrostatic deposition of powder coatings; effect of substrate on performance", BSc final year project report, Department of Metallurgy, University of Aston in Birmingham, 1978.
- (147) Treverton, J.A., "Production and use of coil-coated strip", Proc. Int. Conf., The Metals Society, 1981.
- (148) Mittal, K.L., "Adhesion measurement: Recent progress, unsolved problems and prospects", K.L. Mittal ed., ASTM, 1978, 5.
- (149) BS 3900: "Cross-cut test", Part E6: 1974.
- (150) BS 3900 "Pull-off test for adhesion", Part E10: 1979.
- (151) P.A. Engel, and D.D., Roshow, "Indentation debonding of an adhered surface layer", J. Adhesion, 1979, 10, 237.

- (152) Murphy, J.F., "The Finishing of Aluminium" Ed., G.H. Lissin Reinhold, 1963, 68.
- (153) Treverton, J.A., and Amor, M.P., "The structure and surface composition of chromate conversion coating; an XPS and SEM study", Trans. Inst. Met. Fin., 1982, 60, 92.
- (154) Hoffmann, E. "Measurement of adhesion of paint films by the Schmidt test", J. Oil Colour Chemist Assoc., 1960, 43, 583.
- (155) Bullett, T.R., and Prosser, J.L., Progress in Organic Coating, Elsevier Publishing Company, Asterdam, 45.
- (156) Zettlemoyer A.C., Siddig, M., and Micale, F.J., "Surface properties of heat treated chromium of narrow particle size distribution", J. of Colloid & interface science, 1978, 66, 173.
- (157) Paatsch, W., Galvananotecknic, 1977, 68, 392.
- (158) Good, R.J. "Adhesion Measurement of thin coating, Thick films, and bulk coatings", ASTM STP 640, K.L. Mittal Ed., American Society for testing and materials, 1978, 18.
- (159) Bikerman, J.J., The Science of Adhesive joints, 2nd edition, Academic Press, New York, 1968.